W&M ScholarWorks

Dissertations, Theses, and Masters Projects

Theses, Dissertations, & Master Projects

2013

Modeling the formation of periodic hypoxia in partially mixed estuaries and its response to oligotrophication and climate change

Samuel J. Lake
College of William and Mary - Virginia Institute of Marine Science

Follow this and additional works at: https://scholarworks.wm.edu/etd

Part of the Climate Commons, Ecology and Evolutionary Biology Commons, Environmental Sciences Commons, and the Marine Biology Commons

Recommended Citation

Lake, Samuel J., "Modeling the formation of periodic hypoxia in partially mixed estuaries and its response to oligotrophication and climate change" (2013). *Dissertations, Theses, and Masters Projects.* Paper 1539616727.
https://dx.doi.org/doi:10.25773/v5-vc5q-j389

This Dissertation is brought to you for free and open access by the Theses, Dissertations, & Master Projects at W&M ScholarWorks. It has been accepted for inclusion in Dissertations, Theses, and Masters Projects by an authorized administrator of W&M ScholarWorks. For more information, please contact scholarworks@wm.edu.

MODELING THE FORMATION OF PERIODIC HYPOXIA IN PARTIALLY MIXED ESTUARIES AND ITS RESPONSE TO OLIGOTROPHICATION AND CLIMATE CHANGE

A Dissertation

Presented to

The Faculty of the School of Marine Science

The College of William and Mary in Virginia

In Partial Fulfillment

Of the Requirements for the Degree of

Doctor of Philosophy

By

Samuel Joseph Lake

2013

APPROVAL SHEET

This Dissertation is Submitted in Partial Fulfillment of

The Requirements for the Degree of

Doctor of Philosophy

Samuel J Lake

Samuel J. Lake

Approved, by the Committee, April 2013

Mark J. Brush, Ph.D.
Committee Chairman, Advisor

Iris C. Anderson, Ph.D.

Robert J Diaz

Robert J. Diaz, Ph.D.

Howard Kator

Howard I. Kator, Ph.D.

Jian Shen, Ph.D.

Erik M. Smith, Ph.D.
Baruch Institute for Marine and Coastal Science and the
North Inlet-Winyah Bay National Estuarine Research Reserve
Georgetown, South Carolina

TABLE OF CONTENTS

ACKNOWLEDGEMENTS viii

LIST OF FIGURES ix

LIST OF TABLES xiii

ABSTRACT 1

INTRODUCTION 2

- EUTROPHICATION AND HYPOXIA IN COASTAL MARINE SYSTEMS 3
- HYPOXIA IN CHESAPEAKE BAY AND ITS TRIBUTARIES 5
- CARBON SOURCES FUELING HYPOXIA 8
- HYPOXIA SIMULATION MODELS 11
- OBJECTIVES 13
  - CHAPTER 1 14
  - CHAPTER 2 15
  - CHAPTER 3 16
  - CHAPTER 4 17
- LITERATURE CITED 18

CHAPTER 1: INTERNAL VERSUS EXTERNAL DRIVERS OF PERIODIC HYPOXIA IN A COASTAL PLAIN TRIBUTARY ESTUARY: THE YORK RIVER, VIRGINIA. 29
- TITLE PAGE 30
- ABSTRACT 31
- INTRODUCTION 32
- METHODS 35
  - SITE DESCRIPTION 35
  - ACROBAT MONITORING 36
  - SPRING-NEAP DISCRETE SURVEYS 37
  - METABOLIC INCUBATIONS 39
  - COMPUTED OXYGEN TRAJECTORIES 42
  - CARBON BUDGET 44
  - ESTIMATING AND SCALING UNCERTAINTY 47
- RESULTS 48
  - WATER COLUMN VARIABILITY AND THE SPRING-NEAP CYCLE 48
  - METABOLIC INCUBATIONS 50
  - COMPUTED OXYGEN TRAJECTORIES: ADVECTION VERSUS INTERNAL CONSUMPTION 51
  - CARBON BUDGET: INTERNAL VERSUS EXTERNAL SOURCES 52
- DISCUSSION 54
  - DRIVERS OF WATER COLUMN DYNAMICS 54
  - METABOLIC RATE MEASUREMENTS 55
  - COMPUTED OXYGEN TRAJECTORIES 56
  - SUMMER INTEGRATED GPP AND R 58
  - SPATIAL AND TEMPORAL VARIATIONS IN NEM 60
  - SUMMER TOTAL ORGANIC CARBON BUDGET 62
- CONCLUSIONS 65
- ACKNOWLEDGEMENTS 66
- LITERATURE CITED 67
- FIGURES 75
- TABLES 94

CHAPTER 2: MODELING THE CONTRIBUTION OF MULTIPLE ORGANIC MATTER SOURCES TO HYPOXIA IN A TRIBUTARY ESTUARY: THE YORK RIVER, VIRGINIA. 99
TITLE PAGE 100
ABSTRACT 101
INTRODUCTION 102
METHODS 106
SITE DESCRIPTION 106
EUTROPHICATION MODEL 107
FORCING FUNCTION DATA 110
WATER QUALITY CALIBRATION DATA 112
MODEL CALIBRATION AND SKILL ASSESSMENT 114
MODEL SIMULATIONS 115
RESULTS 116
MODEL CALIBRATION AND SKILL ASSESSMENT 116
CONTRIBUTION OF OM SOURCES TO HYPOXIA 118
NUTRIENT AND ORGANIC MATTER SCENARIOS 120
DISCUSSION 122
MODEL SKILL ASSESSMENT 122
CURRENT CONDITIONS 125
CONTRIBUTION OF INTERNAL AND EXTERNAL ORGANIC MATTER SOURCES TO HYPOXIA 126
SIMULATED CHANGES IN NUTRIENT AND ORGANIC MATTER LOADING 129
CONCLUSIONS 132
ACKNOWLEDGEMENTS 134
LITERATURE CITED 135
FIGURES 144
TABLE 161

CHAPTER 3: MODELING THE RESPONSE TO EXTERNAL LOAD REDUCTIONS IN A WARMER CLIMATE: PRIMARY PRODUCTION, NET ECOSYSTEM METABOLISM, AND HYPOXIA IN THE YORK RIVER ESTUARY, VIRGINIA. 164
TITLE PAGE 165
ABSTRACT 166
INTRODUCTION 168
METHODS 173
  SITE DESCRIPTION 173
  LINKAGE BETWEEN AIR AND WATER TEMPERATURE 174
  INTERMEDIATE COMPLEXITY EUTROPHICATION MODEL 175
  MODEL CALIBRATION AND SKILL ASSESSMENT 178
  CLIMATE SIMULATIONS 179
RESULTS 180
  LINKAGE BETWEEN AIR AND WATER TEMPERATURE 180
  CHANGES IN PRIMARY PRODUCTION AND NET ECOSYSTEM METABOLISM 181
  EFFECT OF A WARMER CLIMATE ON HYPOXIA 183
  LOAD REDUCTION SCENARIOS 184
DISCUSSION 185
  LINKAGE BETWEEN AIR AND WATER TEMPERATURE 185
  PREDICTED ECOSYSTEM FUNCTION UNDER A WARMER CLIMATE 186
  EFFECT OF WARMER TEMPERATURE ON HYPOXIA 190
  MANAGEMENT SCENARIOS UNDER A WARMER CLIMATE 192
  FUTURE CLIMATE CHANGE 193
CONCLUSIONS 195
ACKNOWLEDGEMENTS 197
LITERATURE CITED 198
FIGURES 209

CHAPTER 4: THE CONTRIBUTION OF MICROPHYTOBENTHOS TO TOTAL PRODUCTIVITY IN UPPER NARRAGANSETT BAY, RHODE ISLAND. 228
- TITLE PAGE 229
- ABSTRACT 230
- INTRODUCTION 231
- METHODS 234
  - SITE DESCRIPTION 234
  - LIGHT ATTENUATION AND WATER QUALITY 235
  - SEDIMENT CHLOROPHYLL-A SAMPLING AND PROCESSING 236
  - PHOTOSYNTHESIS-IRRADIANCE (P-I) AND METABOLISM EXPERIMENTS 237
  - DATA ANALYSIS AND INTERPOLATION 238
- RESULTS 240
  - SEDIMENT CHLOROPHYLL-A 240
  - BENTHIC PRODUCTION 241
- DISCUSSION 243
  - REGIONAL COMPARISON OF SEDIMENT CHLOROPHYLL-A 243
  - GROSS PRIMARY PRODUCTION 244
  - BENTHIC NET COMMUNITY METABOLISM 246
  - FUTURE ROLE OF MICROPHYTOBENTHOS 247
- CONCLUSIONS 249
- ACKNOWLEDGEMENTS 250
- LITERATURE CITED 251
- FIGURES 255
- TABLES 266

APPENDIX 272

VITA 337

ACKNOWLEDGEMENTS

The efforts and support of countless people led to the completion of this dissertation. It would be impossible for me to fully express my immense gratitude to all those that have lent their support, encouragement, and guidance over the past several years. However, in a humble effort to do so I would like to recognize some of those people here. First, I would like to thank my advisor, Dr. Mark Brush, who has not only given me the opportunity to follow my research interests, but also provided his endless support, encouragement, knowledge and also patience throughout the past six years. His passion and excitement for coastal marine ecology has been absolutely contagious and continually motivates me to strive harder. Additionally, his friendship has made the entire process absolutely enjoyable! I would also like to thank the rest of my academic committee: Drs. Iris Anderson, Robert Diaz, Howard Kator, Jian Shen, and Erik Smith who have helped guide me, have always been very generous with their time and have truly helped me improve the quality of my research.

I am also particularly grateful to Drs. Eric Koepfler and Richard Dame, who inspired me to study marine ecology shortly after entered the marine science program at Coastal Carolina University. Thank you for giving me the momentum which was to be the start of my career! Additionally, I owe many thanks to the Virginia Institute of Marine Science, the VIMS GK-12 Perfect Program, along with countless other funding sources for all of their support, which made this research possible.

I am also grateful to the members of the Brush Lab (Team *dN/dT*) for all of their support, assistance, laughter, and advice. To Beth Condon, Lisa Ott, Juliette Giordano, Brittani Koroknay, Britt Dean and Michael Kuschner thank you for all of your support, encouragement, stimulating discussions, countless impromptu meetings, and much more. I am also very grateful to all my friends in the VIMS community including (but definitely not limited too): Daniel Maxey, Lindsey Kraatz, Stephanie Salisbury, and Lori Sutter. And thank you to all of my friends both within the Williamsburg community and points farther away.

To my parents and family I am forever grateful for your continued support. To my mom and dad, I would not be where I am today without your guidance and encouragement through all of the challenges that I have taken on over the years. Thank you for instilling drive and determination into me all those years ago! I would not be here without your continued support.

Finally, it is impossible to spend the majority of your adult life in school without continual support from family and friends. I give endless thanks to my wife Calandra, and our daughter Naia. They definitely give my life meaning, and I cannot possibly express enough love and appreciation. To Naia, you have given up more than you will ever know, thank you for being so wonderful! Always smiling, laughing and happy to see me when I walk in the door, even when it was late at night. Your energy was all the motivation I would have needed to finish in itself. To my loving wife Calandra, who has sacrificed the most to allow me to follow my dreams, provided unwavering and unconditional love and support, THANK YOU! You have supported me and our family through it all, and have given up the most. I will never be able to express how much I truly appreciated everything that you have done… but I will do my best to express my gratitude and love every day!

LIST OF FIGURES

CHAPTER 1

Figure 1-1. Map of the York River estuary including: sampling region boundaries, sampling stations, and Acrobat^{TM} monitoring survey cruise tracks. 77

Figure 1-2. Interpolated dissolved oxygen concentrations from Acrobat^{TM} surveys, from June 2007 and June 2008. 79

Figure 1-3. Time-series of environmental conditions during the weekly spring-neap surveys in 2008. Precipitation at the Taskinas Creek meteorological station, combined river flow of the Mattaponi and Pamunkey Rivers, wind speed, daily tidal range, observed strength of stratification (bottom – surface, sigma-*t*), and observed mean bottom water dissolved oxygen concentrations. 81

Figure 1-4. Nutrient and water column chlorophyll-*a* concentrations from spring-neap surveys sampled weekly in each sampling region during 2008. 83

Figure 1-5. Time-series of water column and sediment maximum gross photosynthetic rate (in the absence of photoinhibition) measured during light box metabolic incubations following the spring-neap surveys. Mean respiration rates for surface (0.5m) and bottom water, and shallow and deep channel sediments. 85

Figure 1-6. Mean water column and sediment gross primary production calculated from 1000 Monte Carlo simulations where chlorophyll-*a*, k_D, and P-I parameters were randomly selected from their normal distributions. 87

Figure 1-7. Computed and observed dissolved oxygen trajectories during spring to post-neap tide transitions. 89

Figure 1-8. Interpolated daily water column and sediment gross primary production, and water column and sediment respiration for each sampling region. 91

Figure 1-9. Estimated total organic carbon budget for the York River estuary over the sampling season (June – September 2008) including physical inputs and outputs and biological production and respiration. All values are x 10^9 g C. 93

CHAPTER 2

Figure 2-1. Map of the York River estuary and the Chesapeake Bay, including box model boundaries, the surrounding watershed, and long-term Chesapeake Bay Program monitoring stations. 146

Figure 2-2. Diagram of the intermediate-complexity eutrophication model. 148

Figure 2-3. Measured and modeled surface water column chlorophyll-*a*, surface and bottom dissolved oxygen, and surface dissolved inorganic nitrogen and phosphorus for Boxes 4 and 8, respectively. 150

Figure 2-4. Measured and modeled rates of phytoplankton net daytime production, surface and bottom layer water column respiration, MPB gross primary production within the surface layer, and surface and bottom layer sediment respiration. 152

Figure 2-5. Percent change in predicted dissolved oxygen concentrations (deviation from baseline model simulation) for eight scenarios in which individual organic matter sources were removed. 154

Figure 2-6. Annual number of hypoxic ($< 2\text{mg L}^{-1}$) and low oxygen days ($< 3 \text{ mg L}^{-1}$) within each model box predicted under various watershed and tributary loading scenarios, averaged over a four year simulation. 156

Figure 2-7. Annual number of hypoxic ($< 2\text{mg L}^{-1}$) and low oxygen days ($< 3 \text{ mg L}^{-1}$) within each model box predicted under various Chesapeake Bay input scenarios, averaged over a four year simulation. 158

Figure 2-8. Relative seasonal (May – September) contribution of various organic matter sources to the reduction of bottom water oxygen concentrations along the York River estuary. 160

CHAPTER 3

Figure 3-1. Map of the York River estuary and the Chesapeake Bay, including box model boundaries, small ungauged watersheds, and corresponding long-term Chesapeake Bay Program monitoring stations. 211

Figure 3-2. Diagram of intermediate-complexity eutrophication model, highlighting variables and rates that are temperature dependent. State variables, major flows, and major connections are depicted. 213

Figure 3-3. Polyhaline Chesapeake Bay surface and bottom water temperatures plotted against mean monthly air temperatures measured at Norfolk International Airport, between 1949 – 1982 and 1984 – 2012. York River estuary surface and bottom water temperatures at Chesapeake Bay Program sites located in Boxes 1 – 3 and 4 – 8 from 1984 to 2012, plotted against mean monthly air temperatures measured at Norfolk International Airport. 215

Figure 3-4. Modeled percent change in daytime water column net primary production relative to the baseline model simulation under a series of scenarios with increasing temperatures. Results were averaged over a four year simulation. 217

Figure 3-5. Modeled percent change in net ecosystem metabolism relative to the baseline model simulation, under a series of scenarios with increasing temperatures. Results were averaged over a four year simulation. 219

Figure 3-6. Predicted annual number of hypoxic (< 2 mg L^{-1}) and low oxygen days (< 3 mg L^{-1}) within each model box under a range of temperature scenarios. Values represent the average number of days over a four year simulation. 221

Figure 3-7. Predicted annual number of hypoxic (< 2 mg L^{-1}) days within each model box under various scenarios in which nutrient and organic matter (dissolved and particulate) loads from the tributaries and ungauged watersheds were reduced. 223

Figure 3-8. Predicted annual number of hypoxic (< 2mg L^{-1}) days within each model box under various scenarios in which nutrients, phytoplankton biomass, and organic matter (dissolved and particulate) loads from Chesapeake Bay were reduced. 225

Figure 3-9. Predicted annual number of hypoxic (< 2mg L^{-1}) days within the upper (Boxes 1 – 4 combined) and lower (Boxes 5 – 8 combined) York River estuary, under a range of temperature warming scenarios (+ 1, + 2, + 3, and + 5 °C) and external load reductions. 227

CHAPTER 4

Figure 4-1. Location of sediment chlorophyll-*a* depth profiles and sediment core sampling sites, and single depth benthic chlorophyll-*a* survey sites within the different segments of upper Narragansett Bay. 257

Figure 4-2. PI curve displaying minimum, average, and maximum estimated curves for Greenwich Bay from September 2010. 259

Figure 4-3. Sediment chlorophyll-*a* biomass (top 3 mm) with depth at four sites within upper Narragansett Bay. 261

Figure 4-4. Interpolated 5 day moving average GPP_B and daytime NPP_{WC} (modified from Oviatt et al. 2002). 263

Figure 4-5. Interpolated daily NCM_B within each segment of upper Narragansett Bay. 265

LIST OF TABLES

CHAPTER 1

Table 1-1. Monthly and seasonal mean rates of integrated gross primary production, respiration, and net ecosystem metabolism for the entire York River estuary. 96

Table 1-2. Monthly and seasonal mean net ecosystem metabolism for each region of the York River estuary. 98

CHAPTER 2

Table 2-1. Skill assessment metrics for all parameters where measured concentrations or rates were available, averaged over all model boxes and Boxes 5 – 8 where hypoxia occurs. 163

CHAPTER 4

Table 4-1. Percent of total surface area in each sampling regions: Providence River estuary, upper Narragansett Bay, Greenwich Bay, and Greenwich Cove. Numbers represent the percent of surface area below each depth contour. Depths are relative to mean sea level. 268

Table 4-2. Percent of total primary production attributed to microphytobenthos in upper Narragansett Bay. Values outside brackets represent the contribution from benthic production based on the average model, while the bracketed values represent the minimum and maximum models respectively. Total primary production was computed from GPP_B (calculated in this study) and daytime NPP_{WC} (from Oviatt et al. 2002) at 5 sites (site numbers correspond to the bay survey stations from Oviatt et al. 2002) in upper Narragansett Bay from April to October. 270

ABSTRACT

The development of hypoxia represents one of the most common and ecologically detrimental effects of anthropogenic nutrient enrichment in coastal marine ecosystems. Due to the physiological importance of oxygen as a key component of metabolic processes, the development and persistence of hypoxia can reduce the distribution of important species, modify food webs, decrease diversity and richness, and sub-lethally affect growth and reproductive rates. While many recent studies have focused on the global increase in hypoxia and highlighted the need for nutrient reduction strategies, some key processes associated with hypoxia remain understudied. Of particular importance is the resolution of the major carbon sources fueling hypoxia in tributary estuaries, which receive inputs from the upland watershed, internal primary production, and advection from the main estuary, which may also be a source of hypoxic water. Development of well-constrained, intermediate complexity ecosystem models is also needed to provide realistic predictions of the response of hypoxia to nutrient reduction strategies, and to understand the interactive effects of these load reductions with ongoing climate change.

The recent implementation of high spatial and temporal resolution water quality sampling instruments has confirmed the importance of the spring-neap tidal cycle and its effect on the formation and disruption of stratification and hypoxia in the York River estuary (YRE). However, these results have indicated that the advection of high-salinity hypoxic water into the lower YRE from the Chesapeake Bay (CB) may be as important as internal oxygen consumption. Additionally, previous studies have suggested that phytoplankton production in the YRE and similar tributary estuaries may be insufficient to explain the magnitude of hypoxia observed. This study synthesized *in-situ* measurements and high resolution water quality monitoring with an intermediate complexity model to examine the significance of these factors and how they interact to cause hypoxia within the YRE. Simulations were used to determine the magnitude of nutrient and/or organic matter (OM) reductions required to reduce the extent and severity of hypoxia in the presence of increasing temperatures resulting from climate change.

A comparison of *in-situ* and computed oxygen concentrations for the YRE indicated that internal respiration was sufficient to drive hypoxia under stratified conditions, without the need for advection of hypoxic water from the CB. Phytoplankton production was the major source of organic carbon to the YRE and 1.5 times greater than advective inputs from CB, which were roughly balanced by exports. Watershed sources and microphytobenthos contributed comparatively little carbon to the whole system. Model simulations indicated that lower portions of the YRE tributaries are strongly influenced by watershed OM loading during summer, while the low mesohaline region is influenced by internal primary production and OM from the tributaries. The high meso- and polyhaline regions responded primarily to advected dissolved organic carbon from CB. Results indicate that different regions of the YRE require separate management strategies to control hypoxia, with the key issue in the lower estuary being the "far field" source of labile OM from outside the system. The model predicted increasing primary production under warmer conditions in winter and spring throughout most of the YRE, but decreasing production in summer and fall in the lower estuary. These changes together with increasing respiration resulted in increased autotrophy in the upper YRE, while NEM was predicted to decrease throughout the rest of the estuary. Warmer temperatures increased both the temporal and spatial extent of hypoxia in the model, suggesting the need for additional nutrient and OM load reductions in order to achieve the same level of improvement predicted without warming.

INTRODUCTION

Eutrophication and Hypoxia in Coastal Marine Ecosystems

Coastal eutrophication, defined here as "an increase in the rate of supply of organic matter to an ecosystem" (Nixon 1995, 2009), is one of the leading causes of water quality impairment around the world (Nixon 1995; Selman 2007; Diaz and Rosenberg 2008). Although both external nutrient inputs and internal nutrient recycling can increase the amount of organic matter production within coastal marine systems, the principle factor contributing to eutrophication in these systems today is excess anthropogenic nutrients entering from the surrounding watersheds (Nixon 1995, 2009; Diaz and Rosenberg 2008). Anthropogenic nitrogen and phosphorous enrichment has been linked to a number of degradative effects in marine ecosystems including an increase in phytoplankton (including toxic and harmful species) and macroalgae blooms, changes to benthic community structure, loss of submerged aquatic vegetation, hypoxia (≤ 2.0 mg O_2 L^{-1}), and in some cases severe and prolonged anoxia (≤ 0.2 O_2 mg L^{-1}) (Rabalais 2002; Kemp et al. 2005; Diaz and Rosenberg 2008). Of these deleterious effects it has been suggested that hypoxia and anoxia represent the most serious threats from eutrophication (Diaz and Rosenberg 1995, 2008).

The susceptibility of coastal marine ecosystems to hypoxia (and anoxia) is controlled by a combination of environmental factors that interact with the physical and biological characteristics of each particular system; these drivers include meteorological cycles, residence time, wind stress, currents, riverine input, water temperature, density stratification, the input of anthropogenic nutrients and organic matter, and the biogeochemical processing of organic matter (Kemp et al. 1992; Diaz 2001; Boesch et al. 2002; Buzzelli 2002). Although a combination of these factors must align to cause bottom water hypoxia, generally prolonged density stratification and warm summer water temperatures are necessary for the formation of hypoxia (Stanley and Nixon 1992; Buzzelli 2002; Bergondo et al. 2005).

Due to the physiological importance of oxygen as a key element in metabolic processes of most marine organisms, the development and persistence of low oxygen zones in marine habitats can detrimentally impact both benthic and pelagic communities (Diaz and Rosenberg 1995; Breitburg et al. 2009), although some resistant and mobile species may benefit initially from hypoxia due to quick individual recruitment rates (Rosenberg et al. 2002; Lim et al. 2006) or short-term increases in exploitation rates of prey species (Pihl et al. 1992). The ecological impact that hypoxia and anoxia has on a coastal ecosystem is directly related to the duration, severity, and historical occurrence of low oxygen periods (Diaz and Rosenburg 1995, 2008). The duration and spatial scale of hypoxia can range from short-term diel and localized events that last a few hours, typically causing hypoxia-resistant species to rely on behavioral adaptations (Diaz and Rosenburg 1995) while less resistant mobile species frequently migrate away (Tyler and Target 2007), up to large scale seasonal dead zones that result in catastrophic losses of all aerobic benthic organisms (Hagy et al. 2004). During periods of severe anoxia, the absence or significant reduction in available oxygen also alters the rate of coupled nitrification-denitrification and enhances the release of iron-bound phosphorous from the sediment into the overlying water (Kemp et al 1990; Cowan and Boynton 1996; Hagy et al. 2004). The resulting efflux of ammonium and phosphate from the sediments creates a positive feedback that prolongs or intensifies hypoxia by increasing surface water production when water column stratification breaks down or when bottom water is transported laterally into shallower regions (Gavis and Grant 1986; Kemp et al 1990; Cloern 2001).

Hypoxia in Chesapeake Bay and its Tributaries

Eutrophication and hypoxia within the Chesapeake Bay and its tributaries have been intensely studied with large-scale monitoring programs and smaller-scale high intensity sampling over the past 25 years following the noticeable decline in water quality, increase in deep water hypoxia and loss of sub-aquatic vegetation between the 1950's and 1980's (Cooper and Brush 1991; Cooper and Brush 1993; D'Elia et al. 2003; Kemp et al. 2005). The seasonal development of anoxia within the mainstem of the Chesapeake Bay has been linked to the input of fresh water (primarily from the Susquehanna and Potomac Rivers) and associated influx of organic matter and nutrients during high flow periods (winter and spring), the production and subsequent deposition of organic matter during the spring phytoplankton bloom, and density driven water column stratification (Taft et al. 1980; Officer et al. 1984; Seliger et al. 1985; de Jonge et al. 1995; Cloern 2001; Hagy et al. 2004; Kemp et al. 2005). The deposited autochthonus and allochthonus organic matter fuels the formation of seasonally persistent summertime anoxia in the bottom water as it is respired by bacteria under warm temperatures (Malone et al. 1986; Kemp et al. 1992; Paerl et al. 1998; Møhlenberg 1999; Rabalais et al. 2007).

In an effort to improve the water quality within the Chesapeake Bay and its tributaries, the U.S. Environmental Protection Agency (EPA) developed the Ambient Water Quality Criteria for Dissolved Oxygen, Water Clarity, and Chlorophyll-*a* in 2003 under requirements by the Clean Water Act and the Chesapeake 2000 agreement (U.S. EPA 2000, 2003). Due primarily to sampling limitations, the existing Bay monitoring program has been shown to be insufficient to cover all of the outlined EPA criteria components, and instead the Chesapeake Bay Program has focused on assessing only the 30 day mean dissolved oxygen (DO) criteria and in some cases instantaneous minimum dissolved oxygen criteria (U.S. EPA 2007). Although this strategy can sufficiently track the temporal fluctuations in DO in the mainstem and northern tributaries, it may prove inadequate to assess the degree of hypoxia in systems characterized by periodic hypoxia, in which hypoxic events typically a few days to a week in duration alternate with periods of normoxia.

While the conceptual model of hypoxia formation in the mainstem Chesapeake is appropriate for a number of systems worldwide, it does not apply as well to the conditions that are present within many of the Bay's shallower tributaries, which are influenced by multiple sources of labile organic matter and advection of high nutrient – low oxygen water from the mainstem, along with variable physical mixing processes, both tidal and wind driven (Haas 1977; Kuo and Nielson 1987; Sharples et al. 1994; Fisher et al. 2006; Boynton et al. 2008; Testa et al. 2008). These drowned river valley systems are characterized by a narrow but deep centralized channel that is flanked by broad, shallow photic shoals, which support a highly productive community of microphytobenthos (MPB) (Rizzo and Wetzel 1985). Of the three major tributaries in the Virginia portion of the Chesapeake Bay, the James River represents the most hypoxia resistant system because of its shallow river basin, large fetch, and strong tidal mixing due to its proximity to the mouth of the Bay (Kuo and Neilson 1987; Kuo et al. 1991). The Rappahannock River displays the strongest seasonal stratification and most widespread hypoxia, which has been linked to the poor quality of water entering the system from the mainstem and relatively weaker tidal mixing compared to the other two Virginia tributaries (Kuo and Neilson 1987). The York River estuary (YRE) is in a physical state between the James and Rappahannock Rivers, and oscillates between stratified and well-mixed conditions due to the variation in physical mixing energy associated with the spring-neap tidal cycle (Haas 1977; Hayward et al. 1982; Kuo and Neilson 1987; Diaz et al. 1992). This cyclical physical forcing creates the potential for continued formation and disruption of bottom water hypoxia from June to early September within the lower half of the river. Additionally, these destratification events also have the potential to resupply nutrients to the surface water, dynamically affecting phytoplankton production throughout the summer and early fall (D'Elia et al. 1981; Haas et al. 1981). While past studies in the YRE have highlighted the interaction between the spring-neap cycle and the development of hypoxia, we still lack an understanding of how the full suite of physical and biological processes interact to result in hypoxia within the system.

Carbon Sources Fueling Hypoxia

Another as yet unanswered issue surrounding hypoxia in the Chesapeake and particularly its tributaries has to do with the source of organic matter fueling hypoxia. Previous measurements of particulate organic carbon (POC) sedimentation as well as modeling studies conducted in the Chesapeake and its tributaries have shown that the overlying phytoplankton production occurring above the central channels may not be sufficient to support the vertical flux of POC out of the euphotic zone (Malone et al.1986, Testa and Kemp 2008). Malone et al. (1986) attributed this additional carbon source to phytoplankton production occurring over the lateral shoals. Additionally, box model calculations conducted by Testa and Kemp (2008) in the Patuxent River indicated that the export of POC from the surface water was insufficient during parts of the year to support bottom-layer net oxygen uptake. In their discussion, the authors attribute this additional source of POC to more labile, locally produced organic carbon that is vertically and laterally transported to the bottom waters of the estuary rather than the influx of older and less labile organic matter from the Chesapeake Bay mainstem (Testa and Kemp 2008).

It is apparent that additional carbon sources beyond phytoplankton in the main channel may be fueling hypoxia within the tributary estuaries of Chesapeake Bay. Although it is well known that summer phytoplankton blooms can contribute to annual production within estuarine systems (Malone et al. 1988; Pinckney et al. 1998), it is unlikely that these smaller phytoplankton blooms are playing a dominant role in the formation of hypoxia in the YRE due to their historically low chlorophyll-*a* concentrations, relatively small biomass, and dominance by smaller phytoplankton species, primarily dinoflagellates. One potential source of additional organic matter that may prove to be an important factor driving oxygen consumption within the polyhaline region of the YRE may be advection of mainstem subpycnocline water entering via estuarine circulation. In an analysis of chlorophyll-*a* concentrations in the Chesapeake over the past 50 years, Harding and Perry (1997) found that the lower polyhaline mainstem has exhibited the largest increase in chlorophyll-*a* within the bay, with a 5 – 10 fold increase from 1950 to 1994. It is likely that this increase in phytoplankton biomass, which deposits an average of 277 mg chl-*a* m^{-2} (20.8 g C m^{-2}, C:Chl-*a*) ratio of 75) in the lower bay (Hagy et al. 2005), has directly increased biological oxygen demand (BOD) within the polyhaline mainstem. Although the shallow depths, large fetch, and strong tidal and wind mixing in the lower Bay prevent it from becoming hypoxic throughout the summer, it is likely that when this water mass is transported into more stratified regions, like the deeper channels of the lower estuary (Kuo et al. 1993), the oxygen consumption rate can increase beyond the vertical oxygen diffusion rate.

Another source of organic material entering the YRE is from the surrounding watershed primarily delivered by the Mattaponi and Pamunkey Rivers. Although terrestrially-derived organic matter can account for a large quantity of carbon at the head of the estuary, it has been shown that these sources of fixed carbon are not as dominant nor readily utilized as phytoplankton sources within the higher mesohaline and polyhaline regions of the river (McCallister et al. 2006a). This is likely due to several important biological and physical factors including high initial removal rates at the head of the estuary due in part to flocculation and removal to the sediments, rapid rates of microbial degradation, and the long freshwater residence time of the estuary (Shen and Haas 2004; McCallister et al. 2006b; Countway et al. 2007).

A final likely source of organic matter fueling bottom water hypoxia is the highly productive MPB community present throughout the shallow shoal regions of the YRE (< 2 m), which comprise approximately 40 % of the system by area (Rizzo and Wetzel 1985). The micrcophytobenthic community in the YRE varies little spatially regardless of habitat or substrate type within the mesohaline and polyhaline regions of the river or seasonally from late spring to early fall (Rizzo and Wetzel 1985; Lake and Brush unpublished data). MPB is a viable primary producer throughout the year (Pinckney and Zingmark 1993; Reay et al. 1995; Buzzelli 1998), producing an estimated 128.6 (+/- 65.108) g C m^{-2} or 1.7 x 10^7 kg C annually (Rizzo and Wetzel 1985). Extracellular release of organic material (in the form of POC, dissolved organic carbon (DOC), and colloidal organic carbon) relative to total primary production by MPB is also high compared to phytoplankton (Goto et al. 1999), and has been identified as a possible source of missing carbon driving deep water microbial respiration in other systems (Graf et al. 1982). A study conducted by de Jonge and van Beusekom (1995) showed that wind speeds at low as 1-2 m s^{-1} (2.2 – 4.5 mph) are capable of suspending MPB and sediment within the shallow regions of the Ems estuary. Furthermore, their results showed that over 50% of MPB biomass occurring within the top 0.5 cm of sediment was transported to the main channel when wind speeds reached 12 m s^{-1} (26 mph) and 14 – 25% of total benthic diatom biomass was suspended at average wind speeds (4.5 – 6.5 m s^{-1}, 10 – 15 mph) (de Jonge and van Beusekom 1995). While the initial availability of this organic material is most likely limited to the surrounding shallow regions, it is likely that high energy periods resulting in a repeated cycle of particle suspension and subsequent re-settling, eventually transports this organic matter both down the estuary and laterally into the channel where it would be subject to microbial degradation.

Hypoxia Simulation Models

Numerical simulation models have been applied to a number of coastal marine systems over the past 40 years to study how these important marine ecosystems function and to provide critical insight into key ecological processes (Kremer and Nixon 1978; Boesch et al 2001; Brush 2004). More recently, there has been an increasing effort to design models to inform environmental management related primarily to anthropogenic eutrophication and the associated response of the ecosystem (Brush and Harris 2010). The complexity of these ecosystem models range from simple empirical relationships to highly specialized 3-dimensional hydrodynamic-eutrophication models (Giblin and Vallino 2003). Traditional water quality eutrophication models in the Chesapeake Bay have focused on complex 3D models containing nearly 13,000 grid cells and up to 17 depth layers (CBP 2001). Frequently many of the complex ecosystem models have been further adapted to contain sediment transport, larval distribution, atmospheric (airshed), watershed, land-use, and tributary sub-models in an attempt to increase their utility and predictability. Although this increase in parameterization is often implemented in an effort to increase model accuracy, a number of recent studies have highlighted a correlation between model complexity and error propagation (Reckhow 1999). Due to these inherent difficulties, many recent researchers have begun advocating for the use of intermediate complexity models for management and policy applications, instead of highly complex ecosystem models (Pace 2001; Duarte et al. 2003).

Large scale monitoring programs and ecosystem models have been utilized to study the ecological effects of eutrophication in a number US estuaries including the Neuse River, Chesapeake Bay, Long Island Sound, and Narragansett Bay. Some of these systems are currently facing a new phase shift that represents a transition from eutrophication towards oligotrophication (Kemp et al. 2009; Nixon 2009). Oligotrophication or "the reduction in the supply of organic matter to an ecosystem" (Nixon 2009) has been typically linked to a reduction in point source nutrient and terrestrial organic matter loading. Although documentation of oligotrophication is more common for freshwater lakes and rivers (Jeppesen et al. 2005), there are a few temperate coastal marine systems that have shown modest improvements including the Black Sea, the Hudson and East Rivers, and Tampa Bay in the United States, and the Thames River in England (Greening and Janicki 2006; Diaz and Rosenberg 2008). Additionally, a number of other systems have shown smaller improvements in water quality including the Patuxent River, MD (Testa et al. 2008) and New River Estuary, NC (Mallin et al. 2005). However, these studies have also indicated that other regional watershed improvements are necessary in order to facilitate further improvements in local water quality.

Models have proven to be an important synthesis tool for understanding the strategies necessary to facilitate these water quality improvements, and also for identifying gaps in our current understanding of these dynamic systems. Currently, many of these models are being used to assess potential mitigation strategies, to offset eutrophication mainly through nutrient load reductions. Their role in systems ecology will continue to be influential as we begin to focus more on the response of coastal systems to oligotrophication and climate change. One of their many assets is the ability to tease out the interactions of multiple stressors that are often difficult or impossible to resolve with other experimental techniques, since ecosystem trajectories will depend on watershed management practices acting in concert with ongoing climate change.

OBJECTIVES

Given the increasing prevalence and importance of hypoxia in coastal systems, unanswered questions regarding the significance of various organic matter sources and formation of hypoxia in Chesapeake tributaries (particularly the YRE), and the increasing need for well-calibrated ecosystem models to predict system response to changing nutrient loads in concert with climate change, the following objectives were developed to guide this dissertation research. Chapter 1 has been submitted to *Marine Ecology Progress Series*, reviews have been received, and re-submission is pending. Chapter 4 has been published in *Estuarine, Coastal and Shelf Science* (2011, 95:289-297). Chapters 2 and 3 have been written for journal publication and submission is planned in 2013.

Chapter 1

Previous studies in the YRE have highlighted the interaction between the spring-neap cycle and the occurrence of low oxygen bottom water, however we still lack an understanding of how the full suite of biological processes and sources of organic carbon interact with physical stratification in the system. To establish a better understanding of the biological and physical factors controlling organic matter production and subsequent development of hypoxia in the YRE, a multi-faceted sampling program was undertaken in the YRE during the summers of 2007 and 2008. A series of high-resolution two- and three-dimensional surveys of water quality were performed using an Acrobat^{TM} (Sea Sciences, Inc.) towed undulating platform to document the conditions that lead to the formation and disruption of bottom water hypoxia within the YRE. Additionally, weekly discrete sampling and metabolic incubations were conducted to assess the effect of the spring-neap cycle on surface water column nutrient concentrations, chlorophyll-*a* concentrations, and surface and bottom water metabolic rates. Monthly metabolic incubations were conducted to quantify production, respiration, and microphytobenthic biomass in shallow sediments, and respiration in deep channel sediments.

Objective 1: Synthesize data collected from in-situ measurements, metabolic incubations, and high-resolution water quality monitoring into spatially-explicit, temporally-integrated mass balances of carbon and oxygen to examine the significance of multiple organic matter sources and oxygen sinks in relation to hypoxia in the estuary.

Chapter 2

The YRE presents a unique case where physical stratification and destratification, controlled by the spring-neap tidal cycle, combines with a multitude of other potential physical and biological processes that lead to bottom water hypoxia (respiration of phytoplankton-, MPB-, and watershed-derived carbon as well as advection of hypoxic water and organic carbon from the lower bay). However, the individual significance of each of these processes and their collective effect on the system is still largely unknown. This study combined data collected from *in-situ* measurements and metabolic incubations with long-term water quality and meteorological monitoring data into an intermediate complexity eutrophication model. All organic matter sources were isolated to evaluate the individual importance of each source and its contribution to bottom water hypoxia. Additionally, the effectiveness of a range of potential nutrient and organic matter load reductions were tested to determine what actions are necessary to mitigate current water quality concerns.

Objective 2: Utilize an intermediate-complexity model to determine the potential carbon sources and cycles that contribute to the formation of bottom water hypoxia, and assess the potential for nutrient and carbon load reductions to mitigate hypoxia.

Chapter 3

The climate-induced warming of coastal marine ecosystems has the potential to complicate ongoing efforts to mitigate hypoxia, which focus primarily on nutrient load reductions. Increasing water temperatures will directly affect a number of ecosystem processes including: primary production by phytoplankton and MPB, respiration in the water column and sediments, and remineralization and cycling rates of nutrients and organic matter. The effect of these future changes will be further complicated within shallow tributary estuaries because of increased benthic-pelagic coupling along with the advection of nutrients, labile organic matter, and hypoxic water from adjacent coastal marine systems via estuarine circulation. To date, little effort has been focused on determining how current watershed management practices and associated increases and decreases in nutrient loading will interact with future climate warming. This study analyzed past temperature records to examine how Chesapeake Bay surface and bottom waters have fluctuated with atmospheric temperatures over time, and used projected increases in air temperature in the Chesapeake region to drive an intermediate complexity eutrophication model for the YRE. The model was used to quantify potential changes in water column primary production, net ecosystem metabolism, and the prevalence of hypoxia within this sub-estuary under warmer climate conditions, both with and without concurrent changes in nutrient and organic matter loading.

Objective 3: Predict ecosystem response of the York River Estuary to a warming climate with a focus on primary production, ecosystem metabolism, and hypoxia, both with and without concurrent changes in nutrient and organic matter loading.

Chapter 4

In many coastal marine ecosystems, MPB can contribute a significant fraction of total system primary production, particularly in shallow lagoons or systems with broad photic shoals. While the role of MPB has been quantified in several shallow systems around the world, their contribution to primary production on the extensive shoals that line a number of deeper estuaries has often been overlooked. This study assessed the contribution of MPB to total primary production within four regions of upper Narragansett Bay, RI to quantify the significance of benthic production on the extensive shallow shoals that line this relatively deep estuarine system. Results have been used to inform development of a related intermediate complexity ecosystem model for Narragansett Bay with a focus on hypoxia, and will enable simulations of climate warming concurrent with nutrient load reductions in this more heavily loaded, northern estuary for comparison to results from the YRE.

Objective 4: Evaluate the contribution of microphytobenthos to total system production in upper Narragansett Bay, RI.

LITERATURE CITED

Bergondo D. L., D. R. Kester, H. E. Stoffel, and W. L. Woods. 2005 Time-Series Observations during the Low Sub-Surface Oxygen Events in Narragansett Bay During Summer 2001. *Marine Chemistry* 97: 90-103.

Boesch, D. F., R. B. Brinsfield and R. E. Magnien. 2001 Chesapeake Bay Eutrophication: Scientific Understanding, Ecosystem Restoration, and Challenges for Agriculture. *Journal of Environmental Quality* 30: 303-320.

Boesch, D. F.. 2002. Challenges and Oppoortunities for Science in Reducing Nutrient Over-Enrichment of Coastal Ecosystems. *Estuaries* 25: 886-900.

Boynton, W. R., J. D. Hagy, J. C. Cornwell, W. M. Kemp, S. M. Greene, M. S. Owens, J. E. Baker, and R. K. Larsen. 2008. Nutrient Budgets and Management Actions in the Patuxent River Estuary, Maryland. Estuaries and Coasts 31: 623-651.

Breitburg, D. L., D. W. Hondorp L. A. Davias, and R. J. Diaz. 2009. Hypoxia, Nitrogen, and Fisheries: Integrating Effects Across Local and Global Landscapes. *Annual Review of Marine Science* 1: 329-349.

Brush, M. J. 2004. Application of the Greenwich Bay ecosystem model to the development of the Greenwich Bay SAMP (Special Area Management Plan). Final report to the Rhode Island Coastal Resources Center, University of Rhode Island, Narragansett, RI.

Brush, M. J., and L. A. Harris. 2010. Advances in Modeling Estuarine and Coastal Ecosystems: Approaches, Validation, and Applications. *Ecological Modelling* 221: 965-968.

Buzzelli, C.P. 1998. Dynamic Simulation of Littoral Zone Habitats in Lower Chesapeake Bay: I. Habitat Characterization Related to Model Development. *Estuaries* 21: 673-389.

Buzzelli, C.P., R.A. Luettich, S.P. Powers, C.H. Peterson, J.E. McNinch, J.L Pinckney, and H.W. Paerl. 2002. Estimating the Spatial Extent of Bottom-Water Hypoxia and Habitat Degradation in a Shallow Estuary. *Marine Ecology Progress Series* 230: 103-112.

Cerco, C.F., Cole, T.M., 1994. Three-Dimensional Eutrophication Model of Chesapeake Bay, Vol. I: Main Report. Technical report EL-94-4, Waterways Experiment Station, U.S. Army Corps of Engineers, Vicksburg, MS

Cerco, C.F., Noel, M.R., 2004. The 2002 Chesapeake Bay Eutrophication Model. Report 903-R-04-004, Chesapeake Bay Program Office, U.S. Environmental Protection Agency, Annapolis, MD

Chesapeake Bay Program. 2001. Modeling the Chesapeake Bay. *Backgrounder Fact Sheet.* Region III Chesapeake Bay Program Office, Annapolis, MD.

Cloern, J.E. 2001. Our evolving Conceptual Model of the Coastal Eutrophication Problem. *Marine Ecology Progress Series* 210: 223-253.

Cooper, S. R. and G. S. Brush. 1991. Long-Term History of Chesapeake Bay Anoxia. *Science* 254: 992-996.

Cooper, S. R. and G. S. Brush. 1993. A 2,500-Year History of Anoxia and Eutrophication in Chesapeake Bay. *Estuaries* 16: 617-626.

Countway, R.E., E.A. Canuel, and R.M. Dickhut. 2007. Sources of Particulate Organic Matter in Surface Waters of the York River, VA estuary. *Organic Geochemistry*. 38: 365-379.

Cowan, J. L. and W. R. Boynton. 1996. Sediment-Water Oxygen and Nutrient Exchanges Along the Longitudinal Axis of Chesapeake Bay: Seasonal Patterns, Controlling Factors and Ecological Significance. Estuaries 19: 562-580.

Deacutis, C. F., D. Murray, W. Prell, E. Saarman, and L. Korhun. 2006. Hypoxia in the Upper Half of Narragansett Bay, RI, During August 2001 and 2002. *Northeastern Naturalist*. 13: 173-198

de Jonge, and J. E. E. van Beusekom. 1995. Wind- and Tide-induced Resuspension of Sediment and Microphytobenthos from Tidal Flats in the Ems Estuary. Limnology and Oceanography. 40: 766-778.

D'Elia C.F., K.L. Webb and R.L. Wetzel. 1981. Time-Varying Hydrodynamics and Water Quality in an Estuary, pp. 597-606. In: B.J. Neilson and L.E. Cronin [eds.], Estuaries and Nutrients. Humana Press. Clifton, N.J.

D'Elia, C. F., W. R. Boynton, and J. G. Sanders. 2003. A Watershed Perspective on Nutrient Enrichment, Science, and Policy in the Patuxent River, Maryland: 1960-2000. *Estuaries* 26: 171-185.

Diaz, R. J., R. J. Neubauer, L. C. Schaffner, L. Pihl, and S. P. Baden. 1992. Continuous Monitoring of Dissolved Oxygen in an Estuary Experiencing Periodic Hypoxia and the Effects of Hypoxia on Macrobenthos and Fish. *Science in the Total Environment* (Supplement 1992): 1055-1068.

Diaz, R. J. and R. Rosenberg. 1995. Marine Benthic Hypoxia: A Review of its Ecological Effects and the Behavioural Responses of Benthic Macrofauna. *Oceanography and Marine Biology Annual Review* 33: 245-303.

Diaz, R. J. 2001. Overview of Hypoxia Around the World. *Journal of Environmental Quality* 30: 275-281.

Diaz, R. J. and R. Rosenberg. 2008. Spreading Dead Zones and Consequences for Marine Ecosystems. *Science*. 321: 926-929.

Dauer, D.M. H.G. Marshall, J.R. Donat, M.F.Lane, S.C.Doughten,P.L. Morton, and F.A. Hoffman. 2005. Status and Trends in Water Quality and Living Resources in the Virginia Chesapeake Bay: James River (1985-2004).Final Report to the Virginia Department of Environmental Quality, Richmond, Virginia. Applied Marine Research Laboratory, Norfolk VA., 1-63.

Fisher, T. R., J. D. Hagy III, W. R. Boynton, and M. R. Williams. 2006. Cultural Eutrophication in the Choptank and Patuxent Estuaries of Chesapeake Bay. *Limnology and Oceanography* 51: 435-447.

Friedrichs, M. A. M., J. Dusenberry, L. Anderson, R. Armstrong, F. Chai, J. Christian, S.C. Doney, J. Dunne, M. Fujii, R. Hood, D. McGillicuddy, K. Moore, M. Schartau, Y. H. Sptiz, and J. Wiggert. 2007. Assessment of Skill and Portability in Regional Marine Biogeochemical Models: Role of Multiple Phytoplankton Groups. *Journal of Geophysical Research* 112, C08001, doi:10.1029/2006JC003852.

Gavis, J., and V. Grant. 1986. Sulfide, Iron, Manganese , and Phosphate in the Deep water of the Chesapeake Bay During Anoxia. Estuarine, Coastal and Shelf Science 23: 451-463.

Giblin, A. E. and J. J. Vallino. 2003. The Role of Models in Addressing Coastal Eutrophication. pp. 327-343 in C. D. Canham, J. J. Cole, and W. K. Laurenroth [eds.], Models in Ecosystem Science. Princeton University Press. Princeton, NJ

Goto, N., T. Kawamura, O. Mitamura, and H. Terai. 1999. Importance of Extracellular Organic Production in the Total Primary Production by Tidal-flat Diatoms in Comparison to Phytoplankton. *Marine Ecological Progressive Series* 190: 289-295.

Graf, G., W. Bengtsson, U. Duenser, R. Schulz, and H. Theede. 1982. Benthic Response to Sedimentation of a Spring Phytoplankton Bloom: Process and Budget. *Marine Biology* 67: 201-208.

Greening, H., and A. Janicki. 2006. Toward Reversal of Eutrophic Conditions in a Subtropical Estuary: Water Quality and Seagrass Response to Nitrogen Loading Reductions in Tampa Bay, Florida, USA. *Environmental Management* 38: 163-178.

Gregg, W. W. A. M. Friedrichs, Marjorie, A. R. Robinson, K.A. Rose, R. Schlitzer, K.R. Thompson, and S. C. Doney. 2009. Skill Assessment for Coupled Biological/Physical Models of Marine Systems. Journal of Marine Systems 76: 16-33.

Haas, L. W. 1977. The Effect of the Spring-Neap Tidal Cycle on the Vertical Salinity Structure of the James, York, and Rappahannock Rivers, Virginia, U.S.A. *Estuarine and Coastal Marine Science* 5: 485-496.

Haas, L. W., S. J. Hastings and K. L. Webb. 1981. Phytoplankton Response to a Stratification-Mixing Cycle in the York River Estuary During Late Summer, pp. 619-635. In: B.J. Neilson and L.E. Cronin [eds.], Estuaries and Nutrients. Humana Press. Clifton, N.J.

Hagy, J.D., W. R. Boynton, C. W. Keefe, K.V. Wood. 2004. Hypoxia in Chesapeake Bay, 1950 – 2001: Long-term Changes in Relation to Nutrient Loading and River Flow. *Estuaries* 27: 634-658.

Hagy, J.D., W. R. Boynton, and D. A. Jasinski. 2005. Modelling Phytoplankton Deposition to Chesapeake Bay Sediments During Winter–Spring: Interannual Variability in Relation to River Flow. *Estuarine, and Coastal Shelf Science*. 62: 25-40.

Harding Jr, L. W., and E. S. Perry. 1997. Long-Term Increase of Phytoplankton Biomass in Chesapeake Bay, 1950 – 1994. *Marine Ecological Progressive Series* 157: 39-52.

Hayward D., C. S. Welch, and L. W. Haas. 1982. York River Destrtification: An Estuary-Subestuary Interaction. *Science*. 216: 1413-1414.

HydroQual, Inc. 1987. A Steady-State Coupled Hydrodynamic/Water Quality Model of the Eutrophication and Anoxia Process in Chesapeake Bay. Final report to the U.S. E.P.A. Chesapeake Bay Program, HydroQual Inc., Mahwah, NJ

Jeppesen, E., M. Søndergaard, J. P. Jensen, K. E. Havens, O. Anneville, L. Carvalho, M. F. Coveney, R. Deneke, M. T. Dokulil, B. FOY, D. Gerdeaux, S. E. Hampton, S. Hilt, K. Kangur, J. Köhler, E. H. H. R. Lammens, T. L. Lauridsen, M. Manca, M. R. Miracle, B. Moss, P. Nõges, G. Persson, G. Phillips, R. Pprtielje, S. Romo, C. L. Schelske, D. Straile, I. Tatrai, E. Willén, and M. Winder. 2005. Lake Responses to Reduced Nutrient Loading – an Analysis of Contemporary Long-term Data from 35 Case Studies. *Freshwater Biology* 50: 1747-1771

Kemp, W. M., P. Sampou, J. Caffrey, M. Mayer, K. Henriksen, and W. Boynton. 1990. Ammonium Recycling Versus Denitrification in Chesapeake Bay Sediments. *Limnology and Oceanography*. 35: 1545-1563.

Kemp, W. M., P. A. Sampou, J. Garber, J. Tuttle, and W. R. Boynton. 1992. Seasonal Depletion of Oxygen from Bottom-Waters of Chesapeake Bay: Roles of Benthic and Planktonic Respiration and Physical Exchange Processes. *Marine Ecology Progress Series* 85: 137-152.

Kemp, W. M., J. M. Testa, E. M. Smith, and W. R. Boynton. 2005. Eutrophication of the Chesapeake Bay: Historical Trends and Ecological Interactions. *Marine Ecological Progressive Series* 303:1-29

Kemp, W. M., J. M. Testa, D. J. Conley, D. Gilbert, and J. D. Hagy. 2009. Temporal Responses of Coastal Hypoxia to Nutrient Loading and Physical Controls. *Biogeosciences* 6: 2985-3008.

Kremer, J. N., and S. W. Nixon. 1978. A Coastal Marine Ecosystem: Simulation and Analysis. Springer-Verlag, New York, NY.

Kuo, A.Y. and B.J. Neilson. 1987. Hypoxia and Salinity in Virginia Estuaries. *Estuaries* 10:277-283.

Kuo, A.Y., K. Park, and M. Z. Moustafa. 1991. Spatial and Temporal Variabilities of Hypoxia in the Rappahannock River, Virginia. *Estuaries*. 14: 113-121.

Kuo, A. Y., B. J. Neilson, J. Brubaker, and E. P. Ruzecki. 1993. Data Report: Hypoxia in the York River, 1991. Virginia Institute of Marine Science Data Report No. 47. Gloucester Point, Virginia.

Lim, H., R. J. Diaz, J. Hong, L. Schaffner. 2006. Hypoxia and Benthic Community Recovery in Korean Coastal Waters. *Marine Pollution Bulletin*. 52: 1517-1526.

Mallin, M. A., M. R. McIver, H. A. Wells, D. C. Parson, and V. L. Johnson. 2005. Reversal of Eutrophication Following Sewage Treatment Upgrades in the New River Estuary, North Carolina. *Estuaries* 28: 750-760.

Malone, T.C., W.M. Kemp, H.W. Ducklow, W.R. Boynton, J.H. Tuttle, and R.B. Jonas. 1986. Lateral Variation in the Production and Fate of Phytoplankton in a Partially Stratified Estuary. *Marine Ecology Progress Series* 32: 149-160.

Malone, T. C., L. H. Crocker, S. E. Pike, and B. W. Wendler. 1988. Influences of River Flow on the Dynamics of Phytoplankton Production in a Partially Stratified Estuary. Marine Ecology Progressive Series 48: 235-249.

McCallister, S. L., J. E. Bauer, and E. A. Canuel. 2006a. Bioreactivity of Estuarine Dissolved Organic Matter: A Combined Geochemical and Microbiological Approach. *Limnology and Oceanography* 51: 94-100.

McCallister, S. L., J. E. Bauer, H. W. Ducklow, and E. A. Canuel. 2006b. Sources of Estuarine Dissolved and Particulate Matter: A Multi-Tracer Approach. *Organic Geochemistry* 37: 454-468.

Møhlenberg, F. 1999. Effect of Meteorology and Nutrient Load on Oxygen Depletion in a Danish Micro-Tidal Estuary. *Aquatic Ecology* 33: 55-64.

Nixon, S.W. 1995. Coastal Marine Eutrophication: A definition, social causes, and future concerns. *Ophelia* 41: 199-219.

Nixon, S. W. 2009. Eutrophication and the Macroscope. *Hydrobiologia* 629: 5-19.

Officer, C.B., R.B. Biggs, J.L. Taft, L.E. Cronin, and M.A. Tyler. 1984. Chesapeake Bay Anoxia: Origin, Development, and Significance. *Science* 223: 22-27.

Pace, M. L. 2001. Prediction and the Aquatic Sciences. *Canadian Journal of Fisheries and Aquatic Sciences*. 58: 63-72.

Paerl, H.W., J.L. Pinckney, J.M. Fear, and B.L. Peierls. 1998. Ecosystem Responses to Internal and Watershed Organic Matter Loading: Consequences for Hypoxia in the Eutrophying Neuse River Estuary, North Carolina, USA. *Marine Ecology Progress Series* 166: 17-25.

Pinckney, J. L., and R. G. Zingmark. 1993. Modeling the Annual Production of Intertidal Benthic Microalgae in Estuarine Ecosystems. *Journal of Phycology* 29: 396-407.

Pinckney, J. L., H. W. Paerl, M. B. Harrington, and K. E. Howe. 1998. Annual Cycles of Phytoplankton Community-Structure and Bloom Dynamics in the Neuse River Estuary, North Carolina. *Marine Biology*. 131: 371-381

Pihl, L. S., S. P. Baden, R. J. Diaz, and L. C. Schaffner. 1992. Hypoxia-Induced Structural Changes in the Diet of Bottom-Feeding Fishes and Crustacea. Marine Biology 112: 349-361.

Rabalais, N. N. 2002 Nitrogen in Aquatic Ecosystems. *Ambio* 31: 102-112.

Rabalais N. N., R. E. Turner, B. K. S. Gupta, D. F. Boesch, P. Chapman, and M. C. Murrell. 2007. Hypoxia in the Northern Gulf of Mexico: Does the Science Support the Plan to Reduce, Mitigate and Control Hypoxia. *Estuaries and Coasts* 30: 753-772.

Reay, W. G., D. L. Gallagherl, and G. M. Simmons. 1995. Sediment-Water Column Oxygen and Nutrient Fluxes in Nearshore Environments of the Lower Delmarva Peninsula, USA. *Marine Ecological Progressive Series*. 118: 215-227.

Reckhow, K. H. 1999. Water Quality Prediction and Probability Network Models. *Canadian Journal of Fisheries and Aquatic Sciences*. 56: 1150-1158.

Rizzo, W. M. and R. L. Wetzel. 1985. Intertidal and Shoal Benthic Community Metabolism in a Temperate Estuary: Studies of Spatial and Temporal Scales of Variability. *Estuaries*. 8: 342-351.

Rosenberg, R., A. Agrenius, B. Hellman, H. C. Nilsson, and K. Norling. 2002. Recovery of Marine Benthic Habitats and Fauna in a Swedish Fjord Following Improved Oxygen Conditions. *Marine Ecological Progressive Series*. 234: 43-53.

Selamn, M. 2007. Eutrophication: An Overview of Status, Trends, Policies and Stratagies. World Resourses Institute.

Seliger, H. H., J. A. Boggs, and W. H. Buggley. 1985 Catastrophic Anoxia in the Chesapeake Bay in 1984. Science 228: 70-73

Sharples J., J. H. Simpson, and J. M. Brubaker. 1994. Observations and Modelling of Periodic Stratification in the Upper York River Estuary, Virginia. *Estuaries, Coastal and Shelf Science* 38: 301-312.

Shen, J. and L. Haas. 2004. Calculating Age and Residence Time in the Tidal York River Using Three-Dimensional Model Experiments. *Estuaries, Coastal and Shelf Science* 61: 449-461.

Sisson, G. M., J. Shen, S. Kim, J. D. Boon, and A. Y. Kuo. 1997. VIMS Three-Dimensional Hydrodynamic-Eutrophication Model (HEM-3D): Application of the Hydrodynamic Model to the York River System. Special Report in Applied Marine Science and Ocean Engineering. No 327. Virginia Institute of Marine Science, College of William and Mary, Gloucester Point, VA.

Stanley, D.W. and S.W. Nixon. 1992. Stratification and Bottom-Water Hypoxia in the Pamlico River Estuary. *Estuaries* 15: 270-281.

Taft, J. L., E. O. Hartwig, and R. Loftus. 1980. Seasonal Oxygen Depletion in Chesapeake Bay. *Estuaries*. 3: 242-247.

Testa, J. M. and W. M. Kemp. 2008. Variability of Biogeochemical Processes and Physical Transport in a Partially Stratified Estuary: a Box-Modeling Analysis. *Marine Ecology Progressive Series* 356: 63-79.

Tyler, R. M., and T. E. Targett. 2007. Juvenile Weakfish *Cynoscion regalis* Distribution in Relation to Diel-cycling Dissolved Oxygen in an Estuarine Tributary. *Marine Ecological Progressive Series* 333: 257-269.

U.S. Environmental Protection Agency. 2000. Chesapeake 2000. US Environmental Protection Agency Region III, Chesapeake Bay Program Office, Annapolis MD.

U.S. Environmental Protection Agency. 2003. Ambient Water Quality Criteria for Dissolved Oxygen, Water Clarity and Chlorophyll a for Chesapeake Bay and Its Tidal Tributaries. EPA 903-R-03-002. Region III Chesapeake Bay Program Office, Annapolis, MD.

U.S. Environmental Protection Agency. 2007. Ambient Water Quality Criteria for Dissolved Oxygen, Water Clarity and Chlorophyll a for Chesapeake Bay and Its Tidal Tributaries – 2007 Addendum. EPA 903-R-07-003. Region III Chesapeake Bay Program Office, Annapolis, MD.

CHAPTER 1

Submitted to *Marine Ecology Progress Series*

Internal Versus External Drivers of Periodic Hypoxia in a Coastal Plain Tributary Estuary: the York River, Virginia

Samuel J. Lake[1], Mark J. Brush, Iris C. Anderson and Howard I. Kator
Virginia Institute of Marine Science
College of William and Mary, Gloucester Point, VA 23062 USA

[1] Corresponding author:

Email: sjlake@vims.edu

Phone Number: (804) 684-7918

Fax: (804) 684-7293

Keywords: York River, Hypoxia, Production, Respiration, Net Ecosystem Metabolism, Carbon Budget

ABSTRACT

The seasonal formation of periodic hypoxia within tributary estuaries, and its relationship to the spring-neap tidal cycle, has been well documented in a number of systems along the U.S. east coast. However, the importance and scale of other key physical and biological processes, which ultimately control the frequency and spatial extent of hypoxia, are less well understood. This study synthesized *in-situ* measurements, metabolic incubations, and high-resolution water quality monitoring into a spatially-explicit, temporally-integrated mass balance to examine the significance of multiple organic matter sources and oxygen sinks in relation to hypoxia in the York River estuary (YRE), VA, USA. The results highlight episodic peaks in gross primary production (GPP) mostly unrelated to the spring-neap cycle, with phytoplankton accounting for the bulk of total GPP within the system. Despite extensive shoals, microphytobenthos contributed under 20% of total GPP and typically accounted for less than 10%. While GPP in much of the estuary appeared to be relatively balanced with water column and sediment respiration, results indicated an area at the boundary of the mesohaline and polyhaline zones that was net heterotrophic. Observed rates of respiration were sufficient to drive bottom waters to observed levels of hypoxia during transitions from spring to neap tides. Phytoplankton production dominated the estimated inputs of organic carbon from the tributaries and surrounding watersheds, and was 1.5 times greater than advective inputs from the Chesapeake Bay, which were roughly balanced by exports. Results indicate that management efforts to alleviate hypoxia in the YRE should focus on reducing internal phytoplankton production, although the input of labile organic matter across the mouth of the estuary with the Chesapeake Bay represents an important source that can only be controlled by more regional efforts.

INTRODUCTION

Hypoxia represents one of the most common and ecologically detrimental outcomes of anthropogenic nutrient enrichment in coastal marine ecosystems (Diaz and Rosenberg 1995, 2008). Hypoxia (defined here as ≤ 2.0 mg O_2 L^{-1}) and eutrophication within the Chesapeake Bay and its tributaries have been intensively studied with large-scale monitoring programs and smaller-scale high intensity sampling over the past 25 years in response to declining water quality, increasing deep water hypoxia, and loss of submerged aquatic vegetation between the 1950's and 1980's (Cooper and Brush 1991; Cooper and Brush 1993; D'Elia et al. 2003; Kemp et al. 2005). The seasonal development of anoxia within the mainstem of the Chesapeake Bay has been linked to the input of fresh water (primarily from the Susquehanna and Potomac Rivers) and associated influx of organic matter and nutrients during high flow periods (winter and spring), the production and subsequent deposition of organic matter during the spring phytoplankton bloom, and density driven water column stratification (Taft et al. 1980; Officer et al. 1984; Seliger et al. 1985; de Jonge and van Beusekom 1995; Cloern 2001; Hagy et al. 2004; Kemp et al. 2005). Bacterial respiration of the deposited autochthonous and allochthonous organic matter fuels the formation of seasonally persistent summertime anoxia in the bottom water under warm summer temperatures (Malone et al. 1986; Kemp et al. 1992; Paerl et al. 1998; Møhlenberg 1999; Rabalais et al. 2007).

Although this mainstem conceptual model of hypoxia formation is appropriate for a number of estuarine systems worldwide, it does not apply as well to conditions that are present within some of the Chesapeake Bay's shallower tributaries, which are influenced by multiple sources of labile organic matter, advection of high nutrient / low oxygen water from the mainstem, and variable physical mixing processes, both tidally and wind driven (Haas 1977; Kuo and Nielson 1987; Sharples et al. 1994; Fisher et al. 2006; Boynton et al. 2008; Testa and Kemp 2008). Additionally, recent studies have demonstrated the importance of estuarine circulation in advection of nutrients and sometimes hypoxic water from the mainstem into these sub-estuaries (Jordan et al. 1991; Boynton et al. 2008; Testa et al. 2008) as well as in other coastal marine systems (de Jonge 1997; Brush 2004).

The York River estuary (YRE) (Fig. 1) oscillates between stratified and well-mixed conditions due to the physical mixing of the spring-neap tidal cycle (Haas 1977; Hayward et al. 1982; Kuo and Neilson 1987; Diaz et al. 1992). This unique physical mechanism creates the potential for continued formation and disruption of bottom water hypoxia from late May to early September within the lower half of the estuary. Destratification events have the potential to supply regenerated nutrients to the surface water, stimulating phytoplankton production throughout the summer and early fall (D'Elia et al. 1981; Haas et al. 1981).

While previous studies in the YRE have highlighted the interaction between the spring-neap cycle and the occurrence of low oxygen bottom water, we still lack an understanding of how the full suite of biological processes interact with physical stratification in the system (Countway et al. 2007). Until now there has not been an attempt to establish a constrained carbon budget for the York River, examining the multiple organic matter sources that ultimately drive this system to hypoxia. In addition to internal phytoplankton production, and riverine and offshore inputs of dissolved (DOC) and particulate (POC) organic carbon, contributions to this system from the extensive microphytobenthic community are not well known. An additional driver of hypoxia in the YRE could be advection of water with low dissolved oxygen (DO) concentrations from the lower Chesapeake Bay mainstem as indicated by high-resolution surveys in the lower estuary (Fig. 2 a & b). Although the lower mainstem portion of the Chesapeake Bay is not typically considered as a potential source of low DO water, it was classified as an area of low oxygen water in the 1950's (Officer et al. 1984) and more recently identified as an area of hypoxic water separate from the mesohaline mainstem hypoxic/anoxic zone in 1999 (Hagy et al. 2004).

To establish a better understanding of the biological and physical factors controlling organic matter loading and subsequent development of hypoxia in the YRE, a multi-faceted sampling program was undertaken during the summers of 2007 and 2008. A series of high-resolution two- and three-dimensional surveys of water quality were performed using an Acrobat^{TM} (Sea Sciences, Inc.) towed undulating platform as part of a larger program to determine the conditions that lead to the formation and disruption of bottom water hypoxia within the estuary. Discrete sampling and metabolic incubations were conducted to assess the effect of the spring-neap cycle on surface water column nutrient concentrations, chlorophyll-*a* concentrations, and surface and bottom water metabolic rates. Measured rates of oxygen consumption were compared to empirical trajectories of oxygen decline over multiple spring to neap tide transitions to assess the potential for internal respiration to account for observed levels of hypoxia in the system, or if advection of hypoxic water from the Chesapeake had to be invoked to fully account for the observed declines. Finally, data were synthesized into a spatially-explicit, temporally-integrated mass balance of carbon to examine the significance of multiple organic matter sources in relationship to hypoxia in the estuary.

METHODS

Site Description

The YRE is formed by the confluence of the Mattaponi and Pamunkey Rivers near West Point, Virginia, approximately 55 km from where the river enters the mainstem of the Chesapeake Bay on its western edge (Shen and Haas 2004) (Fig. 1). The polyhaline segment of the river extends from the mouth to Catlett Islands (approximately 19 km), and the mesohaline region continues from this point approximately 16 km upstream to the confluence of the Mattaponi and Pamunkey Rivers. Although the surrounding watershed has the second highest population density of the three larger Virginia tributaries, the overall land use surrounding the York River proper is predominantly rural with 62% forested and 16% agricultural land (Dauer et al. 2005).

For this study the lower York River was sub-divided into four primary sampling regions along its axis (Fig. 1). These regions were designated based on the presence of hypoxia observed during 2007 Acrobat^{TM} monitoring cruises and to cover the portion of the river that has historically experienced hypoxia based on long term water quality monitoring by the EPA Chesapeake Bay Program (CBP). The two upstream mesohaline sites located near Clay Bank (CB) and Catlett Islands (CI) were characterized as having little to no signs of hypoxia, while the two downstream polyhaline sites Mumfort Island (MI) and the lower York River (LYR) were observed to develop periodic hypoxia during 2007 Acrobat^{TM} monitoring surveys and in previous studies (Kuo and Neilson 1987; Kuo et al. 1993).

Acrobat Monitoring

As part of a larger water quality monitoring program, the YRE was surveyed during the summers of 2007 and 2008 using an Acrobat^{TM} system equipped with a CTD (Falmouth Scientific Seabird), SCUFA fluorometer/turbidometer (Turner Designs), and a rapid response (300 ms) dissolved oxygen (DO) sensor (Analysenmeßtechnik GmbH, Rostock, Germany). Acrobat^{TM} sensors collected spatially-referenced data four times a second with a horizontal resolution of 6-8 m and a vertical resolution of 5-10 cm, for a total of 40,000-50,000 data scans per survey. Prior to deployment and immediately following each cruise a two-point calibration was performed on the DO sensor (0% and 100% saturated water). Additionally, DO grab samples were collected at the beginning and end of each cruise and analyzed (standard Winkler titrations) to ensure sensor accuracy (+/- 0.5 mg/L).

Monitoring surveys along a zig-zag path were conducted bimonthly (2007) to monthly (2008) to capture the spatial extent of hypoxia in 3-dimensions (Fig. 1). A second straight-line, temporally-intensive sampling strategy was used to capture the development, spread, and disruption of individual hypoxic events during June and August of each year. These intensive surveys were conducted every 2-3 days for 2.5 weeks through a neap-spring-neap tidal cycle, sampling the deepest section of the main channel. For the 2008 sampling season the intensive Acrobat^{TM} cruises were extended approximately 15 km into the lower mainstem of the Chesapeake Bay to identify possible sources of hypoxic water that could be advected into the YRE.

Spring-Neap Discrete Surveys

To collect data on additional water quality parameters and to develop metabolic budgets, a series of 13 water quality surveys and metabolic incubations were conducted from June to September 2008. Sampling dates were selected with a three day lag behind the apex of spring and neap tides in order to sample the river at the peak of mixing and stratification, respectively, as indicated by previous studies (Haas 1977; Hass et al. 1981; Hayward et al. 1986) and past Acrobat™ surveys.

At each channel site (Fig. 1) a YSI 6600 series V2 sonde was used to measure temperature, salinity, chlorophyll-*a*, and DO at the surface (0.5 m) and at one meter intervals starting at one meter below the surface to the bottom of the river. All YSI probes were cleaned and calibrated prior to each survey in accordance with YSI, Inc. operating manual methods. Conductivity and DO were calibrated using a 0.2 molar standard solution of potassium chloride and 100% air saturated water, respectively. Additionally, a 2-point calibration was performed on the optical turbidity and chlorophyll-*a* probes using deionized water and YSI conductivity standard or a rhodamine dye standard, respectively. A LiCor LI-1400 was used to measure irradiance through the water column at an intermediate site between the channel and nearshore sites for computation of vertical attenuation coefficients (k_D). Readings were taken just below the surface (<0.1 m) and at 1 meter. All YSI and LiCor measurements were obtained in triplicate at each depth.

Surface water samples (0.25 m below surface) were collected at each channel site in 500 mL amber Nalgene bottles and immediately placed on ice until they were transported to the lab. Water column chlorophyll-*a* (WC chl-*a*) was determined by filtering 15 or 20 mL (depending on concentration) through a Whatman 0.7 µm glass microfiber filter, sealed in aluminum foil, and placed in the freezer. Samples were later removed and extracted in the dark for 24 hours in 8 ml of 45:45:10 dimethyl sulfoxide: acetone: reagent water with 1% diethylamine (Shoaf and Lium 1976), and read on a 10 AU Turner Design fluorometer before and after acidification. All WC chl-*a* samples were run in triplicate and processed within one month after the initial sampling date. Nutrient samples were filtered through pre-rinsed 0.45 µm Acrodisc filters and frozen until analysis for dissolved inorganic nitrogen (NH_4^+, NO_3^- and NO_2^-), phosphorus (PO_4^{3-}), and silica (Si) on a Technicon AAII Continuous Flow Autoanalyzer.

At each nearshore site (Fig. 1), three replicate sediment samples were collected by pole corer for sediment chlorophyll-*a* (SED chl-*a*) analysis at a depth of one meter below mean lower water (MLW), taking into account the daily tidal range. Subsamples of the 0-0.3 cm depth fraction of each core were transferred into sterile 15 mL BD Falcon polypropylene centrifuge tubes, and immediately placed in an ice filled cooler and frozen for a maximum hold time of one month. Samples were extracted in 10 mL of a 90% acetone: 10% reagent water (by volume) solution, vortexed for 30 seconds on full power, and sonicated for an additional 30 seconds at 4-5 watts with a Fisher Scientific Dismembranator. After a 24-hour extraction period in the freezer, samples were filtered with PALL Life Science HPLC Acrodisc filters (25 mm filter with a 0.45 µm CR-PTEE) and analyzed spectrophotometrically on a Beckman DU 800 Spectrophotometer before and after acidification using the equations of Lorenzen (1967) to correct chlorophyll-*a* values for phaeophytin.

Metabolic Incubations

Surface water, bottom water, and deep channel sediment cores were collected on each survey at each channel site, and shallow water sediment cores were collected monthly at each nearshore site to develop production-irradiance (P-I) curves and compute metabolic rates. Surface water samples were collected in blackened 2 liter Nalgene bottles at a depth of approximately 0.5 m. Bottom water samples (1 meter above the sediment surface) were collected using a Niskin bottle and immediately transferred into blackened 4 liter Nalgene bottles. Deep channel sediment cores (n=4) were collected during each survey using a box corer, sub-sampled with clear acrylic tubing (height 15 cm: i.d. 4.1 cm) and immediately placed on ice. Nearshore sediment cores (n=13) were collected at 1 meter below mean low water (MLW) in cores of the same size. Sediment height within both the nearshore and deep channel cores was approximately 7 cm, with 8 cm of overlying sample water.

Metabolic rates were determined using the methods of Giordano (2009), Lake and Brush (2011), and Giordano et al. (2012). Water samples were incubated immediately upon returning to the lab. Initial oxygen measurements for metabolic experiments were determined with a HACH HQ 40d oxygen meter with luminescent DO sensors. Ten 60 mL BOD bottles were filled with surface water and incubated at ambient temperatures in temperature-controlled, flow-through light gradient boxes under an increasing gradient of photosynthetically active radiation (PAR, ~50-1600 μE m^{-2} s^{-1}). Four additional surface water samples and four bottom water samples were placed in a corresponding temperature-controlled dark box for determination of respiratory rates. Samples were incubated in the light for 1-2 hours, while dark incubations lasted for 15.5 - 27.5 hours, depending on oxygen uptake rates.

Sediment cores were allowed to acclimate uncapped overnight in gently mixed, filtered seawater. Just prior to incubation, the overlying core water was siphoned out of the nearshore cores taking care to not disturb the sediment surface, and replaced with filtered (0.5 μm) site water with a known DO concentration. Similarly, deep channel cores were siphoned and replaced with unfiltered site water with a known DO concentration. All samples were sealed with polyethylene (Saran Wrap™), which has a low oxygen permeability (5.8×10^{-5} ml cm^{-2} h^{-1}; Pemberton et al. 1996) held in place by a tight rubber band. Once sealed the cores were placed in light gradient boxes and incubated as described above for approximately 1.5-2 hours in the light and 2-3hours in the dark (n=10 for nearshore cores in the light; n=3 for nearshore cores in the dark; and n=4 for deep channel cores in the dark).

Net community production (light) and respiration (dark) rates for the water and sediments were computed from the change in DO concentrations over the incubation period and normalized to chlorophyll-*a* biomass (0-3 mm for cores). Water column metabolic rates were used to develop a series of production-irradiance (P-I) curves using the equation of Platt et al. (1980) in Statistical Analysis Systems (SAS®), which takes into account photoinhibition:

$$P^B = P^B{}_s(1 - \exp(-\alpha^B I / P^B{}_s)) \times (\exp(-\beta^B I / P^B{}_s)) - R^B$$

where net biomass-specific production (P^B, mg O_2 mg chl^{-1} h^{-1}) is dependent on irradiance (I, μE m^{-2} s^{-1}) and four statistically determined variables, a term that corresponds to the maximum gross photosynthetic rate in the absence of photoinhibition ($P^B{}_s$, mg O_2 mg chl^{-1} h^{-1}), the initial slope of the P-I curve (α^B, mg O_2 mg chl^{-1} h^{-1} (μE m^{-2} $s^{-1})^{-1}$), a negative slope characterizing photoinhibition (β^B, mg O_2 mg chl^{-1} h^{-1} (μE m^{-2} $s^{-1})^{-1}$), and the biomass-specific rate of respiration (R^B, mg O_2 mg chl^{-1} h^{-1}). Sediment incubations were used to develop a similar series of P-I curves using the Jassby and Platt (1976) hyperbolic tangent function:

$$P^B = P^B_{max} \tanh (\alpha^B I / P^B_{max}) - R^B$$

where P^B_{max} is the biomass-specific maximum gross photosynthetic rate (mg O_2 mg chl^{-1} h^{-1}).

Computed Oxygen Trajectories

To assess the role of internal respiration versus advection of hypoxic water from the Chesapeake mainstem in the formation of hypoxia within the YRE, bottom water and deep channel sediment respiration rates obtained from the metabolic experiments were combined with *in-situ* measurements of DO from the Acrobat^{TM} surveys to compare observed and computed declines in bottom water oxygen concentrations in the mesohaline and polyhaline segments during spring to neap tide transitions. Data from five Acrobat^{TM} cruises from spring to post neap tidal stage (representing the transition from minimum stratification and highest DO to maximum stratification and lowest DO) during June and August of 2007 and 2008 were used to calculate the volume-weighted change in sub-pycnocline DO concentrations within each segment of the river using the NOAA Chesapeake Bay and Tidal Water Interpolator (http://archive.chesapeakebay.net/cims/interpolator.pdf). Pycnocline depths were set at 5 m and 9 m in the mesohaline and polyhaline regions, respectively, based on Acrobat^{TM} results. Sub-pycnocline respiratory oxygen demands were calculated by averaging the rates of bottom water and deep channel sediment respiration from the corresponding sites in the mesohaline (CB & CI) and polyhaline (MI & LYR) segments. These average rates were then linearly interpolated between sampling dates and scaled up by volume (water column) and area (sediment) to obtain segment-wide rates of daily oxygen consumption. The observed changes in bottom water DO concentrations from the Acrobat^{TM} surveys were then compared to concentrations computed from the interpolated measurements of respiratory oxygen demand. Measured metabolic rates from June and August of 2008 were applied to June and August of 2007, respectively, as metabolic incubations were only conducted in 2008. While this calculation assumes that the bottom water was completely isolated from mixing with the surface water and that GPP in this layer was zero, it provides an estimate of what DO trajectories would have been if internal respiration was the sole factor governing oxygen concentrations. These estimates, therefore, provide a first-order constraint in determining if internal metabolism alone could drive the observed formation of hypoxia below the pycnocline or if other physical processes like the advection of low DO water from the mainstem were required to match the observed DO trajectories.

Carbon Budget

P-I parameters were combined with time series of chlorophyll-*a*, k_D, and incident PAR to generate estimates of daily gross primary production of the water column and benthos (GPP_{WC} and GPP_B, respectively), daily net community production (NCP_{WC} and NCP_B), and daily respiration (R_{WC} and R_B) for each region of the YRE. First, estimated values for $P^B{}_{max}$, $P^B{}_s$, α^B, β^B, R^B, and k_D for each station and cruise were linearly interpolated between sampling dates. Second, YSI depth profiles of WC chl-*a* were binned in 0.5 m intervals from the surface to 5 meters, since measured attenuation coefficients indicated that photic depths (1% of surface irradiance) were less than 5 m at all sites throughout the sampling period. YSI chl-a readings were scaled to extracted chl-*a* by normalizing the YSI values at depth to the surface reading (0.5 m) and multiplying all values by the extracted surface concentration. SED chl-*a* biomass was also binned in 0.5 m intervals by applying a biomass-depth curve developed from extracted samples as part of a larger microphytobenthic (MPB) biomass study along the entire estuary (authors' unpublished data). This biomass-depth curve was developed from three sampling events, at 6 stations in the estuary during the spring, summer, and fall of 2009. SED chl-*a* was measured at 0.25 m below mean low water (MLW), and in 0.5 m intervals from the surface to 2.5 m below MLW. Biomass-depth curves were expressed as a fraction of the maximum SED chl-*a* along each depth transect (values deeper than 2.5 m were calculated based on linear extrapolation of biomass using the rate of change between 2 and 2.5 m MLW); seasonal biomass-depth curves were combined with measured SED chl-*a* concentrations from 2008 at 1 m MLW to reconstruct SED chl-*a* on each sampling date from 0 to 4 m in 0.5 m bins. All water column and sediment chlorophyll-*a* values were then interpolated in each depth bin between sampling dates to generate daily values over the study.

Third, PAR data from the Chesapeake Bay National Estuarine Research Reserve meteorological station at Taskinas Creek, Virginia (May - November 2008) were downloaded (www.neers.noaa.gov) and used to calculate average hourly instantaneous PAR (μE m^{-2} s^{-1}) for the study period. Finally, bathymetric soundings were downloaded from the NOAA National Geophysical Data Center (www.ngdc.noaa.gov) and interpolated using a kriging function in ESRI ArcMAP GIS 9.3, to a 5m x 5m grid with a resolution of 10 cm in the vertical. The surface area and volume within each sampling region (Fig. 1) was computed in 0.5 m depth intervals from mean sea level (MSL) to the bottom.

Interpolated time series of P-I parameters, k_D, chlorophyll-*a* biomass, and hourly PAR were used to compute hourly gross primary production and respiration of water and sediments over 0.5 m depth intervals in each region of the YRE. Metabolic rates from CB were applied to the adjacent upper river (UR) region, from CB up to the head of the estuary (Fig. 1). Constant photosynthetic and respiratory quotients of one were applied to all sites to convert from oxygen to carbon units (Kemp et al. 1997; Smith and Kemp 2003). While photosynthetic and respiratory quotients are variable (Law 1991; Harding et al. 2002), a direct comparison has not been made for the YRE. Hourly metabolic rates were integrated over depth and time to produce site-specific daily values; these rates were then integrated over area, volume, and time to obtain monthly and seasonal region- and estuary-wide estimates of GPP and net ecosystem metabolism (NEM) (GPP minus R). Integrated sediment respiration was computed by area-weighting shallow and deep rates by the sediment surface area above and below the pycnocline, calculated using the NOAA bathymetric data.

To compare these internal carbon sources to external inputs, dissolved organic carbon (DOC) and particulate organic carbon (POC) concentrations at the head (CBP site RET 4.3) and mouth (CBP site WE4.2) of the YRE (Fig. 1) were downloaded from the CBP website (www.chesapeakebay.net). Bottom water DOC concentrations at site WE4.2 were unavailable; values were estimated by multiplying the surface water DOC to POC ratio by the bottom water POC concentration on each sampling date. Daily river flows for the Mattaponi and Pamunkey Rivers were downloaded from the Virginia USGS website (http://va.water.usgs.gov) and scaled to the entire YRE watershed including the area below the fall line. An Officer (1980) box model was used to calculate the exchange rates between the LYR and the Chesapeake Bay using interpolated CBP salinity values measured throughout the system. These freshwater flows and computed exchanges with the Chesapeake were combined with daily interpolated DOC and POC concentrations to estimate input and export of organic carbon across the upstream and downstream boundaries.

Estimating and Scaling Uncertainty

The inclusion of error estimates in budget calculations of this kind are necessary in order to identify the relative uncertainty associated with each term, and are also useful in determining what input terms need to be focused on in future studies. The magnitude of uncertainty related to various input terms (e.g., chlorophyll-*a*, k_D, P-I parameters, respiration rates) used to construct this carbon budget have been included on figures as standard error. These calculations follow the framework laid out in Boynton et al. (2008) and Lehrter and Cebrian (2010). The uncertainty associated with computing daily primary production from input terms with associated standard errors was calculated by performing a series of Monte Carlo simulations where chlorophyll-*a*, k_D, and all associated P-I parameters were randomly selected from their normal distributions. A series of 1000 independent simulations were conducted for both water column and sediment production rates for each site on each sampling date. GPP rates are presented as the mean of those 1000 simulations +/- one standard deviation. Initial testing with the Monte Carlo approach indicated that 500 simulations were sufficient to constrain the standard deviation. This exercise provides estimates of the uncertainty around our measured daily rates, but we have not attempted to propagate error in our daily interpolations between sampling dates or into our seasonal mass balance of organic carbon as that is beyond the scope of the present study.

RESULTS

Water Column Variability and the Spring-Neap Cycle

During the first half of the summer, the York River experienced two periods of strong density stratification (bottom – surface, Δ sigma-t > 2 kg m^{-3}) that were prevalent over consecutive sampling periods (Fig. 3c). These prolonged events were longer in duration and did not follow the typical spring-neap tidal cycle. The first prolonged event during June resulted from storms that initially disrupted stratification during a neap tide, but which was subsequently followed by a significant pulse of fresh water that acted to stratify the system for a two-week period (Fig. 3 a,c). During mid-July a relatively week spring tide did not lead to the complete breakdown of stratification in the two polyhaline sampling sites (Fig. 3 b,c). Finally, during mid-August stratification completely broke down throughout the entire river due to a series of strong storm events that acted to completely mix the water column (Fig. 3 a-c). Although the lower estuary did not experience stratification during each neap tide, hypoxia did develop during each strong stratification event (Fig. 3 c,d). Surface nutrient concentrations did not show an apparent pattern related to the spring-neap cycle (Fig. 4 a-c). DIN concentrations remained low throughout June and July until the middle of August when water column stratification began to break down. DIP concentrations were also low in early June, increased slightly at some locations during the summer before a brief period of decline in mid-August. DIP at all locations increased in late August and throughout September. Silica concentrations remained elevated, compared to DIN and DIP, from June to September 2008. In contrast to nutrients, surface chlorophyll-*a* concentrations displayed oscillations in early summer in part related to the spring-neap cycle, with a tendency for higher concentrations during more stratified neap tides (Fig. 4d). Chlorophyll-*a* concentrations decreased in late August following late summer storm events (Fig.

3b). Measured k_D was lower through the sampling period in the LYR (mean value 1.17 m^{-1}) compared to the other regions in YRE (CB 1.79, CI 1.77, and MI 1.43 m^{-1}). However, photic depth (1% of surface irradiance) never exceeded 5 meters in any region on any sampling date.

Metabolic Incubations

Water column maximum photosynthetic rates and integrated daily production (GPP_{WC}) varied throughout June, July and August with no clear relationship to the spring-neap tidal cycle (Fig. 5a, 6a). Sediment maximum photosynthetic rates and integrated daily production (GPP_B) remained constant at most sites from June to July before decreasing in August and September (Fig. 5b, 6b). Throughout the study the maximum sediment photosynthetic rates in the LYR remained elevated compared to other three regions of the YRE (Fig. 5b). Surface and bottom water column respiration rates exhibited seasonal and shorter-term peaks with the highest rates occurring during mid-summer (Fig. 5 c,d). Similarly, shallow sediment respiration rates peaked in mid-summer, while deep channel rates increased initially in mid June before decreasing at all sites from July to early August (Fig. 5 e,f). During mid August deep channel respiration rates increased slightly as a series of storms broke down stratification throughout the river (Fig. 3 a-c).

Computed Oxygen Trajectories: Advection versus Internal Consumption

Volume-weighted, sub-pycnocline DO concentrations during the 2007 intensive Acrobat™ surveys covering two spring-to-neap transitions declined by an average rate of 0.17 and 0.29 mg O_2 L^{-1} d^{-1} in the mesohaline, and 0.29 and 0.28 mg O_2 L^{-1} d^{-1} in the polyhaline region of the lower YRE during June and August, respectively (Fig. 7 a,b). During the intensive surveys in June 2008, DO concentrations initially increased due to a spring tide mixing event (Fig. 3 b,c), after which they declined at a rate of 3.43 and 0.15 mg O_2 L^{-1} d^{-1} in the mesohaline and polyhaline zones, respectively (Fig. 7c). During August 2008 DO concentrations in the mesohaline and polyhaline continually increased following a neap tide, which corresponded with the breakdown of stratification within both regions (Fig. 3c, 7d). DO trajectories computed using measured rates of respiration in bottom water and deep channel sediments in 2008 matched or fell below the computed decrease in volume-weighted DO based on Acrobat™ data except in the mesohaline region during June 2008 (Fig. 7 a-d). These trajectories were computed starting at the initial observed concentration except in June 2008, where a mixing event occurred following this initial survey that increased bottom water DO concentrations; in that case the trajectories were computed from the second observation, after which hypoxia developed. These trajectories provide a first-order estimate of what oxygen concentrations would have been if they were controlled solely by internal respiration, and suggest that in most cases internal respiration was more than sufficient to cause the observed patterns in bottom water DO. The exception was in the mesohaline zone in June 2008, where respiration could not account for the observed rapid decline in DO concentrations; in this case other mechanisms such as advection of hypoxic water from the polyhaline zone of the estuary must be invoked.

Carbon Budget: Internal versus External Sources

Daily interpolated rates of GPP_{WC} for the YRE oscillated on both weekly and longer time scales throughout the summer of 2008 (Fig. 8a), however the realized effect of the spring-neap tidal cycle was over-shadowed by longer temporal shifts in WC chl-*a* biomass (Fig. 4d) and greater light availability in the LYR during mid summer (which exceeded all other regions during this period). Additionally, interpolated GPP_{WC} initially increased at all sites in late August as stratification broke down before subsequently decreasing for the remainder of the study (Fig. 8a). Although rates varied throughout the summer, mean monthly total gross primary production (GPP_{total}, water column and benthic) generally decreased over the course of the summer (Table 1), with less than 10% of total system gross primary production attributed to the MPB (Fig. 8 a,b).

Daily interpolated rates of R_{WC} in the YRE did not appear to respond to the spring-neap cycle (Fig. 8c). Mean R_{WC} increased from June (1.12 g C m^{-2} d^{-1}) to July and August (1.35 g C m^{-2} d^{-1}), before declining to the lowest seasonal rates in September (0.55 g C m^{-2} d^{-1}) (Table 1, Fig. 8c). Rates at stations CB and CI remained relatively constant throughout the summer with short periods of higher values, while rates at MI and LYR increased in mid June to approximately double the rates of CB and CI, and remained elevated until late August. Daily interpolated rates of benthic respiration (shallow and deep sediments combined) increased slightly from June to August (0.16 g C m^{-2} d^{-1}) with an average seasonal rate of 0.14 g C m^{-2} d^{-1}), which accounted for approximately 11% of total system respiration throughout the summer (Table 1, Fig. 8 c-d).

Regional rates of NEM varied temporally and spatially throughout the river, with the highest rates of net autotrophy occurring during June in MI and LYR, and during September in CB and CI (Table 2). Most regions remained net autotrophic throughout the entire summer, although NEM at UR and LYR decreased to 0.06 and 0.30 g C m^{-2} d^{-1}. At MI NEM, however, decreased from 3.37 g C m^{-2} d^{-1} in June to -0.12 g C m^{-2} d^{-1} in July and remained net heterotrophic through August (-0.53 g C m^{-2} d^{-1}). Seasonal NEM for the whole system decreased from June to August with a rebound in September as water column production increased and respiration rates declined (Table 1).

Since the rates of internal oxygen consumption appeared sufficient to drive development of bottom water hypoxia in the lower YRE, results from the metabolic incubations were used to construct a carbon budget for the system to identify the potential roles of autochthonous and allochthonous carbon sources in driving hypoxia. In addition to phytoplankton and MPB production, this analysis incorporated external sources of organic carbon from the tributaries, surrounding watershed, and the Chesapeake Bay. Results indicated that the monthly average net input of DOC and POC from the two tributaries ranged from 5.5×10^3 - 2.2×10^4 kg C d^{-1} during the summer, with an average seasonal rate of 1.2×10^4 kg C d^{-1}. The smaller watersheds that surround the YRE supplied an average of 866 kg C d^{-1} (monthly means ranging from 200 - 6800 kg C d^{-1}). However, both of these sources were relatively low compared to the seasonal mean import (2×10^5 kg C d^{-1}) and export (2.1×10^5 kg C d^{-1}) of organic carbon from the Chesapeake Bay.

DISCUSSION

Drivers of Water Column Dynamics

The 2008 Acrobat^{TM} and spring-neap surveys confirmed the importance of density stratification and the development of hypoxia within the YRE, however the spring-neap tidal cycle did not completely drive the oscillations between stratified and non-stratified periods (Fig. 3c). A series of strong storms during early June acted to break down stratification over a neap tidal period, while the subsequent freshwater input following the storms stratified the system during a relatively weak semidiurnal spring tide (Fig. 3 a-c). During mid-July stratification in the polyhaline York River did not fully break down until more than 3 days after a weaker spring tide. However, the system remained homogenous through the following neap tide due to stronger than predicted neap tidal amplitudes. Finally, during mid-August stratification completely broke down throughout the entire river due to a series of strong storm events that acted to completely mix the water column (Fig. 3 a-c). High resolution sampling confirmed that the spring-neap cycle has the ability to control stratification and hypoxia, as noted in other previous studies Haas 1977; Hayward et al. 1982; Kuo and Neilson 1987). However, the results also indicated a number of other important physical factors that must also be considered including: strong wind events, freshwater flow, and relative tidal mixing strength.

Metabolic Rate Measurements

The metabolic rates observed in this study were within the range or slightly below those reported from previous studies conducted in the lower polyhaline Chesapeake Bay. Kemp et al. (1997) reported seasonal GPP rates for June – September between 0.75 and 5.25 g C m^{-2} d^{-1} in the lower bay (assuming a PQ = 1). Seasonal mean GPP_{WC} values in this study fell within their range, at 2.11 g C m^{-2} d^{-1} (monthly means from 1.73 - 2.97 g C m^{-2} d^{-1}), with maximum daily values exceeding 4 g C m^{-2} d^{-1} (Fig 8a). The net water column primary production rates in this study ranged from 0.43 - 1.66 g C m^{-2} d^{-1}, which bracketed the summer net ^{14}C primary production value of 1.2 g C m^{-2} d^{-1} reported by Harding et al. (2002) for the lower bay. However, these net rates fell below the daytime net community production values reported by Smith and Kemp (1995) (3.53 +/- 0.83 g C m^{-2} d^{-1}). R_{WC} rates from this study (0.012 - 0.056 mg O_2 l^{-1} h^{-1}) overlapped the mean values reported for the lower bay above 20°C by Smith and Kemp (1995) for the surface layer (0.01 - 0.04 mg O_2 l^{-1} h^{-1}). Similarly, R_{WC} for the bottom layer (0.001 - 0.055 mg O_2 l^{-1} h^{-1}) of the YRE also overlapped Smith and Kemp (1995) lower bay rates (0.01 - 0.04 mg O_2 l^{-1} h^{-1}). The measured deep channel sediment oxygen demand rates bracketed the range reported by Cowan and Boynton (1996) for the lower bay (0.65 - 0.75 g O_2 m^{-2} d^{-1}) (Fig. 5f). However, the scaled YRE monthly average rates were slightly below this range (0.42 - 0.66 g O_2 m^{-2} d^{-1}).

Computed Oxygen Trajectories

Comparing *in-situ* DO concentrations over the intensive Acrobat^{TM} surveys in 2007 and 2008 with trajectories computed using rates from the 2008 metabolic incubations (Fig. 7) provides an estimate of the role of respiration in controlling the observed changes in DO concentrations. While this exercise is admittedly first-order as it excludes mixing of oxygen across the pycnocline and assumes that the rates during 2007 were the same as 2008, it nevertheless provides a method for quantifying the relative importance of internal respiration as opposed to external factors like advection of hypoxic water into the system from the lower Chesapeake Bay. The other major process that was excluded from these calculations is production of oxygen below the pycnocline, but calculations based on measured attenuation of irradiance and P-I curves indicated minimal to no photosynthetic oxygen production below approximately 5 m, the depth used for the mesohaline pycnocline in these calculations (9 m in the polyhaline).

The comparison of *in-situ* and computed DO concentrations within the polyhaline YRE indicated that internal respiration alone was capable of driving this system to hypoxia under stratified conditions without the need for advection of hypoxic water from the Chesapeake Bay (Fig. 7). During the summer of 2007 the interpolated volumetric DO concentrations in the polyhaline declined at rates less than or equal to the combined water column and sediment respiration trajectories. During June of 2008 the DO concentrations in the polyhaline York initially declined slightly faster than suggested by respiratory rates, however this may be due in part to a settling effect of higher density low DO water that was partially mixed into the surface layer during the previous spring tide (Fig. 2 c,d). The 2007 mesohaline oxygen concentrations also declined at rates equal to or less than the oxygen uptake trajectories measured for this region. During June of 2008 however, the observed DO concentrations for the mesohaline York declined much faster than those computed from metabolic rates, which suggests that factors other than internal respiration were required to explain the observed decline. In this instance it appears that the rapid decline in DO concentrations was caused by the advection of low DO water into the mesohaline region from the polyhaline York. Acrobat^{TM} surveys from 2008 appear to confirm this, as higher density, low DO water advanced upriver following a spring tide (data not shown). DO concentrations in both the polyhaline and mesohaline increased throughout the month of August (2008) as fall storms mixed the entire water column for the remainder of the summer (Fig 3 a,b).

Summer Integrated GPP and R

Confirmation that internal respiration within the estuary was generally sufficient to drive hypoxia led to an evaluation of the importance of individual autochthonous and allochthonous organic matter sources and their potential to contribute to hypoxia at monthly and seasonal scales. While uncertainty was not propagated through the daily interpolated estimates of GPP and R (Fig. 8) used to generate the values in Table 1, estimated errors on the rates each day of measurement (Fig. 5c-f; Fig. 6) indicate that the values are sufficiently well constrained to allow order of magnitude comparisons between water column and sediment rates, contributions from phytoplankton and MPB, and relative rates of production and respiration. Results indicated that phytoplankton production dominated total GPP in the system and was more than sufficient to offset the aerobic respiration in the water column and sediments (Table 1). This study did not capture the spring phytoplankton bloom in the tributaries and upper river that precedes seasonal development of hypoxia in the polyhaline segment, which would provide an additional phytoplankton-based source of carbon for fueling hypoxia.

Microphytobenthic production along the shallow photic shoals (< 2m) of the river, which comprise greater than 40% of the YRE surface area (Rizzo and Wetzel 1985), has been suggested to be an important primary producer throughout the year (Pickney and Zingmark 1993; Reay et al. 1995; Buzzelli 1998). These results indicate that benthic production accounted for less than 10% of GPP_{total} throughout the summer, which is similar to the microphytobenthic production contribution for the mainstem Chesapeake Bay estimated by Kemp et al. (1999). However, on a local scale benthic production appeared to be more significant in some regions, specifically CI where GPP_B accounted for up to 20% of GPP_{total} during the month of June, before declining to less than 10% in July. Measured benthic production rates were consistently higher in the LYR throughout the summer compared to the other regions (Fig. 5b); however, the high rates of primary production did not offset the smaller percentage of photic surface area in the polyhaline zone (Fig. 8b).

Water column respiration in the mesohaline remained relatively constant from June to late August 2008 with only short weekly periods of elevated rates, which may be due in part to resuspension of the bottom boundary layer resulting from stronger tidal currents. Bed erodibility in this region, which has been demonstrated to be higher than in the lower polyhaline (Cartwright et al. 2009), likely suspends some labile particular organic matter and pore water nutrients into the overlying water column, increasing water column respiration rates. Within the polyhaline regions R_{WC} rates increased in mid July, as GPP_{WC} decreased, and remained elevated compared to the mesohaline regions throughout the summer (Fig. 8c). Elevated polyhaline R_{WC} rates were approximately double the corresponding rates in the mesohaline during July and August, which likely resulted from the degradation of internally produced organic matter resulting from greater light availability in the LYR, and advected labile DOC and POC water from the lower Chesapeake Bay.

Spatial and Temporal Variations in NEM

NEM varied both temporally and spatially throughout the river during the summer of 2008. During June all sites were found to be net autotrophic with the highest rates of GPP_{total} occurring in MI and LYR (Table 2). With the exception of MI, all regions remained net autotrophic throughout the summer, although the UR and LYR regions decreased to their lowest rates in August. MI however, alternated from net autotrophy to net heterotrophy in July, and remained net heterotrophic through August. Mumfort Island, which is just below the mesohaline – polyhaline transition zone, appears to be a trap for respirable organic matter. This region is also the most upriver location for recurring hypoxia based on previous Acrobat^{TM} surveys (authors' unpublished data). The CI region, just above MI, is a transition zone where the York River channel becomes wider and deeper compared to the broad shallow regions in the upper river. It is possible that estuarine circulation transports and retains labile organic matter in this region, which results in higher respiration rates within the water column and in the sediments (Fig. 8 c,d) without the elevated rates of GPP_{WC} present in the LYR (Fig. 8a).

Seasonal mean NEM for the entire system decreased from June to August with a subsequent increase in September as water column production increased and respiration declined. Interestingly, Raymond et al. (2000) calculated that the York River, including portions of the tributaries, was net heterotrophic using open water DIC measurements. Within Raymond et al. (2000) did note that the LYR region had the lowest rates of heterotrophy with seasonal net autotrophy. The discrepancy between Raymond et al. (2000) and this study may be due in part to the two different approaches used to measure NEM (*in-situ* measurements of DIC vs. component incubations). Although there have only been a limited number of studies that have utilized multiple NEM methods, these studies have highlighted discrepancies in NEM values associated with different techniques (Kemp and Boynton 1980; Kemp et al. 1997; Giordano et al. 2012). It is also likely that the DIC method of Raymond et al. (2000) accounted for excess CO_2 from upriver tidal freshwater marsh systems, rather than water column processes within the estuary (Neubauer and Anderson 2003).

Summer Total Organic Carbon Budget

Measured biological rate processes and computed physical transport of particulate and dissolved organic carbon from the surrounding watershed and lower Chesapeake Bay were combined into a seasonal budget of organic carbon fluxes in the YRE (Fig. 9). As noted above, estimated errors on the rates each day of measurement (Fig. 5c-f; Fig. 6) are sufficiently well constrained to allow order of magnitude comparisons between major terms in the carbon budget even though errors were not propagated through these seasonal integrated values.

During the summer of 2008, internal water column production accounted for over half (57.5%) of all organic carbon inputs to the YRE, with advected POC and DOC from the lower Chesapeake Bay accounting for an additional 37%. It was not surprising that these two sources of organic carbon contributed significantly to this system; past studies of particulate and dissolved organic matter in the YRE have highlighted their significance within the mesohaline and polyhaline portions of the river (Countway et al. 2007; McCallister et al. 2006a; McCallister et al. 2006b). Previous studies also indicate that organic matter from the Chesapeake Bay is important to bacterial secondary production within the LYR, contributing 66-70% of bacterial production during October (McCallister et al. 2004); however, the contribution during the summer was reported to be significantly lower (8-10% in July).

Allochthonous POC and DOC entering from the watershed and tributaries were found to be comparatively low, accounting for less than 3% of organic carbon inputs during the summer. These allochthonous sources of carbon are likely to be more refractory in nature (McCallister et al. 2004; McCallister et al. 2006a; McCallister et al. 2006b), which would further limit their bioavailability. The role of MPB in this system also appeared to be limited, contributing only 3% of seasonal organic matter input. While it is likely that some of this organic matter can be transported to the deep channels of the York following storm events, it is unlikely that this source would contribute significantly to the formation of hypoxia. Future management efforts including nutrient and sediment reduction strategies and improved water clarity may benefit MPB in this system, along with submerged aquatic vegetation, causing these sources to become more significant in the future.

It is interesting to note that the exchanges of POC and DOC to and from the Chesapeake Bay are nearly in balance during the summer. While the net exchange of POC and DOC across the mouth of the estuary appears to currently be in balance, this important exchange should be addressed in future management strategies. Nutrient reduction strategies focused on the tributaries may reduce phytoplankton production in the York River; however, this approach will not reduce POC and DOC entering from the lower Chesapeake Bay. A recent analysis of WC chl-*a* concentrations over the past 50 years by Harding and Perry (1997) found that the lower polyhaline mainstem exhibited the largest increase within any region of the Chesapeake Bay. It is likely that the outcome of nutrient reduction strategies for the York River will be influenced indirectly by the Chesapeake Bay. Similar studies in other sub-estuaries of the Chesapeake Bay have identified the mainstem as a source of labile organic matter, DIN, and DIP (Jordan et al. 1991; Boynton et al. 2008; Testa et al. 2008), which likely contribute to the elevated rates of GPP and net autotrophy in the LYR.

The carbon mass balance indicates that internal water column and benthic respiration is approximately equal to the export of organic matter to the Chesapeake Bay, at 47% and 53% of all loss terms, respectively. Surface (< 5 and < 9 meters for the mesohaline and polyhaline, respectively) water column respiration in this shallow sub-estuary accounted for the majority of internal aerobic respiration (74%), with sub-pycnocline water column respiration accounting for an additional 15%. Benthic respiration along the shallow shoals and in the deep channels was found to be comparatively low (7% and 4%, respectively) compared to other internal sinks within the estuary. However, these measurements of aerobic respiration likely underestimates total benthic respiration, which includes anaerobic respiration occurring in the deep channel under hypoxic conditions and in anaerobic sediments.

CONCLUSIONS

The oxygen mass balance for the YRE indicates that internal respiration is sufficient to drive the system to hypoxia under stratified conditions, without the need for advection of hypoxic water from the Chesapeake Bay to reproduce the observed declines in DO. Although this system is directly affected by multiple organic matter sources, both autochthonous and allochthonous, this analysis indicates that internal water column phytoplankton production is the dominant source of organic carbon to the YRE during the summer. Reducing this labile source of organic material by implementing nutrient reduction strategies could potentially mitigate some current water quality concerns, although a more complete assessment of the magnitude of nutrient reductions necessary to cause these changes is required over multiple years and under a range of climate scenarios. Additionally, the net exchange of labile organic matter between the lower Chesapeake Bay and the YRE should not be discounted given the potential ecological impacts and associated management implications of these inputs.

ACKNOWLEDGEMENTS

This project was funded by a grant from NOAA/UNH Cooperative Institute for Coastal and Estuarine Environmental Technology, NOAA Grant Number NA05NOS4191149. S. J. Lake also received financial support from NSF GK-12 (Division of Graduate Education 0840804). We would also like to thank Larry Haas, Jennifer Stanhope, Hunter Walker, Lisa Ott, Juliette Giordano, and many other VIMS students and staff members for their field and laboratory assistance. This is Virginia Institute of Marine Science contribution no. XXXX.

LITERATURE CITED

Boynton WR, Hagy JD, Cornwell JC, Kemp WM, Greene SM, Owens MS, Baker JE, Larsen RK (2008) Nutrient budgets and management actions in the Patuxent River estuary, Maryland. Estuaries 31:623-651

Brush MJ (2004) Application of the Greenwich Bay ecosystem model to the development of the Greenwich Bay SAMP (Special Area Management Plan). Final report to the Rhode Island Coastal Resources Center, University of Rhode Island, Narragansett, RI.

Buzzelli CP (1998) Dynamic simulation of littoral zone habitats in lower Chesapeake Bay: I. habitat characterization related to model development. Estuaries 21:673-389

Cartwright GM, Friedrichs CT, Dickhudt PJ, Gass T, Farmer FH (2009) Using the acoustic Doppler velocimeter (ADV) in the MUDBED real-time observing system. Proceedings, OCEANS 2009, Institute of Electrical and Electronics Engineers, ISBN 978-1-4244-4960-6:1428-1436.

Cloern JE (2001) Our evolving conceptual model of the coastal eutrophication problem. Mar Eco Prog Ser 210:223-253

Cooper SR, Brush GS (1991) Long-term history of Chesapeake Bay anoxia. Science 254:992-996

Cooper SR, Brush GS (1993) A 2,500-year history of anoxia and eutrophication in Chesapeake Bay. Estuaries 16:617-626

Countway RE, Canuel EA, Dickhut RM (2007) Sources of particulate organic matter in surface waters of the York River, VA estuary. Org Geochem 38:365-379

Cowan JL, Boynton WR (1996) Sediment-water oxygen and nutrient exchanges along the longitudinal axis of Chesapeake Bay: seasonal patterns, controlling factors and ecological significance. Estuaries 19:562-580

Dauer DM, Marshall HG, Donat JR, Lane MF, Doughten SC, Morton PL, Hoffman FA (2005) Status and trends in water quality and living resources in the Virginia Chesapeake Bay: James River (1985-2004). Final Report to the Virginia Department of Environmental Quality, Richmond, Virginia. Applied Marine Research Laboratory, Norfolk VA. 1-63.

de Jonge VN, van Beusekom JEE (1995) Wind- and tide-induced resuspension of sediment and microphytobenthos from tidal flats in the Ems Estuary. Limnol Oceanogr 40:766-778

de Jonge VN (1997) High remaining productivity in the Dutch western Wadden Sea despite decreasing nutrient inputs from riverine sources. *Mar Pollut Bull* 34:427-436

D'Elia CF, Webb KL, Wetzel RL (1981) Time-varying hydrodynamics and water quality in an estuary. In: Neilson BJ, Cronin LE (eds), Estuaries and nutrients. Humana Press, Clifton, N.J.

D'Elia CF, Boynton WR, Sanders JG (2003) A watershed perspective on nutrient enrichment, science, and policy in the Patuxent River, Maryland: 1960-2000. Estuaries 26:171-185

Diaz RJ, Neubauer RJ, Schaffner LC, Pihl L, Baden SP (1992) Continuous monitoring of dissolved oxygen in an estuary experiencing periodic hypoxia and the effects of hypoxia on macrobenthos and fish. Sci Total Environ Supplement 1992:1055-1068

Diaz RJ, Rosenberg R (1995) Marine benthic hypoxia: a review of its ecological effects and the behavioural responses of benthic macrofauna. Oceanogr Mar Biol Annu Rev 33:245-303

Diaz RJ, Rosenberg R (2008) Spreading dead zones and consequences for marine ecosystems. Science 321:926-929

Fisher TR, Hagy JD, Boynton WR, Williams MR (2006) Cultural eutrophication in the Choptank and Patuxent Estuaries of Chesapeake Bay. Limnol Oceanogr 51:435-447

Giordano JCP (2009) Nutrient loading and system response in the coastal lagoons of the Delmarva Peninsula. M.S. thesis, College of William and Mary, Virginia Institute of Marine Science, Gloucester Point, VA

Giordano JCP, Brush MJ, Anderson IC (2012) Ecosystem metabolism in shallow coastal lagoons: patterns and partitioning of planktonic, benthic, and integrated community rates. Mar Ecol Prog Ser 458:21-38

Haas LW (1977) The effect of the spring-neap tidal cycle on the vertical salinity structure of the James, York, and Rappahannock Rivers, Virginia, U.S.A. Est Coast Mar Sci 5:485-496

Haas LW, Hastings SJ, Webb KL (1981) Phytoplankton response to a stratification-mixing cycle in the York River estuary during late summer. In: Neilson BJ, Cronin LE (eds), Estuaries and nutrients. Humana Press, Clifton, N.J.

Hagy JD, Boynton WR, Keefe CW, Wood KV (2004) Hypoxia in Chesapeake Bay, 1950 – 2001: long-term changes in relation to nutrient loading and river flow. Estuaries 27:634-658

Harding Jr. LW, Perry ES (1997). Long-term increase of phytoplankton biomass in Chesapeake Bay, 1950 – 1994. Mar Ecol Prog Ser 157:39-52

Harding Jr. LW, Mallonee ME, Perry ES (2002) Toward a predictive understanding of primary productivity in a temperate, partially stratified estuary. Est Coast Shelf Sci 55:437-463

Hayward D, Welch CS, Haas LW (1982) York River destratification: an estuary-subestuary interaction. Science 216:1413-1414

Hayward D, Haas LW, Boon III JD, Webb KL, Friedland KD (1986). Empirical models of stratification variation in the York River estuary, Virginia, USA. In: Bowman MJ, Yentsch CM, Peterson WT (eds) Lecture notes on coastal and estuarine studies: tidal mixing and plankton dynamics. Springer-Verlag, New York, NY

Jassby AD, Platt T (1976) Mathematical formulations of the relationship between photosynthesis and light for phytoplankton. Limnol Oceangr 21:540-547

Jordan TE, Correll DL, Miklas J, Weller DE (1991) Long-term trends in estuarine nutrients and chlorophyll, and short-term effects of variation in watershed discharge. Mar Ecol Prog Ser 75:121-132

Kemp WM, Boynton WR (1980) Influence of biological and physical processes on dissolved oxygen dynamics in an estuarine system: implications for measurement of community metabolism. Est Coast Mar Sci 11:407-431

Kemp WM, Sampou PA, Garber J, Tuttle J, Boynton WR (1992) Seasonal depletion of oxygen from bottom-waters of Chesapeake Bay: roles of benthic and planktonic respiration and physical exchange processes. Mar Ecol Prog Ser 85:137-152

Kemp WM, Smith EM, Marvin-DiPasquale M, Boynton WR (1997) Organic carbon balance and net ecosystem metabolism in Chesapeake Bay. Mar Ecol Prog Ser 150:229-248

Kemp WM, Puskaric S, Faganeli A, Smith E, Boynton W (1999) Pelagic-benthic coupling and nutrient cycling. In: Malone T, Malej A, Harding L, Smodlaka N, Turner R (eds) Ecosystems at the land-sea margin: drainage basin to coastal sea. American Geophysical Union, Washington, DC.

Kemp, WM, Boynton WR, Adolf JE, Boesch DF, Boicourt WC, Brush G, Cornwell JC, Fisher TR, Glibert PM, Hagy JD, Harding LW, Houde ED, Kimmel DG, Miller WD, Newell RIE, Roman MR, Smith EM, Stevenson JC (2005) Eutrophication of Chesapeake Bay: historical trends and ecological interactions. *Mar Ecol Progr Ser* 303:1-29

Kuo AY, Neilson BJ (1987) Hypoxia and salinity in Virginia estuaries. Estuaries 10:277-283

Kuo AY, Neilson BJ, Brubaker J, Ruzecki EP (1993) Hypoxia in the York River, 1991. Virginia Institute of Marine Science Data Report No. 47. Gloucester Point, Virginia

Lake SJ, Brush MJ (2011) The contribution of microphytobenthos to total productivity in Narragansett Bay, Rhode Island. Est Coast Shelf Sci 95:289-297

Law EA (1991) Photosynthetic quotients, new production and net community production in the open ocean. Deep-Sea Res 38:143-167

Lehrter JC, Cerbian, J (2010) Uncertainty propagation in an ecosystem nutrient budget. Ecol. Appl. 20:508-524

Lorenzen C (1967) Determination of chlorophyll and phaeopigments: spectrophotometric equations. Limnol and Oceanogr 12:343-346

McCallister SL, Bauer JE, Cherrier JE, Ducklow HW (2004) Assessing sources and ages of organic matter supporting river and estuarine bacterial production: a multiple-isotope approach. Limnol and Oceanogr 49:1687-1702

McCallister SL, Bauer JE, Canuel EA (2006a) Bioreactivity of estuarine dissolved organic matter: a combined geochemical and microbiological approach. Limnol Oceanogr 51:94-100

McCallister SL, Bauer JE, Ducklow HW, Canuel EA (2006b) Sources of estuarine dissolved and particulate matter: a multi-tracer approach. Org Geochem 37:454-468

Malone TC, Kemp WM, Ducklow HW, Boynton WR, Tuttle JH, Jonas RB (1986) Lateral variation in the production and fate of phytoplankton in a partially stratified estuary. Mar Ecol Prog Ser 32:149-160

Møhlenberg F (1999) Effect of meteorology and nutrient load on oxygen depletion in a Danish micro-tidal estuary. *Aquat Ecol* 33:55-64

Neubauer SC, Anderson IC (2003) Transport of dissolved inorganic carbon from a tidal freshwater marsh to the York River estuary. Limnol Oceanogr 48:299-307

Officer CB (1980) Box models revisited. In: Hamilton P, MacDonald KB (eds.). Estuarine and wetland processes with emphasis on modeling. Plenum Press. New York, NY

Officer CB, Biggs RB, Taft JL, Cronin LE, Tyler MA (1984) Chesapeake Bay anoxia: origin, development, and significance. Science 223:22-27

Paerl HW, Pinckney JL, Fear JM, Peierls BL (1998) Ecosystem responses to internal and watershed organic matter loading: consequences for hypoxia in the eutrophying Neuse River estuary, North Carolina, USA. Mar Ecol Prog Ser 166:17-25

Pemberton M, Anderson GL, Barker JH (1996) Characterization of microvascular vasoconstriction following ischemia/reperfusion in skeletal muscle using videomicroscopy. Microsurgery 17:9-16

Pinckney JL, Zingmark RG (1993) Modeling the annual production of intertidal benthic microalgae in estuarine ecosystems. J Phycol 29:396-407

Platt T, Gallegos CL, Harrison WG (1980) Photoinhibition of photosynthesis in natural assemblages of marine phytoplankton. J Mar Res 38:687-701

Rabalais NN, Turner RE, Gupta BKS, Boesch DF, Chapman P, Murrell MC (2007) Hypoxia in the northern Gulf of Mexico: does the science support the plan to reduce, mitigate and control hypoxia. Estuaries 30:753-772

Raymond PA, Bauer JE, Cole JJ (2000) Bacterial consumption of DOC during transport through a temperate estuary. Aquat Microb Ecol 22:1-12

Reay WG, Gallagherl DL, Simmons GM (1995) Sediment-water column oxygen and nutrient fluxes in nearshore environments of the lower Delmarva Peninsula, USA. Mar Ecol Prog Ser 118:215-227

Rizzo WM, Wetzel RL. (1985) Intertidal and shoal benthic community metabolism in a temperate estuary: studies of spatial and temporal scales of variability. Estuaries 8:342-351

Seliger HH, Boggs JA, Buggley WH (1985) Catastrophic anoxia in the Chesapeake Bay in 1984. Science 228:70-73

Sharples J, Simpson JH, Brubaker JM (1994) Observations and modelling of periodic stratification in the upper York River estuary, Virginia. Est Coast Shelf Sci 38:301-312

Shen J, Haas L (2004) Calculating age and residence time in the tidal York River using three-dimensional model experiments. Est Coast Shelf Sci 61:449-461

Shoaf WT, Lium BW (1976) Improved extraction of chlorophyll *a* and *b* from algae using dimethyl sulfoxide. Limnol Oceanogr 21:926-928

Smith EM, Kemp WM (1995) Seasonal and regional variations in plankton community production and respiration for Chesapeake Bay. Mar Ecol Prog Ser 116:217-231

Taft JL, Hartwig EO, Loftus R (1980) Seasonal oxygen depletion in Chesapeake Bay. Estuaries 3:242-247

Testa JM, Kemp WM (2008) Variability of biogeochemical processes and physical transport in a partially stratified estuary: a box-modeling analysis. Mar Ecol Prog Ser 356:63-79

Testa JM, Kemp WM, Boynton WR, Hagy III JD (2008) Long-term changes in water quality and productivity in the Patuxent River estuary: 1985 – 2003. Estuaries 31:1021-1037

CHAPTER 1 - FIGURES

Figure 1-1. Map of the York River estuary and the Chesapeake Bay (insert), including boundaries of each sampling region, and corresponding channel (black circles) and nearshore (bulls eyes) sampling stations. Acrobat^{TM} monitoring surveys (grey line) were conducted bi-monthly (2007) and monthly (2008) to examine the spatial extent of hypoxia in 3-dimensions. Intensive (dashed black line) surveys were conducted every 2-3 days for a 2.5 week period during June and August of each year to capture the development, spread, and disruption of hypoxia. The intensive surveys were extended outside the mouth of the York River estuary into the lower Chesapeake Bay for the 2008 sampling season.

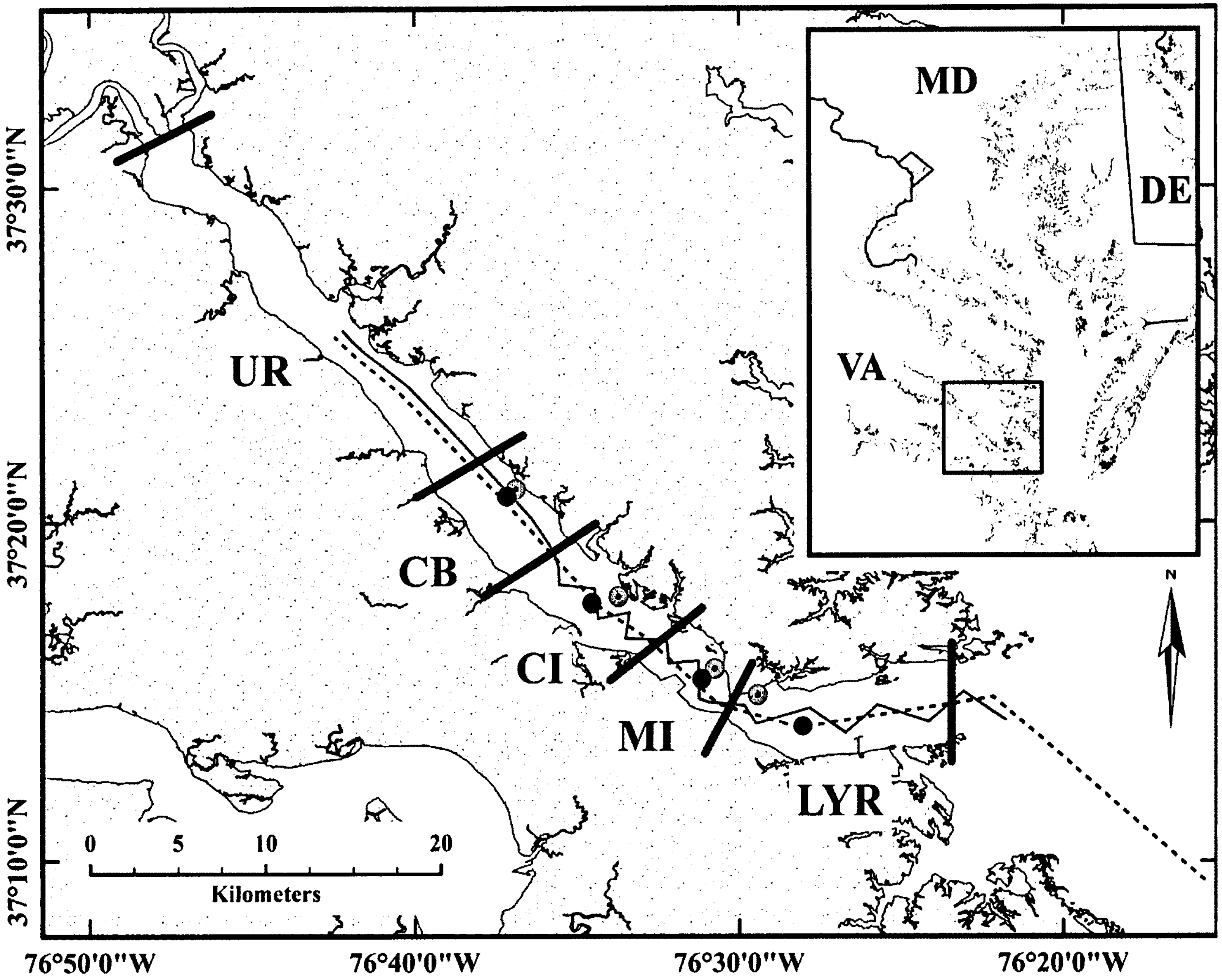

MD
DE
VA
UR
CB
CI
MI
LYR
N
0
5
10
20
Kilometers
37°30'0"N
37°20'0"N
37°10'0"N
76°50'0"W
76°40'0"W
76°30'0"W
76°20'0"W

Figure 1-2. Interpolated dissolved oxygen concentrations from Acrobat^{TM} surveys, from June 2007 (a, b) and June 2008 (c, d). Panels (a) and (b) show hypoxic water appearing in the lower YRE following a neap tide on June 22, 2007. During June 2008 water column stratification and hypoxia persisted after a spring tide on June 19 (c, d). On June 25, 2008 (d), hypoxic water was observed in bottom waters up to 13 km outside the mouth of the YRE. All Acrobat^{TM} interpolations were developed using the Inverse Distance Weighting method in ArcMAP 9.3.

York River Acrobat Surveys

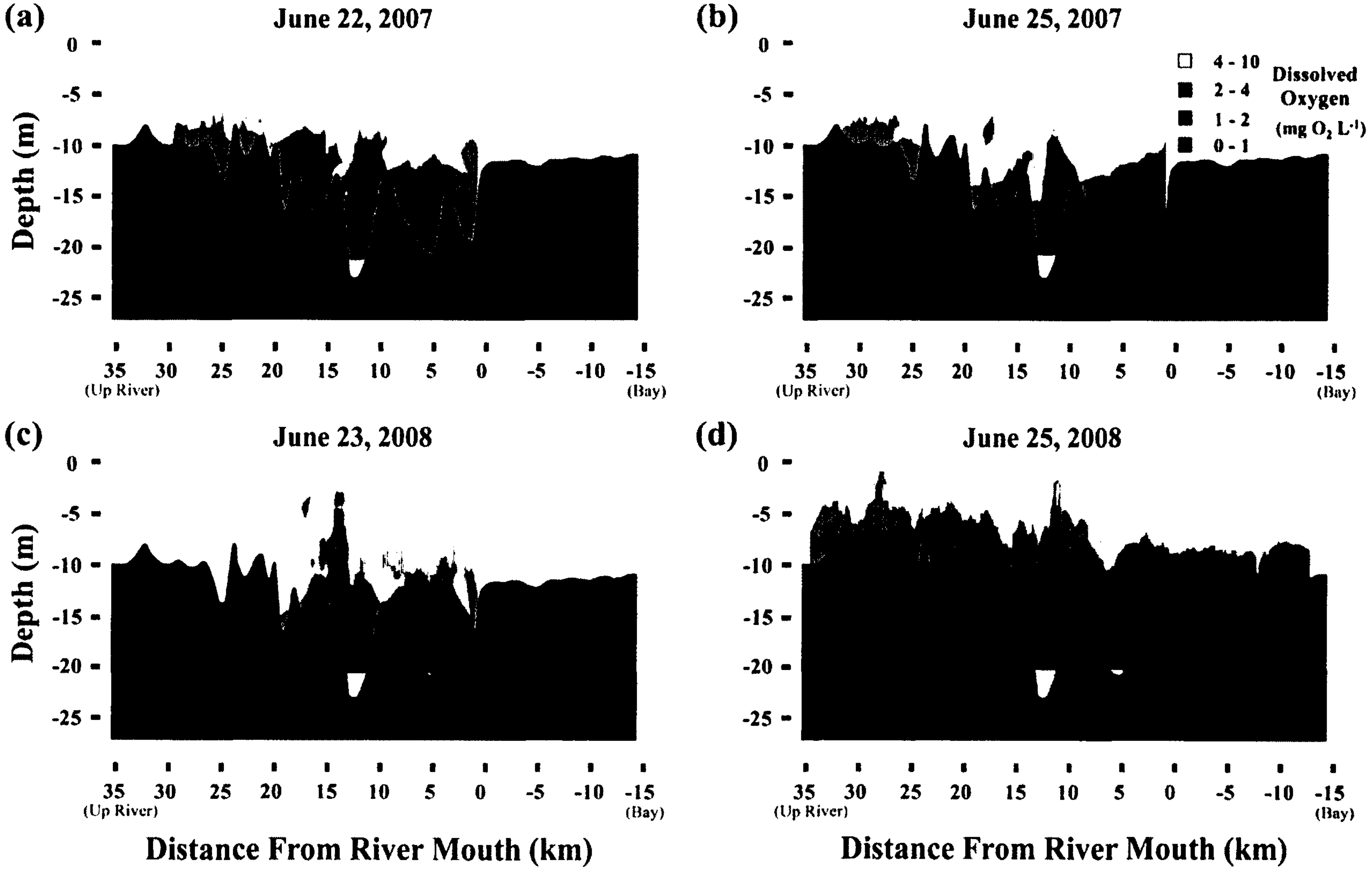

Figure 1-3. Time-series of environmental conditions during the weekly spring-neap surveys in 2008. (a) Precipitation at the Taskinas Creek, VA meteorological station (www.nerrs.noaa.gov) and combined river flow of the Mattaponi and Pamunkey Rivers (waterdata.usgs.gov/nwis), (b) hourly wind speed and daily tidal range measured at the Coast Guard Pier in the lower YRE (tidesandcurrents.noaa.gov), (c) observed strength of stratification (bottom – surface sigma-*t*), and (d) observed mean bottom water dissolved oxygen concentrations. The YRE oscillated between stratified (low oxygen) and well mixed (normoxic) conditions on time scales longer than the spring-neap tidal cycle. Error bars on panels (c) and (d) are standard error. White boxes (outlined in black) highlight a 3-day period beginning at the apex of spring tide; light grey boxes correspond to a 3-day period beginning on neap tides.

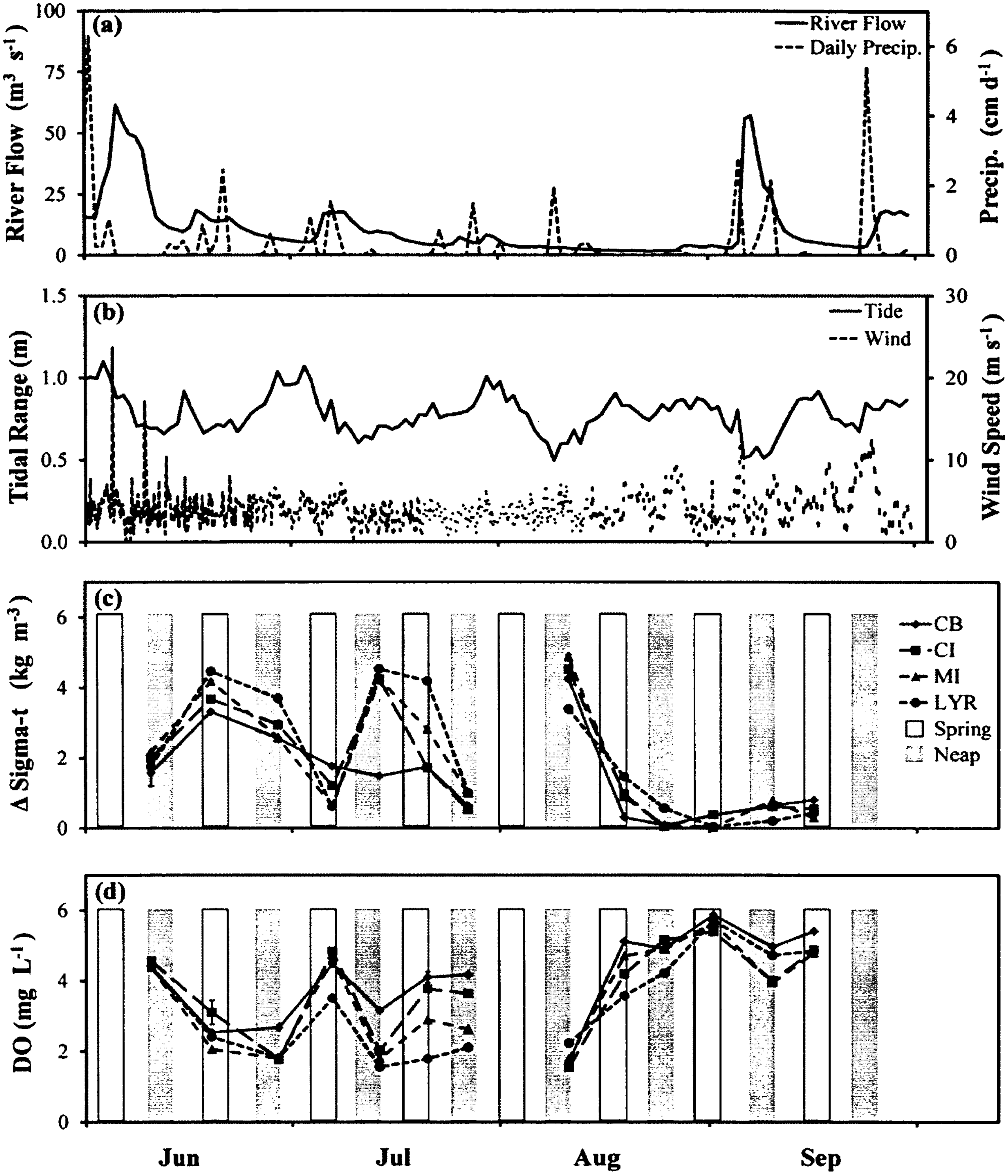
(a)
River Flow
Daily Precip.
River Flow (m^3 s^{-1})
Precip. (cm d^{-1})
100
75
50
25
0
6
4
2
0
(b)
Tide
Wind
Tidal Range (m)
Wind Speed (m s^{-1})
1.5
1.0
0.5
0.0
30
20
10
0
(c)
Δ Sigma-t (kg m^{-3})
CB
CI
MI
LYR
Spring
Neap
6
4
2
0
(d)
DO (mg L^{-1})
6
4
2
0
Jun
Jul
Aug
Sep

Figure 1-4. Nutrient and water column chlorophyll-*a* concentrations from spring-neap surveys sampled weekly in each sampling region during 2008. (a) Dissolved inorganic nitrogen, (b) dissolved inorganic phosphorus, (c) dissolved silica, and (d) chlorophyll-*a* concentrations in the surface water (sampled at 0.25 m). Error bars represent standard error. White boxes (outlined in black) highlight a 3-day period beginning at the apex of spring tide; light grey boxes correspond to a 3-day period beginning on neap tides.

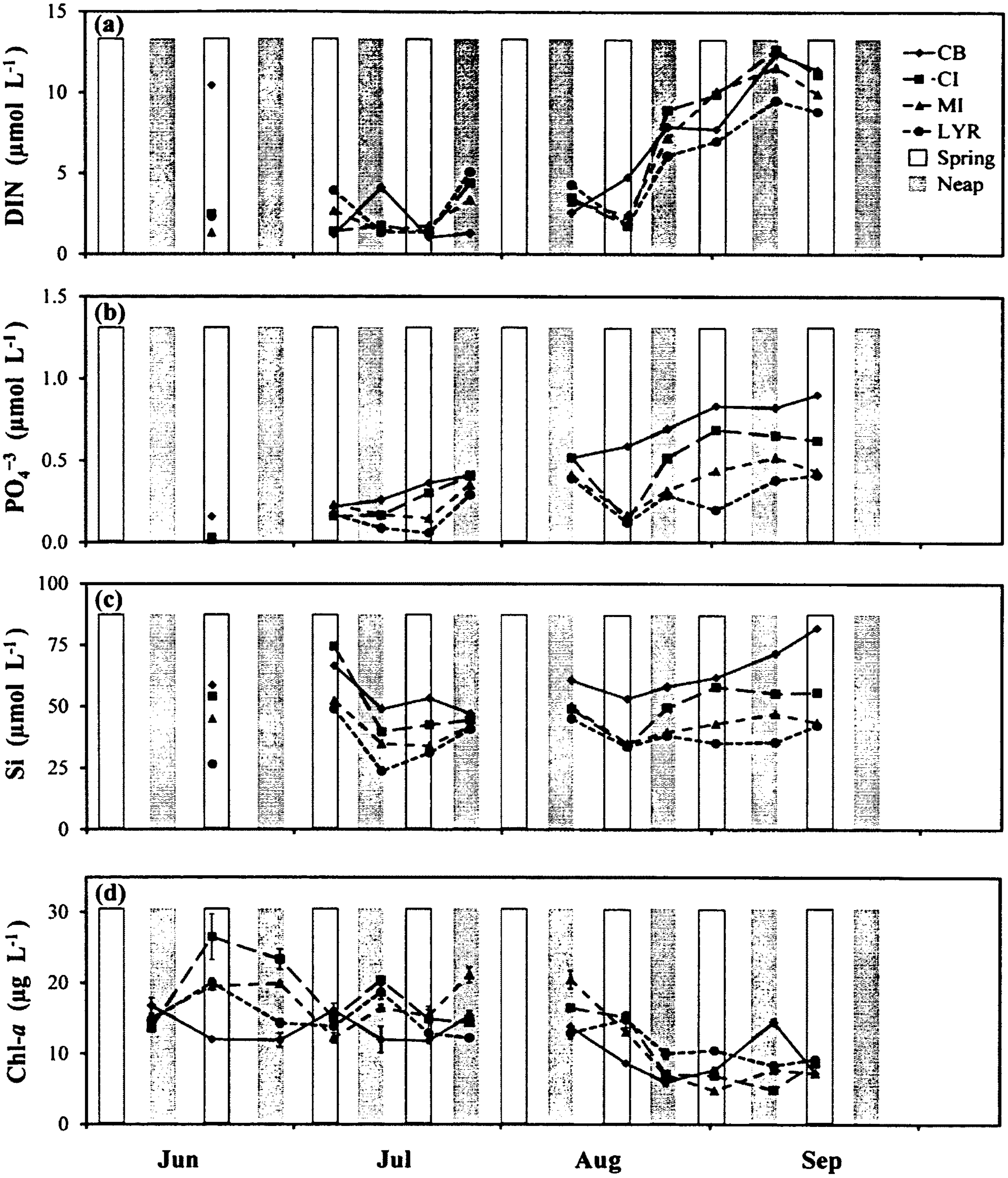

(a)
DIN (µmol L^{-1})
15
10
5
0
CB
CI
MI
LYR
Spring
Neap
(b)
PO$_4^{-3}$ (µmol L^{-1})
1.5
1.0
0.5
0.0
(c)
Si (µmol L^{-1})
100
75
50
25
0
(d)
Chl-a (µg L^{-1})
30
20
10
0
Jun
Jul
Aug
Sep

Figure 1-5. Time-series of (a) water column and (b) sediment maximum gross photosynthetic rate (in the absence of photoinhibition) measured during light box metabolic incubations following the spring-neap surveys. Hourly biomass-specific values were multiplied by chlorophyll-*a* biomass and scaled to daily rates to 24 hours of continuous irradiance. Lower panels show mean respiration rates for (c) surface (0.5m) and (d) bottom water, and (e) shallow and (f) deep channel sediments. Hourly biomass-specific were multiplied by chlorophyll-*a* biomass and scaled to daily rates. Error bars on all panels represent standard error. Open symbols correspond to dates when less than three replicates were available or error estimation was not possible due to lack of required data. Mean rates are offset in time to limit overlap of means and error bars.

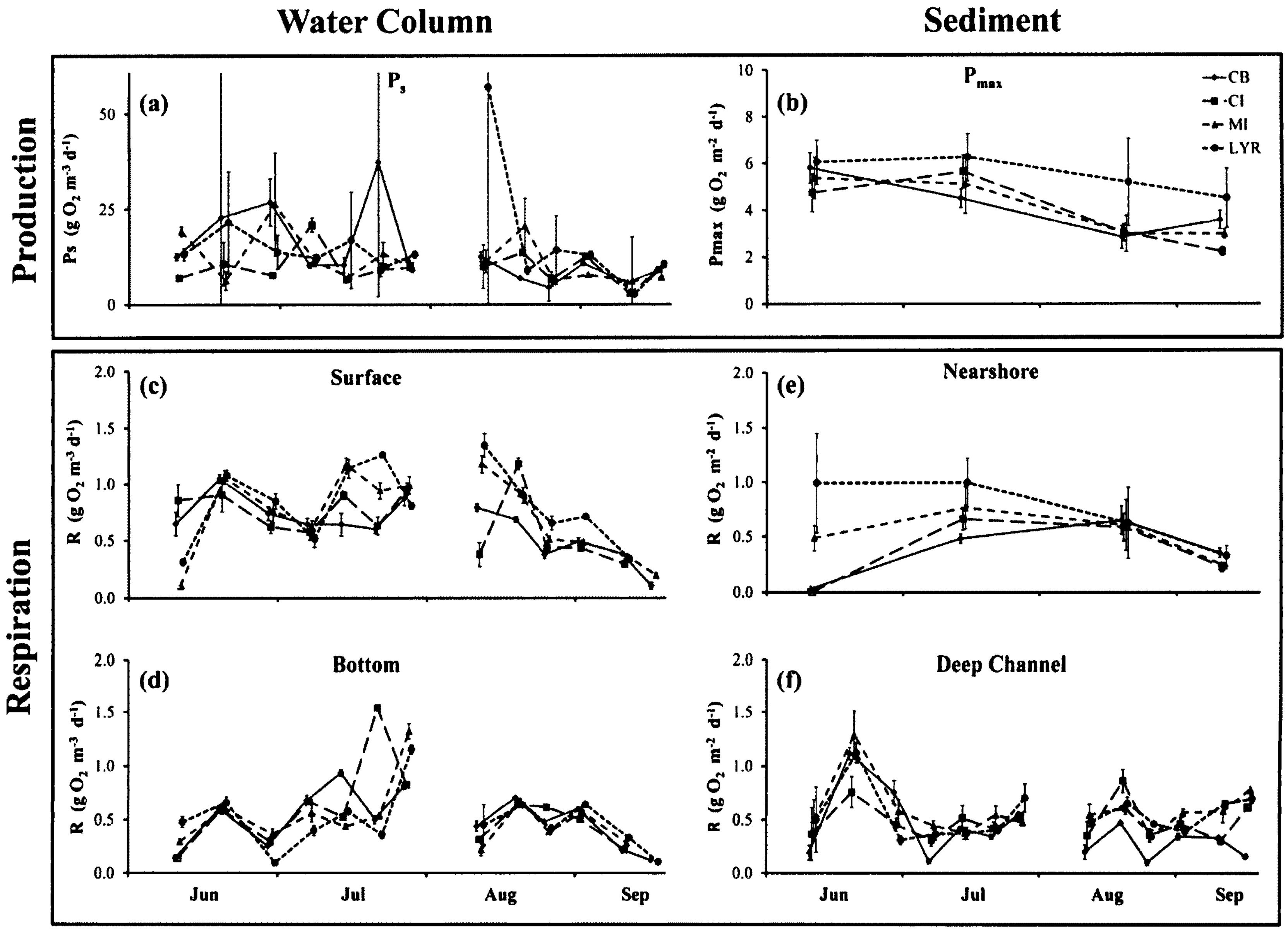
Water Column
Sediment
Production
Respiration
(a)
Ps
Ps (g O$_2$ m^{-3} d^{-1})
0
25
50
(b)
P$_{max}$
Pmax (g O$_2$ m^{-2} d^{-1})
0
2
4
6
8
10
CB
CI
MI
LYR
(c)
Surface
R (g O$_2$ m^{-3} d^{-1})
0.0
0.5
1.0
1.5
2.0
(e)
Nearshore
R (g O$_2$ m^{-2} d^{-1})
(d)
Bottom
R (g O$_2$ m^{-3} d^{-1})
(f)
Deep Channel
R (g O$_2$ m^{-2} d^{-1})
Jun
Jul
Aug
Sep
Jun
Jul
Aug
Sep

Figure 1-6. Mean (a) water column and (b) sediment gross primary production calculated from 1000 Monte Carlo simulations where chlorophyll-*a*, k_D, and P-I parameters were randomly selected from their normal distributions. Error bars represent the standard deviation of all 1000 simulations. Mean rates are offset in time to limit overlap of means and error bars.

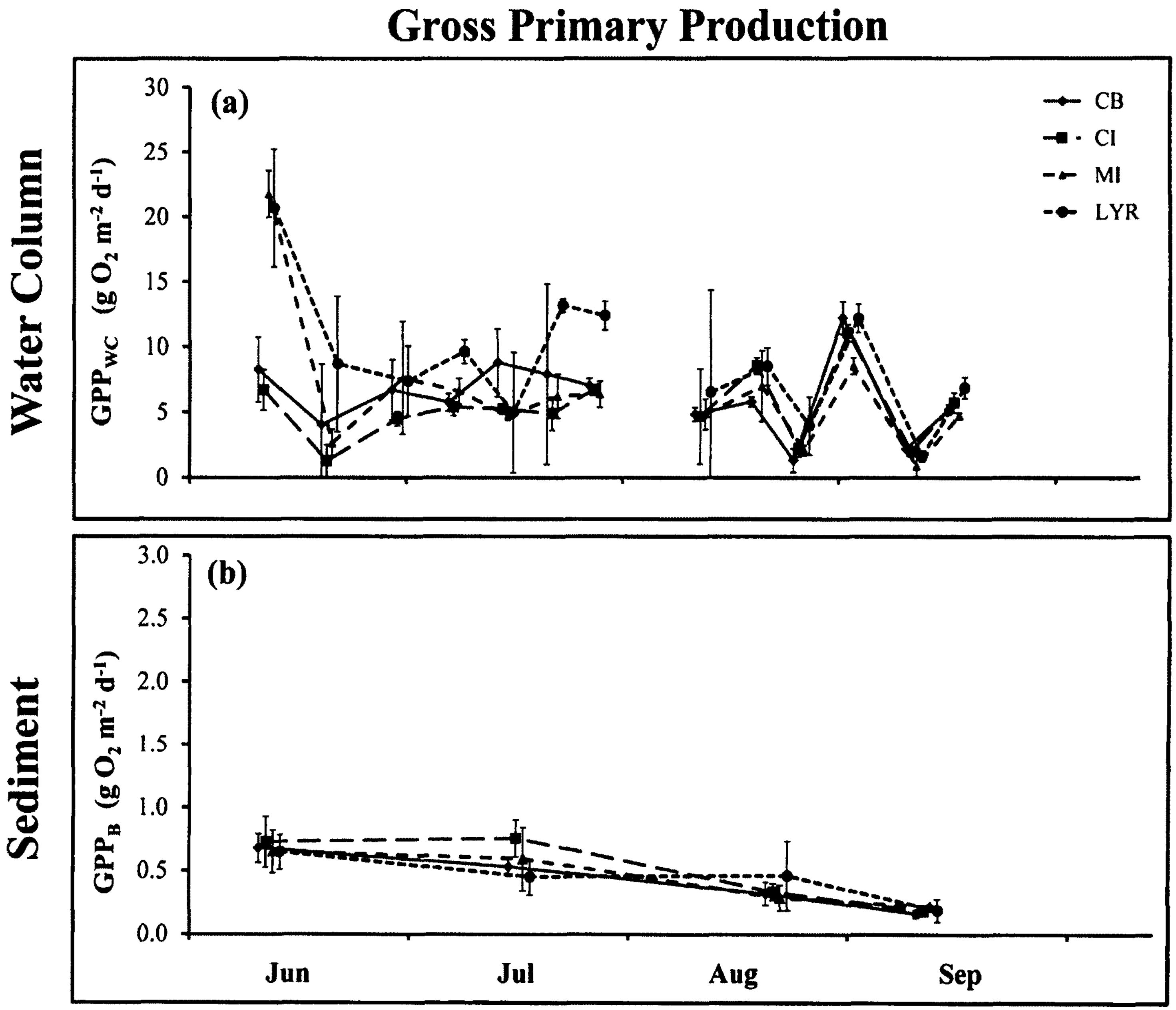
Gross Primary Production
Water Column
(a)
GPP$_{WC}$ (g O$_2$ m^{-2} d^{-1})
30
25
20
15
10
5
0
CB
CI
MI
LYR
Sediment
(b)
GPP$_B$ (g O$_2$ m^{-2} d^{-1})
3.0
2.5
2.0
1.5
1.0
0.5
0.0
Jun
Jul
Aug
Sep

Figure 1-7. Computed and observed dissolved oxygen trajectories during spring to post-neap tide transitions. Points represent sub-pycnocline, volume-weighted concentrations in the mesohaline (grey circles) and polyhaline (black squares) regions of the YRE from ACROBAT^{TM} surveys. Dashed grey (solid black) lines represent the expected dissolved oxygen trajectories based on measured rates of bottom water column and deep channel sediment respiration for the mesohaline (polyhaline) regions of the estuary.

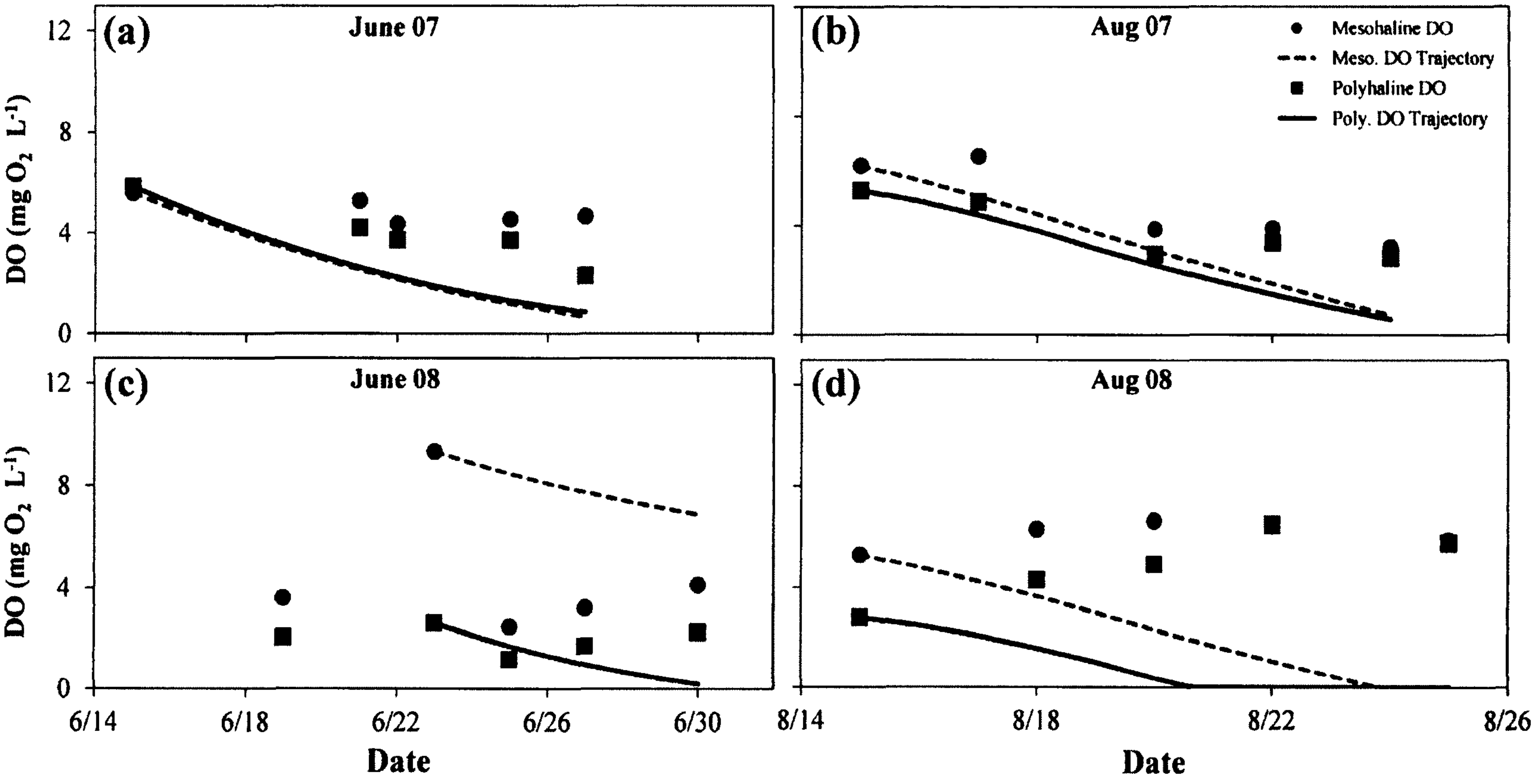
(a)
June 07
(b)
Aug 07
(c)
June 08
(d)
Aug 08
● Mesohaline DO
- - - Meso. DO Trajectory
■ Polyhaline DO
— Poly. DO Trajectory
DO (mg O_2 L^{-1})
0
4
8
12
6/14
6/18
6/22
6/26
6/30
8/14
8/18
8/22
8/26
Date

Figure 1-8. Interpolated daily (a) water column and (b) sediment gross primary production, and (c) water column and (d) sediment respiration for each sampling region. Values are scaled to each region using hourly PAR and interpolated k_D, chlorophyll-*a* in 0.5 m depth bins, and P-I parameters.

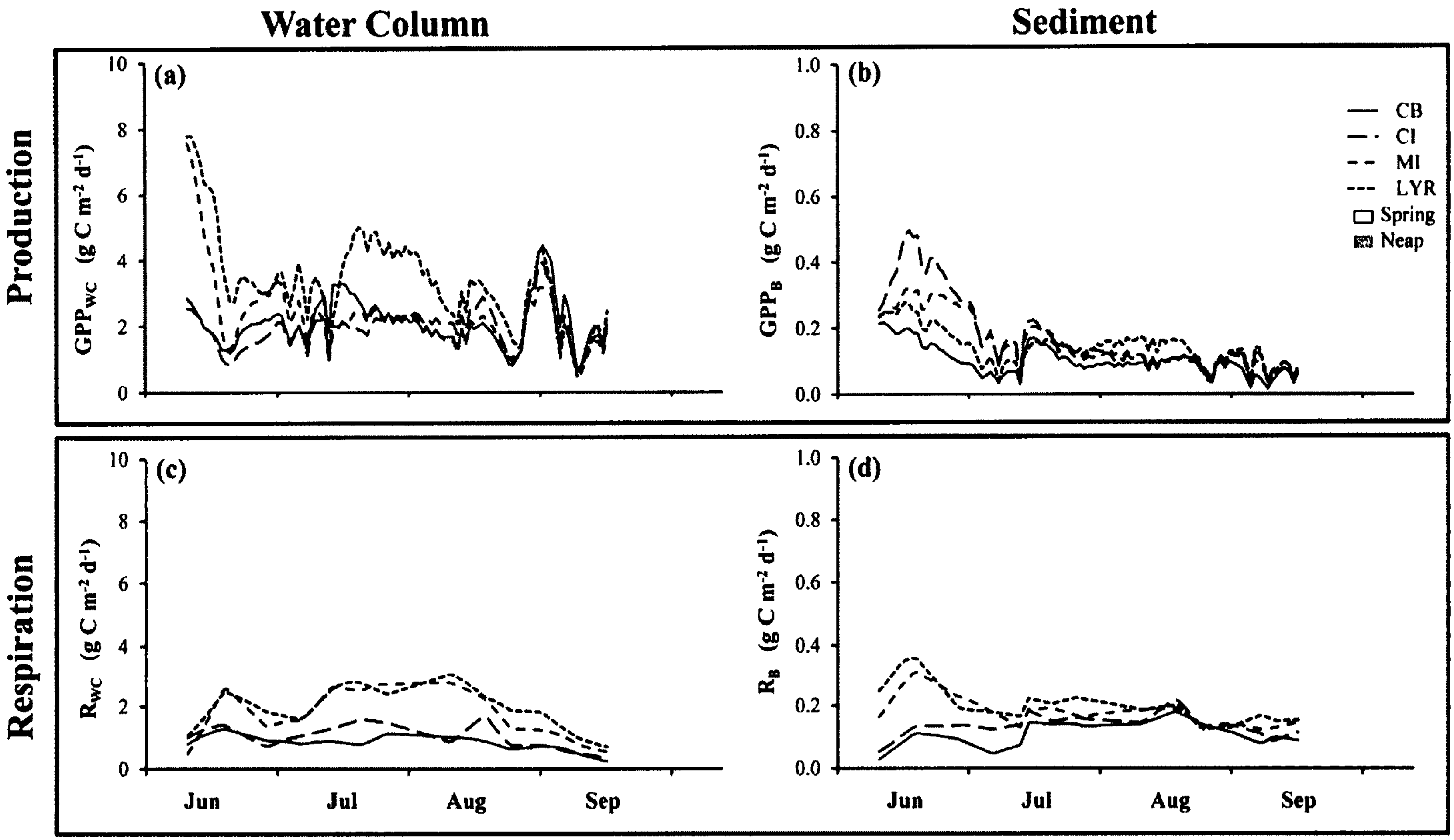
Water Column
Sediment
Production
Respiration
(a)
(b)
(c)
(d)
GPP$_{WC}$ (g C m^{-2} d^{-1})
GPP$_B$ (g C m^{-2} d^{-1})
R$_{WC}$ (g C m^{-2} d^{-1})
R$_B$ (g C m^{-2} d^{-1})
0
2
4
6
8
10
0.0
0.2
0.4
0.6
0.8
1.0
CB
CI
MI
LYR
☐ Spring
▨ Neap
Jun
Jul
Aug
Sep

Figure 1-9. Estimated total organic carbon budget for the York River estuary over the sampling season (June – September 2008) including physical inputs and outputs and biological production and respiration. All values are x 10^9 g C.

York River Estuary

Total Organic Carbon

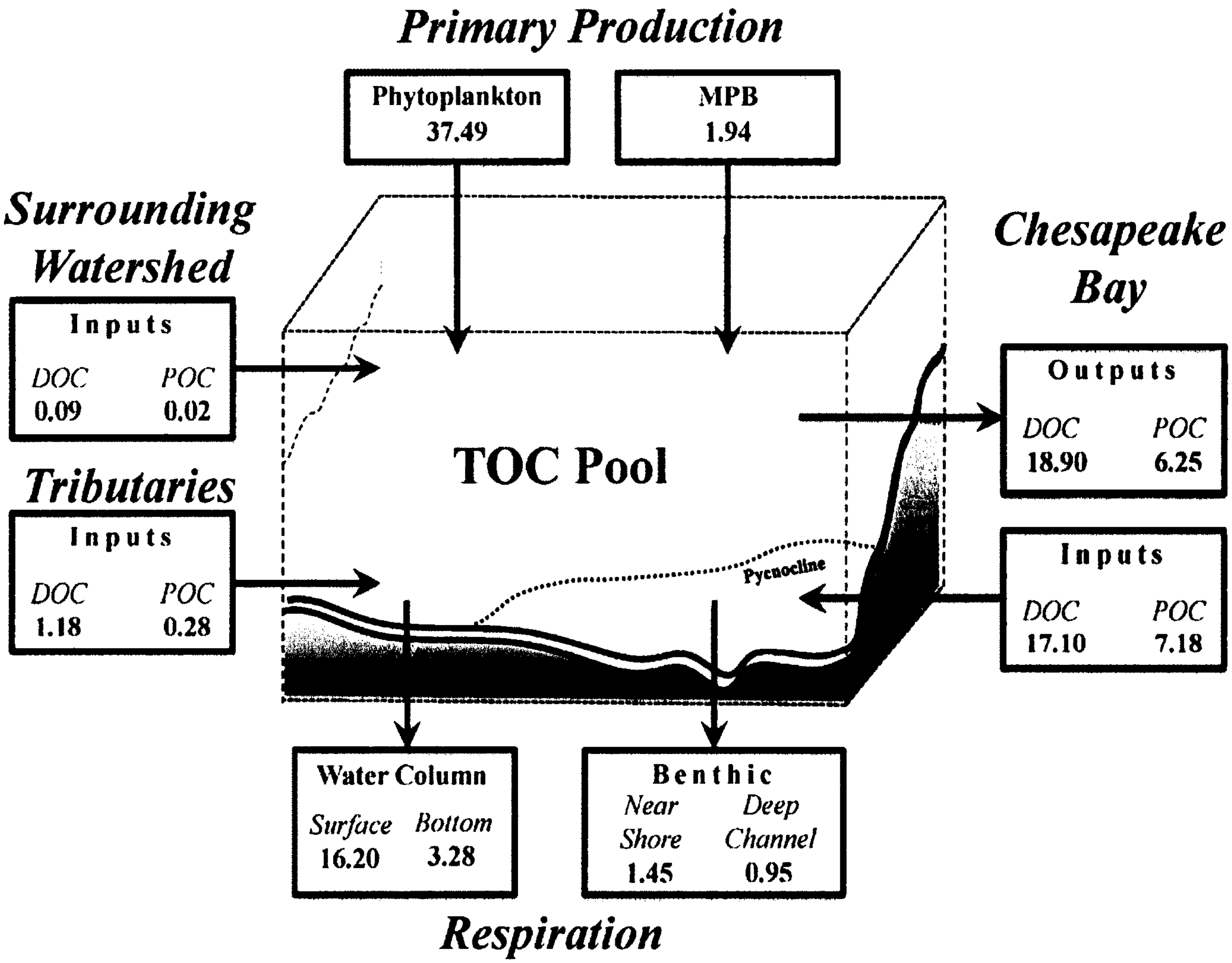

Primary Production

Phytoplankton
37.49

MPB
1.94

Surrounding Watershed

Inputs

DOC	*POC*
0.09	0.02

Tributaries

Inputs

DOC	*POC*
1.18	0.28

TOC Pool

Pycnocline

Chesapeake Bay

Outputs

DOC	*POC*
18.90	6.25

Inputs

DOC	*POC*
17.10	7.18

Water Column

Surface	*Bottom*
16.20	3.28

Benthic

Near Shore	*Deep Channel*
1.45	0.95

Respiration

CHAPTER 1 - TABLES

Table 1-1. Monthly and seasonal mean rates of integrated gross primary production (GPP), respiration (R), and net ecosystem metabolism (NEM, = GPP_{total} - R_{total}) for the entire York River estuary. Total GPP and R are the sum of water column and benthic rates. Values may not sum due to rounding. Seasonal totals are integrated across daily interpolated rates and are not an average of the monthly values.

York River Estuary Metabolic Rates

($\mathrm{g\ C\ m^{2}\ d^{-1}}$)

	June	July	Aug.	Sept.	**Seasonal Mean**
$\mathbf{GPP_{total}}$	**2.97**	**2.31**	**1.87**	**1.73**	**2.22**
$\mathrm{GPP_{WC}}$	**2.78**	**2.21**	**1.78**	**1.67**	2.11
$\mathrm{GPP_{B}}$	**0.20**	**0.10**	**0.09**	**0.05**	0.11
$\mathbf{R_{total}}$	**1.25**	**1.49**	**1.51**	**0.66**	**1.23**
$\mathrm{R_{WC}}$	**1.12**	**1.35**	**1.35**	**0.55**	1.09
$\mathrm{R_{B}}$	**0.13**	**0.14**	**0.16**	**0.11**	0.14
NEM	**1.72**	**0.82**	**0.36**	**1.07**	**0.99**

Table 1-2. Monthly and seasonal mean net ecosystem metabolism (NEM, = GPP_{total} - R_{total}) for each region of the York River estuary. Seasonal totals are integrated across daily interpolated rates and are not an average of the monthly values.

Net Ecosystem Metabolism

(g C m^2 d^{-1})

Region	June	July	Aug.	Sept.	**Seasonal Mean**
UR	0.70	0.53	0.06	0.74	**0.50**
CB	1.21	1.40	0.76	1.55	**1.23**
CI	0.77	0.54	0.86	1.34	**0.88**
MI	3.37	-0.12	-0.53	0.79	**0.86**
LYR	3.74	1.22	0.30	0.96	**1.54**

CHAPTER 2

Modeling the Contribution of Multiple Organic Matter Sources to the Development of Periodic Hypoxia in a Tributary Estuary: the York River, Virginia

Samuel J. Lake[1] and Mark J. Brush
Virginia Institute of Marine Science,
College of William and Mary, Gloucester Point, VA 23062 USA

[1] Corresponding author

Email: sjlake@vims.edu

Phone Number: (804) 684-7918

Fax: (804) 684-7293

Keywords: York River Estuary, Ecosystem Model, Hypoxia, Organic Matter, Primary Production, Respiration

ABSTRACT

The seasonal formation of periodic hypoxia within tributary estuarine ecosystems is directly influenced by multiple organic matter sources, both autochthonous and allochthonous, that are subsequently respired under warm summer temperatures. These dynamic systems are subject to allochthonous inputs from near-field sources in the surrounding watershed, as well as far-field sources that contribute nutrients, labile organic matter, and hypoxic water from adjacent coastal marine systems via estuarine circulation. This study utilized an intermediate complexity eutrophication model to quantify the importance of individual organic matter sources contributing to the development of low oxygen within the York River estuary (YRE), VA, USA, and assess the reductions in external loads necessary to mitigate current hypoxic conditions. Our results indicate that the lower portions of the YRE tributary rivers are most strongly influenced by organic matter loading from the upstream watershed, while the lower mesohaline region is influenced by both internal phytoplankton production and organic matter loading from the tributaries. In the high mesohaline, tributary organic matter and internal phytoplankton production play an equally important role during the spring; however, in summer and fall dissolved oxygen concentrations appear to respond most strongly to dissolved organic carbon (DOC) entering via advection from the lower Chesapeake Bay (CB). The polyhaline region, which is frequently the site of reoccurring bottom water hypoxia throughout the summer, responded primarily to advected DOC from the CB. Results indicate that different regions of the YRE may require different management strategies, and highlight the strong relationship between development of periodic hypoxia in the lower YRE and the advection of labile organic matter from the lower CB, a far field input that requires a more regional approach to management.

INTRODUCTION

Many large estuaries like the Chesapeake Bay (CB) have relatively shallow tributary estuaries draining into them; examples in the CB include the Patuxent, Potomac, Rappahannock, York, and James Rivers. These tributary estuaries are strongly influenced by multiple sources of organic matter, both autochthonous and allochthonous, which results in a complex cycling of organic material throughout these highly productive ecosystems. These drowned river valley systems support autochthonous production by water column phytoplankton and also a highly productive community of microphytobenthos (MPB) along the broad, shallow photic shoals that line these systems (Rizzo and Wetzel 1985). Allochthonous sources of organic carbon include inputs from the surrounding watershed of both labile and refractory material derived from terrestrial, freshwater, and anthropogenic sources, as well as material advected across the estuarine mouth (McCallister et al. 2004; Countway et al. 2007). In addition to the multitude of organic matter sources, these systems are frequently subject to high rates of anthropogenic nutrient enrichment, which makes them susceptible to the process of eutrophication (Nixon 1995, 2009) and many associated water quality concerns including the development of bottom water hypoxia (< 2.0 mg O_2 L^{-1}) (Rabalais 2002; Kemp et al. 2005; Diaz and Rosenberg 2008). Several recent studies have also demonstrated the importance of estuarine circulation in advecting nutrients and sometimes hypoxic water from the adjacent systems into these sub-estuaries (de Jonge 1997; Jordan et al. 1991; Brush 2004; Boynton et al. 2008; Testa et al. 2008).

The interaction of all of these factors makes it increasingly difficult to study these dynamic systems using more traditional sampling and experimental techniques. Long-term monitoring studies are limited by temporal and spatial variability, a frequent lack of associated data, changes in sampling methods and analysis, and other compounding factors (Nixon and Buckley 2002).

While numerous comparative and long-term whole-system experiments have been carried out in lakes (Oglesby 1977; Hanson and Leggett 1982), few studies have been attempted in coastal marine systems (see Nixon and Buckley 2002). While the unintended anthropogenic enrichment of coastal marine systems continues today, it is unlikely that large scale ecosystem enrichment studies will be attempted in coastal waters in the foreseeable future. Large mesocosm studies have also been used to simulate estuarine ecosystems, however these are inevitably subject to their own short comings including scaling problems, "bottle effects", sample heterogeneity, and larger-scale physical processes (Nixon 2001).

Ecosystem simulation models are ideally suited to study the ecological function of shallow tributary estuaries and provide insight into the effects of eutrophication. While they are also limited by current knowledge, assumptions, and data availability they represent a valuable hypothesis testing tool. The use of intermediate-complexity models that incorporate both traditional mechanistic approaches and empirical functions that apply across a wide variety of temperate estuaries maximizes the use of available data while limiting excessive parameterization and error propagation from loosely constrained variables (Reckhow 1999; Pace 2001; Brush et al. 2002). Reduced complexity models have been widely used as synthesis tools, to address complex sets of hypotheses related to ecosystem function, and to inform coastal management (Stow et al. 2003; Brush 2004; Scavia et al. 2004, 2006; Swaney et al. 2008; Brush and Nixon *in review*).

The York River estuary (YRE) (Fig. 1) is an ideal system to implement this modeling approach to gain insight into both the biological and chemical cycles that contribute to hypoxia, and potential responses to various management scenarios. The YRE has a long monitoring history and is influenced by multiple sources of labile organic matter, advection of high nutrient /

low dissolved oxygen (DO) water from the mainstem Chesapeake, and variable physical mixing processes, both tidally and wind driven (Haas 1977; Kuo and Nielson 1987; Sharples et al. 1994; Lake et al. *in review*). These characteristics make the YRE a model system that can be used to make inferences into how other shallow tributary estuaries function. While this system has been historically well studied, we still lack an understanding of how the full suite of biological, chemical and physical processes interact within this system (Countway et al. 2007; Lake et al. *in review*), which can be directly addressed with this approach.

Recent work focused on establishing a seasonal carbon budget for the YRE indicated that internal water column phytoplankton production was the dominant source of organic carbon to the estuary, and highlighted the importance of the net exchange of organic matter between the lower Chesapeake Bay and the YRE (Lake et al. *in review*). This analysis suggested that reducing internal phytoplankton production by implementing nutrient reduction strategies might mitigate some of the current water quality concerns, but a more complete assessment is required to determine the magnitude of reductions necessary to cause improvements. It is likely that different regions of the YRE will respond differently to reductions in nutrient and organic matter loading, which may require multiple management strategies that focus on various sources entering this estuary, rather than a single approach.

The goal of the current study is to develop a more complete understanding of how various organic matter and nutrient sources contribute to the development of hypoxia within different regions of the YRE, and determine what management scenarios might be appropriate to mitigate the negative effects of hypoxia. To do this we incorporated data collected from *in-situ* measurements with long-term water quality and meteorological monitoring and metabolic incubations into an intermediate complexity eutrophication model. Following calibration, a series of scenarios were run to isolate the individual importance of each source to bottom water hypoxia. Finally, we evaluated the effectiveness of a range of nutrient and organic matter load reductions to determine what actions may be necessary to meet established water quality criteria (e.g., US EPA 2003) in different parts of the system.

METHODS

Site Description

The YRE is formed by the confluence of the Mattaponi and Pamunkey Rivers near West Point, Virginia, approximately 55 km from where the river enters the mainstem of the Chesapeake Bay on its western edge (Shen and Haas 2004) (Fig. 1). The overall land use surrounding the YRE is predominantly rural with 62% forested and 16% agricultural land (Dauer et al. 2005). The estuary is flanked by shallow photic shoals (< 2m), which comprise 40% of the estuary by area (Rizzo and Wetzel 1985). The YRE oscillates between stratified and well-mixed conditions due to the physical mixing of the spring-neap tidal cycle, which has been well documented in past studies (Haas 1977; Hayward et al. 1982; Kuo and Neilson 1987; Diaz et al. 1992). This physical forcing creates the potential for continued formation and disruption of bottom water hypoxia from late May to early September within the lower half of the estuary (Kuo and Neilson 1987; Kuo et al. 1993; Lake et al. *in review*).

For this study the YRE was sub-divided into eight regions along its axis (Fig. 1). These regions were designated based on long term water quality monitoring by the EPA Chesapeake Bay Program (CBP) and the presence of hypoxia during monitoring surveys. The two upstream boxes (1 and 2) are located within the lower Mattaponi and Pamunkey Rivers, respectively. Boxes 3 and 4 are located in the low mesohaline and Boxes 5 and 6 in the high mesohaline portions of the estuary, which are typically characterized as having little to no signs of hypoxia. The two downstream polyhaline boxes (7 and 8) have been observed to develop periodic hypoxia during past monitoring surveys and in previous studies (Kuo and Neilson 1987; Kuo et al. 1993; Lake et al. *in review*).

Eutrophication Model

We applied a previously developed model that combines the benefits of both empirical and mechanistic modeling approaches into an intermediate-complexity, shallow marine ecosystem model (Brush 2002, 2004; Brush et al. 2002; Brush and Brawley 2009; Brush and Nixon 2010, *in review*). The model includes only those state variables and rate processes that are of primary importance to the process of estuarine eutrophication, and integrates robust empirical relationships that have been shown to apply across multiple temperate estuaries to predict key rate processes. State variables include pools of carbon (C), nitrogen (N), and phosphorous (P) in phytoplankton (PHYTO) and MPB, water column pools of organic carbon (C_{WC}) and its associated N and P, dissolved inorganic nitrogen (DIN) and phosphorous (DIP), DO (O_2), and a pool of recently deposited, labile organic carbon in the sediments (C_{SED}) and its associated N and P (Fig. 2). In the following paragraphs we outline modifications that have been made to adapt the model to the YRE, since details on the other formulations have been published elsewhere (see above).

The original model remineralizes N and P and denitrifies N from the sediment organic pool using temperature-dependent functions constrained during calibration. Given the current focus on hypoxia, the formulations were modified to account for the effects of low DO on coupled nitrification-denitrification and resulting release of NH_4^+. A denitrification efficiency function was developed using data presented in Kemp et al. (2005) to reduce the rate of denitrification under declining DO concentrations and increase the remineralization of NH_4^+:

$$\text{DENIT EFF} = 0.4 + (0.0518 * \text{DO})$$

where the denitrification efficiency (DENIT EFF) is a dimensionless term dependent on DO (mg O_2 L^{-1}) concentrations overlying water column. A similar function was developed to reflect the enhanced release of phosphate from sediments under anoxic conditions using data from Boynton and Bailey (2008) measured in the mesohaline and polyhaline Chesapeake Bay and the Patuxent, Potomac, and York Rivers:

$$\text{DIP FLUX} = 0.0286 * \exp(-0.6271 * \text{DO})$$

where the low oxygen sediment DIP flux (DIP FLUX) is a dimensionless term dependent on DO (mg O_2 L^{-1}) concentrations in the overlying water column.

Given the extensive photic shoals and active MPB community in the YRE, we added a newly developed MPB sub-model (Brush et al. *in prep*), developed using metabolic rates measured in the YRE, the New River estuary, NC and lagoons of the Delmarva Peninsula. MPB production and respiration were simulated at 0.5 meter depth intervals within each box, as a function of irradiance at depth and temperature. Nutrient limitation was not included since MPB have the ability to obtain nutrients from overlying water as well as pore water within the sediments. For this study we have excluded production from seagrass and macroalgae, due to their limited spatial distribution within the estuary under current conditions (Moore et al. 2000; Moore et al. 2001).

The ecosystem model is coupled to an Officer (1980) two-layer box model, which computes both advective (gravitational circulation) and non-advective (tidal) volumetric exchanges among coarse spatial elements as a function of forced salinity and freshwater inputs. Surface and bottom boxes were delineated based on pycnocline depth as determined from CBP monitoring data and Acrobat™ monitoring surveys; these depths were set at 4 m (Boxes 1 and 2), 5 m (Boxes 3 - 6), and 9 m (Boxes 7 and 8). Although box models necessarily lose spatial resolution compared to higher resolution 3-D hydrodynamic circulation models, they nonetheless reproduce typical down-estuary and surface to bottom gradients, operate at the typical scale of available monitoring data (e.g., Fig. 1), are driven by exchanges that are constrained by observations, and enable fast run times (minutes on personal computers), which makes possible the multiple runs required for adequate calibration, sensitivity analysis, and forecasting scenarios. Recent work has confirmed the utility of boxed approaches (Ménesguen et al. 2007; Testa and Kemp 2008; Kremer et al. 2010).

Forcing Function Data

Photosynthetically active radiation (PAR), precipitation, air temperature, relative humidity, and wind speed at the Chesapeake Bay National Estuarine Research Reserve in Virginia (CBNERRVA) meteorological station at Taskinas Creek (January 2007 - December 2010) were downloaded (www.nerrs.noaa.gov) and used to calculate total daily PAR and average daily temperature, humidity and wind speed. Daily river flow from the Mattaponi and Pamunkey Rivers over the same period were downloaded from the Virginia USGS website (va.water.usgs.gov) and expressed as yields per area of watershed. These yields were scaled up to the entire area of the Mattaponi and Pamunkey watersheds including the area below the Fall Line, and combined with the areas of the smaller, ungauged watersheds surrounding the YRE to estimate freshwater inputs to those boxes (Fig. 1). Concentrations of DIN and DIP measured at the USGS gauging stations were linearly interpolated between sampling dates and combined with scaled up flows to each box to compute daily material loads..

Bi-weekly to monthly (depending on location and season) monitoring data for water temperature, salinity, turbidity (NTU), water column chlorophyll-*a* (WC Chl-*a*), and particulate (POC) and dissolved organic carbon (DOC) were downloaded from the CBP website (www.chesapeakebay.net). Surface and bottom temperature, salinity, and turbidity were linearly interpolated between sampling dates and forced into each box of the model. Concentrations of POC and DOC at CBP stations TF 4.2 and TF 4.4 in the tidal fresh portions of the Mattaponi and Pamunkey Rivers were linearly interpolated between sampling dates and combined with scaled up watershed flows to estimate daily loads to each box. Surface and bottom concentrations of WC Chl-*a*, POC, DOC, DIN, and DIP in Chesapeake Bay (CBP station WE 4.2) were similarly interpolated and combined with box model estimates of advection into the YRE to estimate inputs across the mouth. Advected CB chlorophyll-*a* was converted to phytoplankton biomass utilizing a carbon to chlorophyll-*a* ratio of 90.4 g g^{-1}, which was calculated based on surface POC and WC Chl-*a* concentrations measured at CBP sites LE 4.3 and WE 4.2 from 2006 to 2010. Advected CB POC was reduced by this amount to avoid double counting phytoplankton carbon. Bottom water DOC concentrations were unavailable at station WE 4.2; values were estimated by multiplying the surface water DOC to POC ratio by the bottom water POC concentration for each sampling date.

A series of 480 light attenuation (k_D) measurements collected by the CBNERRVA (between January 2006 to November 2011) and an additional 62 measurements made by the CBP were used to develop multiple regression models for light attenuation in three regions within the YRE (Boxes 1-4, 5-6, and 7-8). Regressions were developed using extracted WC Chl-*a*, turbidity (NTU), and salinity as a proxy for chromophoric dissolved organic matter (CDOM) (Xu et al. 2005).

Bathymetric soundings were downloaded from the NOAA National Geophysical Data Center (www.ngdc.noaa.gov) and interpolated using a kriging function in ESRI® ArcMAP 9.3, to a 5m x 5m grid with a resolution of 10 cm in the vertical. The surface area and volume within each box (Fig. 1) was binned in 0.5 m depth intervals from mean sea level (MSL) to the bottom.

Water Quality Calibration Data

The model was calibrated to CBP monitoring data over a four year period (2007-2010) for WC Chl-*a*, DIN, DIP, and DO for boxes containing stations (Fig. 1), along with data from three other sources. A series of 13 water quality surveys (WQS) were conducted from June to September 2008 by Lake et al. (*in review*). Sampling dates were selected with a three day lag behind the apex of spring and neap tides in order to sample the river at the peak of mixing and stratification, respectively, as indicated by previous studies (Haas 1977; Hass et al. 1981; Hayward et al. 1986) and past surveys. Parameters measured include temperature, salinity, WC Chl-*a*, DO, k_D, and rates of water column primary production, pelagic respiration (surface and deep water), and deep channel sediment respiration using oxygen incubations. This study also measured sediment primary production and respiration at shoal sites four times (approximately monthly) at a depth of one meter below mean lower water (MLW), taking into account the daily tidal range.

As part of a larger water quality monitoring program, the YRE was surveyed during the summers of 2007 and 2008 using an Acrobat^{TM} tow body (Sea Sciences, Inc.) equipped with a CTD (Falmouth Scientific Seabird), SCUFA fluorometer/turbidometer (Turner Designs), and a rapid response (300 ms) DO sensor (Analysenmeßtechnik GmbH, Rostock, Germany). Acrobat^{TM} sensors collected spatially-referenced data four times a second with a horizontal resolution of 6-8 m and a vertical resolution of 5-10 cm, for a total of 40,000-50,000 data scans per survey. Additional sampling and calibration details can be found in Lake et al. (*in review*). Data from five Acrobat^{TM} monitoring surveys from spring to post neap tidal stage (representing the transition from minimum stratification and highest DO to maximum stratification and lowest DO) during June and August of 2007 and 2008 were used to calculate the volume-weighted (above and below the pycnocline) DO concentrations within high mesohaline and polyhaline segments of the estuary using the NOAA Chesapeake Bay and Tidal Water Interpolator (http://archive.chesapeakebay.net/cims/interpolator.pdf). Pycnocline depths were set at 5 m and 9 m in the high mesohaline and polyhaline regions, respectively, based on Acrobat^{TM} results.

MPB chlorophyll-*a* (MPB Chl-*a*) biomass was measured bi-weekly from May 2008 to December 2008, and monthly from January 2009 to December 2010 at 7 near shore sites along the middle and lower portions of the estuary (Boxes 4-8). At each site three replicate samples were collected (0-0.3 cm depth fraction), using a pole corer, at a depth of one meter below mean lower water (MLW). During the spring, summer, and fall of 2009 additional samples were conducted at 30 randomly selected sites, along with depth profile samples at 6 sites collected in triplicate at 0.25, 0.5, 1, 1.5, and 2 meters below MLW. All samples were processed as outlined in Lake et al. (*in review*) and used to calibrate the microphytobenthos (MPB) submodel.

Model Calibration and Skill Assessment

The YRE eutrophication model was calibrated to k_D, WC Chl-*a*, MPB Chl-*a*, and surface and bottom water concentrations of O_2 (DO_S and DO_B), DIN (DIN_S and DIN_B), and DIP (DIP_S and DIP_B) using data sources described above. Phytoplankton net primary production (PHYTO NPP_S), MPB gross primary production (MPB GPP_S), and water column and sediment respiration rates in the surface and bottom layers (WC R_S, WC R_B, SED R_S, and SED R_B) were calibrated to rates measured by Lake et al. (*in review*). Denitrification rates were calibrated to measurements made in the mainstem Chesapeake Bay and Bay tributaries (Jenkins and Kemp 1984; Kemp et al. 1990; Boynton et al 1995; Kana et al. 1998; Kana et al 2006; Boynton et al 2008; Cornwell and Owens 2011).

A detailed skill assessment was conducted on all model parameters where measured rates and concentrations were available to quantify the degree to which the model predicted the observations. Absolute (ABS Error), percent (% Error), and root mean square error (RMS Error) were calculated for each term. While no single metric is suitable for assessing the uncertainty related to all parameters, this combination of multiple quantitative measurements helps to define specific areas of uncertainty with the model.

Model Simulations

The calibrated model simulation under current conditions (CC) (2007 - 2010) was used as a baseline comparison for all subsequent simulations. In order to identify the individual contribution of each organic matter source to the development of bottom water hypoxia, a series of model simulations were conducted where each internal and external source was removed from the model run. For example, internal phytoplankton biomass and production was set (and held) at zero throughout the four year simulation. Similarly, MPB, tributary nutrients and organic carbon, surrounding watershed nutrients and organic carbon, and CB nutrients, phytoplankton biomass (utilizing WC Chl-*a* as a proxy for biomass), DOC, and POC were sequentially set and held at zero. A final model simulation was conducted without any organic matter sources to simulate conditions when controlled only by physical circulation of water and air-sea gas exchange.

Once the individual contribution of each organic matter source was isolated, model runs were conducted to determine how future changes in nutrient and organic matter loading into the YRE would affect the development of hypoxia. These simulations focused on increasing and decreasing tributary, watershed, and CB sources from 0.5 to 2 times current conditions to determine the potential for various management scenarios to mitigate hypoxia within different regions of the system. Rates and concentrations were averaged across the four year simulations to account for interannual variability.

RESULTS

Model Calibration and Skill Assessment

Model predictions of WC Chl-*a* followed the CBP observations within all boxes throughout all four years (Fig. 3 a,b). Percent error between observations and predictions was relatively low for the system as a whole (11.2%), and lower for Boxes 5 – 8 (5.4%) where hypoxia occurs (Table 1). Dissolved oxygen concentrations in both the surface and bottom water also followed the observed concentrations from both the CBP and Acrobat^{TM} surveys (Fig. 3 c-f). Absolute error associated with bottom water DO in Boxes 5 – 8 was less than a 0.5 mg L^{-1} (0.33 mg L^{-1}, Table 1). Modeled nutrient concentrations (DIN and DIP) were within the range of measured concentrations and followed the overall seasonal cycles (Fig. 3 g-j). While the percent error for DIN and DIP were relatively large compared to other terms due to the overall low concentrations, the absolute error was less than or equal to 0.1 and 0.01 for DIN and DIP, respectively (Table 1). Modeled MPB Chl-*a* (0.5 - 1 m) was within the range and near the mean seasonal values of the observed biomass from 2008 to 2010 in Boxes 5 – 8 (Fig. 3 k,l). Observed MPB Chl-*a* concentrations displayed high variability throughout the sampling period, which was not fully captured by the model as it is likely driven by fine-scale sediment heterogeneity not captured by this or other traditional models; thus model error was higher at 21.7% (Table 1).

Model rates of PHYTO NPP_S varied seasonally with the highest rates in spring (March – May mean of 0.76 ± 0.57 (s.d.) g C m^{-2} d^{-1}) and summer (June – Aug. mean of 0.86 ± 0.62 (s.d.) g C m^{-2} d^{-1}), with a gradual decrease through the fall (Sept. – Nov. mean of 0.38 ± 0.24 (s.d.) g C m^{-2} d^{-1}) and into winter (Dec. – Jan. mean of 0.19 ± 0.13 (s.d.) g C m^{-2} d^{-1}) (Fig. 4 a,b). These values were generally within the range of rates measured during summer of 2008, but slightly below some of the higher rates measured in Boxes 7 and 8. Absolute error associated with modeled PHYTO NPP in Boxes 5 – 8 was 0.23 g C m^{-2} d^{-1} (Table 1). Modeled surface water respiration was also within the range of the measured rates from 2008 for Boxes 5 and 6, and within the lower end of the range for Boxes 7 and 8 (mean rates for Boxes 5-8 were 0.31, 0.51, 0.24, and 0.11 g C m^{-2} d^{-1} during spring, summer, fall, and winter, respectively) (Fig. 4 c,d). Modeled bottom water respiration increased moving downstream from the mesohaline to the polyhaline region during the summer (0.41, 0.44, 0.51, 0.64, 0.69, and 0.62 g C m^{-2} d^{-1} in Boxes 3 – 8, respectively). The absolute errors associated with modeled rates of surface and bottom water respiration in Boxes 5 – 8 were 0.31 and 0.09 g C m^{-2} d^{-1}, respectively (Table 1). Modeled MPB GPP_S along the photic shoals was variable throughout the year with the highest rates during the summer (mean rates for Boxes 5-8 were 0.41, 0.61, 0.47, and 0.29 g C m^{-2} d^{-1} during spring, summer, fall and winter, respectively) (Fig. 4 g,h). Modeled sediment respiration in the surface layer increased in spring (mean 0.12 g C m^{-2} d^{-1}) and summer (mean 0.16 g C m^{-2} d^{-1}) and was relatively low in the fall and winter (mean 0.06 and 0.02 g C m^{-2} d^{-1}, respectively) (Fig. 4 i,j). Similarly modeled sediment respiration in the bottom layer was highest during spring and summer (mean 0.17 and 0.25 g C m^{-2} d^{-1}, respectively) and lower in the fall and winter (mean 0.09 and 0.04 g C m^{-2} d^{-1}, respectively) (Fig. 4 k,l). The absolute errors associated with benthic rates of MPB GPP_S, and surface and bottom layer respiration were 0.10, 0.09, and 0.04 g C m^{-2} d^{-1}, respectively (Table 1).

Contribution of OM sources to Hypoxia

The contribution of internal and external organic matter sources to hypoxia varied temporally and spatially throughout the YRE (Fig. 5 a-h). In the two tributary boxes (1 and 2), upstream inputs of organic matter had the greatest impact on hypoxia in May and June, with more than a 20% and 25% increase in DO concentrations in Boxes 1 and 2, respectively, when this source was removed (Fig. 5 a,b). This contribution decreased slightly in July and August as internal phytoplankton production accounted for an additional 5% increase in July and 10% increase in August in both boxes. In the low mesohaline boxes (3 and 4), the effect of removing organic matter entering from the tributaries equaled that of internal phytoplankton production during spring and summer, with a 10-30% increase in DO when each source was removed (Fig. 5 c,d). Additionally, within this region the response of removing DOC from the Chesapeake began to play an important role in improving DO concentrations, particularly from mid-summer to late-fall. In the high mesohaline (Boxes 5 and 6), the contribution of internal phytoplankton production was equal to or slightly less than the contribution from CB DOC in late spring and early summer (Fig. 5 e,f). However, the contribution of CB DOC surpassed that of phytoplankton from July to October with an average DO increase of 30% and > 50% in Boxes 5 and 6, respectively. While internal phytoplankton production and advection of POC and phytoplankton biomass from the Chesapeake contributed significantly during the spring, summer and fall (resulting in a 5-15 % increase in DO concentrations during the summer), these improvements were much lower than the percent increase obtained by removing DOC entering from the lower Chesapeake Bay (> 50% increase in DO concentrations during the summer; Fig. 5 g,h).

Contrary to these positive effects on DO associated with removing various organic matter sources, model simulations predicted that removal of MPB would result in lower DO concentrations throughout the entire YRE during summer and fall (Fig. 5 c-g). This response was greatest in the mesohaline region (in particular Boxes 3 – 7) during the summer. A similar but much smaller response was predicted when phytoplankton were removed from the model during winter and spring. In the absence of all organic matter sources, summer average DO concentrations were predicted to increase from 4.4 to 84% depending on box (Fig. 5 c).

Nutrient and Organic Matter Scenarios

Reducing nutrient loading from both the tributaries and smaller adjacent watersheds surrounding the YRE to 0.5 and 0.75 times current conditions did not lead to large predicted decreases in the average number of hypoxic or low DO days (Fig 6 a,c). Similarly, an increase of 1.5 and 2 times current nutrient concentrations from these two sources did not greatly increase the number of days predicted to be hypoxic within any region of the YRE.

When watershed nutrient reductions were combined with reductions in organic matter loads, however, the predicted number low DO days decreased in both tributary boxes (Fig 6 b,d). This response diminished further down-river with small improvements in the number of low oxygen days in Box 6 (6 and 3 days for 0.5x and 0.75x, respectively), and a slight improvement in Boxes 7 and 8 (1-3 days). An increase in both watershed nutrient and organic matter loading resulted in a predicted increase in both hypoxic and low DO days throughout the estuary with the largest response in the tributaries and mesohaline regions of the estuary (Fig. 6 b,d). A doubling of current loads resulted in an increase in the spatial extent of low oxygen within the YRE, with hypoxia developing in mesohaline Boxes 4, 5, and 6, which did not occur in the baseline model simulation. The predicted number of low DO days in Boxes 6 and 7 increased by 5-15 days under these higher loads, but only by 2-4 days in Box 8 (Fig 6 b,d).

Chesapeake Bay nutrient and phytoplankton reductions did not result in a large decrease in the number of days predicted to be hypoxic; however, these reductions did result in an improvement in the number of low DO days in Box 6 (5 and 2 days for 0.5x and 0.75x) and to a lesser extent Boxes 7 and 8 (Fig. 7 a,c). Conversely, increasing nutrients and phytoplankton entering from the lower CB resulted in a predicted increase in both hypoxic and low DO days in Boxes 6 – 8. This increase did not result in an increase in the number of hypoxic days above

Box 6, although a doubling of current loads resulted in a slight increase in the number of low oxygen days in Boxes 4 and 5.

Modeled reductions in nutrients, phytoplankton and organic matter (DOC and POC) entering from the lower CB resulted in the largest improvement in hypoxic and low oxygen days (Fig. 7 b,d). A reduction to 0.75 times current conditions to all three of these sources eliminated hypoxia within the polyhaline segment of the YRE, and reduced the number of low DO days to 1 and 9 in Boxes 7 and 8, respectively. However, increasing these inputs to 1.5 and 2 times current conditions resulted in very large increases in the number of hypoxic days as well as a predicted increase in the spatial extent of hypoxia up to Box 4.

DISCUSSION

Model Skill Assessment

The model captured the seasonal cycle of phytoplankton throughout the spring, summer and fall, and was within the correct magnitude during each season (Fig. 3 a,b). However, in some instances it did fail to capture some unusually high WC Chl-*a* concentrations in the spring (Fig. 3 a). Modeled MPB Chl-*a* concentrations, in the 0.5 to 1 meter depth segment, for Boxes 4 – 8 were all within the range of concentrations measured from 2008 to 2010 (Fig. 3 k,l). The modeled concentrations were near the seasonal mean values throughout the four year simulation; however, due to the patchiness of MPB on the sediment surface it is not surprising that the error associated with this component was larger than other state variables.

The model also captured the seasonal cycle of dissolved oxygen in the surface water, which is calculated based on temperature-salinity solubility and air-water gas exchanges, as well as internal oxygen production by primary producers and water column and sediment respiration (Fig 3 c,d). The model does particularly well in the summer in Boxes 5 – 8, although predicted winter surface DO concentrations were frequently lower than *in-situ* measurements, which may be due in part to stronger physical mixing by winter storms that acts to significantly mix the surface water over relatively short time scales. Since the model utilizes average daily wind speed and interpolated temperature and salinity between discrete sampling events, these short-term, intense storm events are not fully captured by the model. More important to the present application is that the model captured both the seasonal cycle of low dissolved oxygen in the bottom water, along with shorter-term weekly and bi-weekly oscillations in DO as would be expected with the spring-neap cycle (Fig. 3 e,f).

While the DIN concentrations simulated by the model were within the correct magnitude, there are periods of time, specifically when observed concentrations are low, when the model overestimated the concentrations within the surface water. This could be due in part to the rapid uptake of nutrients in the surface water by phytoplankton that may not be fully captured by the reduced complexity of the model formulations. The model also captured the seasonal cycle of DIP with lower concentrations in the spring and high concentrations in the fall and winter (Fig 3 i,j).

The metabolic rates calculated by the model were calibrated to our own measurements in summer of 2008; however modeled rates were also within the range or slightly below those reported in previous studies conducted in the lower polyhaline Chesapeake Bay. The mean seasonal rates of water column NPP in this study were 0.76, 0.86, and 0.38 g C m^{-2} d^{-1} (s.d. 0.57, 0.62, and 0.24, respectively), which were near or below the seasonal rates reported by Harding et al. (2002) for net ^{14}C primary production (0.70, 1.24, and 0.89 g C m^{-2} d^{-1} for the spring, summer and fall) in the lower bay. These mean seasonal rates fell below the average seasonal values calculated from Smith and Kemp's (1995) estimates of daytime net community production during the spring (March to May = 2.17 g C m^{-2} d^{-1}) and summer (June to August = 3.23 g C m^{-2} d^{-1}) (using a PQ of 1). The range of modeled daily rates did however, overlap the spring (0.03 - 3.64 g C m^{-2} d^{-1}) and summer (0.002 - 3.34 g C m^{-2} d^{-1}) ranges reported by Smith and Kemp (1995). Additionally, the average fall rates were close to the average of the rates reported for September and November (0.41 g C m^{-2} d^{-1}) by Smith and Kemp (1995).

Model estimates of MPB GPP_S were within the range of rates measured during the 2008 metabolic experiments. These rates varied on both daily and seasonal timescales, and were primarily controlled by the amount of light reaching the sediment surface. It should be noted that these rates were normalized to the sediment surface area within each surface box (i.e. sediment surface area above the pycnocline), rather than the total surface area of each box, which would also include the deep channel.

Modeled SED R_B rates for Boxes 5 – 8 overlapped the range reported by Cowan and Boynton (1996) for the lower bay stations (0.12 and 0.29 g C m^{-2} d^{-1}) (using an RQ = 1). The modeled spring (mean = 0.17 g C m^{-2} d^{-1}) and summer (mean = 0.25 g C m^{-2} d^{-1}) rates from this study matched the calculated seasonal rates reported in Cowan and Boynton (1996) (0.17 and 0.27 g C m^{-2} d^{-1}, respectively). However, the fall and winter rates from this study were below their reported rates for September-November (mean = 0.21 g C m^{-2} d^{-1}) and December-February (mean = 0.16 g C m^{-2} d^{-1}). While the seasonal average rates from this study were below the range reported by Boynton and Kemp (1985) for the lower Bay site in May (0.45 g C m^{-2} d^{-1}) and August (0.45 g C m^{-2} d^{-1}) (RQ = 1), they were near the monthly average rates for Box 8 from this study (May = 0.31, Aug. = 0.39 g C m^{-2} d^{-1}).

Current Conditions

Utilizing our baseline model simulations to represent current conditions within the YRE, the average yearly number of hypoxic days (< 2 mg L^{-1}) over the four year simulation was 7 and 12 for Boxes 7, and 8, respectively. While the effect that these low oxygen conditions have on the species that utilize the deep-water of the YRE varies from species to species, the EPA set the minimum 1-day mean for deep-water at > 2.3 mg L^{-1} (US EPA 2003) . This minimum DO concentration is cited as the theoretical minimum for the survival and recruitment of open-water juvenile and adult fish. In addition to violating this 1-day mean criterion, the lowest modeled daily DO concentrations also violated the deep-water instantaneous minimum criterion of 1.7 mg L^{-1} in the months of July, August and September in Boxes 7 and 8.

Average modeled monthly DO in all boxes did remain above the 30-day mean EPA criterion of 3.0 mg L^{-1}. However, average monthly concentrations for Boxes 7 and 8 were only just above this criterion at 3.49 and 3.10 mg L^{-1} during July, and 3.76 and 3.57 mg L^{-1} during August, respectively. This 30-day mean criterion is cited as the minimum necessary for the survival and recruitment of bay anchovy eggs and larvae. The baseline model run from 2007 to 2010 simulated an average of 10, 18, and 29 days below 3.0 mg L^{-1} for Boxes 6, 7, and 8, respectively. While the effect that low oxygen conditions has on a species utilizing these deeper regions of the Bay is continuing to be studied, this baseline analysis indicates that bottom water oxygen conditions need to improve in order to provide essential habitat for multiple species within the bay.

Contribution of Internal and External Organic Matter Sources to Hypoxia

By isolating the individual contributions of each organic matter source to its associated reduction in DO concentrations, this analysis was able to determine how these multiple sources contributed to oxygen uptake both spatially within the YRE, and also temporally throughout the year (Fig. 5). The lower portions of the Mattaponi and Pamunkey Rivers were most strongly influenced by organic matter entering from the upstream watershed. This effect was particularly important in May and June when eliminating tributary organic matter resulted in a > 1 mg L^{-1} increase in DO concentrations in both boxes. Internal phytoplankton production was also an important source that reduced bottom water oxygen concentrations within these two boxes; however, its contribution was relatively more important later in the summer; potentially after the high winter and spring organic matter loads from the tributaries began to decrease following the annual spring freshet.

The low mesohaline region (Boxes 3 – 4) responded most significantly to the removal of tributary derived organic matter and internal phytoplankton production. This is not surprising since this area, as well as the adjacent tributary boxes upstream, are the primary location of the annual spring bloom based on CBP data. While average monthly oxygen concentrations in these two boxes remained above 3.0 mg L^{-1} throughout the year, the minimum July DO concentration in Box 4 was 3.75 mg L^{-1}. Additionally, the contribution of advected DOC from the lower Chesapeake Bay played an equally important role in reducing DO concentrations in Box 4, particular in the mid-summer and into the fall. The model simulations suggest that this labile material is continually respired as it is transported upriver (via estuarine circulation), resulting in bottom water oxygen concentrations in Boxes 3 and 4 that are 1 – 1.5 mg L^{-1} lower than simulations where CB DOC is removed.

The high mesohaline region (Boxes 5 and 6) represent a transition zone where the influence of the organic matter being advected in from the lower Chesapeake Bay begins to surpass the contribution of both internal phytoplankton production and tributary derived organic matter. Within Box 5, removing phytoplankton increased DO concentrations by 0.7, 1.2, and 0.9 mg L^{-1} during June, July and August, respectively. During this time period removal of CB DOC resulted in a 1.3, 1.9, and 1.7 mg L^{-1} increase in DO. This trend was further emphasized down river in Box 6 where removal of CB DOC surpassed the effect of all other sources throughout the year. Removal of CB DOC improved oxygen concentrations in Box 6 by 1.9, 2.7, and 2.5 mg L^{-1} during June, July and August, respectively. In comparison the combined effect of removing both tributary organic matter and internal phytoplankton production was 1.3, 1.2, and 0.9 mg L^{-1} over the same period.

The contribution of CB DOC in the polyhaline region (Boxes 7 and 8) was sufficient to reduce DO concentrations in this region by approximately 1.8, 2.9, and 2.7 mg L^{-1} during June, July and August, respectively. This result emphasizes the strong interconnection between these shallow tributary estuaries and the mainstem Chesapeake Bay. Harding and Perry's (1997) analysis of long-term phytoplankton biomass in the CB indicated that WC Chl-*a* in the seaward region of the Bay increased 5-10 fold from 1950 to 1994. They related this increase in biomass to the increase in nitrogen loading and continually lessening of nitrogen limitation within the CB. This phytoplankton biomass consequently increases the concentration of DOC and POC as this labile material sinks out of the photic zone. Once this material sinks into the bottom water it is subject to up estuary transport via estuarine circulation, where it can enter the adjacent sub-estuaries.

The organic matter reduction simulations also illustrated the importance of MPB within this shallow tributary estuary. We had originally hypothesized that MPB on the extensive photic shoals in this system could be a major source of carbon that is resuspended and advected laterally into the deep channels where it would contribute to hypoxia. However, our recent carbon budget for the YRE indicated that MPB only contributes approximately 10 % of total summer primary production within the system (Lake et al. *in review*), and model simulations actually indicated lower DO in the absence of MPB (Fig. 5). This result suggests that despite their relatively small contribution to production of organic carbon, the ecological role of MPB in the YRE is likely much more significant. The decrease in modeled DO in the absence of MPB is probably due to their ability to acquire nutrients from both the sediments and also the overlying water column. In recent years, a number of MPB studies along the mid-Atlantic U.S. have provided insight into the ecological importance of MPB in very shallow embayments, serving as a sediment cap that retains nutrients in the sediment and prevents their release into the overlying water column where they can fuel phytoplankton growth (Underwood and Kromkamp 1999; Anderson et al. 2003; Tyler et al. 2003). Model results suggest that if MPB were not present along the shallow photic shoals, oxygen conditions would be lower as a result of additional sediment nutrient releases being available to the water column phytoplankton community. This additional phytoplankton biomass would ultimately be respired within both the water column and sediments in the shallow and deep portions of the YRE, driving higher respiration rates and consequently lower bottom water DO.

Simulated Changes in Nutrient and Organic Matter Loading

Simulations in which external loading was increased and decreased indicated that changes in nutrient loads from the tributaries and surrounding watersheds did not have a substantial effect on the number of low oxygen or hypoxic days (Fig. 6a,c). This is likely due in part to the largely forested, rural land use in the YRE watershed, which is unique for a CB tributary. This is not to suggest that increasing nutrient loads did not have any effect on the system; these scenarios resulted in an increase in predicted chlorophyll-*a*, sediment carbon concentrations, and respiration rates (results not shown). However, these ecological changes did not combine to decrease the oxygen concentrations sufficiently to increase the number of days below 3 or 2 mg L^{-1}.

Changing both nutrient and organic matter loading from the tributaries and watershed by the same magnitude did result in large changes in both tributary boxes, with sizeable but diminishing effects downstream (Fig. 6b,d). This indicates that organic matter load reductions obtained by improving shoreline buffer zones and reducing watershed runoff (along with other mitigation strategies) may help alleviate low oxygen conditions in the tributaries and to a lesser extent improve conditions in the mesohaline portion of the system. The continued development of the upper watershed and wetland loss/degradation has the potential to result in an increase in the amount of organic matter entering the YRE which is predicted to have a negative impact on the degree of hypoxia.

In contrast to the effect of changes in watershed loads, nutrient and phytoplankton reductions from the lower CB into the YRE primarily benefited Boxes 6 – 8, although reducing these sources to half of their current concentrations did not change the number of hypoxic days in this region (although it did decrease the number of days with DO < 3 mg L^{-1}) (Fig. 7a,c).

Increasing these loads did however have a large impact on conditions in these boxes. While current management efforts are focused on reducing nutrients entering the CB by implementing best management practices and improving wastewater treatment facilities, the short-term realized effect of these reductions may be diminished initially due to the legacy effect from nutrient regeneration within Bay sediments. If past trends of increasing chlorophyll-*a* in the lower CB continue the model simulations suggest that the severity and extent of hypoxia will increase in the near term, potentially doubling the number of hypoxic days in Boxes 6 – 8, while also acting to drive oxygen concentrations below 3 mg L^{-1} in Boxes 4 and 5 (Harding and Perry 1997).

As with tributary scenarios, organic matter (DOC and POC) inputs from the Chesapeake Bay had a much larger effect on oxygen concentrations in the lower YRE and all the way to Box 4 (Fig. 7b,d). Assuming that current and future management plans begin to reduce the concentrations of nutrients, phytoplankton biomass, and organic matter (DOC and POC) entering from the CB, model simulations indicated that a 25% reduction in all of these sources will eliminate hypoxia in the mesohaline and polyhaline regions. Additionally, this reduction would reduce the number of low oxygen days to 1 and 9 in Boxes 7 and 8, respectively.

The realized effect of reducing both watershed and Chesapeake Bay sources will likely be initially diminished due to a corresponding legacy effect that the model does not account for in these simulations. While point source reductions can directly limit the contribution from specific sources (i.e. wastewater treatment facilities), other important sources including atmospheric exchange, septic tank leaching, ground water discharge, nutrient regeneration within the sediments, and other positive feedbacks will likely delay the predicted improvements discussed above. Future studies will be needed to determine the appropriate CB reductions strategies needed to yield the improvements require to eliminate bottom water hypoxia in this tributary estuary. The results of this study indicate that if past trends are not reversed that future increases in organic matter and nutrients from the CB will lead to lower oxygen conditions throughout the mesohaline and polyhaline regions of the YRE. This is particularly true in the face of future climate change, which will likely affect freshwater input to this system, modify density driven stratification, during a period of time when atmospheric and water temperatures are increasing.

CONCLUSIONS

The results of this study highlight the contribution of various organic matter sources to the reduction of bottom water oxygen concentrations along the YRE (Fig. 8). Model simulations indicate that a multifaceted management strategy may be required to adequately mitigate hypoxia within this shallow tributary estuary. Watershed and tributary derived organic matter loading reductions are required to mitigate low oxygen conditions in the tributaries and low mesohaline region, and may also benefit the high mesohaline region. However, to mitigate periodic hypoxia in the most susceptible region, the polyhaline, management strategies need to focus on reducing advective inputs of labile organic matter from the lower mainstem Chesapeake Bay.

While most management approaches have historically focused on near field, controllable inputs in the upland watershed, the YRE appears to be a case where the far field sources are more important, which may be a common issue in other tributary estuaries that drain into highly impacted systems like the Chesapeake. Controlling these far field sources is more difficult than near field sources because they require more of a regional management effort. The YRE also appears to be a case where external inputs of fixed carbon, rather than watershed nutrient inputs (or nutrients advected into the system) are the primary cause of hypoxia. However, model simulations indicate that without nutrient uptake by MPB , it is likely that controlling these external nutrient sources would become more important; for this reason it is increasingly important to control sediment inputs to maintain adequate light penetration to support MPB photosynthesis. Finally, we need a better understanding of how these potential management scenarios will be affected by ongoing climate change, which will likely affect freshwater input to this system and modify density driven stratification during a period of time when atmospheric and water temperatures are increasing. These climate changes will likely alter the potential improvements in DO predicted by our model under the load reduction scenarios.

ACKNOWLEDGEMENTS

This project was funded by a grant from_________________ #_________________. S. J. Lake also received financial support from NSF GK-12 (Division of Graduate Education 0840804). We thank the Chesapeake Bay National Estuarine Research Reserve, and specifically Ken Moore and Dave Parrish would provide valuable light attenuation data for multiple sites along York River estuary. Additionally, we would like to thank Walter Boynton for provide us access to the UMCES sediment oxygen and nutrient flux data. We would also like to thank Iris Anderson, Larry Haas, Jennifer Stanhope, Hunter Walker, Lisa Ott, Juliette Giordano, and many other VIMS students and staff members for their field and laboratory assistance. This is Virginia Institute of Marine Science contribution no. XXXX.

LITERATURE CITED

Anderson, I. C., K. J. McGlathery, and A. C. Tyler. 2003. Microbial Mediation of 'Reactive Nitrogen' Transformations in a Temperate Lagoon. *Marine Ecological Progressive Series* 246: 73-84.

Boynton, W. R. and W. M. Kemp. 1985. Nutrient Regeneration and Oxygen Consumption by Sediments Along an Estuarine Salinity Gradient. *Marine Ecology Progress Series* 23: 45-55.

Boynton, W. R., J. H. Garber, R. Summers, and W. M. Kemp, 1995. Inputs, Transformations, and Transport of Nitrogen and Phosphorus in Chesapeake Bay and Selected Tributaries. *Estuaries* 18: 285-314.

Boynton, W. R., J. D. Hagy, J. C. Cornwell, W. M. Kemp, S. M. Greene, M. S. Owens, J. E. Baker, and R. K. Larsen. 2008. Nutrient Budgets and Management Actions in the Patuxent River Estuary, Maryland. *Estuaries and Coasts* 31: 623-651.

Boynton, W. R. and E. M. Bailey. 2008. Sediment Oxygen and Nutrient Exchange Measurements from Chesapeake Bay, Tributary Rivers, and Maryland Coastal Bays: Development of a Comprehensive Database & Analysis of Factors Controlling Patterns and Magnitude of Sediment-Water Exchanges. University of Maryland, Center for Enviromental Science Technical Report Series. TS-542-08.

Brush, M. J. 2002. Development of a Numerical Model for Shallow Marine Ecosystem with Applications to Greenwich Bay, R.I. Ph.D. Dissertation. University of Rhode Island, Kingston, RI

Brush, M. J. 2004. Application of the Greenwich Bay Ecosystem Model to the Development of the Greenwich Bay SAMP (Special Area Management Plan). Final report to the Rhode Island Coastal Resources Center, University of Rhode Island, Narragansett, RI.

Brush, M. J., J. W. Brawley, S. W. Nixon, and J. N. Kremer. 2002. Modeling Phytoplankton Production: Problems with the Eppley Curve and an Empirical Alternative. *Marine Ecology Progress Series* 238: 31-45.

Brush, M.J. and J.W. Brawley. 2009. Adapting the light • biomass (BZI) models of phytoplankton primary production to shallow marine ecosystems. *Journal of Marine Systems* 75: 227–235.

Brush, M.J., and S.W. Nixon. 2010. Modeling the Role of Macroalgae in a Shallow Sub-Estuary of Narragansett Nay, RI (USA). *Ecological Modelling* 221: 1065-1079.

Brush, M. J. and S. W. Nixon. *In review*. An Intermediate Complexity, Hybrid Empirical-Mechanistic Eutrophication Model For Shallow Marine Ecosystems. Submitted to *Ecological Modelling.*

Brush M. J., S. J. Lake, and J. C. P Giordano. *In prep.* Constraining a Model of Microphytobenthos in a Temperate Estuary. In preparation for *Estuarine, Coastal and Shelf Science*.

Cornwell, J. C., and M. S. Owens. 2011. Quantifying Sediment Nitrogen Releases Associated with Estuarine Dredging. *Aquatic Geochemistry* 17: 499-517.

Countway, R.E., E.A. Canuel, and R.M. Dickhut. 2007. Sources of Particulate Organic Matter in Surface Waters of the York River, VA Estuary. *Organic Geochemistry* 38: 365-379.

Cowan, J. L. and W. R. Boynton. 1996. Sediment-Water Oxygen and Nutrient Exchanges Along the Longitudinal Axis of Chesapeake Bay: Seasonal Patterns, Controlling Factors and Ecological Significance. *Estuaries* 19: 562-580.

Dauer, D.M., H.G. Marshall, J.R. Donat, M.F. Lane, S.C. Doughten, P.L. Morton, and F.A. Hoffman. 2005. Status and Trends in Water Quality and Living Resources in the Virginia Chesapeake Bay: James River (1985-2004). Final Report to the Virginia Department of Environmental Quality, Richmond, Virginia. Applied Marine Research Laboratory, Norfolk VA. 1-63.

de Jonge, V. N. 1997. High Remaining Productivity in the Dutch Western Wadden Sea Despite Decreasing Nutrient Inputs from Riverine Sources. *Marine Pollution Bulletin* 34: 427-436.

Diaz, R. J., R. J. Neubauer, L. C. Schaffner, L. Pihl, and S. P. Baden. 1992. Continuous Monitoring of Dissolved Oxygen in an Estuary Experiencing Periodic Hypoxia and the Effects of Hypoxia on Macrobenthos and Fish. *Science in the Total Environment* (Supplement 1992): 1055-1068.

Diaz, R. J. and R. Rosenberg. 2008. Spreading Dead Zones and Consequences for Marine Ecosystems. *Science* 321: 926-929.

Haas, L. W. 1977. The Effect of the Spring-Neap Tidal Cycle on the Vertical Salinity Structure of the James, York, and Rappahannock Rivers, Virginia, U.S.A. *Estuarine and Coastal Marine Science* 5: 485-496.

Haas, L. W., S. J. Hastings and K. L. Webb. 1981. Phytoplankton Response to a Stratification-Mixing Cycle in the York River Estuary During Late Summer, pp. 619-635. In: B.J. Neilson and L.E. Cronin [eds.], Estuaries and Nutrients. Humana Press. Clifton, NJ.

Hanson, J. M., and W. C. Leggett. 1982. Empirical Prediction of Fish Biomass and Yield. *Canadian Journal of Fisheries and Aquatic Sciences* 39: 257-263

Harding Jr., L. W., and E. S. Perry. 1997. Long-term Increase of Phytoplankton Biomass in Chesapeake Bay, 1950 – 1994. *Marine Ecological Progressive Series* 157: 39-52.

Harding Jr., L. W., M. E. Mallonee, and E. S. Perry. 2002. Toward a Predictive Understanding of Primary Productivity in a Temperate, Partially Stratified Estuary. *Estuarine, Coastal and Shelf Science* 55: 437-463.

Hayward D., C. S. Welch, and L. W. Haas. 1982. York River Destratification: An Estuary-Subestuary Interaction. *Science* 216: 1413-1414.

Hayward, D., L. W. Haas, J. D. Boon III, K. L. Webb, and K. D. Friedland. 1986. Empirical Models of Stratification Variation in the York River Estuary, Virginia, USA. , pp. 346-367. In: M. J. Bowman, C. M. Yentsch, and W. T. Peterson [eds.], Lecture Notes on Coastal and Estuarine Studies: tidal mixing and plankton dynamics. Springer-Verlag. New York, NY.

Jenkins, M. C. and W. M. Kemp. 1984. The Coupling of Nitrification and Denitrification in Two Estuarine Sediments. *Limnology and Oceanography* 29: 609-619.

Jordan, T. E., D. L. Correll, J. Miklas, and D. E. Weller. 1991. Long-term Trends in Esturine Nutrients and Chlorophyll, and Short-term Effects of Variation in Watershed Discharge. *Marine Ecological Progressive Series* 75: 121-132.

Kana, T. M., M. B. Sullivan, J. C. Cornwell and K. M. Groszkowski. 1998. Denitrification in Estuarine Sediments Determined by Membrane Inlet Mass Spectrometry. *Limnology and Oceanography* 43: 334-339.

Kana, T. M., J. C. Cornwell, L. Zhong. 2006. Determination of Denitrification in the Chesapeake Bay from Measurements of N_2 Accumulation in Bottom Water. *Estuaries and Coasts* 29: 222-231.

Kemp, W. M., P. Sampou, J. Caffrey, M. Mayer, K. Henriksen, and W. R. Boynton 1990. Ammonium Recycling Versus Denitrification in Chesapeake Bay Sediments. *Limnology and Oceanography* 35: 1545-1563.

Kemp, W. M., J. M. Testa, E. M. Smith, and W. R. Boynton. 2005. Eutrophication of the Chesapeake Bay: Historical Trends and Ecological Interactions. *Marine Ecological Progressive Series* 303:1-29.

Kremer, J. N., J. Vaudrey, D. Ullman, D. Bergondo, N. LaSota, C. Kincaid, D. Codiga, and M. J. Brush. 2010. Simulating Property Exchange in Estuarine Ecosystem Models at Ecologically Appropriate Scales. *Ecological Modelling* 221:1080-1088.

Kuo, A.Y. and B.J. Neilson. 1987. Hypoxia and Salinity in Virginia Estuaries. *Estuaries* 10: 277-283.

Kuo, A. Y., B. J. Neilson, J. Brubaker, and E. P. Ruzecki. 1993. Data Report: Hypoxia in the York River, 1991. Virginia Institute of Marine Science Data Report No. 47. Gloucester Point, Virginia.

Lake, S. J., M. J. Brush, I. C. Anderson, and H. I. Kator. *In review*. Internal Versus External Drivers of Periodic Hypoxia in a Coastal Plain Tributary Estuary: the York River, Virginia. *Marine Ecological Progressive Series*. Submitted for publication 2012.

McCallister, S.L., J.E. Bauer, J.E. Cherrier, and H.W. Ducklow. 2004. Assessing Sources and Ages of Organic Matter Supporting River and Estuarine Bacterial Production: A Multiple-Isotope ($\Delta^{14}C$, $\delta^{13}C$, and $\delta^{15}N$) Approach. Limnology and Oceanography 49(5): 1687-1702.

Ménesguen, A., Cugier, P., Loyer, S., Vanhoutte-Brunier, A., Hoch, T., Guillaud, J-F., Gohin, F., 2007. Two- or Three-Layered Box-Models Versus Fine 3D Models for Coastal Ecological Modelling? A Comparative Study in the English Channel (Western Europe). *Journal of Marine Systems* 64: 47-65.

Moore, K. A., D. J. Wilcox, and R. J. Orth. 2000. Analysis of the Abundance of Submersed Aquatic Vegetation Communities in the Chesapeake Bay. *Estuaries* 23:115-127.

Moore, K., D. Wilcox, and B. Anderson. 2001. Analysis of Historical Distribution of Submerged Aquatic Vegetation (SAV) in the York and Rappahannock Rivers as Evidence of Historical Water Quality Condictions. Special Report in *Applied Marine Science and Ocean Engineering* 375.

Nixon, S.W. 1995. Coastal Marine Eutrophication: A Definition, Social Causes, and Future Concerns. *Ophelia* 41: 199-219.

Nixon, S. W. 2001. Some Reluctant Ruminations on Scales (and Claws and Teeth) in Marine Mesocosms. pp.183-195. *in:* Gardner, R. H., W. M. Kemp, V. S. Kennedy, and J. E. Petersen (eds.). Scaling Relations in Experimental Ecology. Columbia University Press, New York.

Nixon, S. W. 2009. Eutrophication and the Macroscope. *Hydrobiologia* 629: 5-19.

Nixon, S. W., and B. A. Buckley. 2002. "A strikingly rich zone"—Nutrient Enrichment and Secondary Production in Coastal Marine Ecosystems. *Estuaries and Coasts* 25: 782-796.

Odum, H. T. 1994. Ecological and General systems: an Introduction to Systems Ecology (2nd ed.) University Press of Colorado, Niwot, Colorado, USA.

Officer, C. B. 1980. Box Models Revisited. pp. 65-114 *in*: Hamilton, P. and K. B. MacDonald (eds.). Estuarine and Wetland Processes with Emphasis on Modeling. Plenum Press, New York.

Oglesby, R. T. 1977. Relationships of Fish Yield to Lake Phytoplankton Standing Crop, Production, and Morphoedaphic Factors. *Journal of the Fisheries Research Board of Canada* 34: 2271-2279.

Pace, M. L. 2001. Predictions and the Aquatic Sciences. *Canadian Journal of Fisheries and Aquatic Sciences* 58: 63-72.

Rabalais, N. N. 2002 Nitrogen in Aquatic Ecosystems. *Ambio* 31: 102-112.

Reckhow, K. H. 1999. Water Quality Prediction and Probability Network Models. *Canadian Journal of Fisheries and Aquatic Sciences* 56: 1150-1158.

Rizzo, W. M. and R. L. Wetzel. 1985. Intertidal and Shoal Benthic Community Metabolism in a Temperate Estuary: Studies of Spatial and Temporal Scales of Variability. *Estuaries* 8: 342-351.

Scavia, D., D. Justic, and V. J. Bierman Jr. 2004. Reducing Hypoxia in the Gulf of Mexico: Advice from Three Models. *Estuaries* 27: 419-425.

Scavia, D., E.L.A. Kelly, and J.D. Hagy III. 2006. A Simple Model for Forecasting the Effects of Nitrogen Loads on Chesapeake Bay Hypoxia. *Estuaries and Coasts* 29: 674–684.

Sharples J., J. H. Simpson, and J. M. Brubaker. 1994. Observations and Modelling of Periodic Stratification in the Upper York River Estuary, Virginia. *Estuaries, Coastal and Shelf Science* 38: 301-312.

Shen, J. and L. Haas. 2004. Calculating Age and Residence Time in the Tidal York River Using Three-Dimensional Model Experiments. *Estuaries, Coastal and Shelf Science* 61: 449-461.

Smith, E. M., and W. M. Kemp. 1995. Seasonal and Regional Variations in Plankton Community Production and Respiration for Chesapeake Bay. *Marine Ecology Progressive Series* 116: 217-231.

Stow, C.A., Roessler, C., Borsuk, M.E., Bowen, J.D., Reckhow, K.H., 2003. Comparison of Estuarine Water Quality Models for Total Maximum Daily Load Development in Neuse River Estuary. *Journal Water Resources Planning and Management* 129: 307-314.

Swaney, D.P., D. Scavia, R.W. Howarth, and R.M. Marino. 2008. Estuarine Classification and Response to Nitrogen Loading: Insights from Simple Ecological Models. *Estuarine, Coastal and Shelf Science* 77: 253–263

Testa, J.M., and W. M. Kemp. 2008. Regional, Seasonal, and Inter-Annual Variability of Biogeochemical Processes and Physical Transport in a Partially Stratified Estuary: A Box-Modeling Analysis. *Marine Ecology Progress Series* 356: 63-79.

Testa, J. M., W. M. Kemp, W. R. Boynton, and J. D. Hagy III. 2008. Long-term Changes in Water Quality and Productivity in the Patuxent River Estuary: 1985 – 2003. *Estuaries and Coasts* 31: 1021-1037.

Tyler A. C., K. J. McGlathery, and I. C. Anderson. 2003. Benthic Algae Control Sediment-Water Column Fluxes of Organic and Inorganic Nitrogen Compounds in a Temperate Lagoon. *Limnology and Oceanography* 48: 2125-2137.

Underwood, G. J. C. and J. Kromkamp. 1999. Primary Production by Phytoplankton and Microphytobenthos in Estuaries. pp. 93-153 in: Nedwell, D. B., and D. G. Raffaelli (eds.). *Estuaries. Advances in Ecological Research.* Academic Press, London.

U.S. Environmental Protection Agency. 2003. Ambient Water Quality Criteria for Dissolved Oxygen, Water Clarity and Chlorophyll a for Chesapeake Bay and Its Tidal Tributaries. EPA 903-R-03-002. Region III Chesapeake Bay Program Office, Annapolis, MD.

Xu, J., R.R. Hood, and S-Y. Chao. 2005. A simple Empirical Optical Model for Simulating Light Attenuation Variability in a Partially Mixed Estuary. *Estuaries* 28: 572–580.

CHAPTER 2 - FIGURES

Figure 2-1. Map of the York River estuary and the Chesapeake Bay (insert), including box model boundaries, the surrounding watershed, and long-term Chesapeake Bay Program (bulls eyes) monitoring stations. Boxes 1 and 2 are located within the lower Mattaponi and Pamunkey Rivers, respectively. Boxes 3 and 4 are located in the low mesohaline, Boxes 5 and 6 in the high mesohaline, and Boxes 7 and 8 in the polyhaline portion of the estuary.

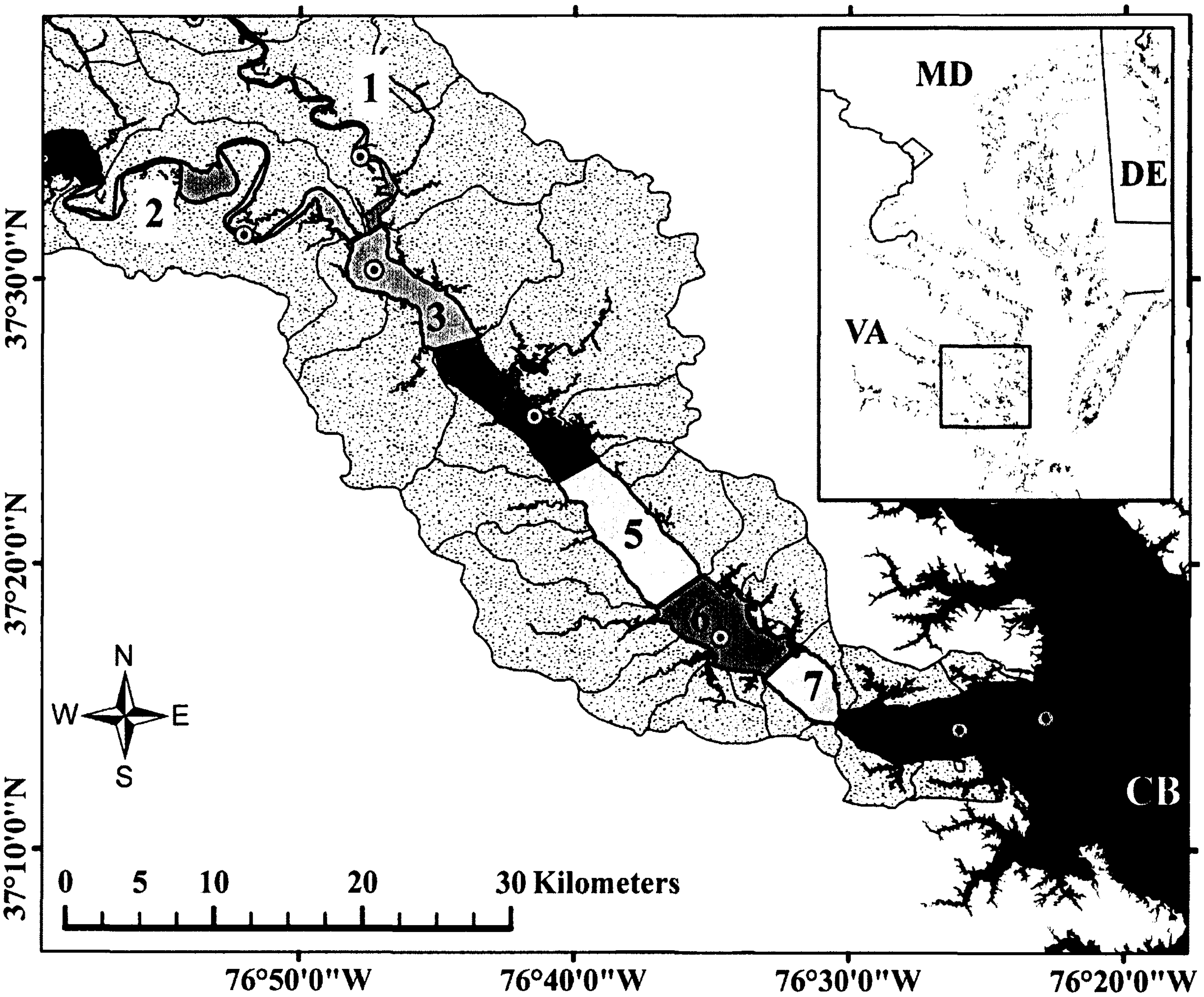
1
2
3
5
6
7
MD
DE
VA
CB
N
W
E
S
37°30'0"N
37°20'0"N
37°10'0"N
76°50'0"W
76°40'0"W
76°30'0"W
76°20'0"W
0
5
10
20
30 Kilometers

Figure 2-2. Diagram of the intermediate-complexity eutrophication model. State variables, major flows (with arrows), and major connections (without arrows) are depicted. Flows that consume material (e.g. nutrient uptake, oxygen consumption, loss of biomass) are shown with solid lines. Flows which produce material (e.g. remineralization, photosynthetic oxygen production) are shown with broken lines. To reduce the complexity of the figure, all respiratory demands are shown as being integrated into an estimate of total water column respiration (R_{WC}), which draws from the oxygen pool and remineralizes N and P. The effect of temperature (T) on most state variables and flows has likewise been excluded. WS = watershed, AT = atmospheric. All other terms are defined in the text. Symbols are those of Odum (1994). Adapted from Brush and Nixon (submitted).

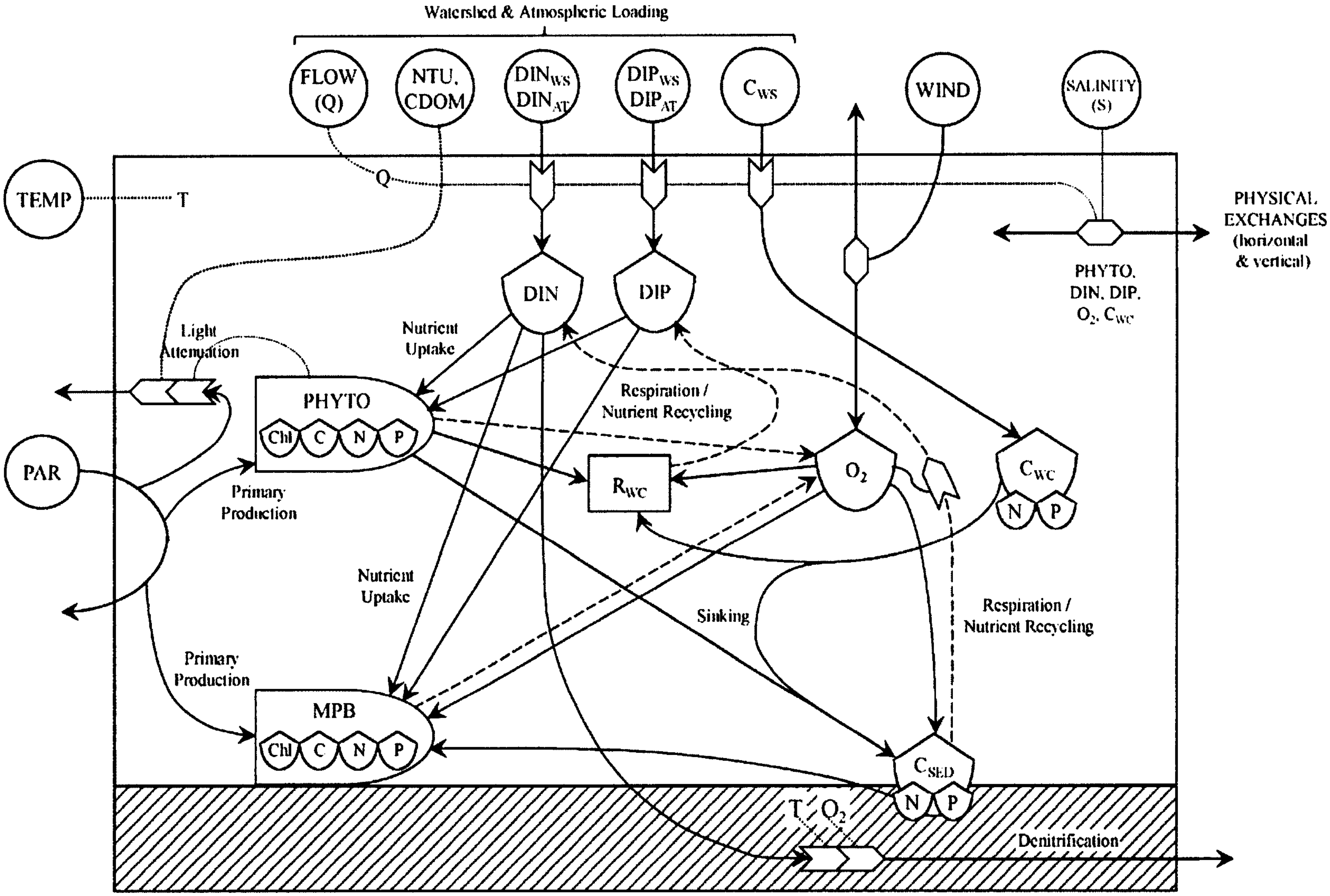
Watershed & Atmospheric Loading
FLOW (Q)
NTU, CDOM
DIN_{WS} DIN_{AT}
DIP_{WS} DIP_{AT}
C_{WS}
WIND
SALINITY (S)
TEMP
T
Q
PHYSICAL EXCHANGES (horizontal & vertical)
PHYTO, DIN, DIP, O_2, C_{WC}
DIN
DIP
Light Attenuation
Nutrient Uptake
PHYTO
Chl
C
N
P
Respiration / Nutrient Recycling
PAR
Primary Production
R_{WC}
O_2
C_{WC}
N
P
Nutrient Uptake
Sinking
Respiration / Nutrient Recycling
Primary Production
MPB
Chl
C
N
P
C_{SED}
N
P
T
O_2
Denitrification

Figure 2-3. Measured (large black points, CBP) and modeled (small gray points) (a, b) surface water column chlorophyll-*a*, (c, d) surface and (e, f) bottom dissolved oxygen, and (g, h) surface dissolved inorganic nitrogen and (i, j) phosphorus for Boxes 4 and 8, respectively. Volume weighted dissolved oxygen concentrations sampled during the 2007 and 2008 Acrobat^{TM} surveys are included as triangles in panels d and f. Dashed lines in panels e and f represent hypoxic conditions (< 2 mg L^{-1}). (k, l) Measured (1 m below mean low water) and modeled (0.5 – 1 m depth segment) MPB chlorophyll-*a* in Boxes 5 and 8, respectively (MPB biomass was not measured in Box 4).

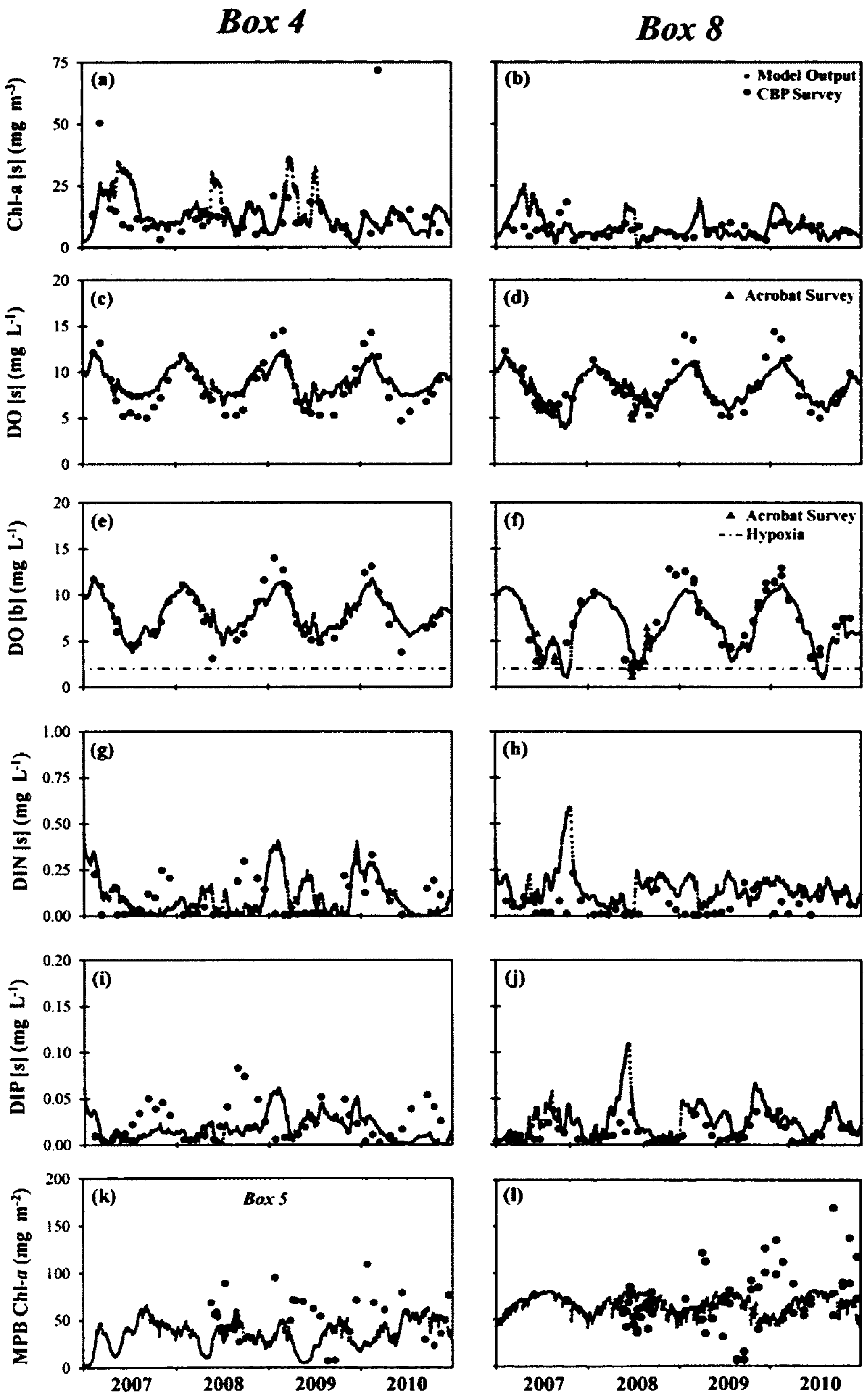
Box 4
Box 8
Chl-a |s| (mg m^{-3})
DO |s| (mg L^{-1})
DO |b| (mg L^{-1})
DIN |s| (mg L^{-1})
DIP |s| (mg L^{-1})
MPB Chl-a (mg m^{-2})
(a)
(b)
• Model Output
● CBP Survey
(c)
(d)
▲ Acrobat Survey
(e)
(f)
▲ Acrobat Survey
-·- Hypoxia
(g)
(h)
(i)
(j)
(k)
Box 5
(l)
75
50
25
0
20
15
10
5
0
1.00
0.75
0.50
0.25
0.00
0.20
0.15
0.10
0.05
0.00
200
150
100
50
0
2007
2008
2009
2010

Figure 2-4. Measured (large black points) and modeled (small gray points) rates of (a, b) phytoplankton net daytime production, (c, d) surface and (e, f) bottom layer water column respiration, (g, h) MPB gross primary production within the surface layer, and (i, j) surface and (k, l) bottom layer sediment respiration. Measured water column and sediment metabolic rates were calculated from samples collected during the 2008 water quality surveys (2008 WQS).

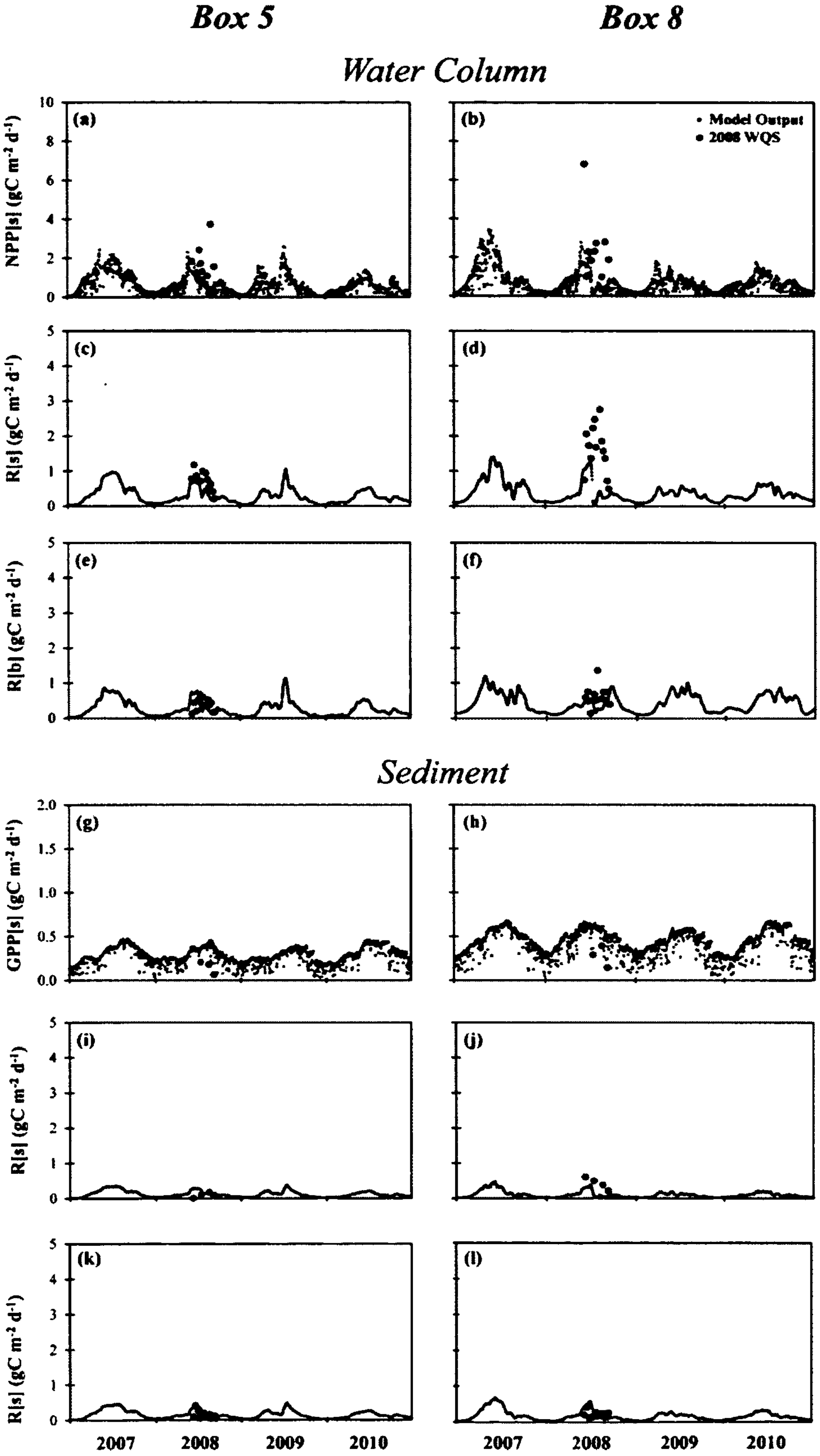
Box 5
Box 8
Water Column
NPP[s] (gC m-2 d-1)
10
8
6
4
2
0
(a)
(b)
• Model Output
● 2008 WQS
R[s] (gC m-2 d-1)
5
4
3
2
1
0
(c)
(d)
R[b] (gC m-2 d-1)
(e)
(f)
Sediment
GPP[s] (gC m-2 d-1)
2.0
1.5
1.0
0.5
0.0
(g)
(h)
R[s] (gC m-2 d-1)
(i)
(j)
R[s] (gC m-2 d-1)
(k)
(l)
2007
2008
2009
2010
2007
2008
2009
2010

Figure 2-5. Percent change in predicted dissolved oxygen concentrations (deviation from baseline model simulation) for eight scenarios in which individual organic matter sources were removed. Values represent mean changes over a four year model simulation. Phyto = water column phytoplankton, MPB = microphytobenthos, Trib OM = tributary dissolved and particulate organic matter, WS OM = watershed dissolve and particulate organic matter, CB POC = particulate organic matter from the Chesapeake Bay, CB DOC = dissolved organic matter from the Chesapeake Bay, CB WC Chl-*a* = chlorophyll-*a* (as a proxy for phytoplankton biomass) from the Chesapeake Bay, and None = all sources removed.

Contribution of OM Sources to Bottom Water DO

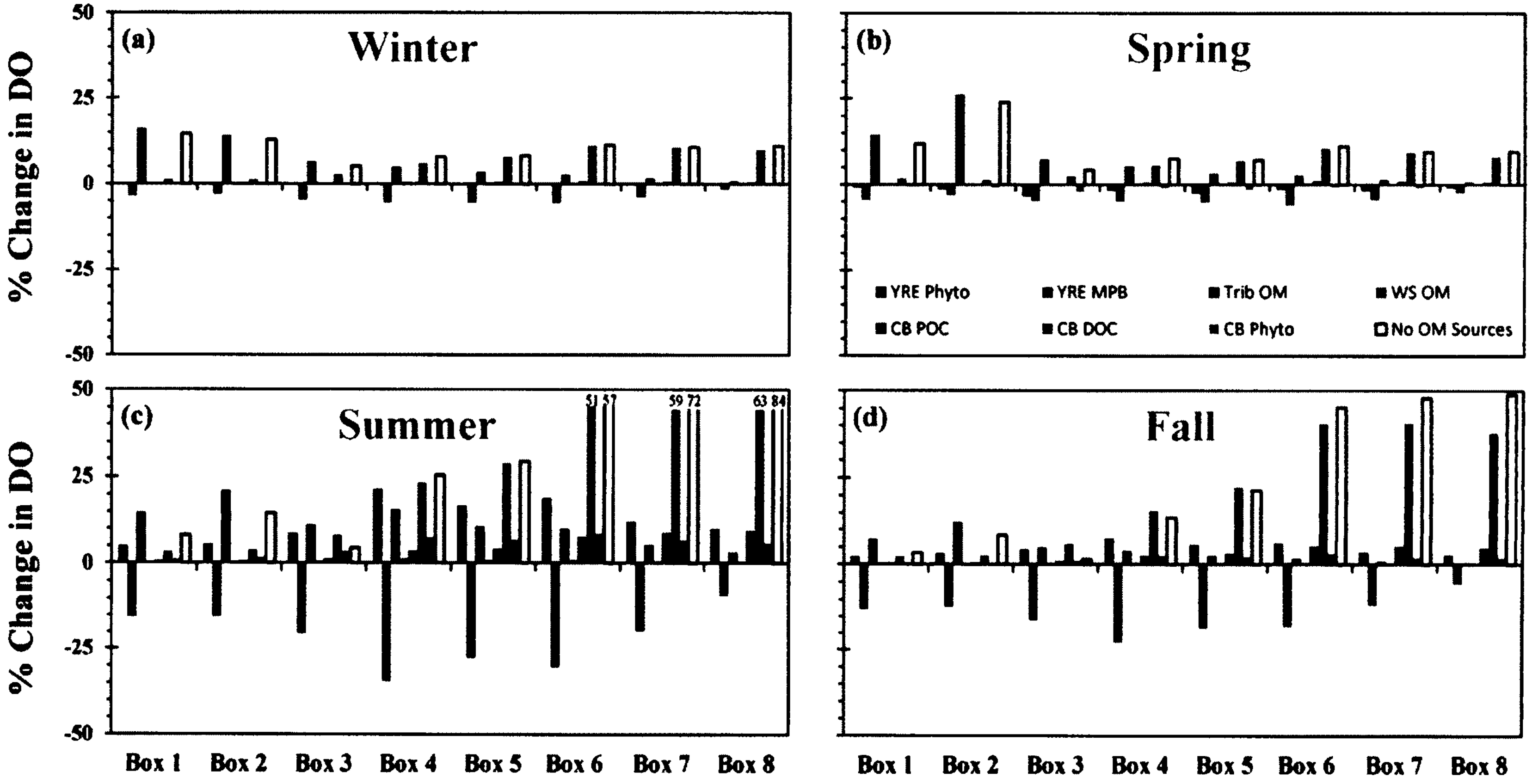

Figure 2-6. Annual number of hypoxic (< 2mg L^{-1}) and low oxygen days (< 3 mg L^{-1}) within each model box predicted under various watershed and tributary loading scenarios, averaged over a four year simulation. Scenarios included changing (a, c) nutrient and (b, d) nutrient and organic matter (DOC, POC) loading from one half (0.5x) to double (2x) the current loads.

Watershed and Tributary Inputs

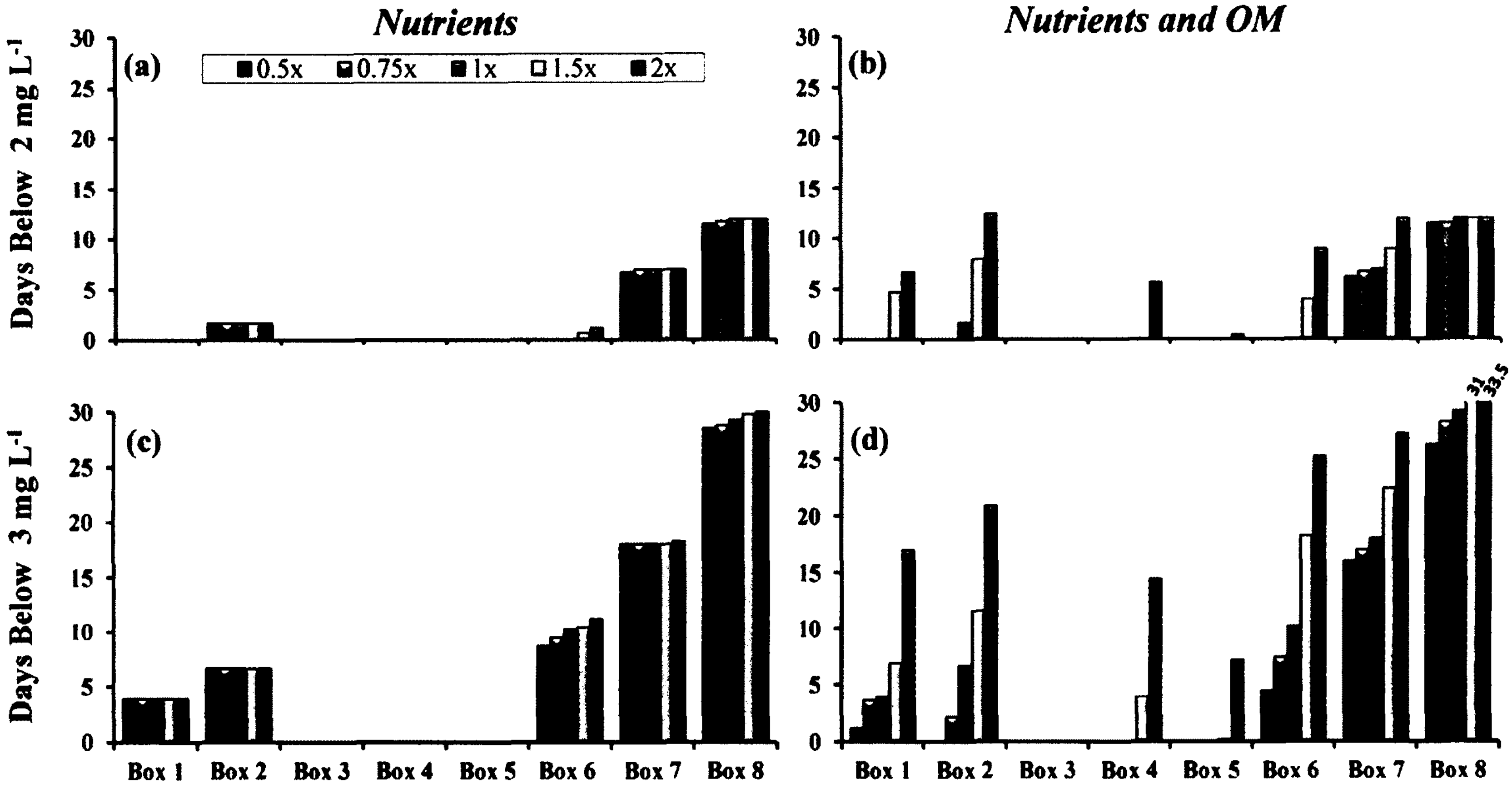

Figure 2-7. Annual number of hypoxic (< 2mg L^{-1}) and low oxygen days (< 3 mg L^{-1}) within each model box predicted under various Chesapeake Bay input scenarios, averaged over a four year simulation. Scenarios included changing (a, c) nutrient and chlorophyll-*a* and (b, d) nutrient, chlorophyll-*a*, and organic matter (DOC, POC) concentrations in the mainstem Chesapeake Bay from one half (0.5x) to double (2x) the current values.

Chesapeake Bay Inputs

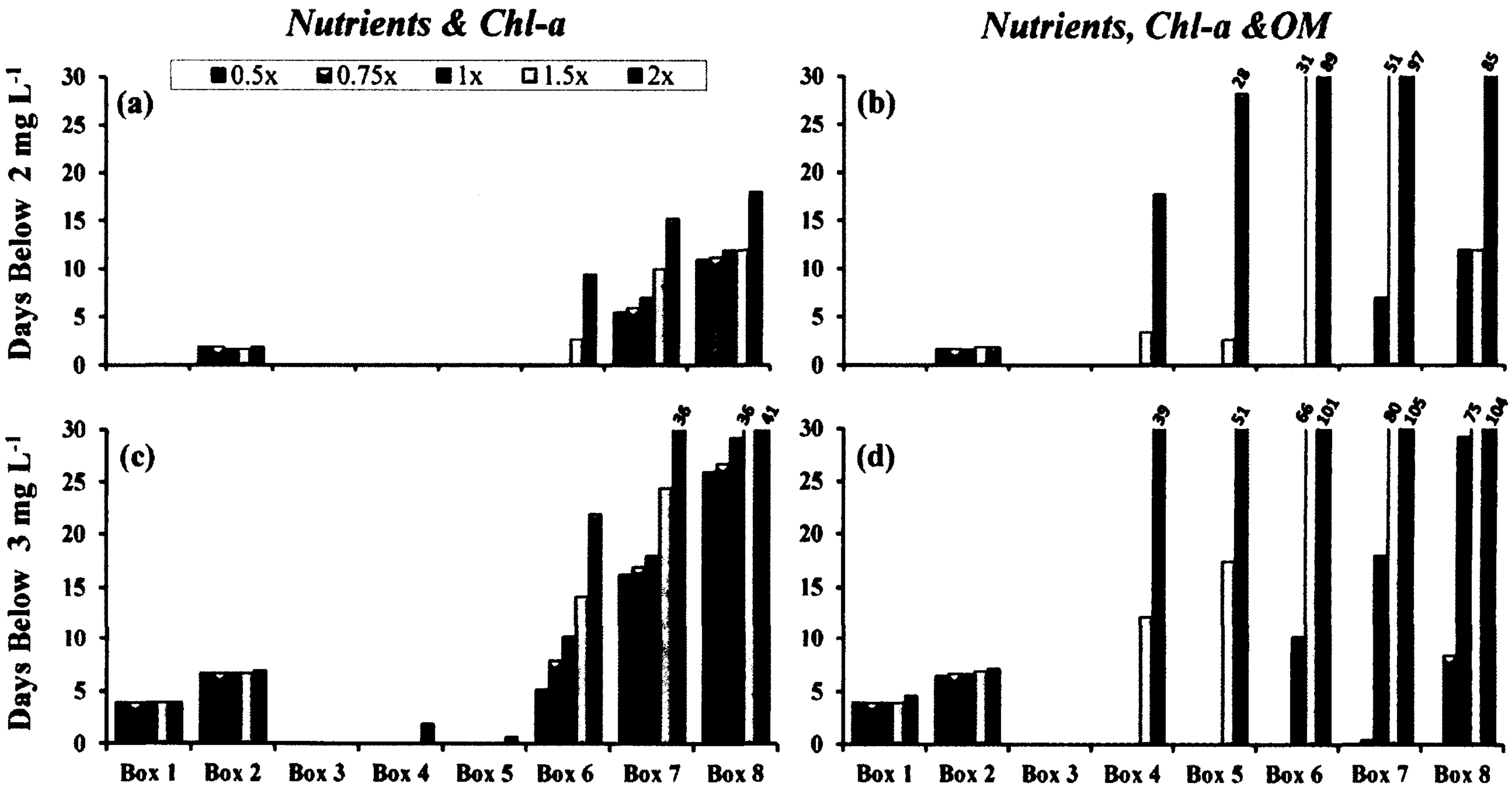

Figure 2-8. Relative seasonal (May – September) contribution of various organic matter sources to the reduction of bottom water oxygen concentrations along the York River estuary (YRE). The thickness of each line corresponds to the percent change in predicted dissolved oxygen concentrations (deviation from baseline model simulation) in each region based on model simulations. Only those sources that contributed to a greater than 1% change in bottom water oxygen concentrations were included. YRE Phyto = water column phytoplankton, YRE MPB = microphytobenthos, Trib OM = tributary dissolved and particulate organic matter, CB POC = particulate organic matter from the Chesapeake Bay, CB DOC = dissolved organic matter from the Chesapeake Bay, and CB Phyto. = phytoplankton biomass (calculated using chlorophyll-*a* as a proxy) from the Chesapeake Bay.

Organic Matter Sources

Relative Contribution to Bottom Water Oxygen

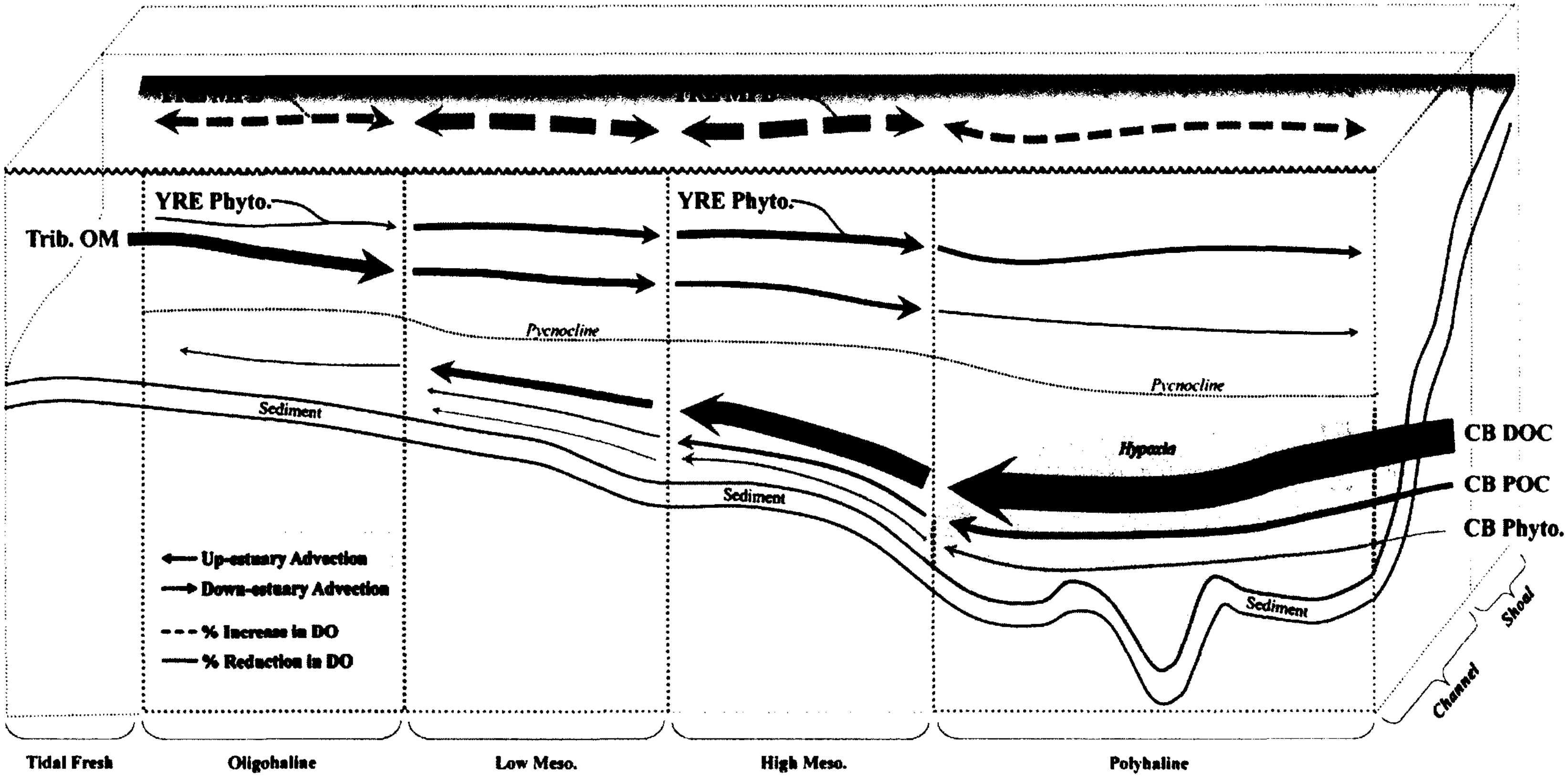

YRE Phyto.
Trib. OM
YRE Phyto.
Pycnocline
Pycnocline
Sediment
Sediment
Sediment
Hypoxia
CB DOC
CB POC
CB Phyto.
Shoal
Channel
← Up-estuary Advection
→ Down-estuary Advection
- - - % Increase in DO
—— % Reduction in DO
Tidal Fresh
Oligohaline
Low Meso.
High Meso.
Polyhaline

Chapter 2 - TABLE

Table 1. Skill assessment metrics for all parameters where measured concentrations or rates were available, averaged over all model boxes and Boxes 5 – 8 where hypoxia occurs. ABS = absolute, % = percent, and RMS = root mean square error. The number of measured and modeled values compared for each parameter is listed at the top of each column. All abbreviated terms are defined in the text.

		K_D	PHYTO Chl-*a*	MPB Chl-*a*	DO_S	DO_B	DIN_S	DIN_B	DIP_S	DIP_B	PHYTO NPP_S	WC R_S	WC R_B	MPB GPP_S	SED R_S	SED R_B
	n =	*449*	*252*	*135*	*249*	*215*	*252*	*244*	*255*	*244*	*52*	*52*	*52*	*16*	*16*	*52*
All Sites	**ABS Error**	**0.27**	**0.78**	**10.72**	**0.69**	**0.63**	**0.03**	**0.05**	**0.01**	**0.01**	**0.23**	**0.31**	**0.09**	**0.10**	**0.09**	**0.04**
	% Error	**17.11**	**11.23**	**21.68**	**8.53**	**9.00**	**38.07**	**52.81**	**37.60**	**39.09**	**46.21**	**38.88**	**17.16**	**26.01**	**44.36**	**24.78**
	RMS Error	**0.55**	**7.92**	**31.77**	**1.63**	**1.77**	**0.08**	**0.10**	**0.02**	**0.02**	**1.28**	**0.79**	**0.36**	**0.13**	**0.15**	**0.08**
	n =	*417*	*81*	*132*	*82*	*61*	*82*	*82*	*84*	*83*	*52*	*52*	*52*	*16*	*16*	*52*
Boxes 5 – 8	**ABS Error**	**0.27**	**0.33**	**10.86**	**0.38**	**0.33**	**0.04**	**0.07**	**0.00**	**0.00**	**0.23**	**0.31**	**0.09**	**0.10**	**0.09**	**0.04**
	% Error	**18.04**	**5.39**	**21.19**	**4.79**	**4.34**	**136.15**	**253.34**	**16.52**	**29.35**	**46.21**	**38.88**	**17.16**	**26.01**	**44.36**	**24.78**
	RMS Error	**0.51**	**3.79**	**32.10**	**1.07**	**1.14**	**0.09**	**0.13**	**0.01**	**0.02**	**1.28**	**0.79**	**0.36**	**0.13**	**0.15**	**0.08**

CHAPTER 3

Modeling the Response to External Load Reductions in a Warmer Climate: Primary Production, Net Ecosystem Metabolism, and Hypoxia in the York River Estuary, Virginia

Samuel J. Lake[1] and Mark J. Brush
Virginia Institute of Marine Science,
College of William and Mary, Gloucester Point, VA 23062 USA

[1] Corresponding author:
Email: sjlake@vims.edu
Phone Number: (804) 684-7918
Fax: (804) 684-7293

Keywords: York River Estuary, Ecosystem Model, Hypoxia, Climate, Primary Production, Net Ecosystem Metabolism

ABSTRACT

Determining the ecological effects of climate induced warming on coastal marine ecosystems will be particularly complicated within shallow tributary estuaries due to the complex cycling of nutrients and organic matter in these systems, diversity of primary producers, enhanced benthic-pelagic coupling, and advection of nutrients, labile organic matter, and hypoxic water from adjacent systems via estuarine circulation. This study utilized an intermediate complexity eutrophication model developed for the York River estuary (YRE), VA, USA to predict how water column primary production, net ecosystem metabolism (NEM), and hypoxia will change within this sub-estuary of Chesapeake Bay under a range of warmer climate conditions. Water column primary production was predicted to respond positively to warmer climate in the winter and spring throughout most of the YRE, while decreasing in the summer and fall within the high mesohaline and polyhaline regions. These changes in primary production, along with increasing rates of water column and sediment respiration, caused the lower portions of the YRE tributaries as well as portions of the low mesohaline YRE to become more autotrophic, presumably due to increased rates of nutrient cycling. However, NEM was predicted to decrease during the spring, summer and fall throughout the rest of the estuary. Warmer temperatures increased both the temporal and spatial extent of hypoxia (< 2 mg L^{-1}) predicted by the model, with the tributaries experiencing a relatively constant increase in the number of hypoxic days during the late spring and early summer. Low oxygen conditions in the polyhaline region, which is currently the most susceptible region to hypoxia, increased more rapidly with increasing temperatures. Offsetting this spatial and temporal increase in low oxygen with climate warming will require additional nutrient and organic matter load reductions from

the tributaries, surrounding watersheds, and the Chesapeake Bay in order to achieve the same level of improvement predicted in the absence of a warming climate.

INTRODUCTION

Estuaries represent some of the most anthropogenically altered marine ecosystems worldwide, which is in large part due to their historical importance as maritime ports that have evolved into present day metropolitan areas (Cooper and Brush 1993; de Jonge et al. 1994; Cloern 2001; Boesch 2002). Many of the initial human impacts on these systems included direct alterations via logging surrounding watersheds, draining wetlands, damming rivers, water diversion projects, and channel dredging (Dynesius and Nilsson 1994; Lotze 2010). By the mid-17th century European settlers had significantly altered the Chesapeake Bay watershed, initiating the cultural eutrophication of the Bay (Cooper 1995; Brush and Davis 1984; Brush 2009). From this period forward the Chesapeake Bay would be directly influenced by continued pollution, and elevated rates of organic matter, nutrient, and sediment loading (Goldberg et al. 1978; Brush and Davis 1984; Zimmerman and Canuel 2000; Kemp et al. 2005).

More recently, these highly productive and economically important systems have been subject to another more indirect human influence, climate change (Nixon et al. 2009; Smith et al. 2010; Doney et al. 2012). The effect of climate change and the associated ecological responses within marine systems is often difficult to directly quantify due to interannual and seasonal variability in climatic conditions, as well as unrelated concurrent ecological changes within the ecosystem (Murdoch et al. 2000; Scavia et al. 2002; Oviatt 2004; Cloern and Jassby 2008; Whitehead et al. 2009). A number of recent studies have begun to link predicted climatological changes to important ecological cycles in an effort to gain insight into how marine systems might respond to future changes (Najjar et al. 2010; Canuel et al. 2012; Doney et al. 2012). While it is important to continue to develop our broad understanding of how multiple stressors related to climate change will impact a range of systems, it is also important to understand how specific systems will respond to the individual effects of climate change. This study focused on quantifying the effect of a warming climate on primary production, net ecosystem metabolism (NEM), and the development of hypoxia in the York River estuary (YRE), a sub-estuary of Chesapeake Bay.

Over the past century, atmospheric temperatures have increased globally by 0.74 °C (± 0.18) (IPCC 2007), while mean global ocean surface temperatures (0-300 m) have increased by 0.31 °C since 1950 (Levitus et al. 2000). Within the Chesapeake Bay, surface waters have increased approximately 1 °C from 1960 to 1990 (Najjar et al. 2010). A recent, multi-model climate analysis for the Bay region, under enhanced greenhouse gas concentrations, predicted an increase of 1.1 ± 0.4, 2.3 ± 0.6, and 3.9 ± 1.1 °C above the 1970-2000 conditions for 2010-2039, 2040-2069, and 2070-2100, respectively (Najjar et al. 2009). While Najjar et al. (2010) did not directly estimate the effect this increase in air temperature would have on water temperatures in the Chesapeake Bay, they did note the positive correlation between water temperatures in the Bay and regional atmospheric and ocean temperatures measured in previous studies, and suggested that these climate model projections could be applied directly to the Bay.

The physical response of the Chesapeake Bay to a warming climate will likely result in relatively higher rates of evaporation, reduced dissolved oxygen saturation, and seasonal changes in density-driven stratification. These physical changes together with enhanced metabolic rates due to elevated temperatures will modify the cycling of nutrients within the Bay, and potentially alter the timing and community composition of phytoplankton blooms, including increases in toxic species (Edwards and Richardson 2004; Oviatt et al. 2002; Paerl and Huisman 2008, 2009; Nixon et al. 2009; Paerl and Otten 2013). The realized effect of these ecological shifts is still largely unknown, however it is likely that rates of primary production will change with warming temperatures, which has been cited as a potential factor causing the decline of the typical winter-spring phytoplankton bloom and reduced rates of annual primary production in Narragansett Bay, RI (Oviatt et al. 2002; Nixon et al. 2009). Increasing temperatures also have the potential to decrease NEM and enhance the degree of net heterotrophy in coastal systems given the strong dependence of pelagic and sediment respiration on water temperature (Hopkinson and Smith 2005) and the greater sensitivity of respiration to temperature compared to production (López-Urrutia et al. 2006; O'Connor et al. 2009). O'Connor et al. (2009) demonstrated that increasing temperature alone could result in increased primary productivity, decreased total biomass, stronger consumer control of primary production, and a shift in pelagic food web structure in planktonic communities. However, this response was limited to nutrient-enriched treatments, indicating an interaction between enrichment and temperature. Additionally, within the Chesapeake Bay it is likely that continued warming will result in the reduction of important habitat including *Zostera marina* beds and marshes, as a result of temperature stress over prolonged warm periods (Moore et al. 2012) and sea level rise (Perry and Hershner 1999; Perry and Atkinson 2009).

Warming air and water temperatures also have the potential to complicate ongoing efforts to restore estuaries through nutrient load reductions (e.g., US EPA 2010) (Moss et al. 2011). This may be especially true in relatively shallow tributary estuaries that drain into larger systems, such as the many sub-estuaries that flow into the Chesapeake Bay, including the York River (Fig. 1). The response of tributary estuaries to a warming climate will be complicated given the complex cycling of nutrients in these systems, the presence of extensive photic shoals which leads to enhanced benthic-pelagic coupling and benthic primary production by microphytobenthos (MPB), and the importance of allochthonous inputs of labile organic matter both from the watershed and via estuarine circulation where the sub-estuaries meets their parent systems. The development of hypoxia in the YRE has long been linked not only to watershed nutrient inputs, but also advection of nutrient and organic matter (OM) rich water from the mainstem Chesapeake Bay, along with variable physical mixing processes, both tidal and wind driven (Haas 1977; Kuo and Nielson 1987; Sharples et al. 1994; Lake et al. *in review*). A recent effort to quantify the major sources of organic carbon to the YRE indicated that phytoplankton production greatly exceeded the estimated inputs of OM from the tributaries and surrounding watershed, but highlighted the large input of OM from the Chesapeake Bay via estuarine circulation which amounted to 65% of internal phytoplankton production (Lake et al. *in review*). Additionally, a recent modeling analysis focused on assessing the role of multiple organic matter sources that drive the YRE to hypoxia indicated that different regions of the system will require different management efforts to offset hypoxia, with localized watershed reductions improving conditions up river and more regionally-driven reductions from the Chesapeake Bay having the greatest impact in the lower river (Lake and Brush *in prep*). Given the many potential impacts of climatic warming on estuarine community composition and rate processes, it is likely that the effect of external load reductions identified in that study to mitigate hypoxia will need to be enhanced in order to achieve the same level of improvement under a warming climate.

The purpose of the present study was to utilize an intermediate-complexity model recently developed for the YRE (Fig. 2) to predict the effect of climate warming on the YRE ecosystem, and expand our previous analysis of external load reductions to include the interactive effects of these reductions with climate warming. The intermediate-complexity approach incorporates both traditional mechanistic approaches and robust, cross-system empirical functions to constrain key rate processes, which helps limit excessive parameterization and error propagation from loosely constrained variables (Reckhow 1999; Pace 2001; Brush et al. 2002). Reduced complexity models have been widely used as synthesis tools, to address complex sets of hypotheses related to ecosystem function, and to inform coastal management (Stow et al. 2003; Brush 2004; Scavia et al. 2004, 2006; Swaney et al. 2008; Brush and Nixon *in review*; Lake and Brush *in prep*). While the effect of climate change on the YRE will not be limited to increasing temperatures, but also include effects of increased precipitation, storminess, and rates of sea level rise (Najjar et al. 2010), our purpose here is to begin with the first order effect of temperature and its interactions with external loading on ecosystem function and hypoxia.

METHODS

Site Description

The YRE is formed by the confluence of the Mattaponi and Pamunkey Rivers near West Point, Virginia, approximately 55 km from where the river enters the mainstem of the Chesapeake Bay on its western edge (Shen and Haas 2004) (Fig. 1). The overall land use surrounding the YRE is predominantly rural with 62% forested and 16% agricultural (Dauer et al. 2005). The estuary is flanked by shallow photic shoals (< 2m), which comprise 40% of the estuary by area (Rizzo and Wetzel 1985). The YRE oscillates between stratified and well-mixed conditions due to the physical mixing of the spring-neap tidal cycle, which has been well documented in past studies (Haas 1977; Hayward et al. 1982; Kuo and Neilson 1987; Diaz et al. 1992). This unique physical mechanism creates the potential for continued formation and disruption of bottom water hypoxia from late May to early September within the lower half of the estuary.

Linkage Between Air and Water Temperature

Current predictions of temperature increases for the Chesapeake region are for air (i.e., 1.1 °C by 2039, 2.3 °C by 2069, and 3.9 °C by 2100; Najjar et al. 2009), so we first needed to assess how these changes in air temperature might translate to water temperature. Chesapeake Bay water temperature measurements from 1949 – 1982 and 1984 – 2012 were downloaded from the CBP website (www.chesapeakebay.net). Measurements made in the polyhaline Chesapeake Bay from 1949 to 1982 were organized into three depth segments: surface water, 2 meters below the surface, and bottom water. Similarly, measurements from 1984 to 2012 were sorted by the same 3 depth segments for the polyhaline Chesapeake Bay and Box Model regions 1 – 3 and 4 – 8. These water temperature measurements were then paired with mean monthly air temperature measurements from Norfolk International Airport, which were downloaded from the NOAA National Climatic Data Center (www.ncdc.noaa.gov/oa/ncdc.html).

Intermediate Complexity Eutrophication Model

Lake and Brush (*in prep*) adapted a model to the YRE that combines the benefits of both empirical and mechanistic modeling approaches into an intermediate-complexity, shallow marine ecosystem model (Brush 2002, 2004; Brush et al. 2002; Brush and Brawley 2009; Brush and Nixon 2010, *in review*). This approach includes only those state variables and rate processes of primary importance to the process of estuarine eutrophication, and integrates robust empirical relationships that have been shown to apply across a wide range of temperate estuaries to predict key rate processes. State variables include pools of carbon (C), nitrogen (N), phosphorous (P) in phytoplankton (PHYTO) and microphytobenthos (MPB), water column pools of labile organic carbon (C_{WC}) and its associated N and P, dissolved inorganic N (DIN) and P (DIP), dissolved oxygen (DO or O_2), and the pool of recently deposited, labile organic carbon in the sediments (C_{SED}) and its associated N and P (Fig. 2). Full details regarding model formulations and specific calibration to the YRE can be found elsewhere (see above). In the following paragraphs we briefly outline the major components of the model and highlight the key processes that are temperature dependent given the focus of this paper on climatic warming; these have been highlighted on Figure 2.

Phytoplankton biomass is simulated as a single aggregated pool, with net primary production (NPP) computed from a temperature dependent "light * biomass" (BZI) function (Brush et al. 2002; Brush and Brawley 2009). The benefit of this approach is that the empirical BZI models are rooted in direct measurements (^{14}C) of productivity that have been shown to apply across a wide range of systems, and produce predicted rates directly comparable to observations (i.e., g C m^{-2} d^{-1} rather than growth rates). Phytoplankton biomass is lost to physical exchange and heterotrophic processes within the water column and sediments, both exponential functions of temperature. In an effort to reduce model uncertainty and eliminate loosely constrained parameters, a single aggregated pelagic heterotrophic function was utilized, which computes plankton community respiration (on both autochthonous and allochthonous OM sources) as a function of temperature and moving-average chlorophyll-*a* biomass. Since shallow marine systems are characterized by strong benthic-pelagic coupling, an empirically-based, well-constrained, system-level relationship between annual sediment carbon remineralization and total annual carbon input from primary production and allochthonous inputs was used to estimate the labile pool of organic carbon reaching the sediment surface (Nixon 1986). Respiration of this labile carbon pool is driven as an exponential function of temperature.

MPB are simulated with a recently developed submodel (Brush et al. *in prep*), formulated using metabolic rates measured in the YRE, the New River estuary, NC and the lagoons of the Delmarva Peninsula. MPB production and respiration are simulated at 0.5 meter depth intervals within each box, as a function of temperature and irradiance at depth (Brush et al. *in prep*). All production and respiration functions described above stoichiometrically produce or consume DO, DIN, and DIP, so these cycling rates are indirectly dependent on temperature. Denitrification rates are also based on a temperature-dependent function calibrated to measurements made in the mainstem Chesapeake Bay and Bay tributaries (Jenkins and Kemp 1984; Kemp et al. 1990; Boynton et al 1995; Kana et al. 1998; Kana et al 2006; Boynton et al 2008; Cornwell and Owens 2011), and modified to account for the effects of low DO as described by Lake and Brush (*in prep*). Finally, air-sea diffusion of oxygen is computed as a function of wind speed and the concentration at saturation, which is in turn a function of water temperature and salinity.

The ecosystem model is coupled to an Officer (1980) two-layer box model, which computes both advective (gravitational circulation) and non-advective (tidal) volumetric exchanges among coarse spatial elements as a function of forced salinity and freshwater inputs. Although box models necessarily lose spatial resolution compared to higher resolution 3-D hydrodynamic circulation models, they nonetheless reproduce typical down-estuary and surface to bottom gradients, operate at the typical scale of available monitoring data (e.g., Fig. 1), are driven by exchanges that are constrained by observations, and enable fast run times (minutes on personal computers), which makes possible the multiple runs required for adequate calibration, sensitivity analysis, and forecasting scenarios. Recent work has confirmed the utility of boxed approaches (Ménesguen et al. 2007; Testa and Kemp 2008; Kremer et al. 2010).

The model was implemented in eight boxes along its axis (Fig. 1). These regions were designated based on long term water quality monitoring by the EPA Chesapeake Bay Program (CBP) and the presence of hypoxia during our own monitoring surveys (see Lake et al. *in review*). The two upstream sites (Boxes 1 and 2) are located within the lower Mattaponi and Pamunkey Rivers, respectively. Boxes 3 and 4 are located in the low mesohaline, while Boxes 5 and 6 are located in the high mesohaline portion of the estuary, which are typically characterized as having little to no signs of hypoxia. The two downstream polyhaline regions (Boxes 7 and 8) have been observed to develop periodic hypoxia during past monitoring surveys and in previous studies (Kuo and Neilson 1987; Kuo et al. 1993; Lake et al. *in review*).

Model Calibration and Skill Assessment

Lake and Brush (*in prep*) calibrated the model to available observations from 2007 to 2010. Model predictions of phytoplankton chlorophyll-*a* and dissolved oxygen followed the measurements made by the CBP within all boxes, throughout all four years. The percent error observed between measured chlorophyll-*a* concentrations and modeled values was relatively low for the whole system (11.2%), and lower for Boxes 5 – 8 (5.4%) where hypoxia occurs. The absolute error associated with bottom water DO in Boxes 5-8 was less than 0.5 mg/L (0.33). Predicted phytoplankton NPP was within the range of metabolic experiments conducted in 2008 and previous studies in the Chesapeake Bay (Smith and Kemp 1995; Harding et al 2002), although the model slightly underestimated some of the higher rates measured in Boxes 7 and 8. Surface water respiration was also within the range of the measured rates from 2008 for Boxes 5 and 6, and within the lower range for Boxes 7 and 8. Bottom water respiration rates, and shoal and deep channel sediment respiration rates were all within the range of the 2008 metabolic experiments, with an absolute error of 0.09, 0.09, and 0.04 g C m^{-2} d^{-1}, respectively. Additionally, deep channel sediment respiration rates overlapped the range reported by Cowan and Boynton (1996) for the lower Chesapeake Bay. Additional details related to model calibration and skill assessment can be found in Lake and Brush (*in prep*).

Climate Simulations

An initial model simulation was conducted under current conditions (CC) between January 2007 and December 2010 to use as a baseline comparison for all subsequent climate simulations. A range of potential warming conditions (1, 2, 3 and 5 °C) were then simulated, rather than specific model projections, in an effort to capture the ecological changes across this range of potential scenarios. This range brackets multi-model climate projections for the Mid-Atlantic under enhanced greenhouse gas concentrations, up to the end of the century (Najjar et al. 2009). Predicted YRE response to a warming climate was quantified as changes in phytoplankton NPP, NEM, and the frequency and extent of hypoxia for each box.

Once the effect of warmer climate conditions was quantified, model runs were conducted to determine how future reductions in nutrient and organic matter loading from the tributaries, surrounding watersheds, and Chesapeake Bay would influence the development of hypoxia under a warming climate. Simulations focused on decreasing these sources by 5, 10, 15, 25, and 50 % relative to current conditions and were conducted over the same range of temperature increases as above (1, 2, 3, and 5 °C). Rates and concentrations from the four year simulations were averaged to account for interannual variability.

RESULTS

Linkage Between Air and Water Temperature

Surface water temperatures in the polyhaline Chesapeake Bay were found to be strongly correlated with regional monthly average air temperatures (Fig. 3a). On average a 1 °C increase in air temperature resulted in a greater than 1 °C increase in surface water temperatures. Chesapeake Bay bottom water temperatures were also found to be tightly coupled to regional air temperatures (Fig. 3b). However, bottom water measurements made between 1984 and 2012 increased on average slightly less than a corresponding increase in air temperatures during this period. Surface water temperatures along the entire axis of the YRE including the lower Mattaponi and Pamunkey Rivers increased linearly with regional air temperatures (near or slightly above a 1:1 ratio) from 1984 to 2012 (Fig. 3c). Similarly, YRE bottom water temperatures for Boxes 1 – 3 and 4 – 8 from 1984 to 2012 exhibited close to a 1:1 correspondence with monthly air temperature (Fig. 3d). These close relationships between air and water temperatures confirm that our model scenarios (+ 1, 2, 3, and 5 °C) should bracket the range of realistic changes based on the projections for air temperature by Najjar et al. (2009).

Changes in Primary Production and Net Ecosystem Metabolism

Rates of phytoplankton NPP were predicted to increase at all sites during winter months (December – February), and in the tributaries and low mesohaline Box 3 during spring (March – May) under all elevated temperature scenarios (Fig 4 a,b). Modeled primary production in spring in most meso- and polyhaline boxes (3 – 8) increased initially under warmer temperatures, however these increases were not as large in the warmest scenario (+5 °C) and in some cases the rates actually decreased relative to current conditions (Fig 4 b). This up-estuary versus down-estuary difference was more pronounced in the summer (June – August) and fall (September – November), as modeled phytoplankton NPP in Boxes 1 – 3 increased with increasing temperatures, while rates in all downstream boxes decreased under warmer conditions (Fig 4 c,d).

Rates of NEM in general followed a similar up-estuary versus down-estuary pattern. During winter months NEM was predicted to increase under warmer temperatures, becoming increasingly net autotrophic with increasing temperatures in Boxes 1 – 5, while NEM in Boxes 6 – 8 decreased (Fig. 5 a). These percent reductions in NEM do not necessarily indicate that NEM became heterotrophic. This was the case during limited time periods in some boxes, but on a seasonal basis the effect of warming in these boxes was to reduce the degree of autotrophy rather than change the metabolic status. During the spring and fall, Boxes 1 – 3 continued to have higher rates of NEM under warmer temperatures (Fig 5 b,d). During both seasons, NEM in mesohaline Boxes 4 and 5 initially increased with temperature, but rates began to decrease under warmer simulations until they were the same or below current conditions. In the polyhaline region, spring and fall NEM generally decreased with increasing temperature. Summer rates of NEM increased in Boxes 1 – 3, as they did during all four seasons (Fig. 5 c). However, the meso- and polyhaline boxes in general had lower NEM values with increasing temperatures throughout the summer. Again, these decreases in NEM reflect less autotrophy rather than a flip to heterotrophy.

Effect of a Warmer Climate on Hypoxia

Increasing temperatures resulted in an increase in the predicted number of hypoxic (< 2 mg L^{-1}) and low oxygen (< 3 mg L^{-1}) days in the upper and lower YRE, although there were limited or no changes mid-estuary (Boxes 3 – 5) (Fig. 6 a,b). However, the effect of warmer temperatures was not equal in the upper and lower estuary. The two tributary boxes (1 and 2) displayed a fairly monotonic increase in the number of both hypoxic and low oxygen days with increasing temperatures, approximately 1 day for every 1 °C increase in temperature (Fig 6 a,b). The number of hypoxic days in the polyhaline region (Boxes 7 and 8) increased at a faster rate than in the oligo- and mesohaline regions upstream (Fig. 6 a). Hypoxia in Box 7 increased by approximately 3 days for each 1 °C increase, for the + 1 to + 3 °C simulations, but only increased another 3 days with an additional two degree increase (+ 5 °C simulation). Within Box 8, the number of hypoxic days increased more exponentially with increasing temperatures, with a 1, 2, 5, and 12 day increase across the scenarios. A similar response was found for the number of days below 3 mg L^{-1}, in the tributaries and polyhaline YRE (Fig. 6 b). Additionally, the + 3 and + 5 °C simulations predicted the occurrence of low oxygen conditions (< 3 mg L^{-1}) in mesohaline Boxes 4 and 5, which under baseline model simulations currently do not develop.

Load Reduction Scenarios

Reduction of nutrients and organic matter entering from both the tributaries and smaller adjacent watersheds surrounding the YRE resulted in a reduction in the number of predicted hypoxic days in both tributary boxes, under all warming scenarios (Fig 7 a-d). However, the amount of reductions necessary to offset the effect of warmer temperatures was different for each tributary box. Tributary and watershed reductions were enough to eliminate hypoxia in Box 1 up to + 5 °C, although higher temperature simulations required up to a 50% reduction of all sources. In Box 2 however, it was not possible to eliminate hypoxia without decreasing these sources by more than 50% after a + 2 °C increase in temperatures. The downstream effect of tributary and watershed load reductions was diminished, resulting in comparatively little improvement in hypoxia (Fig. 7).

Simulated reductions in nutrients, phytoplankton biomass, and organic matter (DOC and POC) entering from the lower CB resulted in the largest improvement in hypoxic days in the high mesohaline and polyhaline regions (Fig. 8 a-d). Warmer temperature simulations of + 1 °C and + 2 °C increased the number of hypoxic days by 2 and 6 in Box 7, and 1 and 3 in Box 8 under current loads. Reducing Chesapeake Bay inputs by 5 and 10%, respectively, was enough to offset this temperature-induced increase in hypoxia. However, to mitigate the development of hypoxia completely in the meso- and polyhaline YRE these reductions would need to be greater than 25%. A + 3 and + 5 °C increase in temperature would require a 15 % and 25% reduction to offset the increase in hypoxic days, respectively, while offsetting an increase of + 3 °C or more would require up to a 50% reduction.

DISCUSSION

Linkage Between Air and Water Temperature

Surface water temperatures in both the polyhaline Chesapeake Bay and the YRE were strongly correlated with regional monthly average air temperatures, and on average increased approximately 1 °C for every 1 °C increase in air temperature (Fig. 3 a,d). While Chesapeake Bay bottom water temperatures between 1984 and 2012 on average increased slightly less than a corresponding increase in air temperature, measurements from the bottom of the YRE increased at a rate similar to the monthly average air temperatures. This analysis confirms that regional atmospheric temperatures can be used to estimate surface and bottom water temperatures in the YRE at approximately a 1:1 ratio, at least within the range of recent atmospheric conditions, as suggested by Najjar et al. (2010). Given this 1:1 correspondence, the range of potential temperature scenarios utilized in this study (+ 1 to + 5 °C) bracket the range of atmospheric predictions for this region (Najjar et al. 2009). However we note that future climate change may alter the linkage between air and water temperatures due to a number of potential feedbacks including increased density stratification isolating the bottom water earlier in the year and higher rates of estuarine circulation advecting relatively cooler coastal ocean water into the bottom of the Bay and subsequently into the tributary estuaries. Nevertheless, we have chosen to utilize these currently strong positive correlations in our climate scenarios until more detailed relationships are developed with hydrodynamic models.

Predicted Ecosystem Function Under a Warmer Climate

Model simulations of phytoplankton NPP displayed two distinct seasonal patterns under warmer temperatures. First, production was predicted to increase during the winter and spring months throughout most of the estuary (Fig. 4 a,b). This increase in winter-spring production was not only a response of temperature-dependent production rates, but also higher phytoplankton biomass and increased respiratory rates that led to higher surface water nutrient concentrations through remineralization of labile organic matter. Secondly, the up-estuary region (Boxes 1 – 3) displayed an increasing response of phytoplankton NPP with increasing temperature during the summer and fall, while rates of production in the down-estuary boxes (4 – 8) decreased with increasing temperatures (Fig. 4 c,d). These responses suggest the potential for dynamic changes in the timing and community composition of future phytoplankton blooms as in Narragansett Bay (Oviatt 2004; Nixon et al. 2009), as well as transfer of this fixed organic matter to adjacent regions of the YRE and to higher trophic levels, as highlighted below.

Modeled phytoplankton NPP during the spring generally increased for all boxes during March and April under increasing temperatures (data not shown). However, model simulations indicated a temporal shift of maximum spring phytoplankton NPP when temperatures were raised above + 1 °C, whereas rates generally increase in March and April, but begin to decrease in May above this temperature scenario. This response is likely a result of increasing production earlier in the spring due to warmer temperatures, and a negative feedback in May as warmer temperatures increase respiration rates as well as heterotrophic consumption. Zooplankton grazing, while not directly accounted for in the model, could potentially be important in terminating the spring bloom under warmer climate conditions, as warmer winter temperatures will likely allow these species to grow faster and reproduce earlier in the season (Oviatt 2004).

Warmer winter temperatures could have an even more complex effect on top-down predation, as species that are normally relatively inactive during cooler winters will instead remain active preying on eggs and larvae, or as warmer water species are capable of extending their range and seasonal distribution (Sullivan et al. 2001; Oviatt 2004; Doney et al. 2012).

During the summer and fall, simulated phytoplankton NPP increased in the up-estuary boxes (1 – 3) during all months, although this effect was greater during the summer. In most of the meso- and polyhaline regions (Boxes 4 – 8) this trend was reversed, with lower production with increasing temperature. It should be noted that during the warmest temperature simulations, phytoplankton production during the summer in Boxes 6 – 8 decreased by more than 20% and 30% during the + 3 and + 5 °C simulations, respectively. This reduction in phytoplankton NPP was most likely a result of lower seasonal phytoplankton biomass in Boxes 4 - 8, as indicated by modeled chlorophyll-*a* concentrations. WC Chl-a during the summer in the + 5 °C simulation, specifically July and August, was approximately half of the modeled concentrations under the CC simulation. Similar decreases occurred during the fall when rates were relatively lower.

Model simulations suggest that relatively more organic material will be fixed into phytoplankton biomass in the up-estuary region of the YRE and subsequently advected down–estuary under warmer temperatures, while less phytoplankton biomass will be produced in the lower YRE. The water column and benthic communities in both of these regions will likely be affected by this change in phytoplankton primary production. Warmer mean winter temperatures have been directly correlated with lower mean monthly phytoplankton bloom biomass in other coastal systems (Oviatt et al. 2002), potentially supplying less organic matter to higher trophic levels, specifically benthic detritivores that rely on organic carbon deposited during intense blooms (Nixon et al. 2009). Indeed, phytoplankton primary production appears to be tightly linked to macrobenthic biomass in cross-system comparisons (Herman et al. 1999; Hagy 2002; Kemp et al. 2005). Additionally, changes in phytoplankton bloom communities to smaller, less-nutritious species has been suggested as a factor reducing bivalve growth and reproductive rates (Tracey et al. 1988). The ecological significance of changes in phytoplankton dynamics can be wide-reaching, as illustrated in Narragansett Bay where the transition from annual winter-spring blooms to more ephemeral and less intense summer-autumn blooms has resulted in a reduction of organic matter reaching the benthos, subsequently reducing rates of benthic metabolism and nutrient regeneration and ultimately turning the sediments from a net nitrogen sink into a source of fixed nitrogen (Fulweiler et al. 2007; Nixon et al. 2009).

Combining these predicted changes in water column production with model predictions of MPB production and water column and benthic respiration further illustrates the region-specific responses characteristic of this system (Lake and Brush *in prep*). Throughout all four seasons, increasing rates of primary production (both water column and benthic) offset the increasing rates of respiration in Boxes 1 - 3, resulting in an increase in NEM (Fig. 5 a-d). However, there were periods of the year, particularly May and September when this region had lower NEM than under current conditions (data not shown). Overall, the model indicated that increasing temperatures in this region will drive this part of the estuary to become more net autotrophic, supplying additional labile organic matter to the rest of the estuary and potentially the lower Chesapeake Bay. The biogeochemical processing of this additional organic material under warmer summer temperatures will act to fuel oxygen consumption in the mesohaline portion of the estuary, which does not presently experience hypoxia.

During the spring, mesohaline Boxes 4 and 5 displayed month to month variation in simulated NEM, with changes over current conditions resulting from increased primary production within these boxes, elevated rates of respiration, and the advection of labile organic matter from both up-estuary boxes and Chesapeake Bay. The latter has been shown to be an important source of organic material leading to reduced oxygen concentrations in this system (Lake and Brush *in prep*). Predicted NEM in this region of the estuary decreased in the summer due to decreasing phytoplankton NPP and increasing respiration rates with warming temperatures (Fig. 4 c). Rates remained relatively constant with increasing temperatures throughout the fall (Fig. 5 d), however rates during September generally decreased with increasing temperature.

While phytoplankton NPP during the winter months were predicted to increase in the polyhaline YRE (Boxes 7 and 8), the relatively higher rates of predicted respiration were more than enough to offset this increase in production under warmer temperature simulations (Fig. 5a). This trend of decreasing NEM with increasing temperatures was fairly consistent for Boxes 6 – 8 throughout the spring, summer, and fall (Fig. 5 b-d). This is likely due to four factors: generally lower rates of phytoplankton NPP (Fig. 4 b-d), relatively lower surface area to volume ratios within this region due to a deeper channel, higher rates of organic matter loading from up-estuary and the lower Chesapeake Bay, and the resulting higher rates of water column and sediment respiration with increasing temperatures. This ecosystem shift in NEM in the lower estuary reinforces predictions from other recent studies indicating that heterotrophic metabolism is more sensitive to changing temperatures than autotrophic production (López-Urrutia et al. 2006; O'Connor et al. 2009).

Effect of Warmer Temperatures on Hypoxia

Warmer temperatures were predicted to increase not only the number of low oxygen days, but also the spatial extent of low oxygen in the YRE (Fig. 6 a,b). The effect of warming in the lower Mattaponi and Pamunkey Rivers was relatively monotonic, with a one day increase in hypoxia for each 1 °C increase in temperature, up to + 5 °C. The development of low dissolved oxygen in this region appeared to be a result of high inputs of watershed-derived organic matter and warmer temperatures driving higher metabolic rates, combined with elevated phytoplankton biomass and NPP during the spring and early summer (April – June), which is when the model predicted the development of low oxygen and hypoxia in the bottom water. A portion of this additional biomass is probably respired within the tributaries, reducing dissolved oxygen concentrations, before this labile organic matter is flushed downstream. While this study did not focus on physical factors that may influence this process, it is likely that strong tidal and wind mixing, along with high river discharge may alter this relationship as the surface and bottom water are mixed more thoroughly, or as material is flushed out of the region more quickly.

The low mesohaline YRE did not reach hypoxic conditions during any of the warming simulations. This is probably due in part to the extensive shoals, higher surface area to volume ratio, and relatively shallow depths in this region, which make it subject to strong mixing by winds. However, the greatest temperature increases (+ 3 and + 5 °C) were enough to produce low oxygen conditions in Box 4. The high mesohaline region of the estuary was a transition zone where hypoxia developed in Box 6 under warmer temperature scenarios; however, oxygen concentrations in Box 5 remained above 2 mg L^{-1} throughout all simulations (Fig 6 a). Both regions did have an increase in the predicted number of low oxygen (< 3 mg L^{-1}) days with increasing temperatures (Fig 6 b).

The polyhaline boxes (7 and 8) represent the most susceptible region to hypoxia under current conditions, as well as warmer climate conditions (Fig. 6 a,b). This is due in part to a variety of factors. First, this region is directly influenced by advection of labile organic matter from the lower mainstem Chesapeake Bay, which has been shown to contribute significantly to decreasing oxygen concentrations in this region (Lake and Brush *in prep*). Secondly, under warmer temperatures, heterotrophic respiration was predicted to increase faster than autotrophic production, resulting in greater consumption of this labile organic material and consequent reductions in oxygen concentrations. Third, warmer water temperatures contain less oxygen per volume than corresponding cooler waters, based on oxygen solubility. Finally, model simulations of phytoplankton NPP indicate that this region will have lower rates of primary production under warmer temperatures (Fig 4 b-d), reducing the production of oxygen in surface waters.

Management Scenarios Under a Warmer Climate

Previous model simulations under current conditions indicated that reducing nutrient and organic matter loading from the tributaries and surrounding watersheds would result in the largest improvements in dissolved oxygen within Boxes 1 – 3 (Lake and Brush *in prep*). While reducing watershed loads again resulted in improvements in these boxes at a given temperature, in many cases the resulting number of annual hypoxic days under elevated temperatures was still greater than under current conditions (Fig. 7 a-d). This finding indicates that greater tributary and watershed load reductions will be required to offset hypoxia in this region of the YRE under a warmer climate, compared to reductions that would be required under current climate conditions (Fig. 9 a-d).

Previous simulations also indicated that the development of hypoxia in the polyhaline YRE is strongly influenced by the supply of nutrient- and organic-rich water advected from the lower Chesapeake Bay via estuarine circulation (Lake and Brush *in prep*). As above, reductions in these inputs at a given temperature resulted in an improvement in hypoxia; however the resulting number of annual hypoxic days under warmer temperatures was in many cases greater than under current conditions (Fig. 8 a-d). This is particularly evident in the CB reduction scenarios under + 3 and + 5 °C temperature increases. Even if concentrations of nutrients, phytoplankton biomass, and organic matter (DOC and POC) entering from the CB are reduced to 75% of their current concentrations, the model simulations indicated that the YRE would still develop hypoxia in the lower estuary with a 2 °C increase in temperature, which is projected to occur between 2040 – 2069 (Najjar et al 2009). This finding again demonstrates that greater load reductions will be required to offset hypoxia under a warmer climate compared to reductions required under current climate conditions (Fig. 9 a-d).

Future Climate Change

While this analysis focused solely on the effect of increased temperature on ecosystem function and hypoxia, it is important to note that these changes will be confounded by regional changes in precipitation, which ultimately control the input of nitrogen, phosphorous, sediments, and organic carbon from the surrounding watershed. Seasonal changes in precipitation and evaporation have the potential to alter the temporal and spatial extent of water column stratification and hypoxia. Kemp et al. (2005) illustrated the tightly-coupled relationship between higher river flow (January to May) from the Susquehanna River and the volume of hypoxia and anoxia in the mainstem Chesapeake Bay. Future climate model predictions indicate that precipitation for the Chesapeake Bay watershed could increase annually by 3, 7, and 9 % above the 1971-2000 period between 2010-2039, 2040-2069, and 2070-2099, respectively (Najjar et al. 2009). While the seasonal timing of this increase in precipitation will determine how this additional freshwater will contribute to hypoxia in the Bay and its tributaries, it will likely lead to greater stratification, increase watershed loading of nutrients and organic matter, and enhance estuarine circulation, thereby advecting more organic matter into the tributaries. These factors will likely fuel greater production and higher respiration rates, contributing to increases in the frequency, severity, and spatial extent of hypoxia. Wind forcing has also been identified as an important mechanism influencing hypoxia in the Chesapeake Bay (Scully 2010); if summertime winds increase as a result of climate change (due to increasing storm activity or regional atmospheric patterns) this direct physical mixing of the system could act to counteract other climatic effects driving hypoxia such as elevated temperatures. Additional climate related changes may also affect ecosystem function and hypoxia including atmospheric composition (in particular CO_2 concentrations), elevated sea level rise, increased storminess, changes in planktonic community composition, and loss of important habitat (e.g., seagrass and marshes) (Najjar et al. 2010; Doney et al. 2012). We still lack a complete understanding of how all these complex climatic changes will interact with ongoing watershed load reductions to shape estuarine responses. Developing this understanding will require additional studies focused on both individual stressors as well as multiple factors acting in combination.

CONCLUSIONS

Model simulations suggest that water column primary production will respond positively to climate warming in the winter and spring throughout most of the YRE, while decreasing in the summer and fall within the high mesohaline and polyhaline regions. These changes in primary production, along with increasing rates of water column and sediment respiration, were predicted to drive the YRE tributaries and portions of the low mesohaline YRE to become more autotrophic, presumably due to increased rates of nutrient cycling. However, NEM was predicted to decrease during the spring, summer and fall throughout the rest of the estuary due to decreased productivity and increased respiration. These changes combined with decreased oxygen solubility at warmer temperatures resulted in marked increases in the predicted duration and spatial extent of bottom water hypoxia (< 2 mg L^{-1}), with the tributaries experiencing a relatively monotonic increase in the number of hypoxic days during the late spring and early summer. Low oxygen conditions in the polyhaline region, which is currently the most susceptible region to hypoxia, were predicted to increase more rapidly with increasing temperatures.

Results confirm those of Lake et al. (*in prep*) that a multifaceted management strategy is needed, in which watershed reductions are required to improve hypoxic conditions in the upper estuary (Boxes 1 – 4) while Chesapeake Bay reductions are necessary to limit the development of hypoxia in the lower estuary (Boxes 5 – 8). However, model simulations suggest that climatic warming will require additional load reductions beyond those required to mitigate hypoxia in the absence of warming. These reductions may need to be significant, and will likely be complicated by losses of wetlands and buffer zones with continued development of the watershed and projected sea level rise. While these findings highlight the potential effect of increasing temperatures on water column primary production, NEM, and hypoxia, these changes will be confounded by other direct and indirect effects of climate change and additional modeling studies are needed to predict the interactive effects of these climatic changes.

ACKNOWLEDGEMENTS

This project was funded by a grant from_________________ #__________________. S. J. Lake also received financial support from NSF GK-12 (Division of Graduate Education 0840804). We would also like to thank Iris Anderson, Larry Haas, Jennifer Stanhope, Hunter Walker, Lisa Ott, Juliette Giordano, and many other VIMS students and staff members for their field and laboratory assistance. This is Virginia Institute of Marine Science contribution no. XXXX.

LITERATURE CITED

Boesch, D. F. 2002. Challenges and Opportunities for Science in Reducing Nutrient Over-Enrichment of Coastal Ecosystems. *Estuaries and Coasts* 25: 886-900.

Boynton, W. R., J. H. Garber, R. Summers, and W. M. Kemp. 1995. Inputs, Transformations, and Transport of Nitrogen and Phosphorus in Chesapeake Bay and Selected Tributaries. *Estuaries* 18: 285-314.

Boynton, W. R., and E. M. Bailey. 2008. Sediment Oxygen and Nutrient Exchange Measurements from Chesapeake Bay, Tributary Rivers, and Maryland Coastal Bays: Development of a Comprehensive Database & Analysis of Factors Controlling Patterns and Magnitude of Sediment-Water Exchanges. University of Maryland, Center for Environmental Science Technical Report Series. TS-542-08.

Brush, G. S., and F. W. Davis. 1984. Stratigraphic Evidence of Human Disturbance in an Estuary. *Quaternary Research* 22: 91-108.

Brush, G. S. 2009. Historical Land Use, Nitrogen, and Coastal Eutrophication: A Paleoecological Perspective. *Estuaries and Coasts* 32: 18-28.

Brush, M. J. 2002. Development of a Numerical Model for Shallow Marine Ecosystem with Applications to Greenwich Bay, R.I. Ph.D. Dissertation. University of Rhode Island, Kingston, RI.

Brush, M. J. 2004. Application of the Greenwich Bay Ecosystem Model to the Development of the Greenwich Bay SAMP (Special Area Management Plan). Final report to the Rhode Island Coastal Resources Center, University of Rhode Island, Narragansett, RI.

Brush, M. J., J. W. Brawley, S. W. Nixon, and J. N. Kremer. 2002. Modeling Phytoplankton Production: Problems with the Eppley Curve and an Empirical Alternative. *Marine Ecology Progress Series* 238: 31-45.

Brush, M.J. and J.W. Brawley. 2009. Adapting the light • biomass (BZI) models of phytoplankton primary production to shallow marine ecosystems. *Journal of Marine Systems* 75: 227–235.

Brush, M.J., and S.W. Nixon. 2010. Modeling the Role of Macroalgae in a Shallow Sub-Estuary of Narragansett Nay, RI (USA). *Ecological Modelling* 221: 1065-1079.

Brush, M. J. and S. W. Nixon. *In review.* An Intermediate Complexity, Hybrid Empirical-Mechanistic Eutrophication Model For Shallow Marine Ecosystems. Submitted to *Ecological Modelling.*

Brush M. J., S. J. Lake, and J. C. P Giordano. *In prep.* Constraining a Model of Microphytobenthos in a Temperate Estuary. In preparation for *Estuarine, Coastal and Shelf Science.*

Canuel, E. A., S. S. Crammer, H. A. McIntosh, and S. R. Pondell. 2012. Climate Change Impacts on the Organic Carbon Cycle at the Land-Ocean Interface. *Annual Review* of *Earth* and *Planetary Science* 40: 685-711.

Cloern, J. E. 2001. Our Evolving Conceptual Model of the Coastal Eutrophication Problem. *Marine Ecology Progress Series* 210: 223-253.

Cloern, J. E., and A. D. Jassby. 2008. Complex Seasonal Patterns of Primary Producers at the Land–Sea Interface. *Ecology Letters* 11: 1294-1303.

Cooper, S. R., and G. S. Brush. 1993. A 2,500-Year History of Anoxia and Eutrophication in Chesapeake Bay. *Estuaries and Coasts* 16: 617-626.

Cooper, S. R. 1995. Chesapeake Bay Watershed Historical Land Use: Impact on Water Quality and Diatom Communities. *Ecological Applications* 5: 703-723.

Cornwell, J. C., and M. S. Owens. 2011. Quantifying Sediment Nitrogen Releases Associated with Estuarine Dredging. *Aquatic Geochemistry* 17: 499-517.

Cowan, J. L., and W. R. Boynton. 1996. Sediment-Water Oxygen and Nutrient Exchanges Along the Longitudinal Axis of Chesapeake Bay: Seasonal Patterns, Controlling Factors and Ecological Significance. *Estuaries* 19: 562-580.

Dauer, D. M., H. G. Marshall, J. R. Donat, M. F.Lane, S. C.Doughten, P. L. Morton, and F. A. Hoffman. 2005. Status and Trends in Water Quality and Living Resources in the Virginia Chesapeake Bay: James River (1985-2004). Final Report to the Virginia Department of Environmental Quality, Richmond, Virginia. Applied Marine Research Laboratory, Norfolk VA. 1-63.

de Jonge, V. N., W. Boynton, C. F. D'Elia, R. Elmgren, and R. L. Welsh. 1994. Responses to Developments in Eutrophication in Four Different North Atlantic Estuarine Systems. *Olsen & Olsen, Fredensborg, Denmark.* 179-196.

Diaz, R. J., R. J. Neubauer, L. C. Schaffner, L. Pihl, and S. P. Baden. 1992. Continuous Monitoring of Dissolved Oxygen in an Estuary Experiencing Periodic Hypoxia and the Effects of Hypoxia on Macrobenthos and Fish. *Science in the Total Environment* (Supplement 1992): 1055-1068.

Doney, S. C., M. Ruckelshaus, J. E. Duffy, J. P. Barry, F. Chan, C.A. English, H. M. Galindo, J. M. Grebmeier, A. B. Hollowed, N. Knowlton, J.y Polovina, N. N. Rabalais, W. J. Sydeman, and L. D. Talley. 2012. Climate Change Impacts on Marine Ecosystems. *Marine Science* 4: 11-37.

Dynesius, M., and C. Nilsson.1994. Fragmentation and Flow Regulation of River Systems in the Northern Third of the World. *Science* 266: 753-753.

Edwards, M., and A. J. Richardson. 2004. Impact of Climate Change on Marine Pelagic Phenology and Trophic Mismatch. *Nature* 430: 881-884.

Fulweiler, R. W., S. W. Nixon, B. A. Buckley, and S. L. Granger. 2007. Reversal of the Net Dinitrogen Gas Flux in Coastal Marine Sediments. *Nature* 448: 180-182.

Goldberg, E. D., V. Hodge, M. Koide, J. Griffin, E. Gamble, O. P. Bricker, G. Matisoff, G.R. Holdren, and R. Braun. 1978. A Pollution History of Chesapeake Bay. *Geochimica et cosmochimica acta* 42: 1413-1425.

Haas, L. W. 1977. The Effect of the Spring-Neap Tidal Cycle on the Vertical Salinity Structure of the James, York, and Rappahannock Rivers, Virginia, U.S.A. *Estuarine and Coastal Marine Science* 5: 485-496.

Hagy, J. D. 2002. Eutrophication, Hypoxia and Trophic Transfer Efficiency in Chesapeake Bay. Ph.D. Dissertation, University of Maryland, College Park, MD.

Harding Jr., L. W., M. E. Mallonee, and E. S. Perry. 2002. Toward a Predictive Understanding of Primary Productivity in a Temperate, Partially Stratified Estuary. *Estuarine, Coastal and Shelf Science* 55: 437-463.

Hayward D., C. S. Welch, and L. W. Haas. 1982. York River Destratification: An Estuary-Subestuary Interaction. *Science* 216: 1413-1414.

Herman, P. M. J., J. J. Middleburg, J. Van De Koppel, C. H. R. Heip. 1999. Ecology and Estuarine Macrobenthos. *Advances in Ecological Research* 29: 195-240.

International Panel on Climate Change (IPCC) 2007. Climate Change 2007: Synthesis Report. Contribution of Working Group to the Fourth Assessment Report of the Intergovernmental Panel on Climate Change.

Jenkins, M. C. and W. M. Kemp. 1984. The Coupling of Nitrification and Denitrification in Two Estuarine Sediments. *Limnology and Oceanography* 29: 609-619

Kana, T. M., M. B. Sullivan, J. C. Cornwell and K. M. Groszkowski. 1998. Denitrification in Estuarine Sediments Determined by Membrane Inlet Mass Spectrometry. *Limnology and Oceanography* 43:334-339.

Kana, T. M., J. C. Cornwell, and L. Zhong. 2006. Determination of Denitrification in the Chesapeake Bay from Measurements of N_2 Accumulation in Bottom Water. *Estuaries and Coasts* 29: 222-231.

Kemp, W. M., P. Sampou, J. Caffrey, M. Mayer, K. Henriksen, and W. R. Boynton 1990. Ammonium Recycling Versus Denitrification in Chesapeake Bay Sediments. *Limnology and Oceanography* 35: 1545-1563.

Kemp, W. M., W. R. Boynton, J. E. Adolf, D. F. Boesch, W. C. Boicourt, G. Brush, J. C. Cornwell, T. R. Fisher, P. M. Glibert, J. D. Hagy, L. W. Harding, E. D. Houde, D. G. Kimmel, W. D. Miller, R. I. E. Newell, M. R. Roman, E. M. Smith, and J. C. Stevenson. 2005. Eutrophication of Chesapeake Bay: Historical Trends and Ecological Interactions. *Marine Ecology Progress Series* 303: 1-29.

Kremer, J. N., J. Vaudrey, D. Ullman, D. Bergondo, N. LaSota, C. Kincaid, D. Codiga, and M. J. Brush. 2010. Simulating Property Exchange in Estuarine Ecosystem Models at Ecologically Appropriate Scales. *Ecological Modelling* 221:1080-1088.

Kuo, A.Y. and B.J. Neilson. 1987. Hypoxia and Salinity in Virginia Estuaries. *Estuaries* 10: 277-283.

Kuo, A. Y., B. J. Neilson, J. Brubaker, and E. P. Ruzecki. 1993. Data Report: Hypoxia in the York River, 1991. Virginia Institute of Marine Science Data Report No. 47. Gloucester Point, Virginia.

Lake, S. J., M. J. Brush, I. C. Anderson, and H. I. Kator. *In review*. Internal Versus External Drivers of Periodic Hypoxia in a Coastal Plain Tributary Estuary: the York River, Virginia. *Marine Ecological Progressive Series*. Submitted for publication 2012.

Lake, S. J., and M. J. Brush. *In prep*. Modeling the Contribution of Multiple Organic Matter Sources to the Development of Periodic Hypoxia in a Tributary Estuary: the York River, Virginia.

Levitus, S., Antonov, J. I., Boyer, T. P., and C. Stephens 2000. Warming of the World Ocean. *Science* 287: 2225-2229

López-Urrutia, Á., E. San Martin, R. P. Harris, and X. Irigoien. 2006. Scaling the Metabolic Balance of the Oceans. *Proceedings of the National Academy of Sciences* 103: 8739-8744.

Lotze, H. K. 2010. Historical Reconstruction of Human-Induced Changes in US Estuaries. *Oceanography and Marine Biology: an annual review*. 48.

Ménesguen, A., Cugier, P., Loyer, S., Vanhoutte-Brunier, A., Hoch, T., Guillaud, J-F., Gohin, F., 2007. Two- or Three-Layered Box-Models Versus Fine 3D Models for Coastal Ecological Modelling? A Comparative Study in the English Channel (Western Europe). *Journal of Marine Systems* 64: 47-65.

Moore, K. A., E. C. Shields, D. B. Parrish, and R. J. Orth. 2012. Eelgrass Survival in Two Systems: Role of Turbidity and Summer Water Temperatures. *Marine Ecology Progressive Series* 448: 247-258.

Moss, B., S. Kosten, M. Meerhof, R.Battarbee, E. Jeppesen, N. Mazzeo, K. Havens, , G.Lacerot, Z. Liu, L. De Meester, H. Paerl, and M. Scheffer. 2011. Allied Attack: Climate Change and Eutrophication. *Inland Waters* 1: 101-105.

Murdoch, P. S., J. S. Baron, and T. L. Miller. 2000. Potential Effects of Climate Change on Surface-Water Quality in North America. *JAWRA Journal of the American Water Resources Association* 36: 347-366.

Najjar, R., L. Patterson, and S. Graham. 2009. Climate Simulations of Major Estuarine Watersheds in the Mid-Atlantic Region of the US. *Climate Change* 95: 139-168.

Najjar, R. G., C. R. Pyke, M. B. Adams, D. Breitburg, C. Hershner, M. Kemp, R. Howarth, M. E. Mulholland, M. Paolisso, D. Secor, K. Sellner, D. Wardrop, R. Wood. 2010. Potential Climate-Change Impacts on the Chesapeake Bay. *Estuarine, Coastal and Shelf Science* 86: 1-20.

Nixon, S. W. 1986. Nutrient Dynamics and the Productivity of Marine Coastal Waters. Pages 97 – 115 *in* R. Halwagy, D. Clayton, and M. Behbehani, editors. Marine Environment and Pollution. The Alden Press, Oxford, United Kingdom.

Nixon, S. W. 2009. Eutrophication and the Macroscope. *Hydrobiologia* 629: 5-19.

Nixon, S. W., R. W. Fulweiler, B. A. Buckley, S. L. Granger, B. L. Nowicki, and K. M. Henry. 2009. The Impact of Changing Climate on Phenology, Productivity, and Benthic–Pelagic Coupling in Narragansett Bay. *Estuarine, Coastal and Shelf Science*, *82*(1), 1-18.

O'Connor, M. I., M. F. Piehler, D. M. Leech, A. Antonand, J. F. Bruno. 2009. Warming and Resource Availability Shift Food Web Structure and Metabolism. *PLoS biology.* 7: e1000178.

Odum, H. T. 1994. Ecological and General systems: an Introduction to Systems Ecology (2nd ed.) University Press of Colorado, Niwot, Colorado, USA.

Officer, C. B. 1980. Box Models Revisited. pp. 65-114 *in*: Hamilton, P. and K. B. MacDonald (eds.). Estuarine and wetland processes with emphasis on modeling. Plenum Press, New York.

Oviatt, C., A. Keller, and L. Reed. 2002. Annual Primary Production in Narragansett Bay with No Bay-Wide Winter–Spring Phytoplankton Bloom. *Estuarine, Coastal and Shelf Science.* 54: 1013-1026.

Oviatt, C. A. 2004. The Changing Ecology of Temperate Coastal Waters During a Warming Trend. *Estuaries and Coasts* 27: 895-904.

Pace, M. L. 2001. Predictions and the Aquatic Sciences. *Canadian Journal of Fisheries and Aquatic Sciences* 58: 63-72.

Paerl, H. W., and J. Huisman. 2008. Blooms Like it Hot. *Science 320* : 57.

Paerl, H. W., and J. Huisman. 2009. Climate Change: A Catalyst for Global Expansion of Harmful Cyanobacterial Blooms. *Environmental Microbiology Reports* 1: 27-37.

Paerl, H. W., and T. G. Otten. 2013. Harmful Cyanobacterial Blooms: Causes, Consequences, and Controls. *Microbial Ecology* 1-16.

Perry, J. E., and C. H. Hershner. 1999. Temporal Changes in the Vegetation Pattern in a Tidal Freshwater Marsh. *Wetlands* 19: 90-99.

Perry, J. E., and R. B. Atkinson. 2009. York River Tidal Marshes. *Journal of Coastal Research* 57: 40-49.

Reckhow, K. H. 1999. Water Quality Prediction and Probability Network Models. *Canadian Journal of Fisheries and Aquatic Sciences* 56: 1150-1158.

Rizzo, W. M. and R. L. Wetzel. 1985. Intertidal and Shoal Benthic Community Metabolism in a Temperate Estuary: Studies of Spatial and Temporal Scales of Variability *Estuaries* 8: 342-351.

Scavia, D., J. C. Field, D. F. Boesch, R.W. Buddemeier, V. Burkett, D.l R. Cayan, M.Fogarty, M. A. Harwell, R. W. Howarth, C. Mason, D. J. Reed, T. C. Royer, A. H. Sallenger, and J. G. Titus. 2002. Climate Change Impacts on US Coastal and Marine Ecosystems. *Estuaries and Coasts* 25: 149-164.

Scavia, D., E.L.A. Kelly, and J.D. Hagy III. 2006. A Simple Model for Forecasting the Effects of Nitrogen Loads on Chesapeake Bay Hypoxia. *Estuaries and Coasts* 29: 674–684.

Scavia, D., D. Justic, and V. J. Bierman Jr. 2004. Reducing Hypoxia in the Gulf of Mexico: Advice from Three Models. *Estuaries* 27: 419-425.

Scully, M. E. 2010. The Importance of Climate Variability to Wind-Driven Modulation of Hypoxia in Chesapeake Bay. *Journal of Physical Oceanography* 40: 1435-1440.

Sharples J., J. H. Simpson, and J. M. Brubaker. 1994. Observations and Modelling of Periodic Stratification in the Upper York River Estuary, Virginia. *Estuaries, Coastal and Shelf Science* 38: 301-312.

Shen, J. and L. Haas. 2004. Calculating Age and Residence Time in the Tidal York River Using Three-Dimensional Model Experiments. *Estuaries, Coastal and Shelf Science* 61: 449-461.

Smith, E. M., and W. M. Kemp. 1995. Seasonal and Regional Variations in Plankton Community Production and Respiration for Chesapeake Bay. *Marine Ecology Progressive Series* 116: 217-231.

Smith, L. M., S. Whitehouse, and C. A. Oviatt. 2010. Impacts of Climate Change on Narragansett Bay. *Northeastern Naturalist* 17: 77-90.

Sullivan, B.K., D. van Keuren, and M. Clancy. 2001. Timing and Size of Blooms of the Ctenophore *Mnemiopsis leidyi* in Relation to Temperature in Narragansett Bay, RI. Hydrobiologia 451: 113-120.

Smith, L. M., S. Whitehouse, and C. A. Oviatt. 2010. Impacts of Climate Change on Narragansett Bay. *Northeastern Naturalist.* 17: 77-90.

Stow, C.A., Roessler, C., Borsuk, M.E., Bowen, J.D., Reckhow, K.H., 2003. Comparison of Estuarine Water Quality Models for Total Maximum Daily Load Development in Neuse River Estuary. *Journal Water Resources Planning and Management* 129: 307-314.

Swaney, D.P., D. Scavia, R.W. Howarth, and R.M. Marino. 2008. Estuarine Classification and Response to Nitrogen Loading: Insights from Simple Ecological Models. *Estuarine, Coastal and Shelf Science* 77: 253–263

Testa, J. M., and W. M. Kemp. 2008. Regional, Seasonal, and Inter-Annual Variability of Biogeochemical Processes and Physical Transport in a Partially Stratified Estuary: A Box-Modeling Analysis. *Marine Ecology Progress Series* 356: 63-79.

Tracey, G. A., P. W. Johnson, R. W. Steele, P. E. Hargraves, and J. M. Sieburth. 1988. Shift in Photosynthetic Picoplankton Composition and its Effect on Bivalve Mollusc Nutrition: The 1985 'Brown Tide' in Narragansett Bay, Rhode Island. *Journal of Shellfish Research JSHRDA* 7: 671-675.

U.S. Environmental Protection Agency (EPA). 2010. Chesapeake Bay Total Maximum Daily Load for Nitrogen, Phosphorus and Sediment. Region III Chesapeake Bay Program Office, Annapolis, MD.

Whitehead, P. G., R. L. Wilby, R. W. Battarbee, M. Kernan, and A. J. Wade. 2009. A Review of the Potential Impacts of Climate Change on Surface Water Quality. *Hydrological Sciences Journal* 54: 101-123.

Zimmerman, A. R., and E. A. Canuel. 2000. A Geochemical Record of Eutrophication and Anoxia in Chesapeake Bay Sediments: Anthropogenic Influence on Organic Matter Composition. *Marine Chemistry* 69: 117-137.

CHAPTER 3 - FIGURES

Figure 3-1. Map of the York River estuary and the Chesapeake Bay (insert), including box model boundaries, small ungauged watersheds, and corresponding long-term Chesapeake Bay Program (bulls eyes) monitoring stations. Boxes 1 and 2 are located within the lower Mattaponi and Pamunkey Rivers, respectively. Boxes 3 and 4 are located in the low mesohaline, while Boxes 5 and 6 are located in the high mesohaline, and Boxes 7 and 8 are in the polyhaline portion of the estuary.

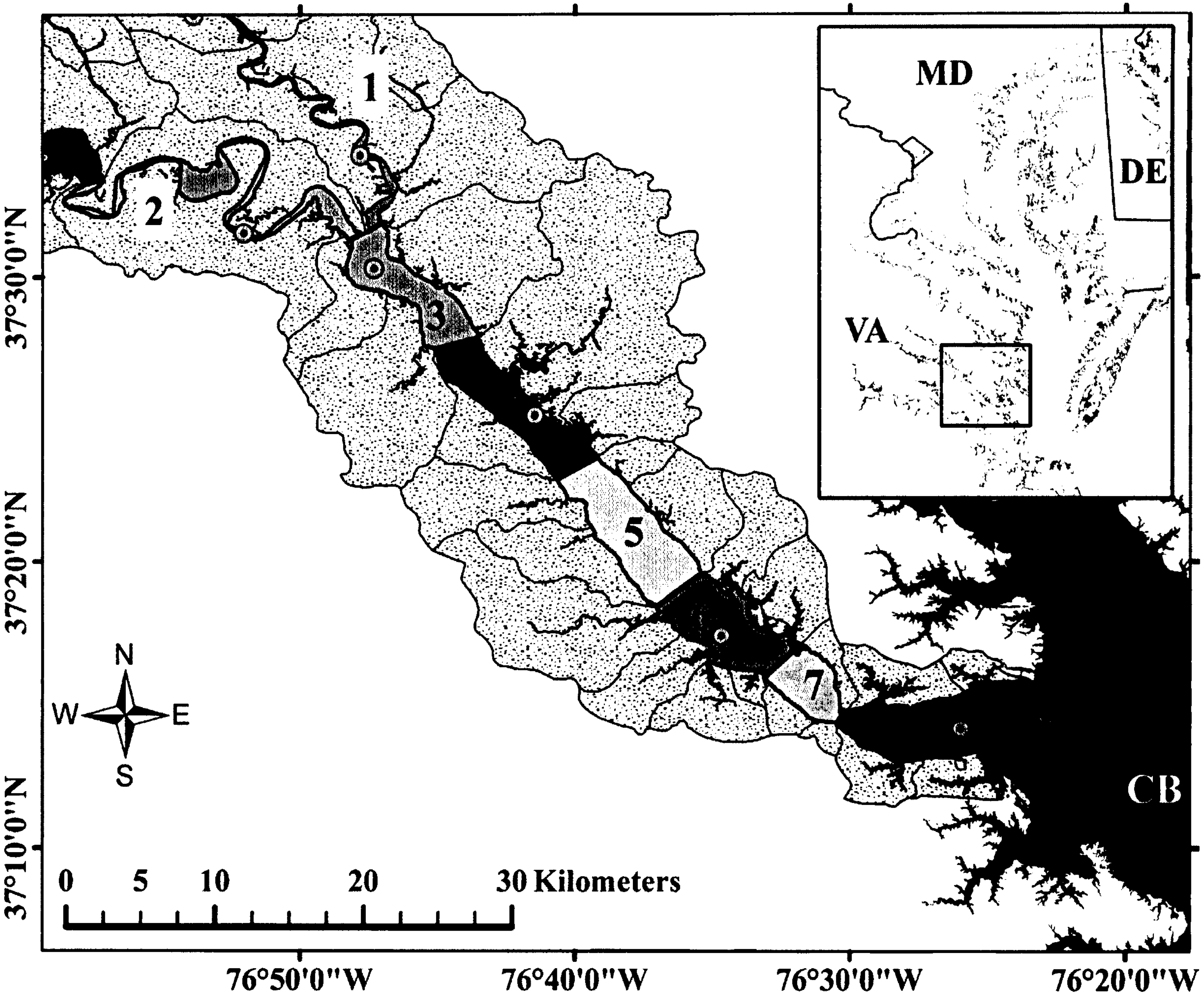
1
2
3
5
7
MD
DE
VA
CB
N
W
E
S
0
5
10
20
30 Kilometers
37°30'0"N
37°20'0"N
37°10'0"N
76°50'0"W
76°40'0"W
76°30'0"W
76°20'0"W

Figure 3-2. Diagram of the intermediate-complexity eutrophication model. State variables, major flows (with arrows), and major connections (without arrows) are depicted. Flows that consume material (e.g. nutrient uptake, oxygen consumption, loss of biomass) are shown with solid lines. Flows which produce material (e.g. remineralization, photosynthetic oxygen production) are shown with broken lines. Red lines and symbols highlight variables (and rates) that are temperature dependent. To reduce the complexity of the figure, all respiratory demands are shown as being integrated into an estimate of total pelagic respiration (R_{WC}), which draws from the oxygen pool and remineralizes N and P. WS = watershed, AT = atmospheric. All other terms are defined in the text. Symbols are those of Odum (1994). Adapted from Brush and Nixon (*in review*) and Lake and Brush (*in prep*).

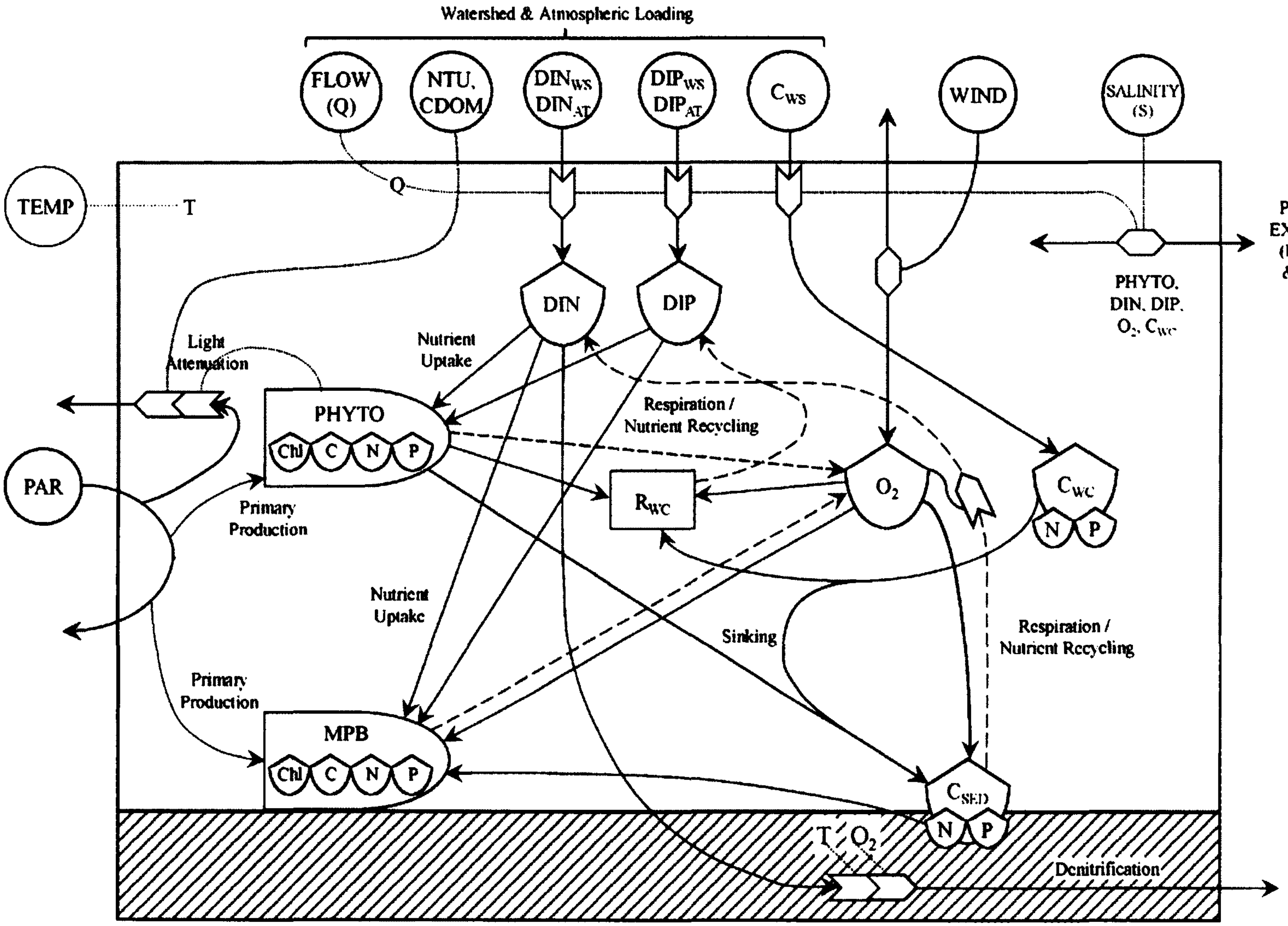
Watershed & Atmospheric Loading
FLOW (Q)
NTU, CDOM
DIN_{WS} DIN_{AT}
DIP_{WS} DIP_{AT}
C_{WS}
WIND
SALINITY (S)
TEMP
T
Q
PHYSICAL EXCHANGES (horizontal & vertical)
PHYTO, DIN, DIP, O_2, C_{WC}
DIN
DIP
Light Attenuation
Nutrient Uptake
PHYTO
Chl
C
N
P
Respiration / Nutrient Recycling
R_{WC}
O_2
C_{WC}
N
P
PAR
Primary Production
Nutrient Uptake
Sinking
Respiration / Nutrient Recycling
Primary Production
MPB
Chl
C
N
P
C_{SED}
N
P
T
O_2
Denitrification

Figure 3-3. Polyhaline Chesapeake Bay (a) surface and (b) bottom water temperatures (CBP) plotted against mean monthly air temperatures measured at Norfolk International Airport, between 1949 – 1982 and 1984 – 2012. York River estuary (c) surface and (d) bottom water temperatures at CBP sites located in Boxes 1 – 3 and 4 – 8 from 1984 to 2012, plotted against mean monthly air temperatures measured at Norfolk International Airport.

Atmospheric vs. Bay Water Temperatures

Polyhaline Chesapeake Bay

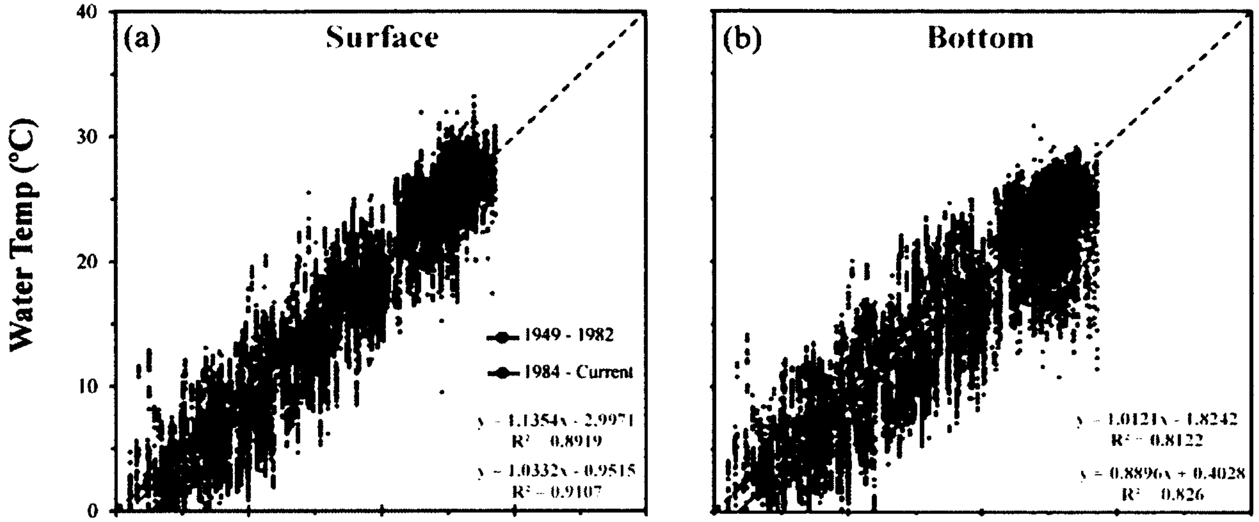

York River Estuary

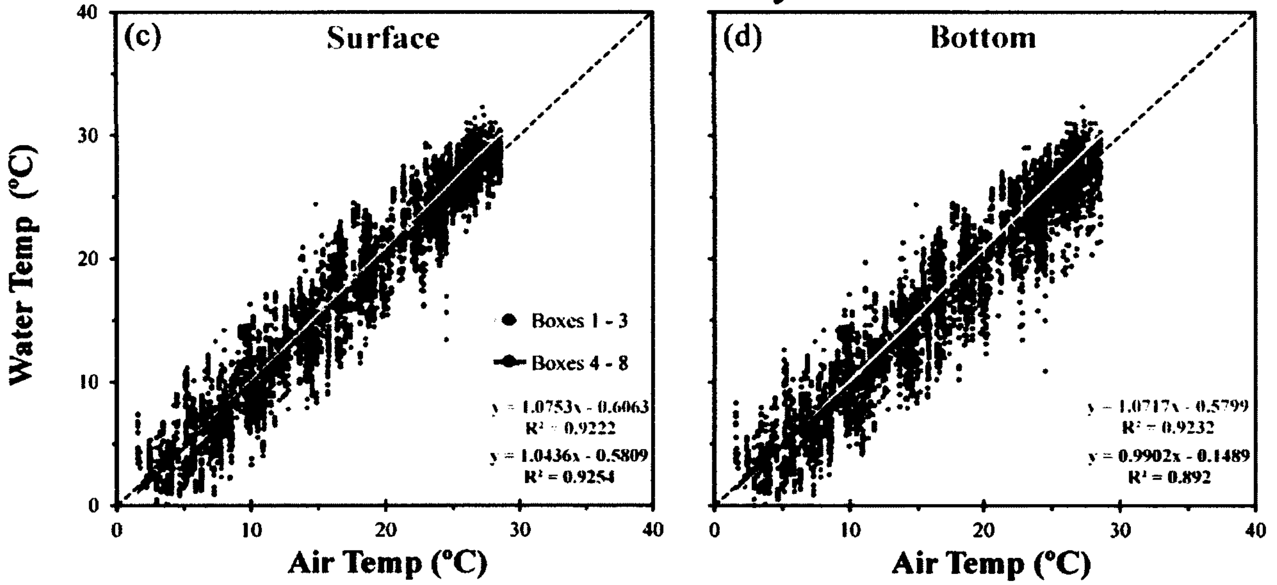

Figure 3-4. Modeled percent change in daytime water column net primary production relative to the baseline model simulation under a series of scenarios with increasing temperatures. Results were averaged over a four year simulation.

Response of NPP_{WC} to Temperature

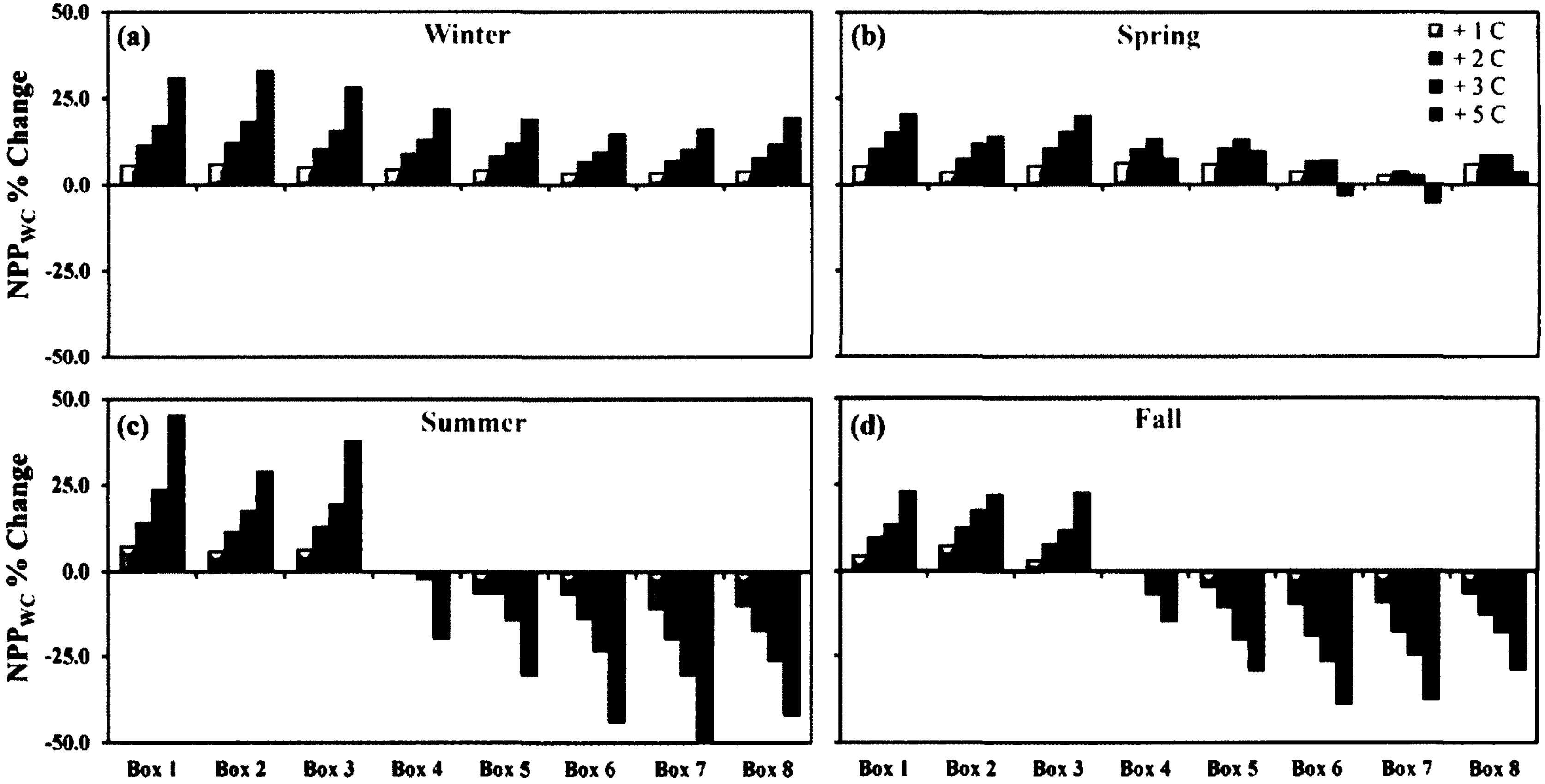

Figure 3-5. Modeled percent change in net ecosystem metabolism (NEM) relative to the baseline model simulation, under a series of scenarios with increasing temperatures. Results were averaged over a four year simulation.

Response of NEM to Temperature

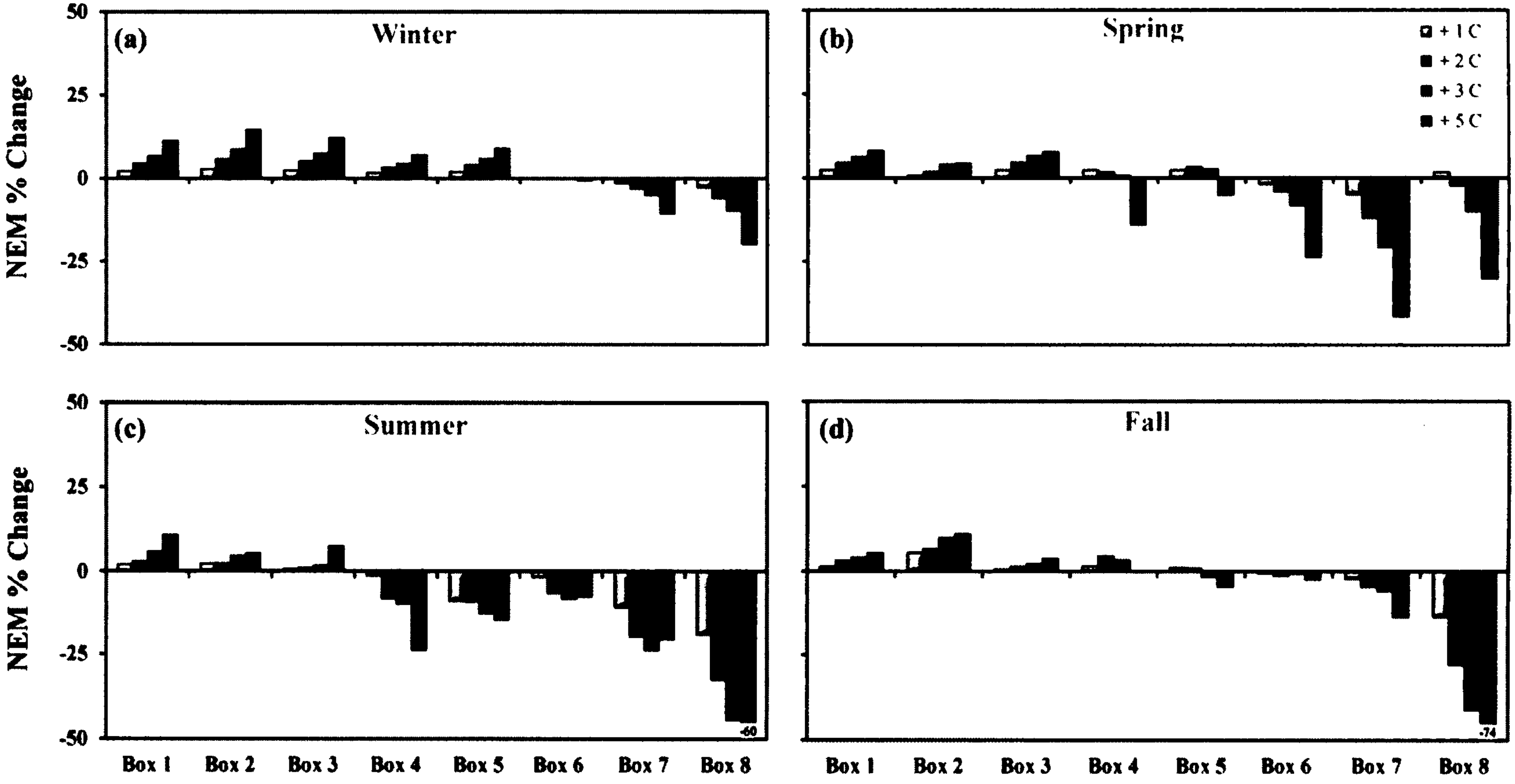

Figure 3-6. Predicted annual number of hypoxic (< 2 mg L^{-1}) and low oxygen days (< 3 mg L^{-1}) within each model box under a range of temperature scenarios. Values represent the average number of days over a four year simulation.

Low Oxygen with Climate Warming

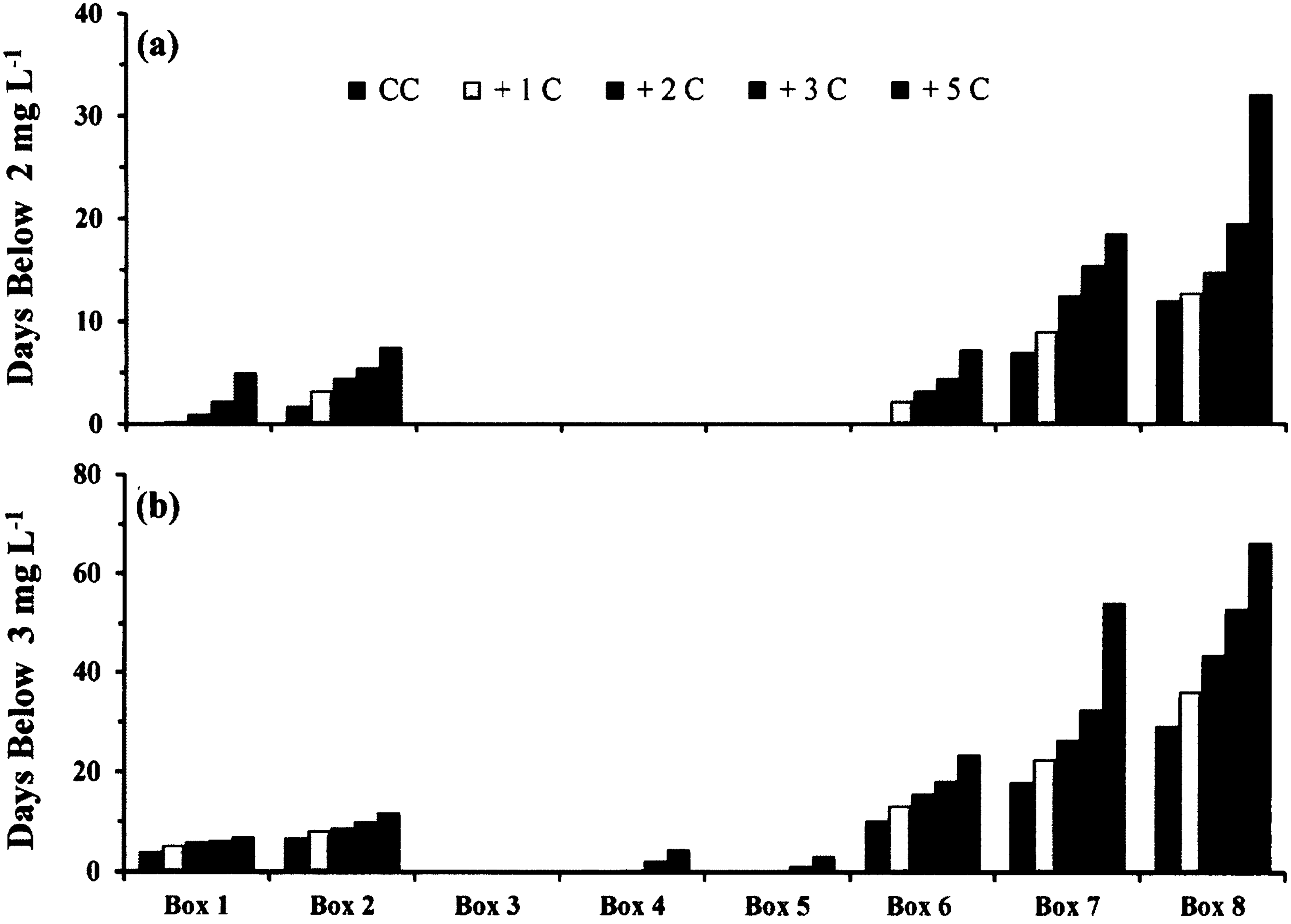

Figure 3-7. Predicted annual number of hypoxic (< 2 mg L^{-1}) days within each model box under various scenarios in which nutrient and organic matter (dissolved and particulate) loads from the tributaries and ungauged watersheds were reduced. Scenarios were run under current conditions (CC) and load reductions (0.5x, 0.75x, 0.85x, 0.90x, 0.95x, and 1.0x) under increasing temperatures of: (a) + 1, (b) + 2, (c) + 3, and (d) + 5 °C. Values represent the average number of days over a four year simulation.

Tributary and Watershed Inputs

Nutrients and OM Reductions

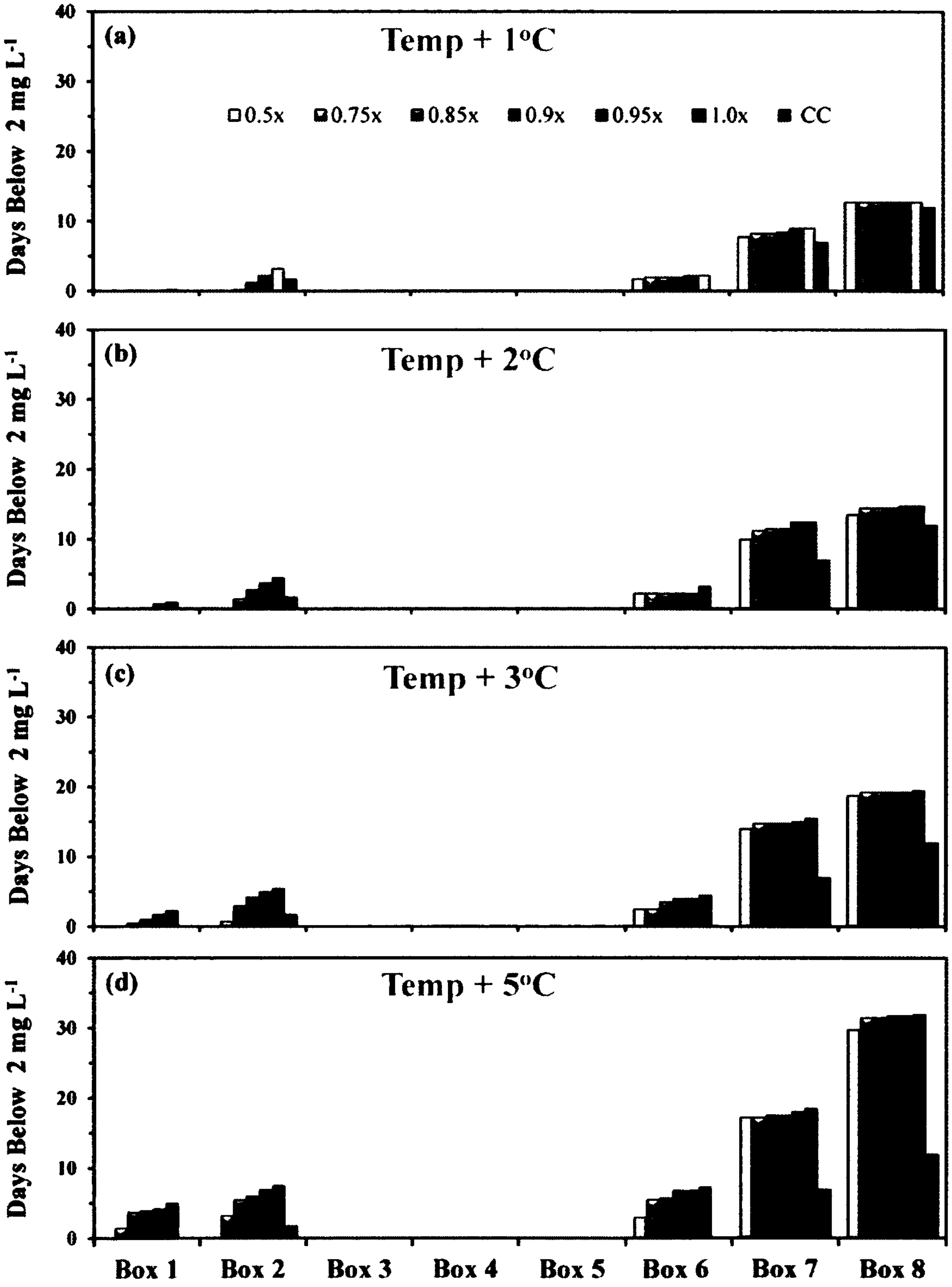

Figure 3-8. Predicted annual number of hypoxic (< 2mg L^{-1}) days within each model box under various scenarios in which nutrients, phytoplankton biomass, and organic matter (dissolved and particulate) loads from Chesapeake Bay were reduced. Scenarios were run under current conditions (CC) and load reductions (0.5x, 0.75x, 0.85x, 0.90x, 0.95x, and 1.0x) under increasing temperatures of: (a) + 1, (b) + 2, (c) + 3, and (d) + 5 °C. Values represent the average number of days over a four year simulation.

Chesapeake Bay Inputs

Nutrients, Chl-a, and OM Reductions

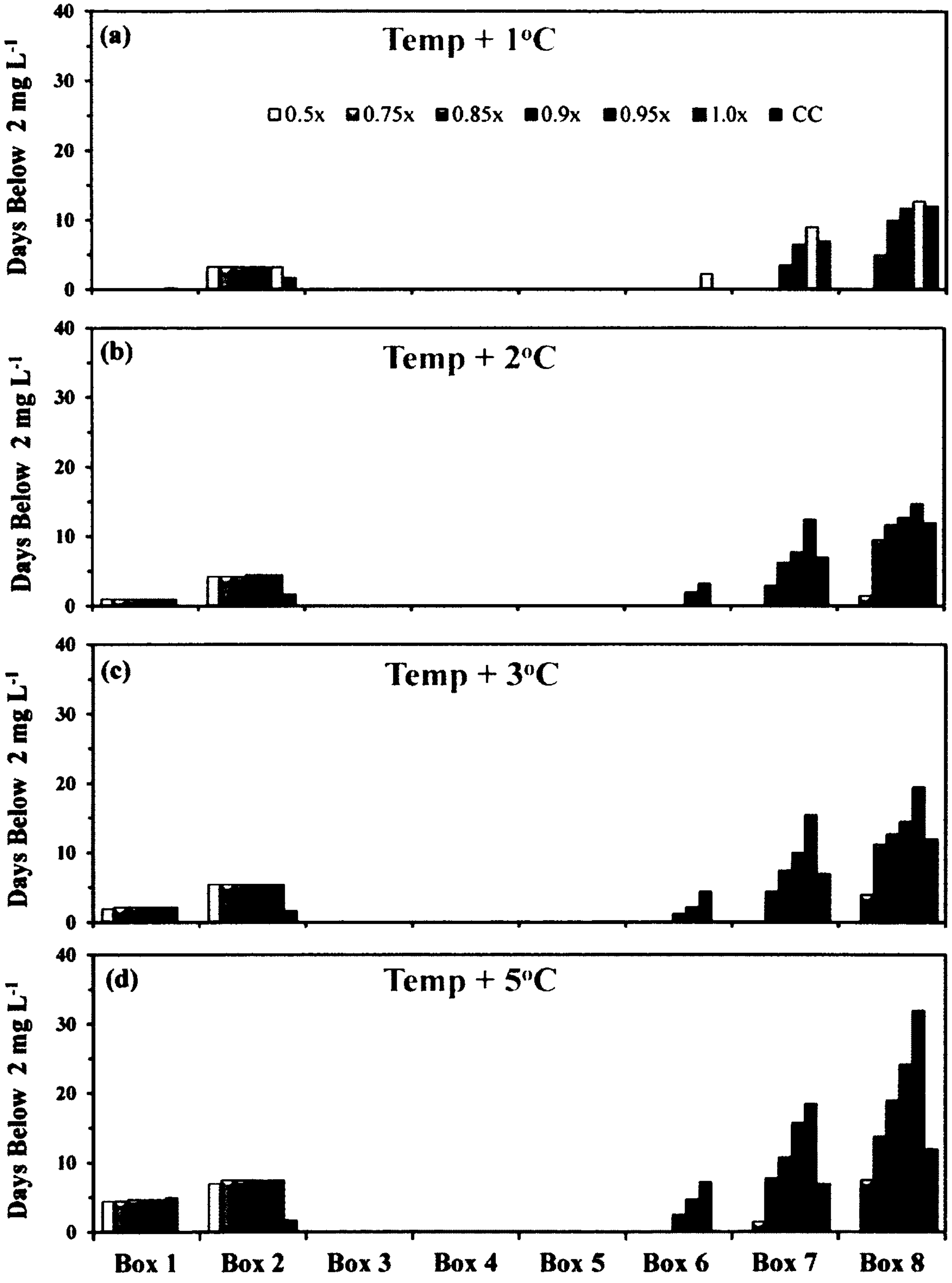

Figure 3-9. Predicted annual number of hypoxic (< 2mg L^{-1}) days within the upper (Boxes 1 – 4 combined) and lower (Boxes 5 – 8 combined) York River estuary, under a range of temperature warming scenarios (+ 1, + 2, + 3, and + 5 °C) and external load reductions. (a, c) Effect of nutrient and organic matter reduction scenarios from the tributaries and ungauged watersheds in the (a) upper and (c) lower estuary. (b, d) Effect of nutrient, phytoplankton biomass, and organic matter reduction scenarios in the (b) upper and (d) lower estuary. Values represent the average number of hypoxic days over a four year simulation. Source reductions were run under current conditions (CC) as well as 5%, 10%, 15%, 25%, and 50% reductions (0.95x, 0.90x, 0.85x, 0.75x, and 0.50x, respectively).

Hypoxic Days with Source Reductions

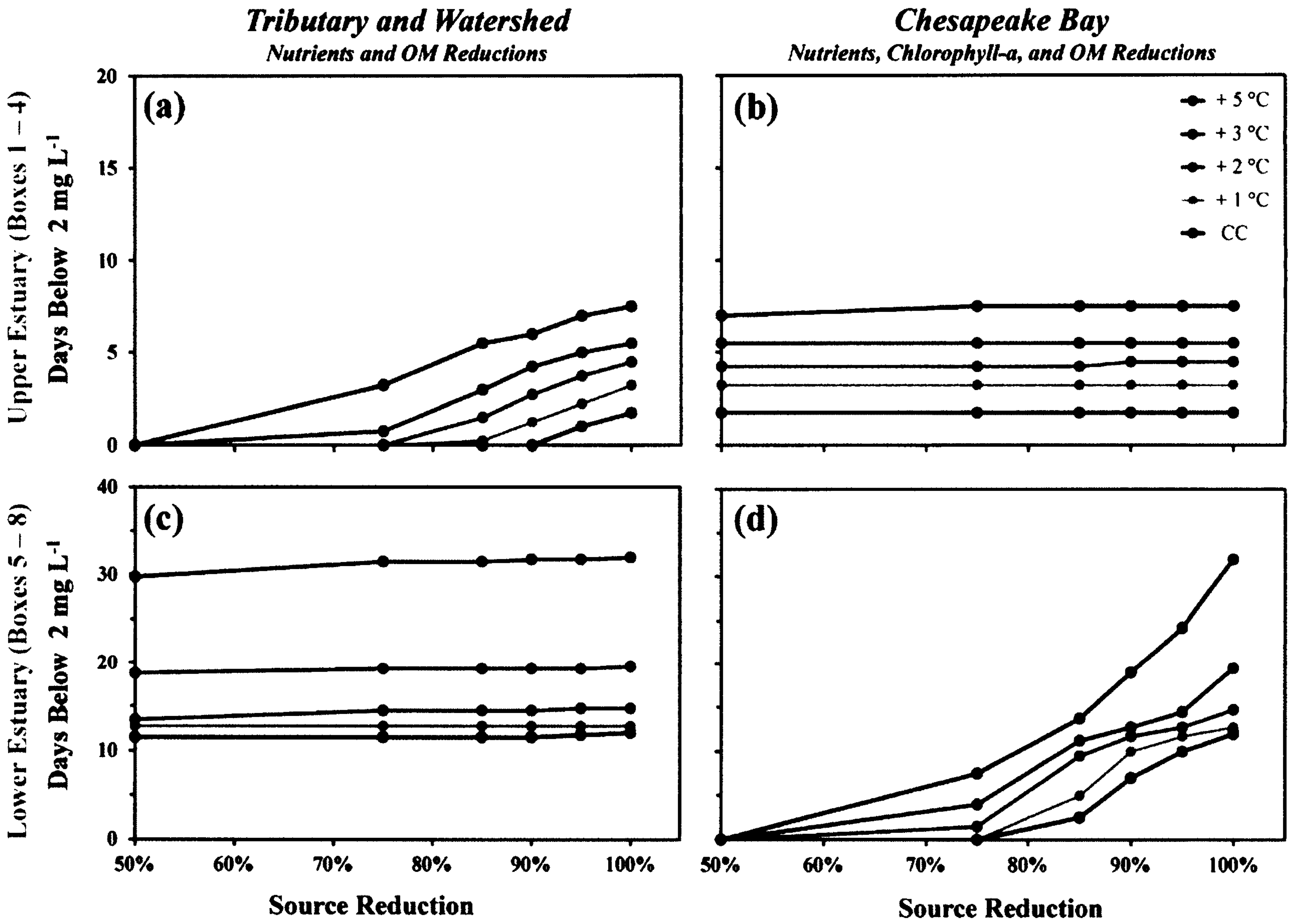

CHAPTER 4

Published in *Estuarine, Coastal and Shelf Science* (2011, 95:289-297)

The Contribution of Microphytobenthos to Total Productivity in upper Narragansett Bay, Rhode Island

Samuel J. Lake[1] and Mark J. Brush

Virginia Institute of Marine Science

College of William and Mary, Gloucester Point, VA 23062 USA

[1] Corresponding author:

Email: sjlake@vims.edu

Phone Number: (804) 684-7918

Fax: (804) 684-7293

Keywords: Microphytobenthos, Primary Production, Narragansett Bay, Sediment Chlorophyll

ABSTRACT

In many coastal marine ecosystems, microphytobenthos (MPB) can contribute a significant fraction of total system primary production, particularly in shallow lagoons or systems with broad photic shoals. While the role of MPB has been quantified in several shallow systems around the world, their contribution to primary production on the extensive shoals that line a number of deeper estuaries has often been overlooked. We assessed the contribution of MPB to total primary production within four regions of upper Narragansett Bay, RI, USA to quantify the significance of benthic production on the extensive shallow shoals that line this relatively deep estuarine system. Our results indicate that surface sediment chlorophyll-*a* concentrations and daily benthic gross primary production rates in shallow portions of upper Narragansett Bay are within the range of previous studies conducted along the northeastern U.S. coast. Despite these high rates, our results when scaled to the system level emphasize the importance of phytoplankton production in most of the upper bay under current conditions, although MPB were found to contribute a significant fraction (up to one third) of total primary production in certain regions at certain times. Despite the high rates of benthic gross primary production in some portions of the upper bay, the benthos remained net heterotrophic throughout the spring, summer, and fall at most sites, although production within the Greenwich Bay sub-estuary was enough to drive the benthos slightly net autotrophic for short periods in the fall. While the current role of MPB appears to be limited in terms of its overall contribution to total gross primary production, the importance of MPB in the future may increase due to changing climate and reductions in anthropogenic nutrient loading.

INTRODUCTION

Previous primary production studies conducted in Narragansett Bay have focused solely on the importance of water column phytoplankton production (Vargo 1979; Oviatt et al. 1981; Oviatt et al. 2002; Oviatt 2008). This is due in large part to the long-standing view that Narragansett Bay is a relatively deep system that has been supported historically by a large winter-spring diatom bloom, in addition to smaller summer time blooms, that sustain a heterotrophic and light limited benthos (Oviatt et al. 2002). In recent years microphytobenthos (MPB) in mid-Atlantic U.S. systems have been shown to contribute significantly to total system primary production throughout the year (McGlathery et al. 2001; Tyler et al. 2003). This work has provided additional insight into the ecological importance of MPB including their ability to work as a sediment cap, retaining nutrients in the sediment and preventing their release to the overlying water column (Underwood and Kromkamp 1999; Anderson et al. 2003; Tyler et al. 2003). The role of microphytobenthos in systems along the Northeastern U.S. coast, however, has not been as extensively examined to determine their quantitative importance in carbon production.

Although a large portion of the bottom of Narragansett Bay lies below the photic zone, there is a significant portion that may receive sufficient light for supporting benthic production, including portions of the Providence River estuary and smaller sub-embayments that surround the bay proper. These shallower regions were historically sites of extensive eelgrass (*Zostera marina*) beds (Deacutis 2008; Nixon et al. 2008). However, a number of factors including increased anthropogenic nutrient loading, changes in land use, increasing regional population densities, and warmer annual water temperatures have been linked to the almost complete loss of eelgrass beds throughout the bay (Deacutis 2008; Nixon et al. 2008). Benthic macroalgae have received increasing attention throughout the bay over the last 15 – 20 years due to the extensive growth and accumulation of nuisance species in portions of some shallow embayments within upper Narragansett Bay; these localized blooms have been shown to end in late summer die-offs that can lead to severe hypoxia and anoxia (Deacutis 2008; Oviatt 2008). Although numerous anthropogenic, and possibly larger climatic changes, have severely limited the ability of vascular plants to grow in the upper bay, the growth and accumulation of macroalgae within portions of the upper bay suggests that enough light reaches the shallow sediment surface to sustain relatively high rates of benthic primary production.

Regionally, there has not been much effort to evaluate the potential importance of microphytobenthos within larger estuarine systems along the coast of New England. There have, however, been a number of smaller studies focused on small embayments and salt ponds conducted over the past few decades. One of the earliest accounts of benthic primary production in southern New England was conducted by Marshall et al. (1971) in four small estuaries along the coasts of Connecticut and Rhode Island in 1969. Their experimental work indicated high levels of sediment chlorophyll-*a* in excess of 100 mg m^{-2} in the top 7.5 mm, with extremely high variability from site to site. Using midday observations to predict mean daily gross benthic primary production they calculated rates of 198 mg C m^{-2} day^{-1}, 431 mg C m^{-2} day^{-1}, and 187 mg C m^{-2} day^{-1} for March-May, June-August, and September-November, respectively. Nowicki and Nixon (1985) reported gross benthic daytime production of 150 g C m^{-2} yr^{-1} with mean chlorophyll-*a* concentrations of 170 and 150 mg m^{-2} for muddy and sandy sediment, respectively, in Potters Pond, a shallow coastal lagoon located near the mouth of Narragansett Bay.

Within Massachusetts there have been a number of studies examining the role of MPB in nutrient enrichment experiments conducted in small estuarine and tidal marsh systems. Van Roalte et al. (1976) examined epibenthic algae in the Great Sippewissett Marsh and noted seasonal patterns in benthic production with peaks in the spring of up to 115 mg C m^{-2} day^{-1} and in the fall of up to 60 mg C m^{-2} day^{-1} with lower summer and winter production rates. Observed rates of benthic production were as high or higher than phytoplankton production in this study on an annual basis. More recently, Tobias et al. (2003) found sediment chlorophyll-*a* concentrations in the Rowley River channel (MA) between 120 – 300 mg m^{-2}, and 240 – 300 mg m^{-2} in the adjacent mud flats. Lever and Valiela (2005) found mean sediment chlorophyll-*a* concentrations between 57 and 109 mg m^{-2} in three Waquoit Bay (MA) estuarine systems and determined that nutrient availability limited benthic biomass within all three systems.

While these studies point to high biomass and productivity of microphytobentos in shallow systems throughout southern New England, the importance of MPB on the shallow shoals of larger, deeper estuarine systems such as Narragansett Bay remains unclear. Chinman and Nixon (1985) calculated that nearly 85% of the bay's sediment surface lies deeper than 2 meters, relative to mean low water (MLW). While portions of upper Narragansett Bay exhibit similar depth profiles, the Providence River estuary and Greenwich Bay represent two relatively shallow sub-basins with 48% and 36% of the sediment surface shallower than two meters relative to mean sea level (MSL) (Table 1), respectively. Recent work has only further highlighted our lack of knowledge surrounding the role of MPB in this system (Deacutis 2008; Nixon et al. 2009; Fulweiler et al. 2010). While this study does not fully describe the role of MPB within Narragansett Bay, we attempt to illuminate the potential contribution of MPB as a viable primary producer under current climate and nutrient conditions.

METHODS

Site Description

The Providence River estuary contains a semi-deep channel (13 - 14 m) that is centered within the middle of the river and flanked on either side by shallow 1 – 2 meter deep shoals south of Fields Point to Conimicut Point (Doering et al. 1990; Asselin and Spaulding 1993) (Fig.1). Below Conimicut Point the surface area to volume ratio of the bay begins to decrease gradually with an average depth of 8.7 m (Nixon et al. 2009). The Bay proper has a number of additional small embayments including Greenwich Bay, a shallow embayment located along the western shoreline of upper Narragansett Bay.

We delineated five sampling regions including: the lower Providence River estuary (PRE), Upper Narragansett Bay (UNB), Greenwich Bay (GB), and Greenwich Cove (GC) (Fig. 1). Additionally a second cove site was selected in Apponaug Cove (AC) for comparison to Greenwich Cove. Four sites within the PRE, UNB and GB were selected, based on accessibility, as sediment chlorophyll-*a* (SED Chl-*a*) sampling sites. One site within each region was randomly selected as a SED Chl-*a* depth profile and photosynthesis-irradiance (P-I) sediment core collection site. A single SED Chl-*a* depth profile and P-I core collection site was selected in GC with a corresponding SED Chl-*a* sampling site in AC. Samples were collected during the late spring/early summer (6/02), summer (7/21) and fall (9/25) of 2010.

Light Attenuation and Water Quality

At each site a YSI 6600 series V2 sonde was used to measure temperature, salinity, and dissolved oxygen at the surface (0.5 m). A LiCor LI-1400 was used to measure irradiance through the water column for computation of vertical attenuation coefficients; measurements were taken above the water surface, just below the surface (<0.1 m) and at 0.5 meter. All YSI and LiCor measurements were taken in triplicate.

Sediment Chlorophyll-*a* Sampling and Processing

At each site three replicate samples were collected for sediment chlorophyll-*a* at a depth of 1 meter below mean lower water (MLW), taking into account the daily tidal range. Four sites were also utilized to develop SED chl-*a* depth profiles within the four sampling regions (Fig. 1, triangles). Depth profile samples were also collected in triplicate at 0.25, 0.5 1.0, 1.5 and 2 meters below MLW and analyzed as described below. All samples were subdivided into two depth fractions, 0 – 0.3 cm and 0.3 – 1.0 cm, transferred into sterile 15 mL BD Falcon polypropylene centrifuge tubes, and immediately placed in an ice filled cooler until they were transferred to a freezer for a maximum hold time of one month.

Samples were extracted in 10 mL of a 90% Acetone: 10% DI water (by volume) solution, vortexed for 30 seconds on full power, and sonicated for an additional 30 seconds at 4-5 watts with a Fisher Scientific Dismembranator. After a 24-hour extraction period in the freezer, samples were filtered with a PALL Life Science HPLC Acrodisk (25 mm filter with a 0.45 μm CR-PTEE) and analyzed spectrophotometrically on a Beckman DU 800 Spectrophotometer before and after acidification using the equations of Lorenzen (1967), which corrects chlorophyll-*a* for phaeophytin.

Photosynthesis-Irradiance (P-I) and Metabolism Experiments

In order to develop shallow sediment production and respiration rates, approximately 16 cores were sampled at each of four sites, one within each of the four regions of upper Narragansett Bay (Fig. 1, triangles). Shoal sediment cores (10 light and 4 dark) were collected in clear acrylic tubing (height 15 cm: i.d. 4.1 cm) at 1 meter below MLW and immediately placed on ice. All cores were covered in black electrical tape below the sediment-water interface to ensure that only the sediment surface was exposed to light during the P-I experiments. Site water was collected at each station in blackened 4 liter Nalgene bottles and later filtered to 0.5 μm. Cores were allowed to acclimate uncapped overnight in a gently mixed water bath filled with site water before incubation. Just prior to incubation, the overlying core water was carefully siphoned out and replaced (as not to disturb the sediment surface) with filtered seawater with a known dissolved oxygen concentration and sealed with polyvinylidene chloride (Saran Wrap), which has been shown to have low oxygen permeability (5.8×10^{-5} ml cm^{-2} h^{-1}; Pemberton et al. 1996), held in place by a tight rubber band. Ten individual cores from each site were incubated at field temperatures in temperature-controlled, flow-through light gradient boxes under a gradient of irradiance (~50 – 1600 μE m^{-2} s^{-1}) for approximately 1.5 - 2 hours. Four additional cores from each site were placed in a corresponding temperature controlled dark box for 2 - 3 hours. Final dissolved oxygen concentrations were measured with a HACH HQ 40d oxygen meter with HACH LDO optical probes and all cores were immediately sub-sampled for chlorophyll-*a* analysis (0-3 mm) to normalize production to biomass.

Data Analysis and Interpolation

Net benthic production was computed from the change in dissolved oxygen concentrations in illuminated and darkened sediment cores. Results were used to develop a series of production-irradiance (P-I) curves using Jassby and Platt's (1976) linear hyperbolic tangent function in SAS® 9.2 software:

$$P = P_{max} \tanh (\alpha I / P_{max}) - R$$

where production (P, mg O_2 mg chl^{-1} h^{-1}) is dependent on irradiance (I, μE m^{-2} sec^{-1}) and three statistically determined variables, the maximum photosynthetic rate (P_{max}, mg O_2 mg chl^{-1} h^{-1}), the slope of the light saturation curve (termed alpha, α, mg 0_2 mg chl^{-1} h^{-1} (μE m^{-2} s^{-1})$^{-1}$), and the rate of respiration (R, mg O_2 mg chl^{-1} h^{-1}). A series of three curves were developed for each site on each sampling date to capture a minimum, average, and maximum possible curve fit, given variability in production between cores at similar irradiance (Fig. 2). The estimated values calculated in SAS for P_{max}, α, and R for each P-I curve were then linearly interpolated between sampling dates in MATLAB R2010b.

Sediment chlorophyll-*a* biomass from the depth profile sampling was combined in ½ meter depth segments to account for variability within each segment. The results from 0.25 and 0.5 m were averaged and used for analysis of the 0-0.5 m depth segment, 0.5 and 1.0 were averaged for 0.5-1.0 m, and so forth. The 1.5 and 2 m values were applied to all depths below 2 meters. These sediment chlorophyll-*a* values and measured attenuation coefficients were also interpolated between sampling dates in MATLAB R2010b.

Hourly total solar radiation received at the Kingston, Rhode Island meteorological station (April - November 2010) was downloaded from the NOAA National Climate Data Center (www.ncdc.noaa.gov/oa/mpp/freedata.html). Total solar radiation values were reduced to 47% of the total, to represent the percentage of total radiation available as PAR, based on previous studies (Vollenweider 1974; Cole and Cloern 1987). Solar radiation was converted from Watts m^{-2} to Einsteins (E) m^{-2} s^{-1} using a mean wavelength of 550 nm.

Bathymetric sounding depths were downloaded from the NOAA National Geophysical Data Center (www.ngdc.noaa.gov) and interpolated using a kriging function in ESRI ArcView GIS 3.3, to a 50m x 50m grid with a resolution of 10 cm in the vertical. The total surface area within each sampling region was calculated for 0.5 m depth intervals from MSL to the bottom. Resulting values were very close to those of Chinman and Nixon (1985).

Gross hourly production was calculated for each region by combining the total surface area at each depth interval, attenuated light reaching that depth, sediment chlorophyll-*a* biomass, and interpolated values of P_{max} and α. Since specific values for PQ and RQ are not available for the benthos of Narragansett Bay we applied a constant PQ (and RQ) of 1 for all sites.

This process was repeated for each depth segment within each region, and then summed for each sampling area to estimate total gross production by MPB. These rates were then compared to water column ^{14}C incubations from Oviatt et al.(2002) for the months of April to October. Net community metabolism for each region was calculated in the same way with the inclusion of the interpolated respiration term (R).

RESULTS

Sediment Chlorophyll-*a*

Microphytobenthic biomass (as sediment chlorophyll-*a*) varied both spatially between sites and with depth (Fig. 3). Sediment chlorophyll-*a* was relatively high at all locations on all sampling dates, with average concentrations of 92.2, 64.1, 98.3, and 72.6 mg m^{-2} within the top 3 mm for PRE, UNB, GB, and GC/AC, respectively. Biomass was characteristically highest in areas shallower than 1 meter in PRE and GC, while it was highest at 1 and 1.5 meters in GB and UNB. The chlorophyll-*a* to phaeophytin ratios for PRE, UNB, and GB were generally highest at depths shallower than 1.5 meters and steadily decreased with depth below this point. Conversely, the ratio at GC decreased continually with depth from the shallowest sampling point and was lower overall than at the other sites.

Benthic Production

The results from the P-I experiments demonstrated varying rates of light-saturated productivity in PRE, UNB, and GB throughout the spring, summer, and fall. Rates were generally higher during the spring and fall, with depressed mid-summer rates. Sediment respiration rates were higher during the warmer summer months than during the spring and fall sampling periods. Sediment core incubations from the GC site did not show a significant relationship between production and irradiance during any sampling period. Due to the lack of a significant trend, a series of constant respiration rates were applied to GC for all sampling periods.

Daily gross benthic primary production (GPP_B), scaled up for each region, varied seasonally with the highest rates occurring during the fall in PRE and GB with maximum estimated monthly rates of 340 and 450 mg C m^{-2} d^{-1}, respectively (Fig. 4). These two sites had lower minimum estimated rates during the July sampling, 6 mg C m^{-2} d^{-1} for PR and 161 mg C m^{-2} d^{-1} for GB. The UNB displayed a similar, but weaker, seasonal trend with maximum estimated monthly GPP_B rates less than 50 mg C m^{-2} d^{-1} during the spring, summer and fall. Due to the lack of measurable benthic production within the incubated sediment cores from GC, an estimate of GPP_B within this region was unavailable.

Benthic net community metabolism (NCM_B) displayed strong net heterotrophy throughout the majority of the spring, summer, and fall within all four regions of upper Narragansett Bay (Fig. 5). Average estimated monthly NCM_B in the PRE decreased from -1000 mg C m^{-2} d^{-1} during June to -1300 mg C m^{-2} d^{-1} July, and then increased steadily to -600 mg C m^{-2} d^{-1} during September. NCM_B in the UNB remained relatively constant throughout the spring, however during the summer the minimum and average estimated rates decreased during June, while the maximum estimated rates began to increase and continued to remain elevated into the early fall. Minimum and average estimated rates in the UNB increased during late July and appeared to peak in early October. NCM_B in GB increased slightly during the early spring before increasing more significantly from mid June to late August, with short (weekly) periods during the fall that were net autotrophic based on maximum estimated rates of production. Greenwich Cove displayed the highest respiration rates of all four sampling sites resulting in NCM_B rates during the spring that were twice that of any other location in upper Narragansett Bay. The average estimated rates increased during the summer from -2400 mg C m^{-2} d^{-1} during May, to -1550 mg C m^{-2} d^{-1} in July and remained relatively constant throughout the fall.

DISCUSSION

Regional Comparison of Sediment Chlorophyll-*a*

Surface sediment chlorophyll-*a* concentrations in upper Narragansett Bay were found to be within the range of previous studies conducted in shallow water systems within this region. Additionally, our concentrations were similar to those of Fulweiler et al. (2010) who collected a limited number of sediment chlorophyll-*a* samples (0-1 cm) at deeper (3m) upper bay sites. They reported relatively higher concentrations in PRE and GB (78.2 mg m^{-2} and 83.6 mg m^{-2}) compared to UNB (42.4 mg m^{-2}). Although no clear seasonal trend was apparent in our samples, the relatively high biomass and high chlorophyll-*a* to phaeophytin ratios within PRE, UNB, and GB indicates that microphytobenthos are not only present within this system, but are also potentially a viable primary producer when sufficient light reaches the sediment surface. This may not be the case for smaller sub-embayments, like the shallow coves surrounding Greenwich Bay. Although chlorophyll-*a* concentrations in GC were above 50 mg m^{-2} (0-3 mm) at the shallowest sampling depths (0.25 and 0.5 m), chlorophyll-*a* concentrations decreased continually with depth, and the corresponding chlorophyll-*a* to phaeophytin ratios indicated that the microalgal biomass in this region was comparatively more degraded than other sampling locations.

Gross Primary Production

Daily gross benthic primary production rates from this study, averaged over each sampling region, ranged from the highest seasonal rates reported by Marshall et al. (1971) to the depressed summer and early winter rates in Van Roalte et al. (1976). In general, GPP_B in PRE and GB were found to be higher than the other areas in upper Narragansett Bay, which is likely a result of expansive shallow, photic shoals (< 5m MSL) in these two basins that represent 79% and 94% of the sediment surface area, respectively (Table 1). Comparatively, the UNB is a deeper embayment that lacks expansive shallow, photic shoals. Although sediment incubations for PRE and UNB produced similar P-I relationships, the relatively large extent (58%) of benthos below the photic zone (> 5m MSL) within the UNB limits the contribution of GPP_B in this region. Benthic production in GC appears to be limited, likely due to a number of factors including degraded MPB biomass and high rates of benthic respiration.

Seasonally GPP_B varied across all sites with peak fall production in PRE, UNB, and GB similar to the results of Van Roalte et al. (1976) with suppressed mid summer rates in UNB and GB. However, results from this study did not display a peak in spring production as seen in the Great Sippewisset Marsh (Van Roalte et al. 1976), which may result from a larger percentage of the benthos being subtidal, a more significant role of phytoplankton communities, and elevated suspended sediment from spring storms that likely limits light availability. The seasonal trends for UNB and GB contrasts with the findings of Marshall et al. (1971) and Nowicki and Nixon (1985), who found maximum rates of gross benthic production in the summer with lower spring and fall rates. However, the maximum production rates for PRE showed a peak in production during the summer that decreased in mid September similar to the results of both Marshall et al. (1971) and Nowicki and Nixon (1985).

Comparison of water column and benthic primary productivity emphasizes the importance of phytoplankton production within the deeper regions of upper Narragansett Bay, particularly in UNB where GPP_B accounted for less than 5% of total primary production (PP_T) from May to September (Fig. 4; Table 2). Although benthic production in PRE can exceed 300 mg C m^{-2} d^{-1}, these rates accounted for less than 10% of PP_T during summer when benthic production was at its maximum. The contribution of GPP_B in GB appeared to be relatively more important than the other regions, particularly during the spring and fall, when GPP_B accounted for 30 – 40 % of total production (Fig. 4; Table 2). However, the contribution of benthic production to total in the summer (June-August) remained at or below 20% of PP_T.

This comparison is somewhat complicated by the different methods (^{14}C vs. O_2) used to measure primary production between our study and that of Oviatt et al. (2002). Oviatt et al. (2002) reported their 2-hour ^{14}C incubation rates as daytime net primary production (NPP_{WC}). A completely accurate comparison would require correcting our O_2-based GPP rates for MPB respiration. Since the fraction of GPP respired by MPB is unknown and impossible to determine from our measurements, we have compared our GPP_B rates directly to Oviatt et al.'s (2002) data as a maximum estimate of the contribution of MPB to total production. Accounting for MPB respiration would lower our estimates by an unknown but likely small amount.

Benthic Net Community Metabolism

Despite the high rates of gross production associated with microphytobenthos in some portions of upper Narragansett Bay, the benthos nevertheless was net heterotrophic throughout the spring, summer, and fall, with the exception of fall in GB where production may be enough to drive the sediments autotrophic over short periods. During the spring, elevated benthic community respiration drove oxygen uptake into the sediment, which resulted in NCM_B rates in PRE, UNB, and GB between -700 and -1300 mg C m^{-2} d^{-1}. This is likely a result of decomposing phytoplankton blooms that frequently exceed 30 μg l^{-1} in upper Narragansett Bay during the spring (Oviatt et al. 2002). Sediment respiration rates in the PRE continued to increase into the summer with rising temperatures, resulting in rates that surpassed the increase in benthic gross primary production, and drove NCM_B to the most heterotrophic rates calculated in this study. Similarly, the minimum and average NCM_B rates for UNB during this period decreased as a result of lower GPP_B and increasing sediment respiration. Net community metabolism in GB increased steadily during the summer as a result of decreasing sediment respiration rates, compared to PRE and UNB. This may be due to lower levels of phytoplankton decomposition in this region compared to the other sites. During the fall sediment respiration decreased to the lowest observed rates for any region within upper Narragansett Bay, which corresponded with the highest rates of GPP_B for GB, resulting in a few short periods during September when NCM_B approached and reached net autotrophy, based on our maximum estimates of production. The shallow photic sediment respiration rates from this study were within the range of previous studies (Nixon et al. 1990; Fulweiler et al. 2010) collected at deeper sites within the upper bay.

Future Role of Microphytobenthos

Under current climate and nutrient conditions the role of MPB in upper Narragansett Bay appears to be limited and in many cases does not appear to offset the high rates of benthic respiration occurring in the sediments. This limited role however may change with the continued oligotrophication of Narragansett Bay (Nixon et al. 2009). This will likely result from both climate change and the implementation of advanced waste water treatment plants, thereby reducing summer nitrogen inputs by 30 – 40% (Nixon et al. 2008). For this study, it should be noted that the water column production rates utilized from Oviatt et al. (2002) were based on surveys and incubations from 1997 – 1998. Although various nutrient reduction strategies have been implemented since this study, recent ^{14}C incubations from 2007 - 2009 indicate that water column production has remained unchanged (Smith 2011), despite other recent studies indicating a reduction in chlorophyll concentrations in the mid and lower bay (Oviatt 2004; Nixon et al. 2008; Nixon et al. 2009). However, if the current trend of oligotrophication continues into upper Narragansett Bay, microphytobenthic production may become proportionately more significant in the future.

While benthic production can sometimes be limited by nutrient availability (Lever and Valiela 2005) similar to water column primary production, Narragansett Bay may exhibit a legacy effect due to its long history of intense fertilization (Nixon et al. 2009). Microphytobenthic communities can take advantage of this legacy effect by utilizing high rates of bacterial mineralization and high pore water concentrations of dissolved nutrients, while working as a sediment cap, retaining nutrients in the sediment and preventing their release to the overlying water column (Underwood and Kromkamp 1999; Tyler et al. 2003). Additionally, a continued decline in phytoplankton biomass will likely increase light availability on the sediment surface. This increase in light availability, combined with legacy supply of nutrients from the sediments could align to create a positive feedback stimulating increased benthic primary production.

CONCLUSIONS

Our results indicate that surface sediment chlorophyll-*a* concentrations and daily benthic gross primary production rates in the shallow portions of upper Narragansett Bay are within the range of previous studies conducted in shallow water systems along the coast of southern New England. While the overall difference in magnitude between water column and benthic production further emphasizes the importance of phytoplankton production in the upper bay, MPB were found to contribute up to one third of total primary production in certain areas of the bay at certain times. Despite the high rates of gross primary production associated with microphytobenthos in some portions of the upper bay, the benthos remains net heterotrophic throughout the spring, summer, and fall, with the possible exception of fall in Greenwich Bay where MPB may drive the sediments slightly net autotrophic over short time periods. While the current role of MPB appears to be limited in terms of its overall contribution to total gross primary production, the importance of MPB in the future may increase due to changing climate and reductions in anthropogenic nutrient loads. Potential increases in MPB production will likely have a significant effect on the benthic communities that rely on phytoplankton and microphytobenthic communities as viable food sources.

ACKNOWLEDGEMENTS

This paper is contribution no. 148 of the National Oceanic and Atmospheric Administration (NOAA) Coastal Hypoxia Research Program (grant no. NA05NOS4781201). S. J. Lake also received financial support from NSF GK-12 (Division of Graduate Education 0840804). We thank Scott Nixon and Candace Oviatt for providing their labs and the facilities necessary to make this work possible. Additionally we would like to thank Courtney Schmidt, Lindsey Kraatz, Jonathan Daniel Maxey, Calandra Waters Lake, Lindsey Fields, Michael Schmidt, and Jason Krumholz for their field and laboratory assistance. This is Virginia Institute of Marine Science contribution no. 3182.

LITERATURE CITED

Anderson, I. C., K. J. McGlathery, and A. C. Tyler. 2003. Microbial Mediation of 'Reactive Nitrogen' Transformations in a Temperate Lagoon. *Marine Ecological Progressive Series* 246: 73-84.

Asselin, S. and M. L. Spaulding. 1993. Flushing Times for the Providence River Based on Tracer Experiements. *Estuaries* 16: 830-839.

Chiman, R. A. and S. W. Nixon. 1985. Depth-Area-Volume Relationships in Narragansett Bay. National Oceanic and Atmospheric Administration / Sea Grant Technical Report 87. Kingston, Rhode Island.

Cole, B. E. and J. E. Cloern. 1987. An Empirical Model for Estimating Phytoplankton Productivity in Estuaries. *Marine Ecology Progress Series* 36: 299-305.

Deacutis, C. F. 2008. Evidence of Ecological Impacts from Excess Nutrients in Upper Narragansett Bay. pp. 349-382 *in*: Desbonnet A., and B. A. Coasta-Pierce (eds.). *Science for Ecosystem-Based Management: Narragansett Bay in the 21st Century*. Springer Science, New York.

Doering, P. H., C. A. Oviatt, and M. E. Q. Pilson. 1990. Control of Nutrient Concentrations in the Seekonk-Providence River Region of Narragansett Bay, Rhode Island. *Estuaries* 14: 418-430.

Fulweiler, R. W., S. W. Nixon, and B. A. Buckley. 2010. Spatial and Temporal Variability of Benthic Oxygen Demand and Nutrient Regeneration in an Anthropogenically Impacted New England Estuary. *Estuaries and Coasts* 33: 1377-1390.

Jassby, A. D. and T. Platt. 1976. Mathematical Formulations of the Relationship Between Photosynthesis and Light for Phytoplankton. *Limnology and Oceanography* 21: 540-547.

Lever, M. A. and I. Valiela. 2005. Response of Microphytobenthic Biomass to Experimental Nutrient Enrichment and Grazer Exclusion at Different Land-Derived Nitrogen Loads. *Marine Ecological Progressive Series* 294: 117-129.

Lorenzen, C. 1967. Determination of Chlorophyll and Phaeopigments: Spectrophotometric Equations. *Limnology and Oceanography* 12: 343-346.

Marshall, N., C. A. Oviatt, and D. M. Skauen. 1971. Productivity of the Benthic Microflora of Shoal Estuarine Environments in Southern New England. Internationale Revue der *gesamten Hydrobiologie* 56: 947-956.

McGathery, K. J., I. C. Anderson, and A. C. Tyler. 2001. Magnitude and Variability of Benthic and Pelagic Metabolism in a Temperate Coastal Lagoon. *Marine Ecological Progressive Series* 216: 1-15.

Nixon, S., B. Nowicki, and B. Buckly. 1990. Report to the Narragansett Bay Project on the Measurement of Sediment Oxygen Demand in Providence River. Rhode Island Sea Grant.

Nixon, S. W., B. A. Buckley, S. L. Granger, L. A. Harris, A. J. Oczkowski, R. W. Fulweiler and L. W. Cole. 2008. Nitrogen and Phosphorous Inputs to Narragansett Bay: Past, Present, and Future. pp. 101-176 in: Desbonnet A., and B. A. Coasta-Pierce (eds.). *Science for Ecosystem-Based Management: Narragansett Bay in the 21st Century.* Springer Science, New York.

Nixon, S. W., R. W. Fulweiler, B. A. Buckley, S. L. Granger, B. L. Nowicki, and K. M. Henry. 2009. The Impact of Changing Climate on Phenology, Productivity, and Benthic-Pelagic Coupling in Narragansett Bay. *Estuarine, Coastal and Shelf Science* 82: 1-18.

Nowicki, B. L. and S. W. Nixon. 1985. Benthic Community Metabolism in a Coastal Lagoon Ecosystem. *Marine Ecology Progressive Series* 22: 21-30.

Oviatt, C. A., B. Buckley, and S. Nixon. 1981. Annual Phytoplankton Metabolism in Narragansett Bay Calculated from Survey Field Measurements and Microcosm Observations. *Estuaries* 4: 167-175.

Oviatt, C., A. Keller, and L. Reed. 2002. Annual Primary Production in Narragansett Bay with No Bay-Wide Winter-Spring Phytoplankton Bloom. *Estuarine, Coastal and Shelf Science* 54: 1013-1026.

Oviatt, C. A. 2004. The Changing Ecology of Temperate Coastal Waters During a Warming Trend. *Estuaries* 27: 895-904.

Oviatt, C. A. 2008. Impacts of Nutrients on Narragansett Bay Productivity: A Gradient Approach. pp. 523-544 in: Desbonnet A., and B. A. Coasta-Pierce (eds.). *Science for Ecosystem-Based Management: Narragansett Bay in the 21st Century*. Springer Science, New York.

Pemberton, M., G. L. Anderson, and J. H. Barker. 1996. Characterization of Microvascular Vasoconstriction Following Ischemia/Reperfusion in Skeletal Muscle using Videomicroscopy. *Microsurgery* 17: 9-16.

Smith, L. 2011. Impacts of Spatial and Temporal Variations of Water Column Production and Respiration on Hypoxia in Narragansett Bay. Ph. D. Dissertation, University of Rhode Island, Narragansett, RI.

Tobias, C. R., M. Cieri, B. J. Peterson, L. A. Deegan., J. Vallino, and J. Hughes. 2003. Watershed-Derived Nitrogen in a Well-Flushed New England Estuary. *Limnology and Oceanography* 48: 1766-1778.

Tyler A. C., K. J. McGlathery, and I. C. Anderson. 2003. Benthic Algae Control Sediment-Water Column Fluxes of Organic and Inorganic Nitrogen Compounds in a Temperate Lagoon. *Limnology and Oceanography* 48: 2125-2137.

Underwood, G. J. C. and J. Kromkamp. 1999. Primary Production by Phytoplankton and Microphytobenthos in Estuaries. pp. 93-153 in: Nedwell, D. B., and D. G. Raffaelli (eds.). *Estuaries. Advances in Ecological Research.* Academic Press, London.

Van Roalte, C. D., I. Valiela, and J. M. Teal. 1976. Production of Epibenthic Salt Marsh Algae: Light and Nutrient Limitation. *Limnology and Oceanography* 21: 862-872.

Vargo, G. A. 1979. The Contribution of Ammonia Excreted by Zooplankton to Phytoplankton Production in Narragansett Bay. *Journal of Plankton Research* 1: 75-84.

Vollenweider, R. A. 1974. Environmental Factors linked with Primary Production. pp. 159-177 in: R. A. Vollenweider (ed.). *A Manual on Methods for Measuring Primary Production in Aquatic Environments.* Blackwell Scientific Publications, Oxford London.

CHAPTER 4 - FIGURES

Figure 4-1. Location of sediment chlorophyll-*a* depth profiles and sediment core sampling sites (triangles), and single depth benthic chlorophyll-*a* survey sites (circles) within the different segments of upper Narragansett Bay. Dark grey dashed lines represent the 2 m contour line (below MSL) and dashed light grey lines represent the 5 m depth contour.

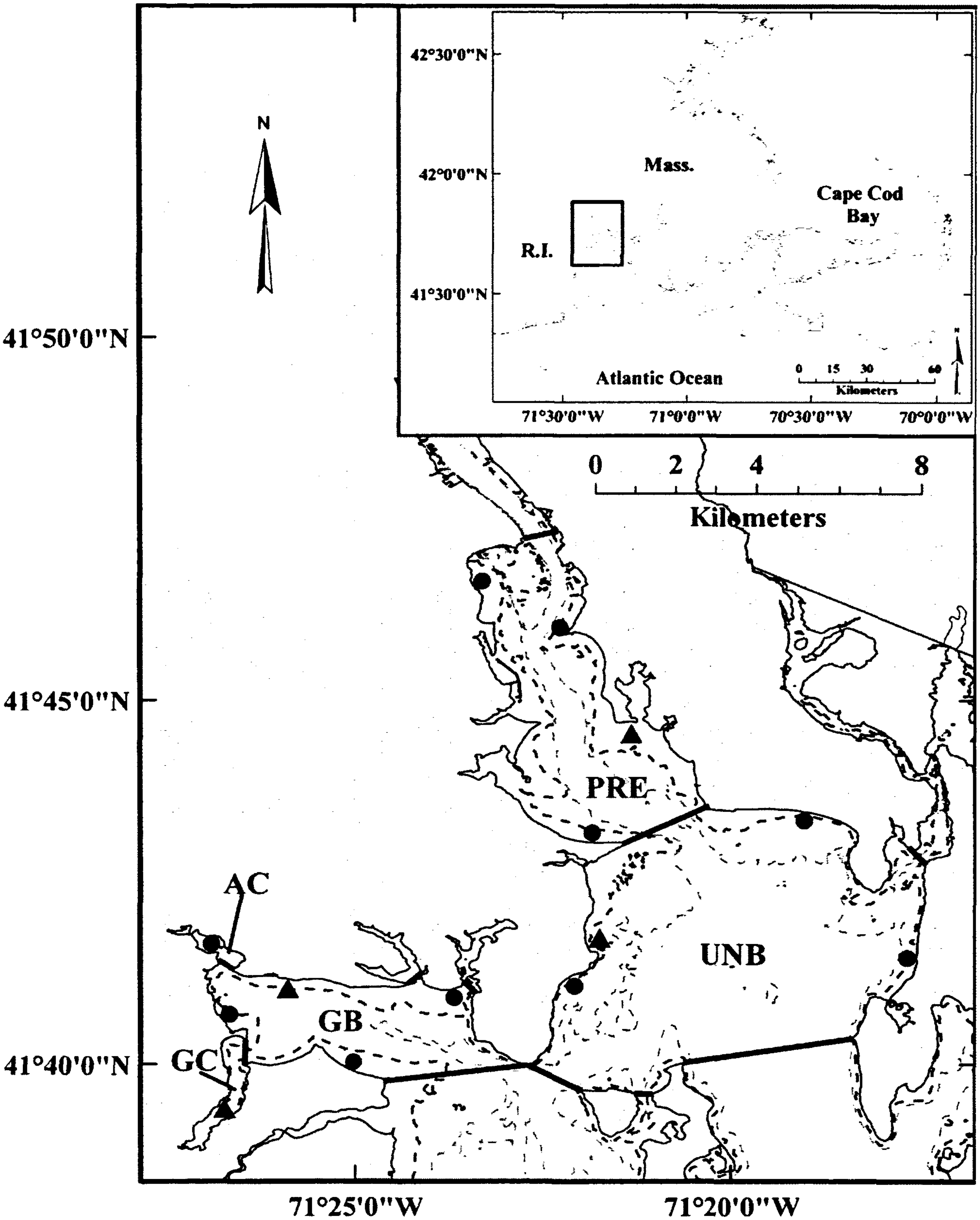
42°30'0"N
42°0'0"N
41°30'0"N
Mass.
Cape Cod Bay
R.I.
Atlantic Ocean
0 15 30 60
Kilometers
71°30'0"W
71°0'0"W
70°30'0"W
70°0'0"W
N
0 2 4 8
Kilometers
41°50'0"N
41°45'0"N
41°40'0"N
PRE
UNB
AC
GB
GC
71°25'0"W
71°20'0"W

Figure 4-2. PI curve displaying minimum, average, and maximum estimated curves for Greenwich Bay from September 2010.

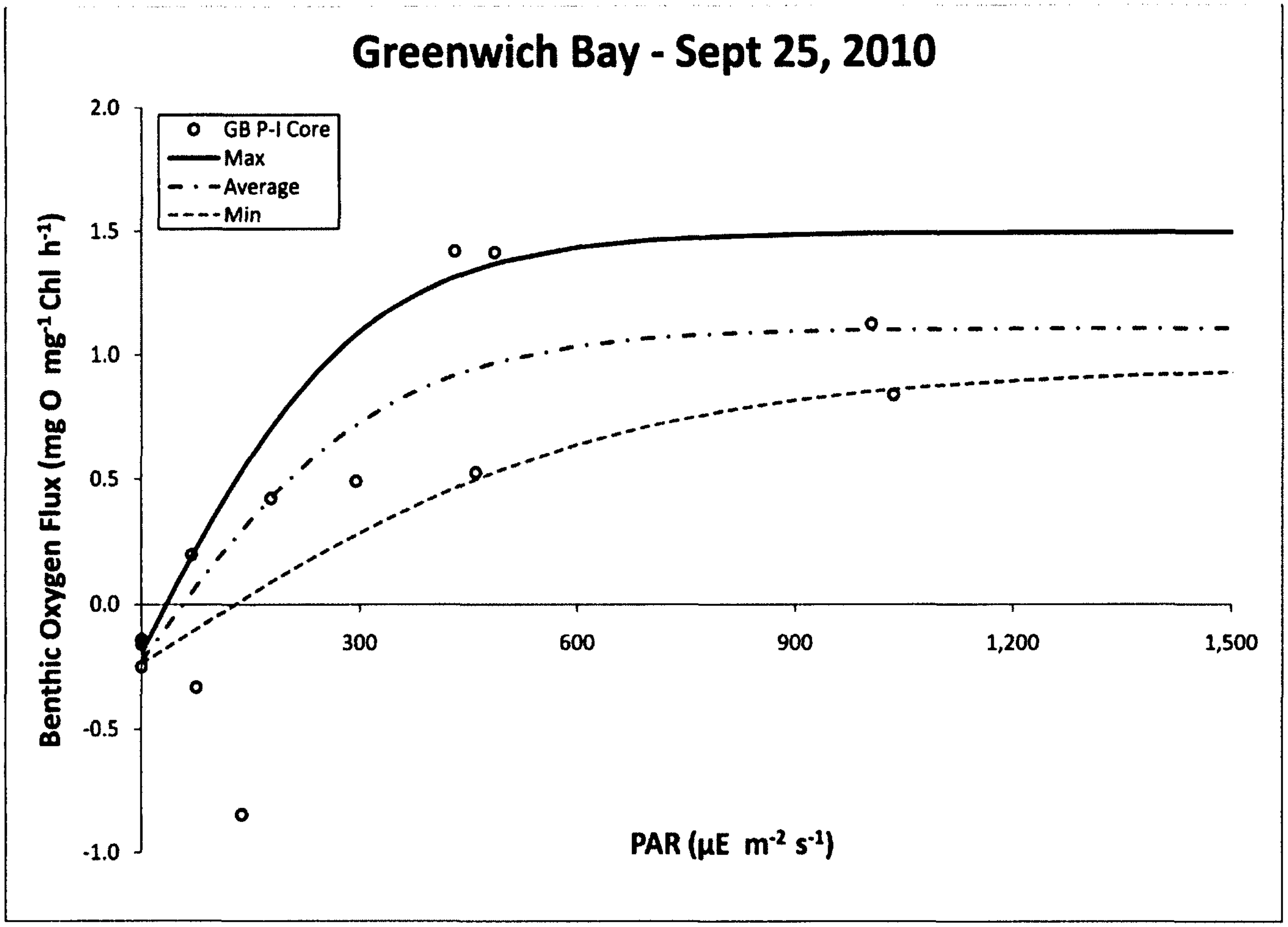
Greenwich Bay - Sept 25, 2010
GB P-I Core
Max
Average
Min
2.0
1.5
1.0
0.5
0.0
-0.5
-1.0
300
600
900
1,200
1,500
Benthic Oxygen Flux (mg O mg^{-1} Chl h^{-1})
PAR (µE m^{-2} s^{-1})

Figure 4-3. Sediment chlorophyll-*a* biomass (top 3 mm) with depth at four sites within upper Narragansett Bay.

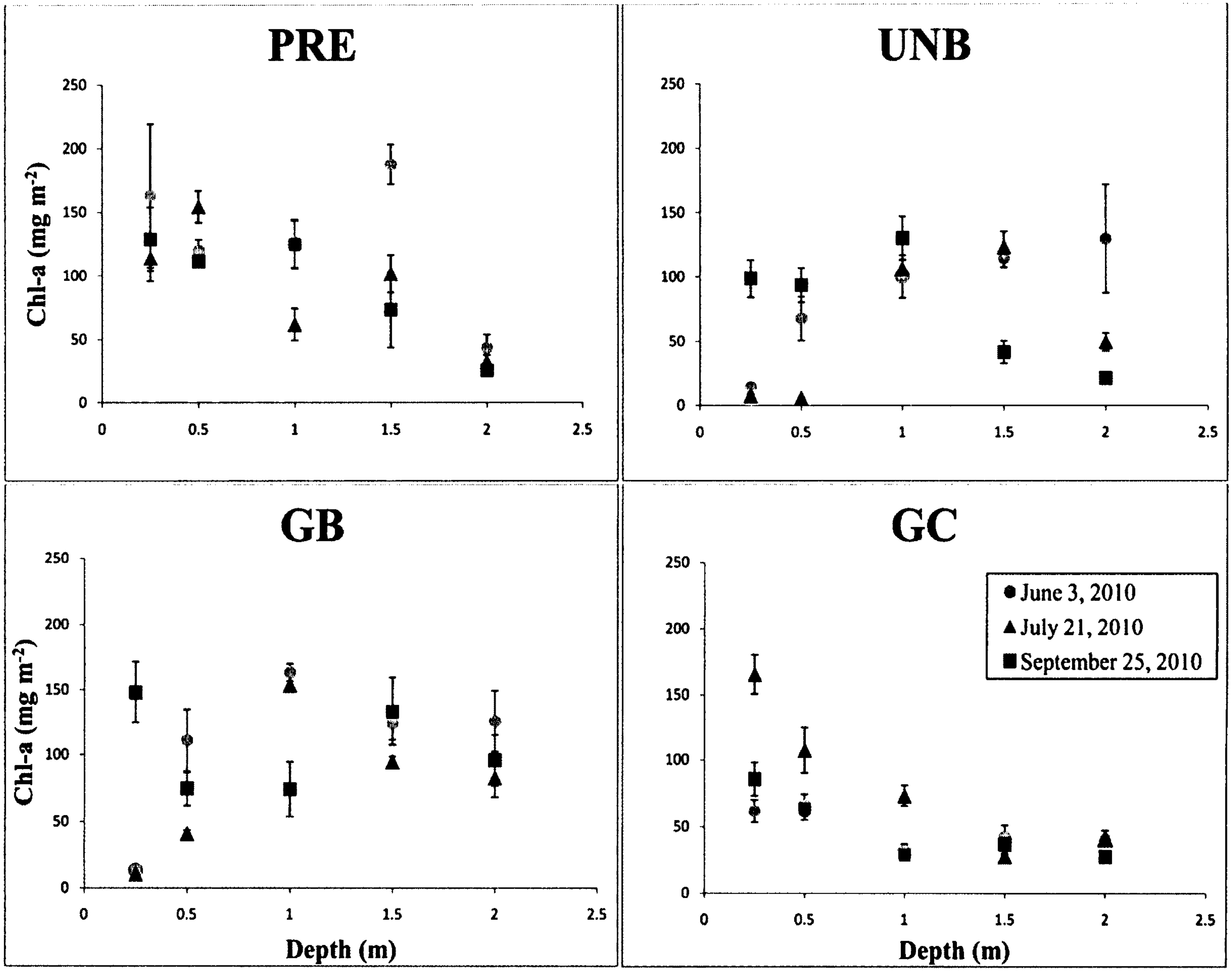
PRE
UNB
GB
GC
Chl-a (mg m^{-2})
0
50
100
150
200
250
0
0.5
1
1.5
2
2.5
Depth (m)
● June 3, 2010
▲ July 21, 2010
■ September 25, 2010

Figure 4-4. Interpolated 5 day moving average GPP_B and daytime NPP_{WC} (modified from Oviatt et al. 2002). Site numbers correspond to the bay survey station numbers from Oviatt et al. (2002).

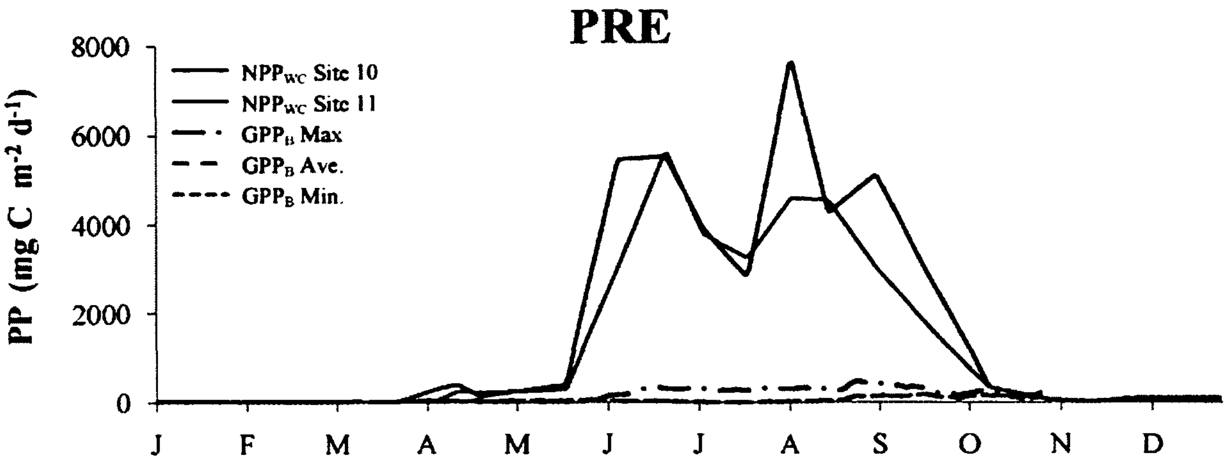
PRE
PP (mg C m^{-2} d^{-1})
8000
6000
4000
2000
0
NPP$_{WC}$ Site 10
NPP$_{WC}$ Site 11
GPP$_B$ Max
GPP$_B$ Ave.
GPP$_B$ Min.
J
F
M
A
M
J
J
A
S
O
N
D

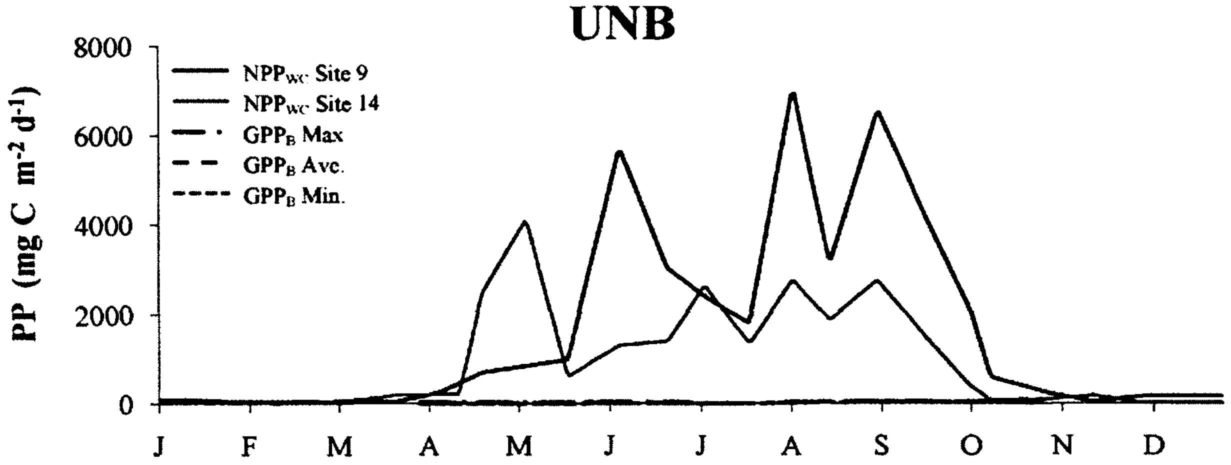
UNB
PP (mg C m^{-2} d^{-1})
8000
6000
4000
2000
0
NPP$_{WC}$ Site 9
NPP$_{WC}$ Site 14
GPP$_B$ Max
GPP$_B$ Ave.
GPP$_B$ Min.
J
F
M
A
M
J
J
A
S
O
N
D

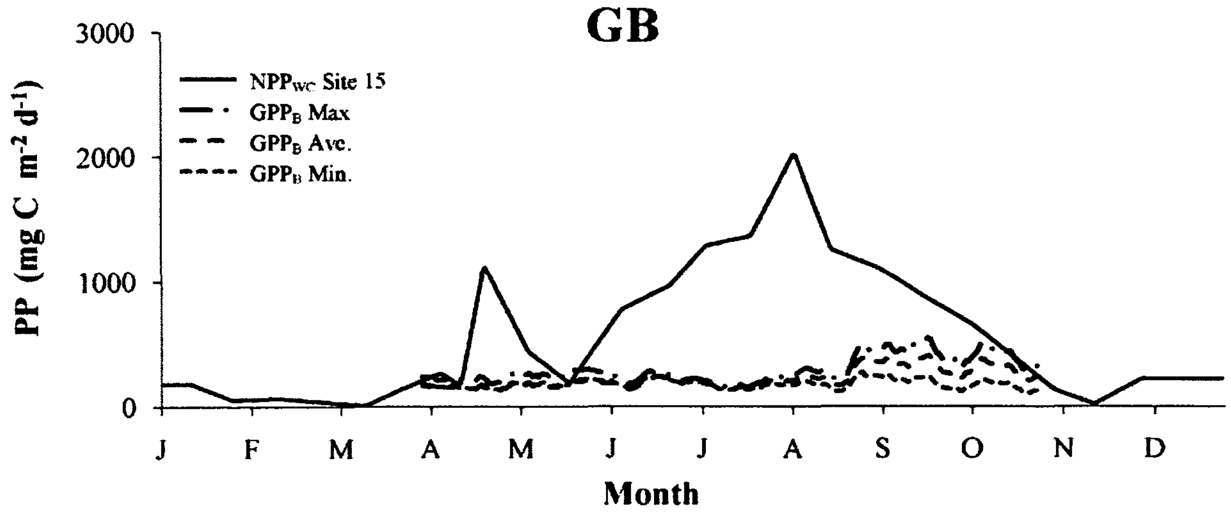
GB
PP (mg C m^{-2} d^{-1})
3000
2000
1000
0
NPP$_{WC}$ Site 15
GPP$_B$ Max
GPP$_B$ Ave.
GPP$_B$ Min.
J
F
M
A
M
J
J
A
S
O
N
D
Month

Figure 4-5. Interpolated daily NCM_B within each segment of upper Narragansett Bay.

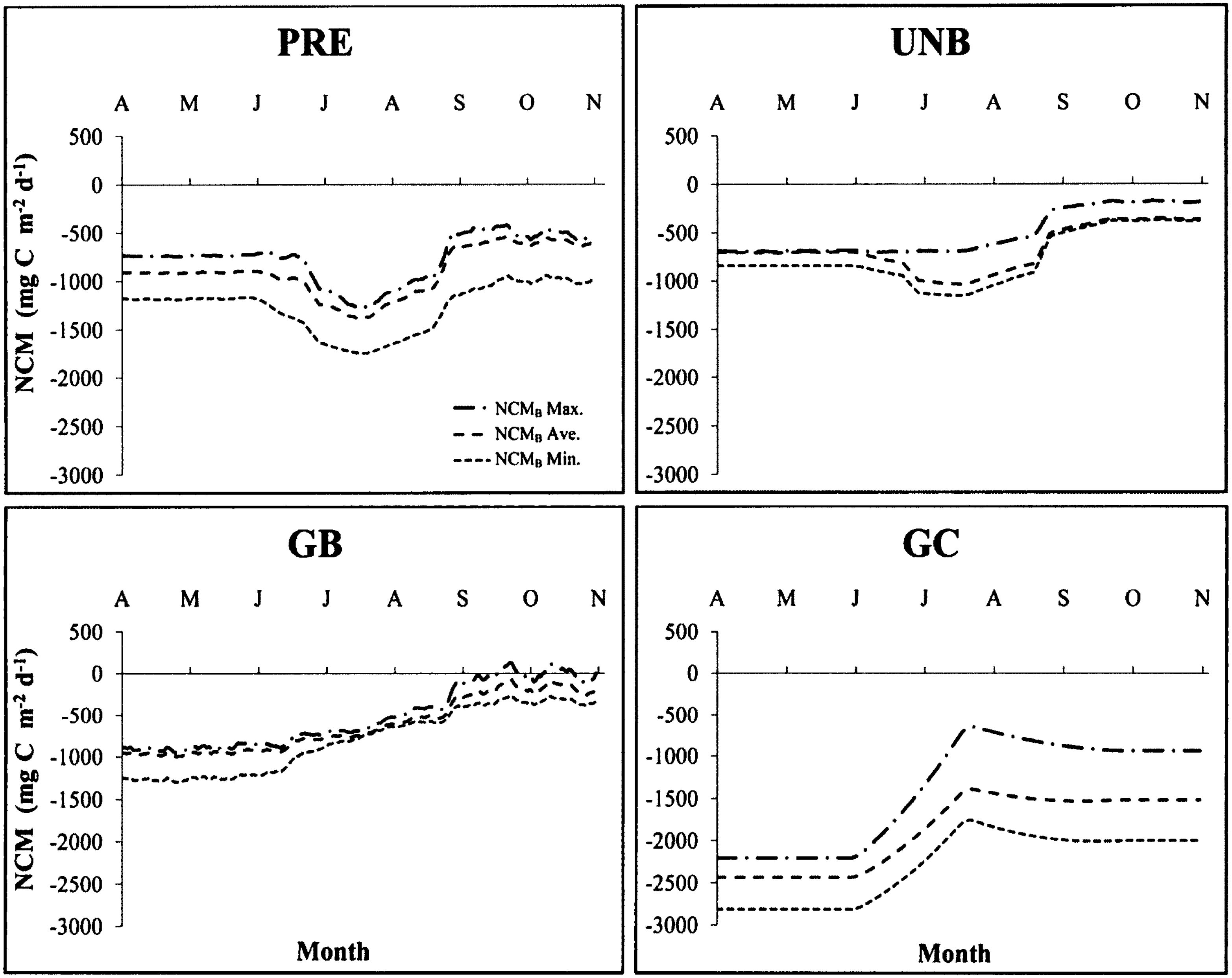
PRE
UNB
GB
GC
A M J J A S O N
500
0
-500
-1000
-1500
-2000
-2500
-3000
NCM (mg C m-2 d-1)
NCMB Max.
NCMB Ave.
NCMB Min.
Month

CHAPTER 4 - TABLES

Table 4-1. Percent of total surface area in each sampling regions: Providence River estuary (PRE), upper Narragansett Bay (UNB), Greenwich Bay (GB), and Greenwich Cove (GC). Numbers represent the percent of surface area below each depth contour. Depths are relative to mean sea level (m).

Depth	**PRE**	**UNB**	**GB**	**GC**
(m)	**(% of total area below each depth segment)**			
1	73	94	80	73
2	52	89	64	43
3	37	81	38	9
4	28	72	13	0
5	21	58	6	0

Table 4-2. Percent of total primary production attributed to microphytobenthos in upper Narragansett Bay. Values outside brackets represent the contribution from benthic production based on the average model, while the bracketed values represent the minimum and maximum models respectively. Total primary production was computed from GPP_B (calculated in this study) and daytime NPP_{WC} (from Oviatt et al. 2002) at 5 sites (site numbers correspond to the bay survey stations from Oviatt et al. 2002) in upper Narragansett Bay from April to October.

Month	PR-10	PR-11	UNB-9	UNB-14	GB-15
Apr	13 *(11-14)*	18 *(16-20)*	3 *(0-6)*	1 *(0-2)*	23 *(22-29)*
May	5 *(5-6)*	8 *(7-9)*	1 *(0-3)*	1 *(0-2)*	33 *(31-40)*
June	3 *(1-4)*	4 *(1-6)*	0 *(0-1)*	1 *(0-2)*	19 *(18-22)*
July	5 *(0-7)*	5 *(0-7)*	0 *(0-0)*	0 *(0-0)*	11 *(11-12)*
Aug	4 *(1-6)*	5 *(1-7)*	1 *(1-1)*	1 *(1-1)*	14 *(11-16)*
Sept	6 *(4-8)*	9 *(6-13)*	1 *(1-1)*	2 *(2-2)*	26 *(18-32)*
Oct	17 *(17-24)*	23 *(22-31)*	3 *(3-4)*	13 *(11-15)*	37 *(25-45)*

APPENDIX

Figure A-1. Modeled daily residence time for the York River estuary (solid lines) for 2007, 2008, 2009, and 2010 calculated by an Officer (1980) type two-layer box model. Dashed lines represent the calculated low, mean and high flow residence times simulated by Shen and Haas (2004).

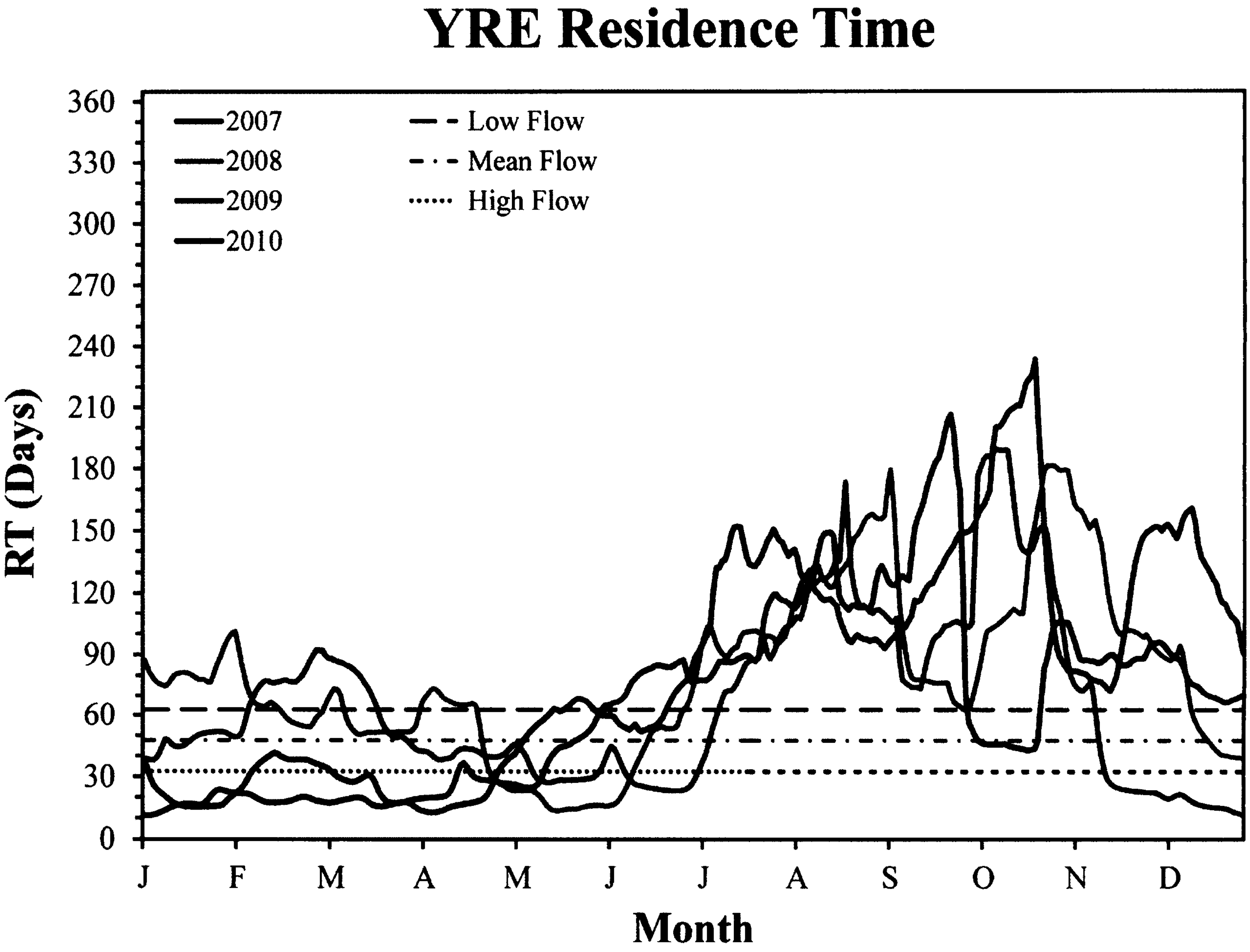
YRE Residence Time
RT (Days)
0
30
60
90
120
150
180
210
240
270
300
330
360
2007
2008
2009
2010
Low Flow
Mean Flow
High Flow
J
F
M
A
M
J
J
A
S
O
N
D
Month

Figure A-2. Measured (large points) and modeled (lines) light attenuation (k_D) for all box model regions. Measured k_D values for Boxes 1 – 8 (a-d) were sampled by the CBP. Additional k_D values measured by the Chesapeake Bay NERR were included for Boxes 5 – 8 (c, d).

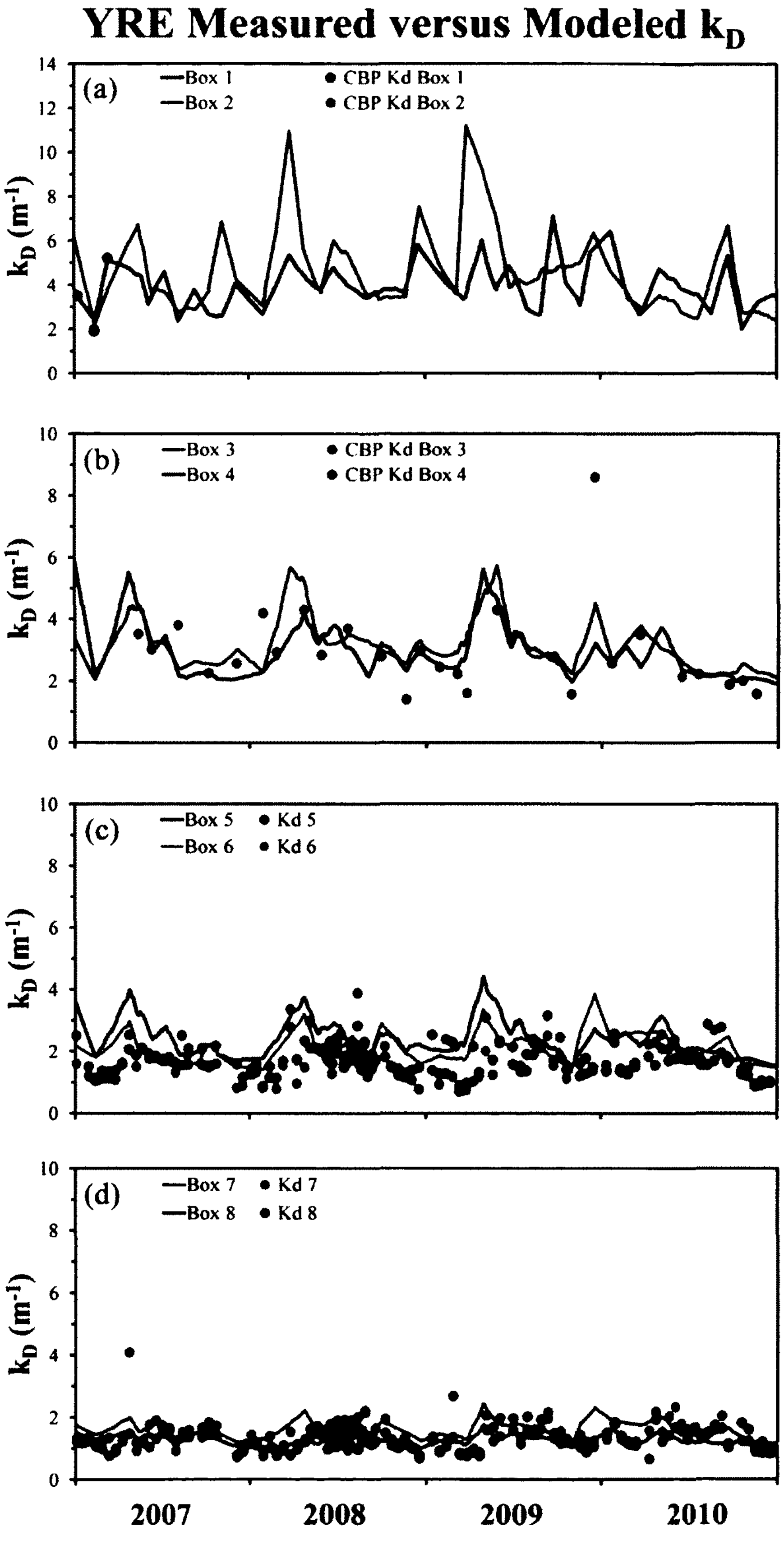
YRE Measured versus Modeled k_D
(a)
—Box 1
—Box 2
● CBP Kd Box 1
● CBP Kd Box 2
(b)
—Box 3
—Box 4
● CBP Kd Box 3
● CBP Kd Box 4
(c)
—Box 5
—Box 6
● Kd 5
● Kd 6
(d)
—Box 7
—Box 8
● Kd 7
● Kd 8
k_D (m^{-1})
0
2
4
6
8
10
12
14
2007
2008
2009
2010

Figure A-3. Measured (large points) and modeled (small grey points) water column chlorophyll-*a* concentrations for the upper estuary boxes (1 – 4). Measured concentrations sampled by the CBP.

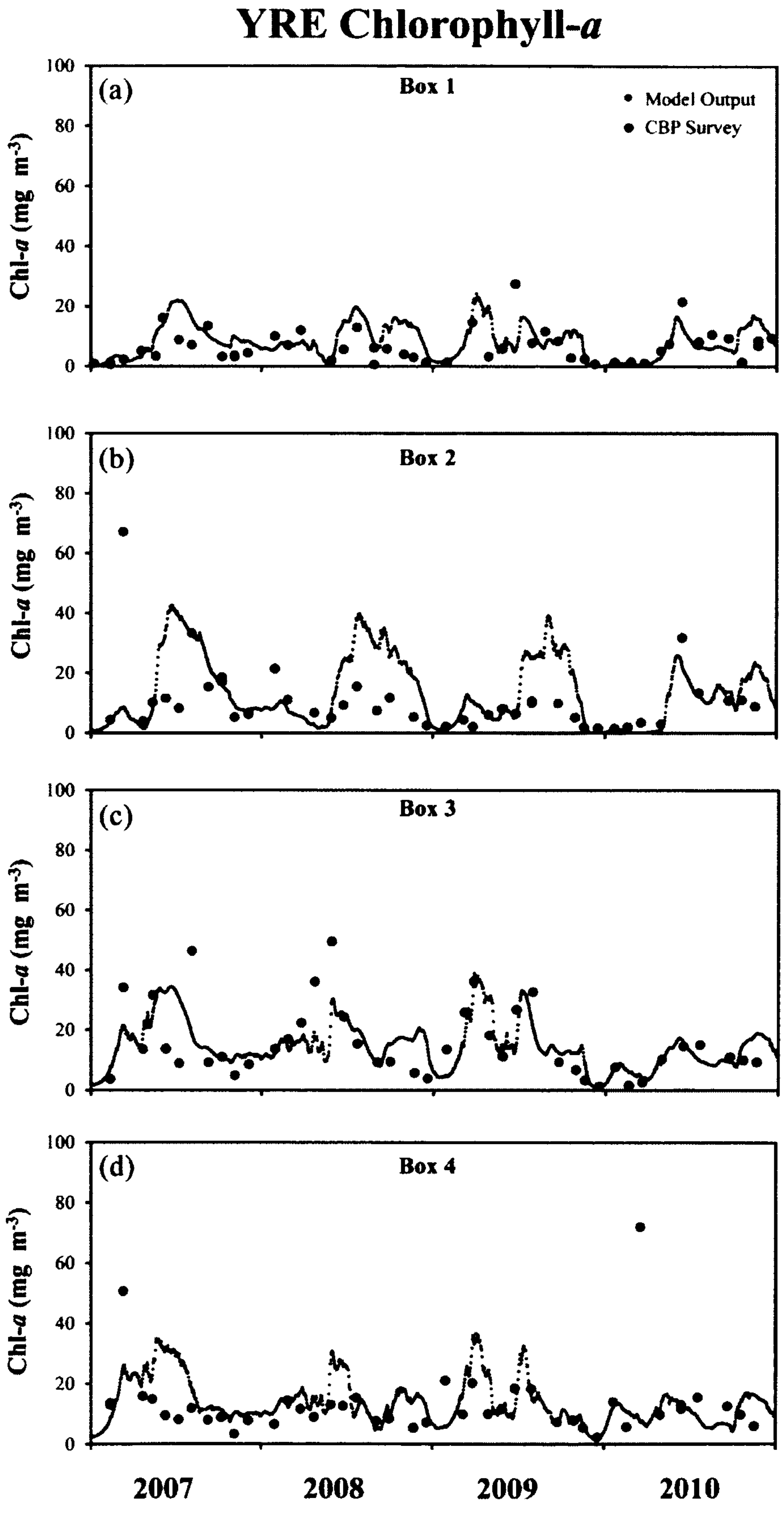
YRE Chlorophyll-*a*
(a)
Box 1
Model Output
CBP Survey
(b)
Box 2
(c)
Box 3
(d)
Box 4
Chl-*a* (mg m-3)
0
20
40
60
80
100
2007
2008
2009
2010

Figure A-4. Measured (large points) and modeled (small grey points) water column chlorophyll-*a* concentrations for the lower estuary boxes (5 – 8). Measured concentrations sampled by the CBP.

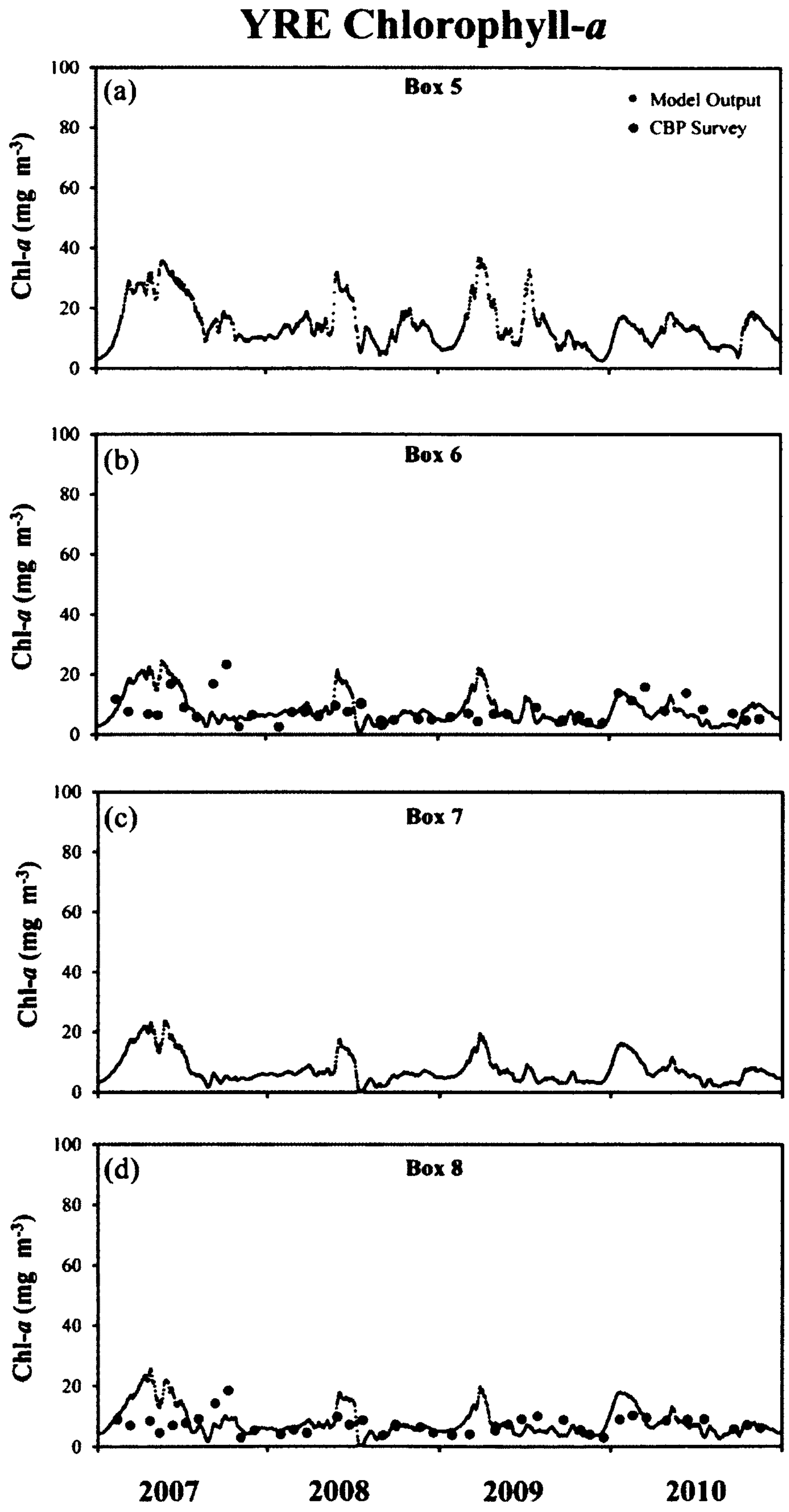
YRE Chlorophyll-a
(a)
Box 5
• Model Output
● CBP Survey
(b)
Box 6
(c)
Box 7
(d)
Box 8
Chl-a (mg m-3)
100
80
60
40
20
0
2007
2008
2009
2010

Figure A-5. Measured (large points) and modeled (small grey points) microphytobenthos chlorophyll-*a* concentrations for the upper estuary boxes (1 – 4). Measured (1 m below mean low water) and modeled (0.5 – 1 m depth segment) concentrations. Microphytobenthos was not measured in Boxes 1 – 3.

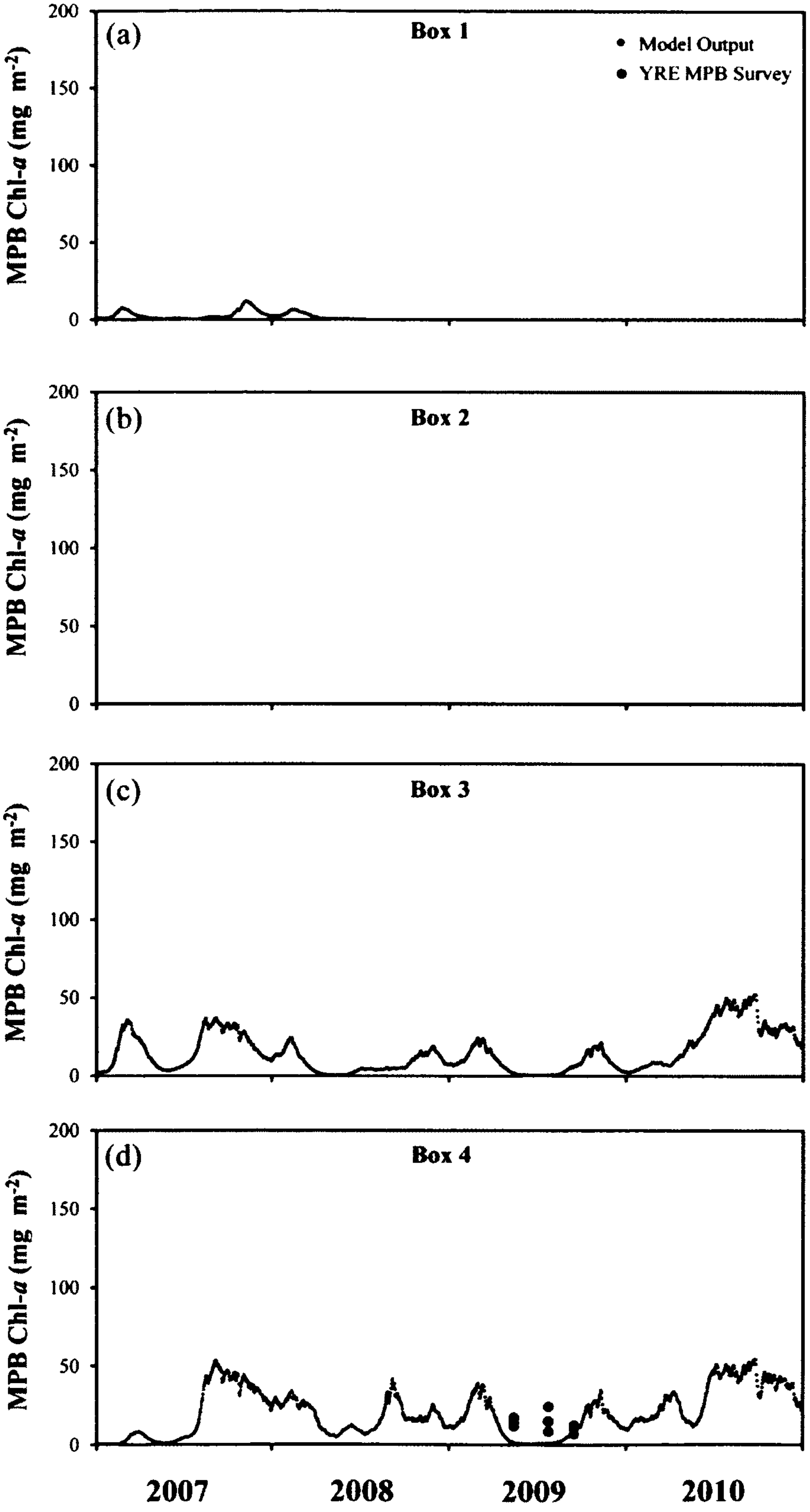

YRE MPB Chl-*a*

(a)
Box 1
• Model Output
● YRE MPB Survey
(b)
Box 2
(c)
Box 3
(d)
Box 4
MPB Chl-a (mg m-2)
0
50
100
150
200
2007
2008
2009
2010

Figure A-6. Measured (large points) and modeled (small grey points) microphytobenthos chlorophyll-*a* concentrations for the lower estuary boxes (5 – 8). Measured (1 m below mean low water) and modeled (0.5 – 1 m depth segment) concentrations.

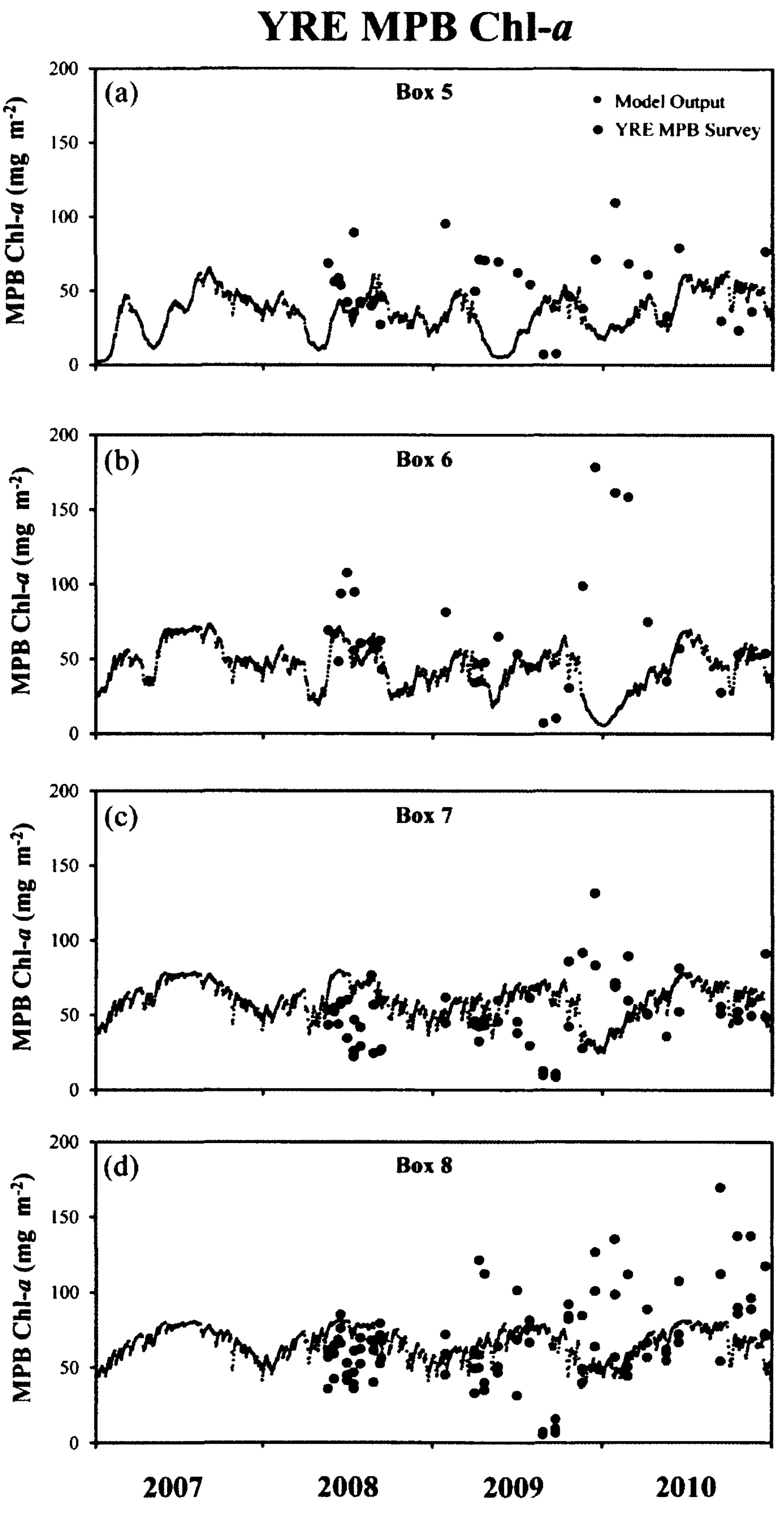
YRE MPB Chl-*a*
(a)
Box 5
(b)
Box 6
(c)
Box 7
(d)
Box 8
● Model Output
● YRE MPB Survey
MPB Chl-*a* (mg m-2)
0
50
100
150
200
2007
2008
2009
2010

Figure A-7. Measured (large points) and modeled (dashed line) microphytobenthos chlorophyll-*a* concentrations with depth for sites within Boxes 4 – 6. Error bars on all panels represent standard error.

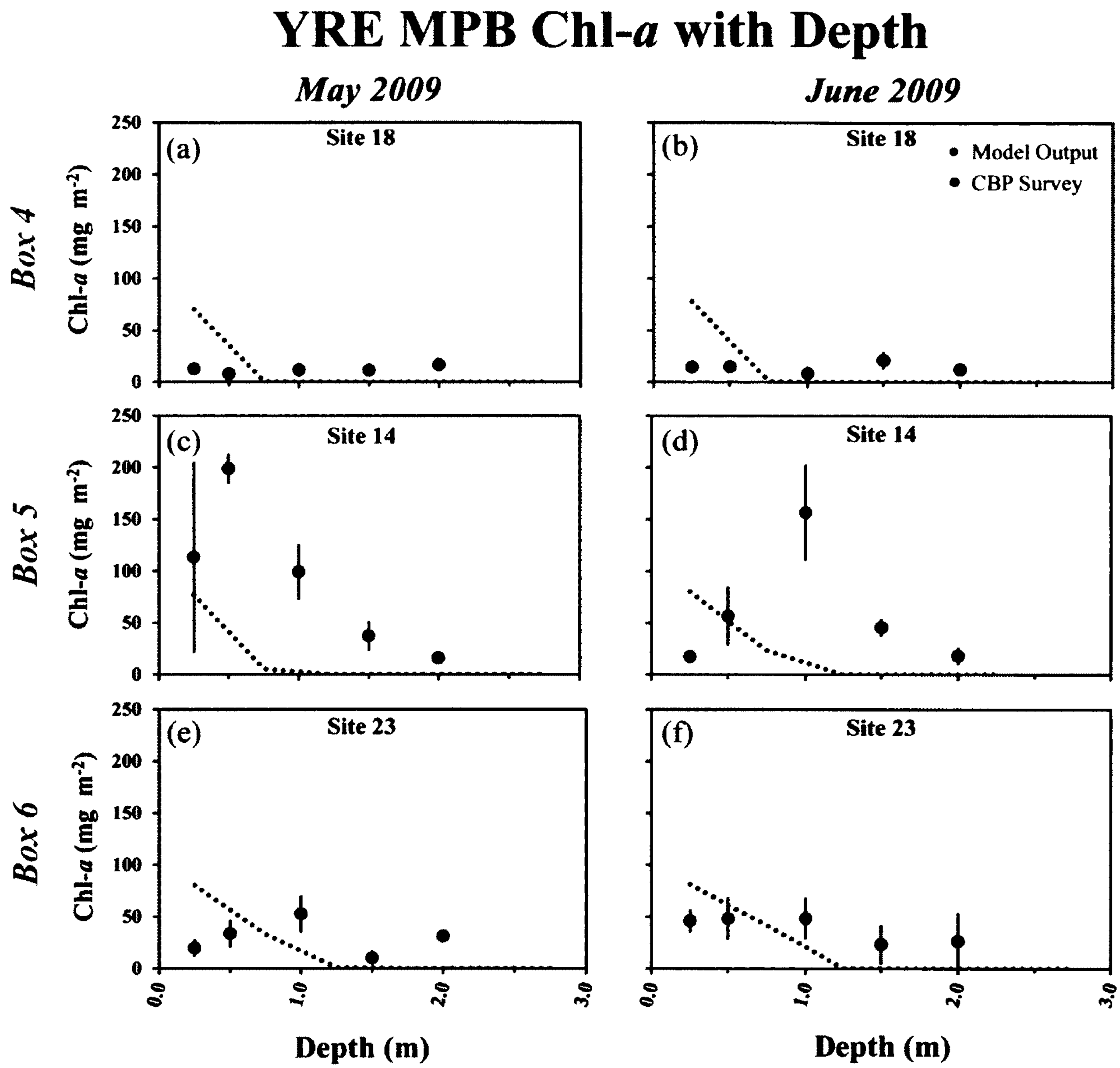
YRE MPB Chl-a with Depth
May 2009
June 2009
Box 4
Box 5
Box 6
Chl-a (mg m-2)
250
200
150
100
50
0
(a)
Site 18
(b)
Site 18
Model Output
CBP Survey
(c)
Site 14
(d)
Site 14
(e)
Site 23
(f)
Site 23
0.0
1.0
2.0
3.0
Depth (m)
Depth (m)

Figure A-8. Measured (large points) and modeled (dashed line) microphytobenthos chlorophyll-*a* concentrations with depth for sites within Boxes 6 – 8. Error bars on all panels represent standard error.

YRE MPB Chl-*a* with Depth

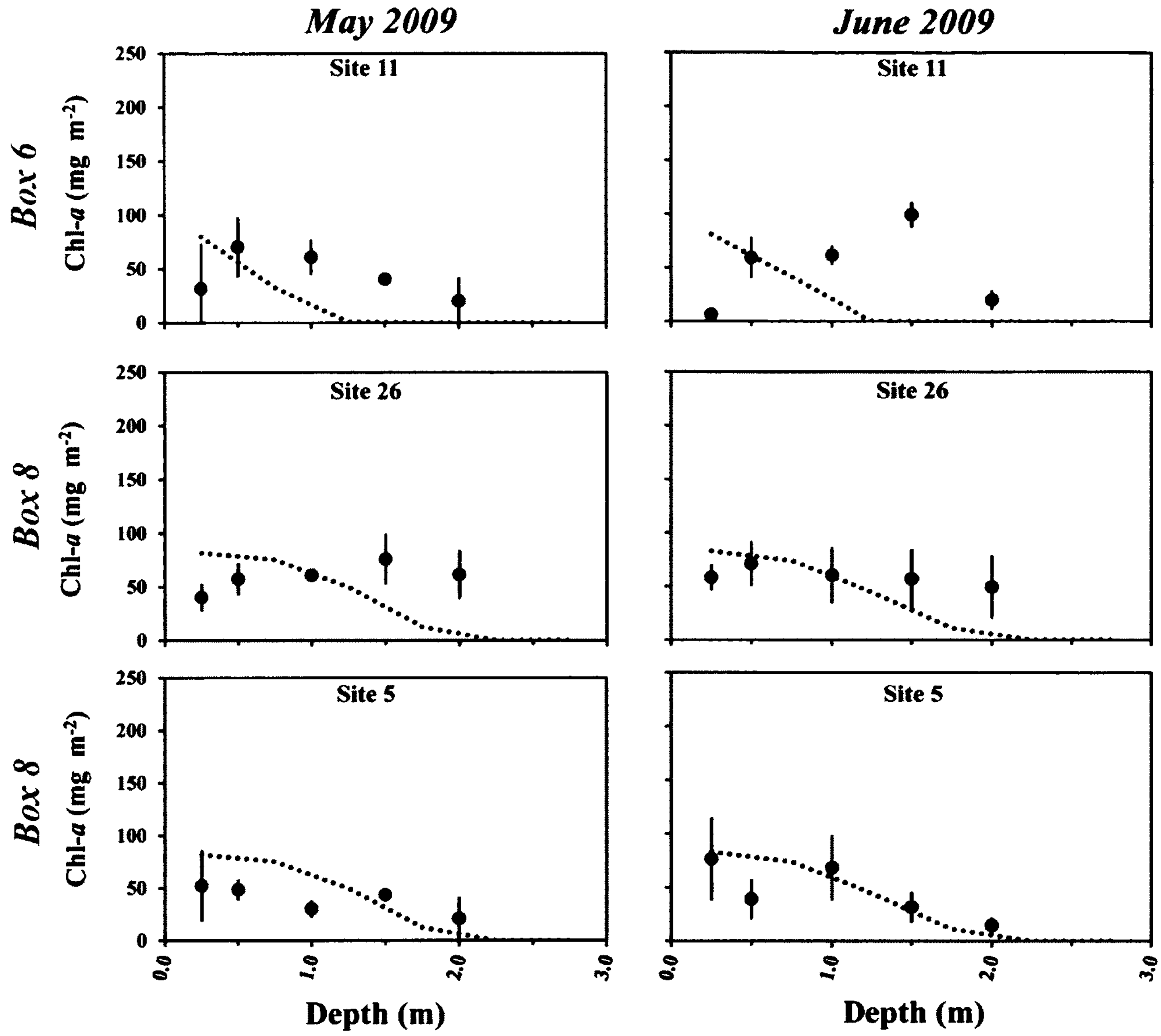

Figure A-9. Measured (large points) and modeled (small grey points) surface layer dissolved oxygen concentrations for the upper estuary boxes (1 – 4). Measured concentrations sampled by the CBP.

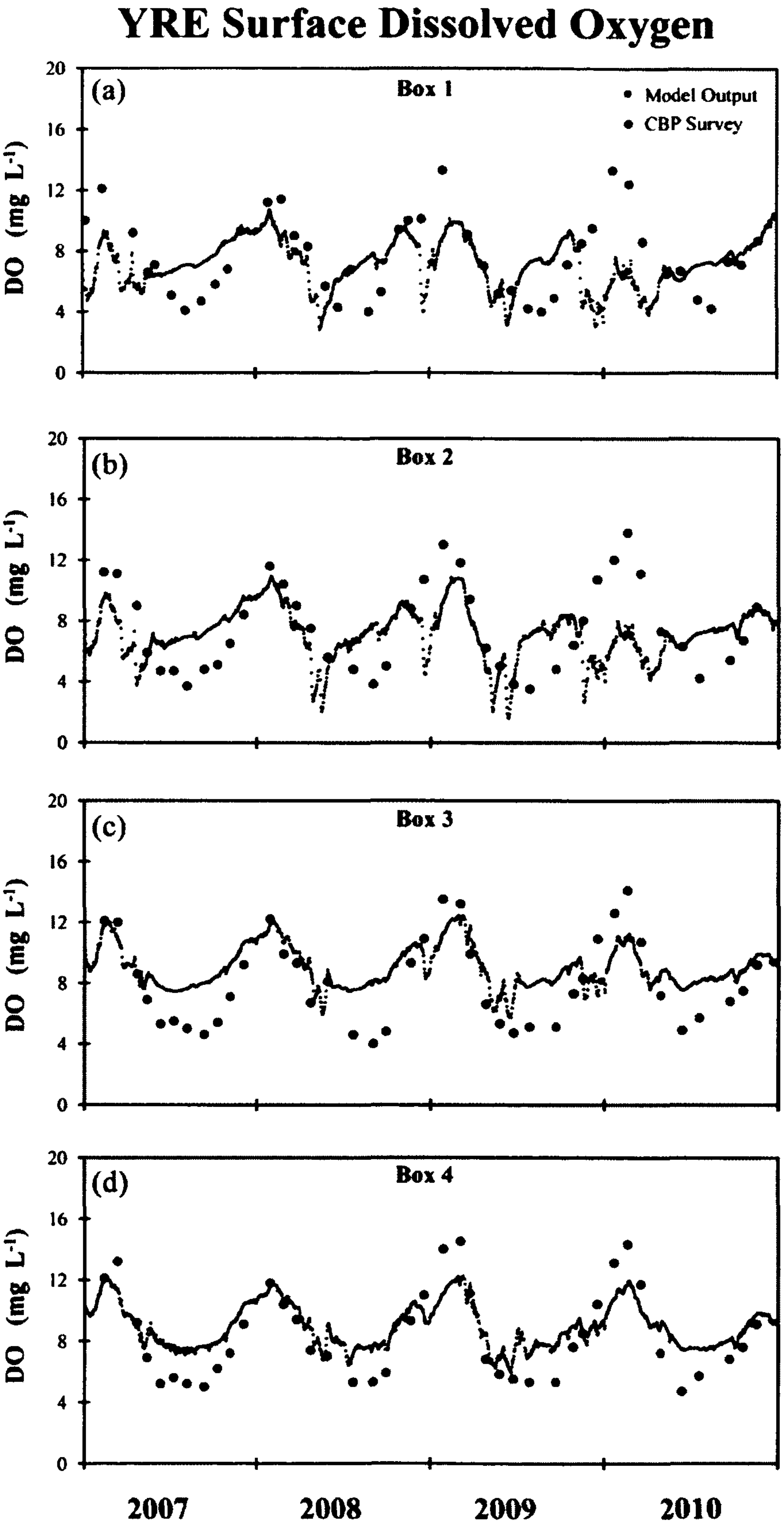
YRE Surface Dissolved Oxygen
(a)
Box 1
Model Output
CBP Survey
(b)
Box 2
(c)
Box 3
(d)
Box 4
DO (mg L^{-1})
0
4
8
12
16
20
2007
2008
2009
2010

Figure A-10. Measured (large points) and modeled (small grey points) surface layer dissolved oxygen concentrations for the lower estuary boxes (5 – 8). Measured concentrations sampled by the CBP. Volume weighted dissolved oxygen concentrations sampled during the 2007 and 2008 Acrobat^{TM} surveys are included as triangles on all panels.

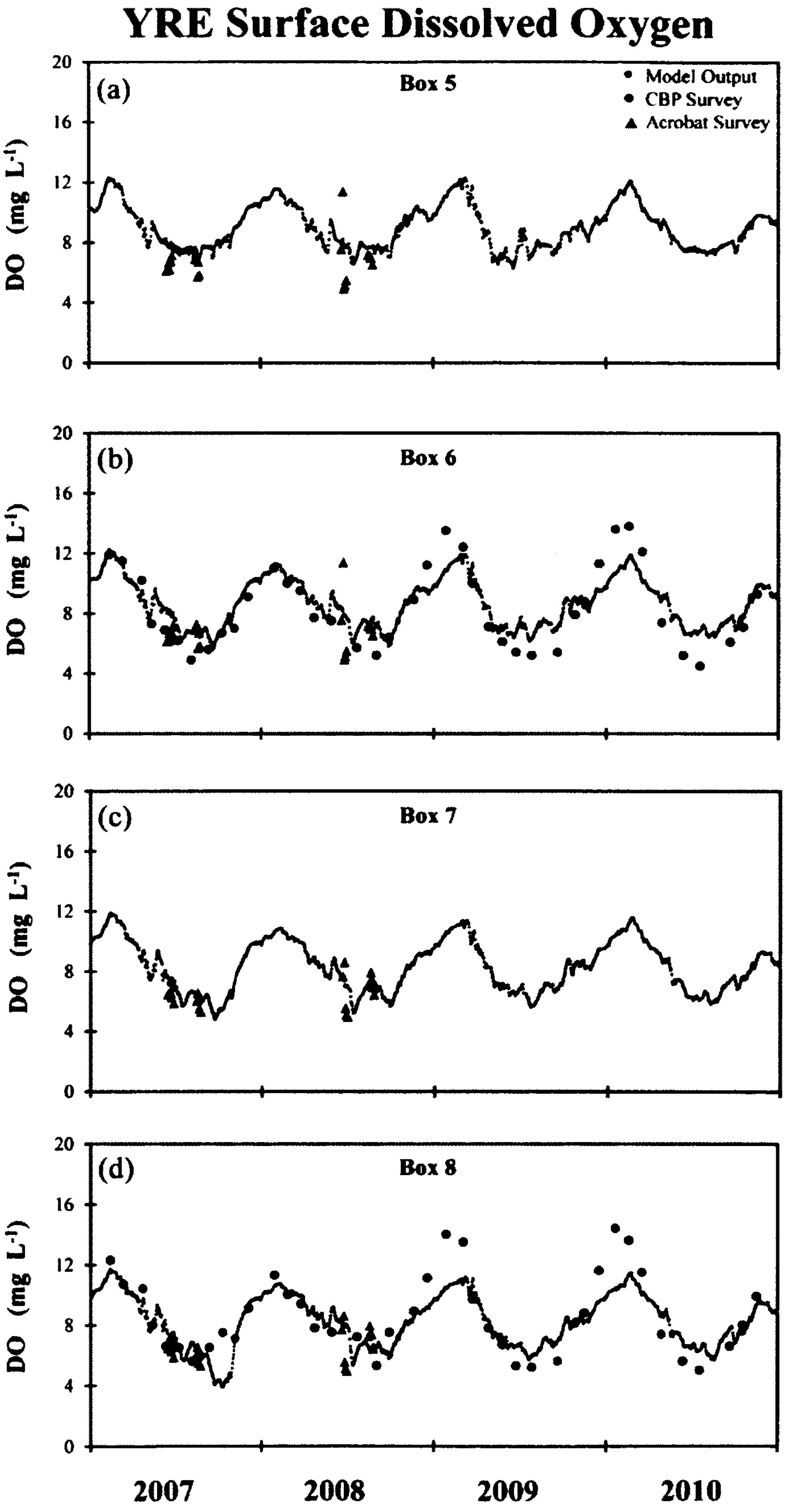
YRE Surface Dissolved Oxygen
(a)
Box 5
• Model Output
● CBP Survey
▲ Acrobat Survey
(b)
Box 6
(c)
Box 7
(d)
Box 8
DO (mg L^{-1})
0
4
8
12
16
20
2007
2008
2009
2010

Figure A-11. Measured (large points) and modeled (small grey points) bottom layer dissolved oxygen concentrations for the upper estuary boxes (1 – 4). Measured concentrations sampled by the CBP.

YRE Bottom Dissolved Oxygen

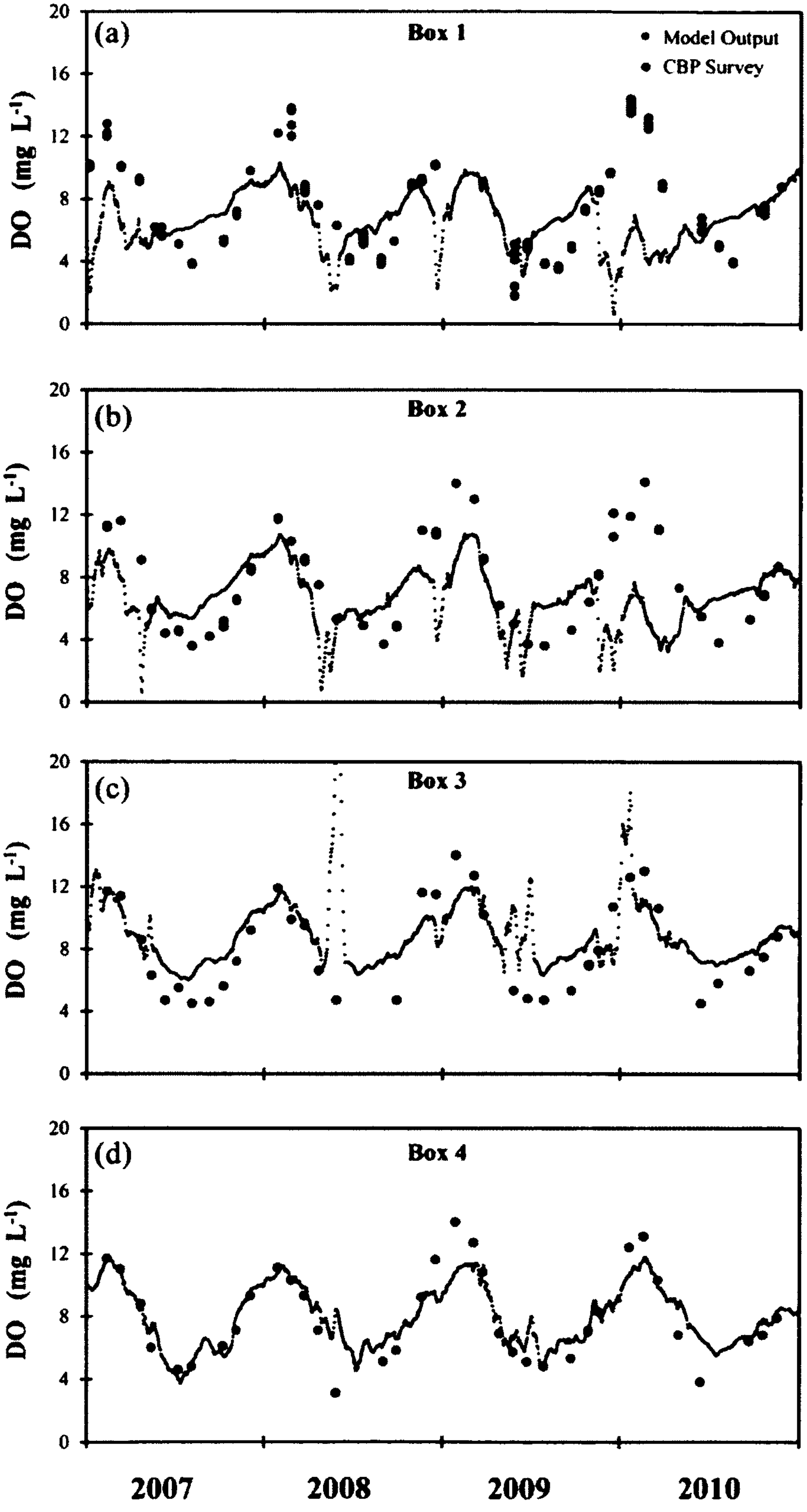

Figure A-12. Measured (large points) and modeled (small grey points) bottom layer dissolved oxygen concentrations for the lower estuary boxes (5 – 8). Measured concentrations sampled by the CBP. Volume weighted dissolved oxygen concentrations sampled during the 2007 and 2008 Acrobat^{TM} surveys are included as triangles on all panels. Dashed lines in all panels represent hypoxic conditions (< 2 mg L^{-1}).

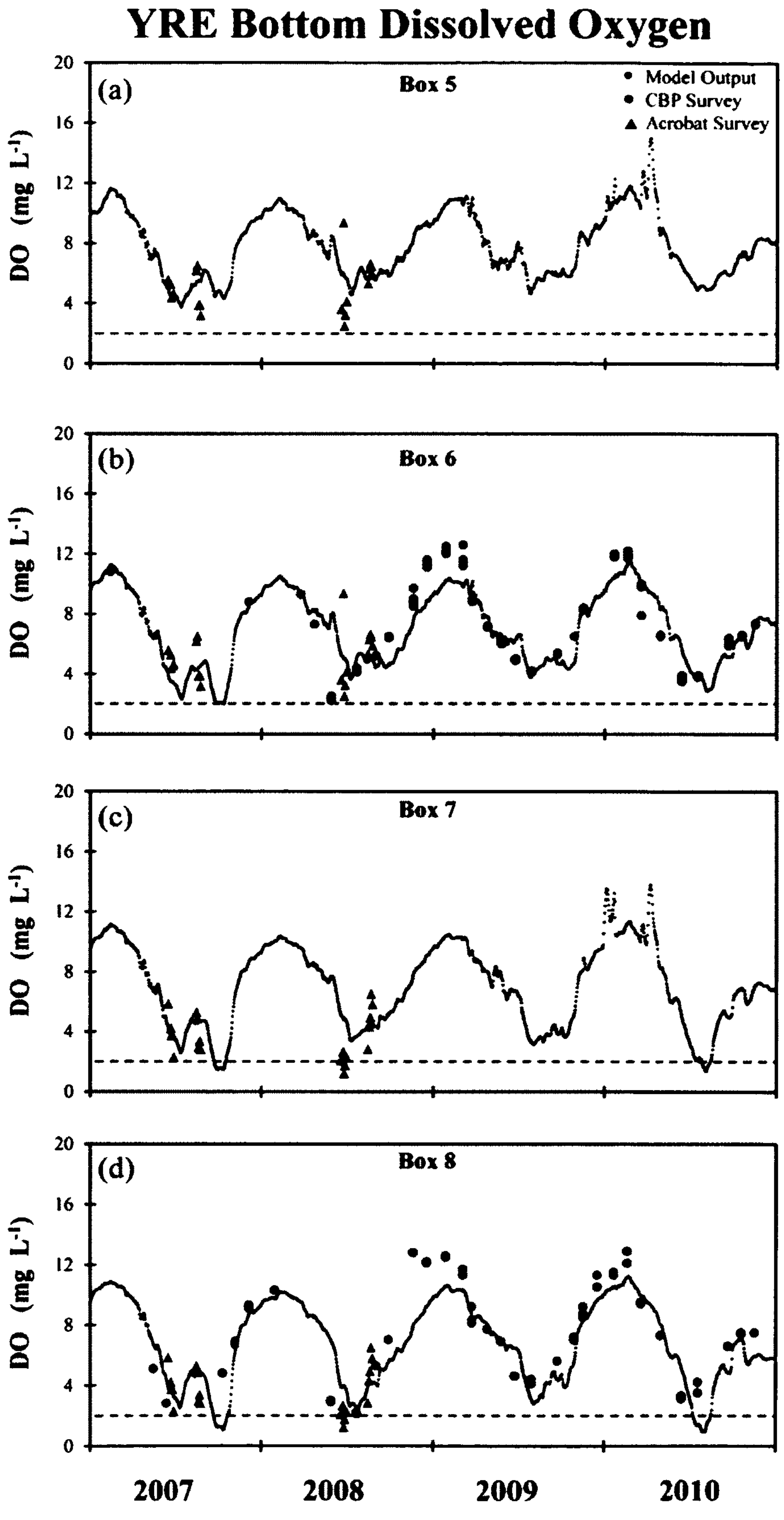
YRE Bottom Dissolved Oxygen
(a)
Box 5
• Model Output
● CBP Survey
▲ Acrobat Survey
(b)
Box 6
(c)
Box 7
(d)
Box 8
DO (mg L-1)
0
4
8
12
16
20
2007
2008
2009
2010

Figure A-13. Measured (large points) and modeled (small grey points) surface layer dissolved inorganic nitrogen concentrations for the upper estuary boxes (1 – 4). Measured concentrations sampled by the CBP.

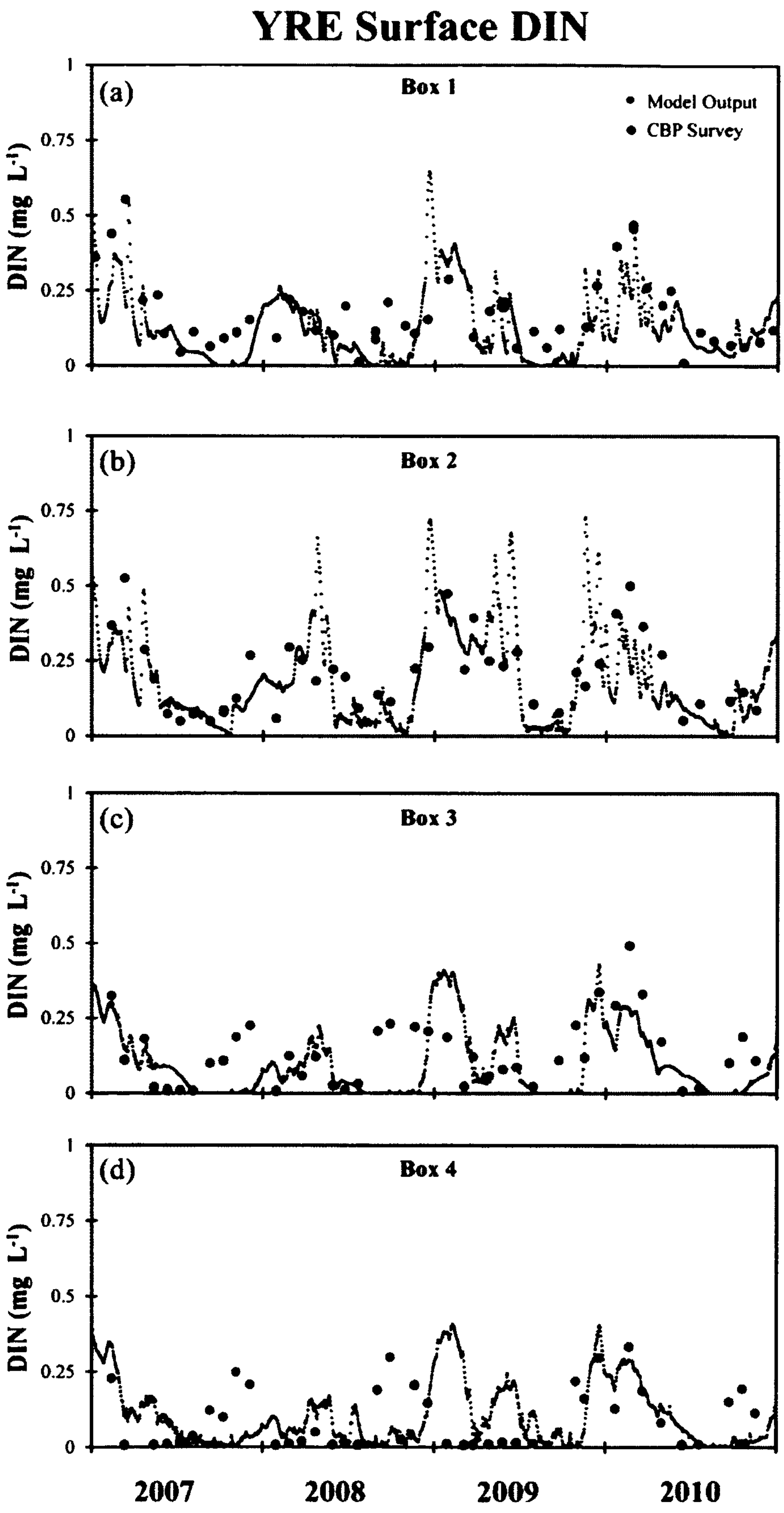
YRE Surface DIN
(a)
Box 1
Model Output
CBP Survey
(b)
Box 2
(c)
Box 3
(d)
Box 4
DIN (mg L^{-1})
0
0.25
0.5
0.75
1
2007
2008
2009
2010

Figure A-14. Measured (large points) and modeled (small grey points) surface layer dissolved inorganic nitrogen concentrations for the lower estuary boxes (5 – 8). Measured concentrations sampled by the CBP.

YRE Surface DIN

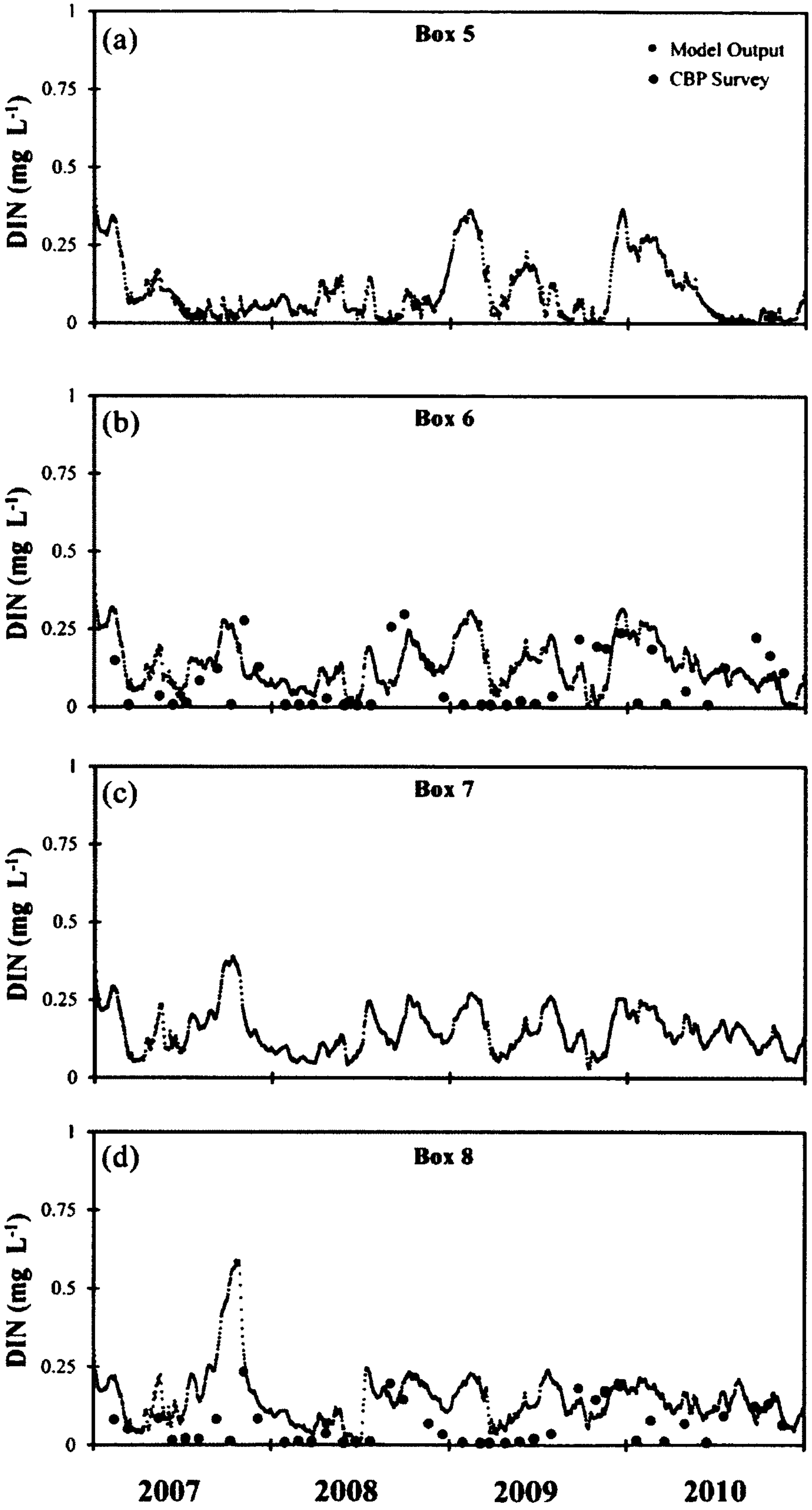

Figure A-15. Measured (large points) and modeled (small grey points) bottom layer dissolved inorganic nitrogen concentrations for the upper estuary boxes (1 – 4). Measured concentrations sampled by the CBP.

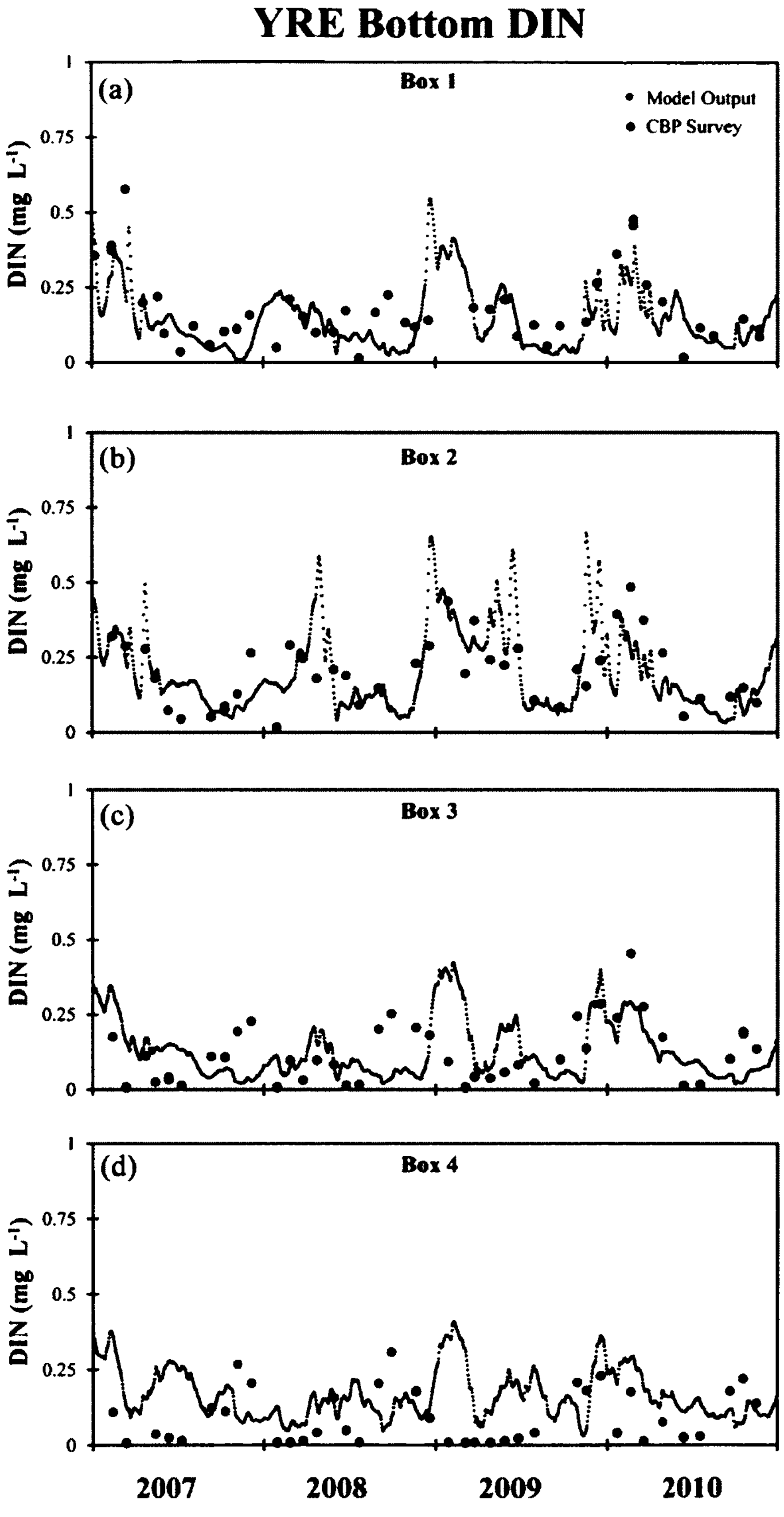
YRE Bottom DIN
(a)
Box 1
Model Output
CBP Survey
(b)
Box 2
(c)
Box 3
(d)
Box 4
DIN (mg L-1)
0
0.25
0.5
0.75
1
2007
2008
2009
2010

Figure A-16. Measured (large points) and modeled (small grey points) bottom layer dissolved inorganic nitrogen concentrations for the lower estuary boxes (5 – 8). Measured concentrations sampled by the CBP.

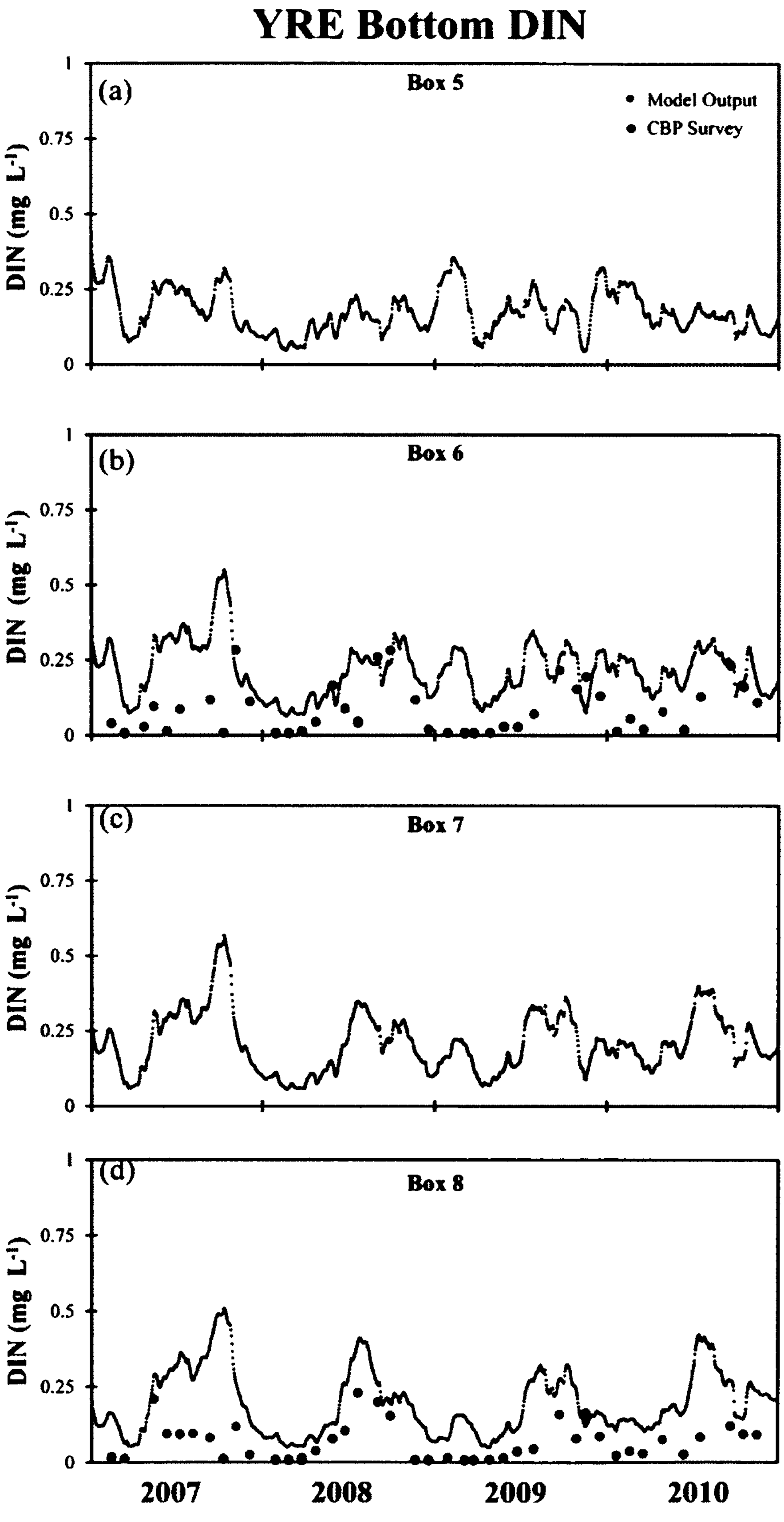
YRE Bottom DIN
(a)
Box 5
Model Output
CBP Survey
(b)
Box 6
(c)
Box 7
(d)
Box 8
DIN (mg L-1)
0
0.25
0.5
0.75
1
2007
2008
2009
2010

Figure A-17. Measured (large points) and modeled (small grey points) surface layer dissolved inorganic phosphorus concentrations for the upper estuary boxes (1 – 4). Measured concentrations sampled by the CBP.

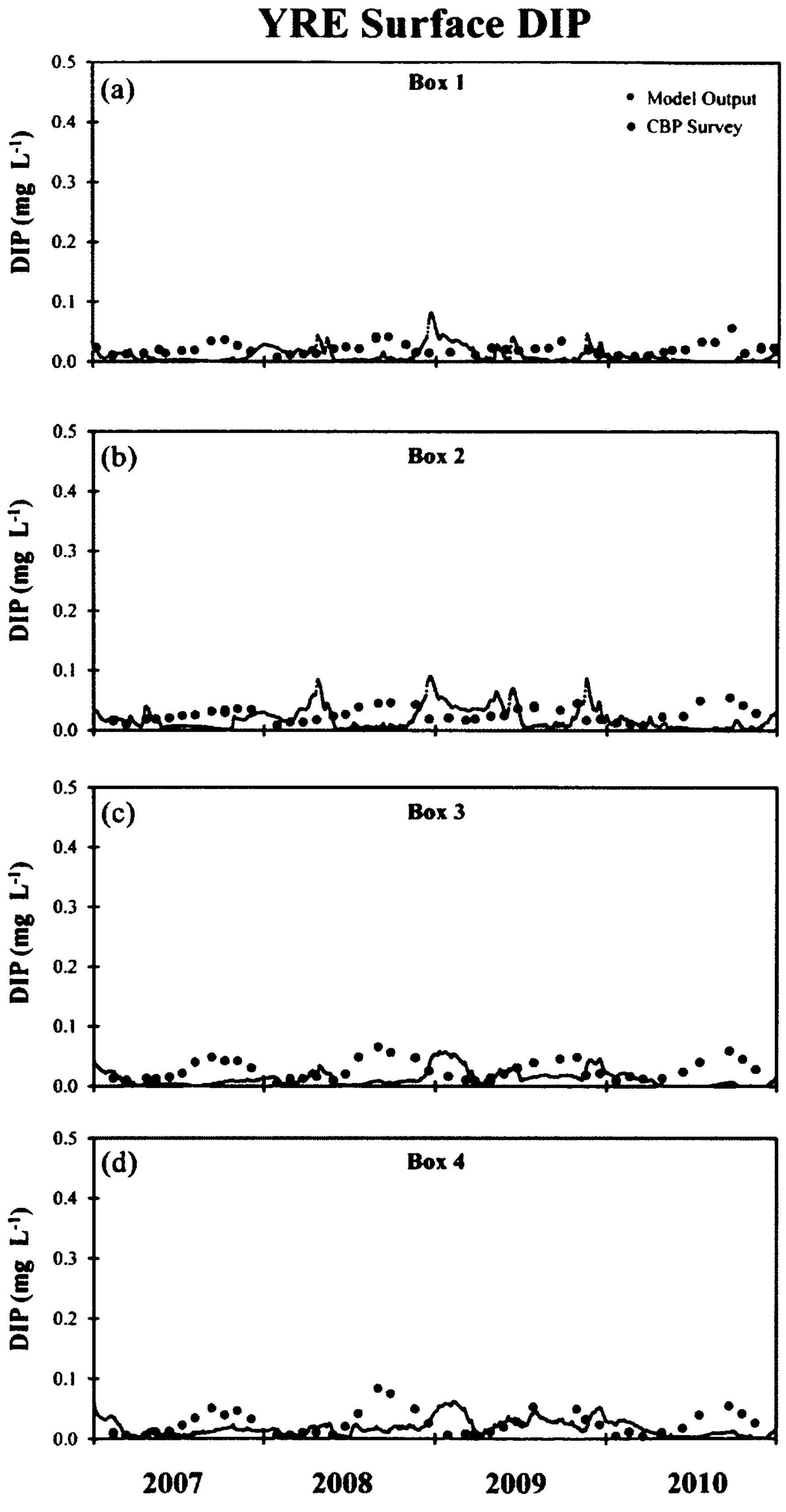
YRE Surface DIP
(a)
Box 1
Model Output
CBP Survey
(b)
Box 2
(c)
Box 3
(d)
Box 4
DIP (mg L-1)
0.5
0.4
0.3
0.2
0.1
0.0
2007
2008
2009
2010

Figure A-18. Measured (large points) and modeled (small grey points) surface layer dissolved inorganic phosphorus concentrations for the lower estuary boxes (5 – 8). Measured concentrations sampled by the CBP.

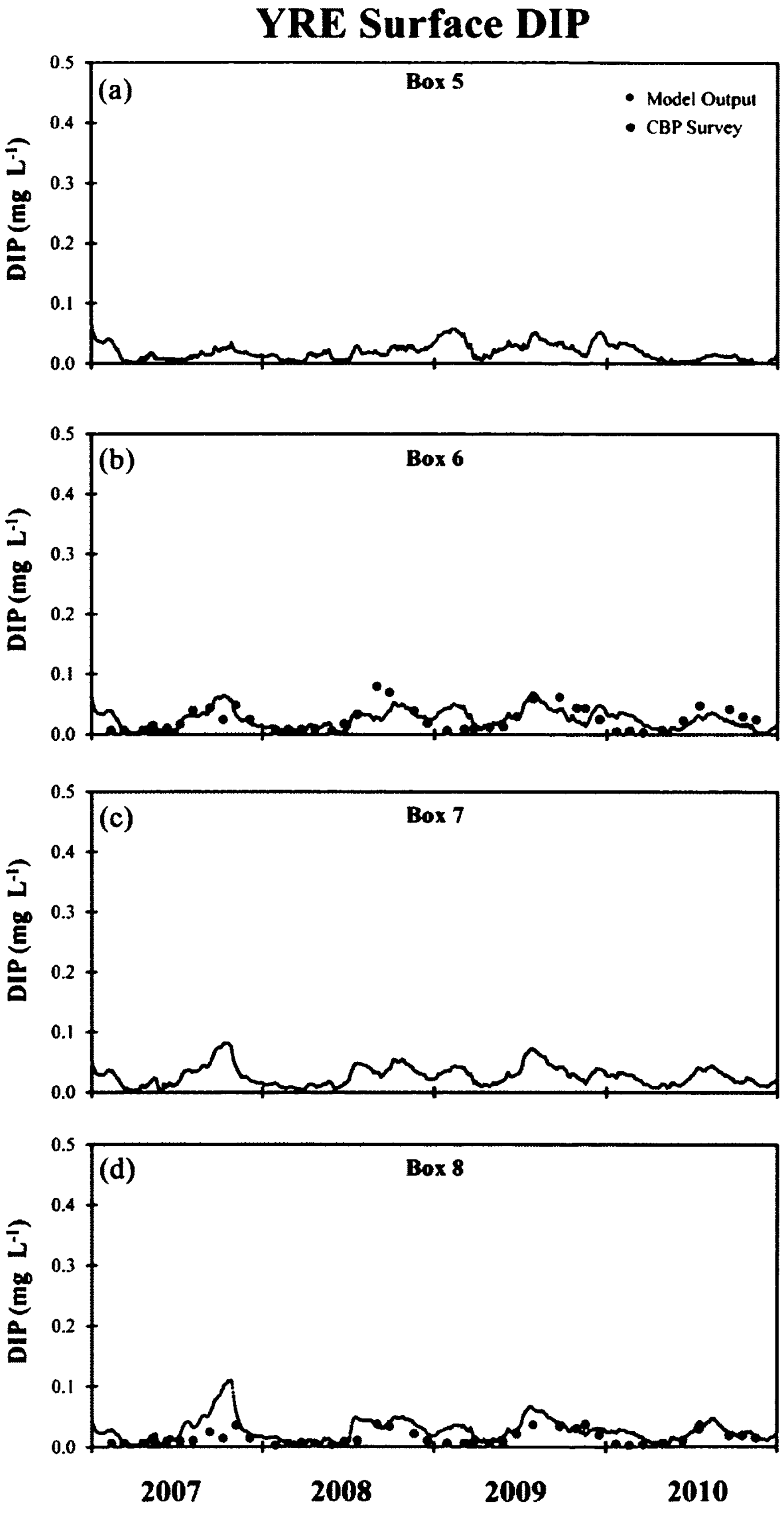
YRE Surface DIP
(a)
Box 5
● Model Output
● CBP Survey
(b)
Box 6
(c)
Box 7
(d)
Box 8
DIP (mg L-1)
0.5
0.4
0.3
0.2
0.1
0.0
2007
2008
2009
2010

Figure A-19. Measured (large points) and modeled (small grey points) bottom layer dissolved inorganic phosphorus concentrations for the upper estuary boxes (1 – 4). Measured concentrations sampled by the CBP.

YRE Bottom DIP

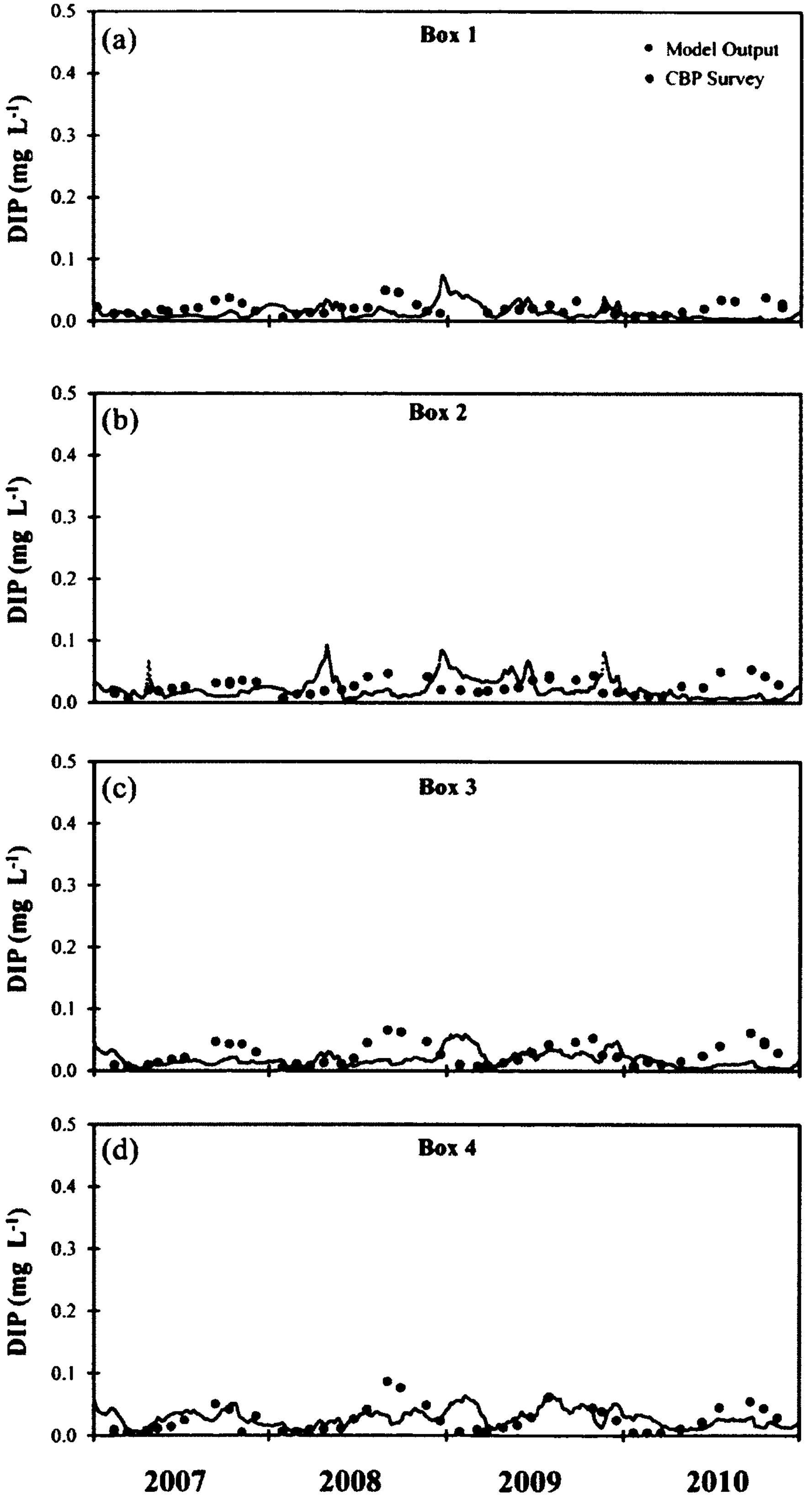

Figure A-20. Measured (large points) and modeled (small grey points) bottom layer dissolved inorganic phosphorus concentrations for the lower estuary boxes (5 – 8). Measured concentrations sampled by the CBP.

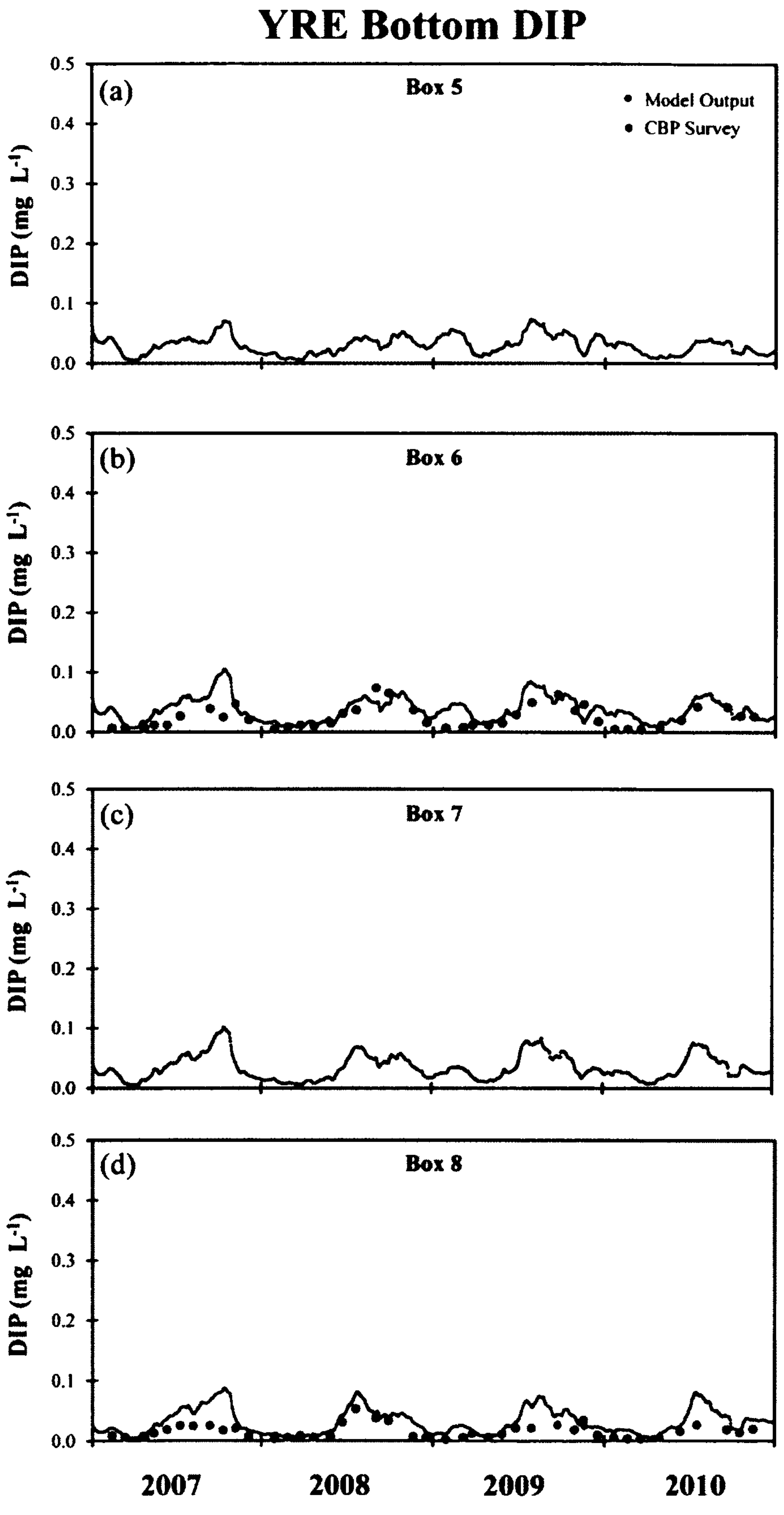
YRE Bottom DIP
(a)
Box 5
Model Output
CBP Survey
(b)
Box 6
(c)
Box 7
(d)
Box 8
DIP (mg L-1)
0.0
0.1
0.2
0.3
0.4
0.5
2007
2008
2009
2010

Figure A-21. Modeled (small grey points) surface layer water column net primary production for the upper estuary boxes (1 – 4).

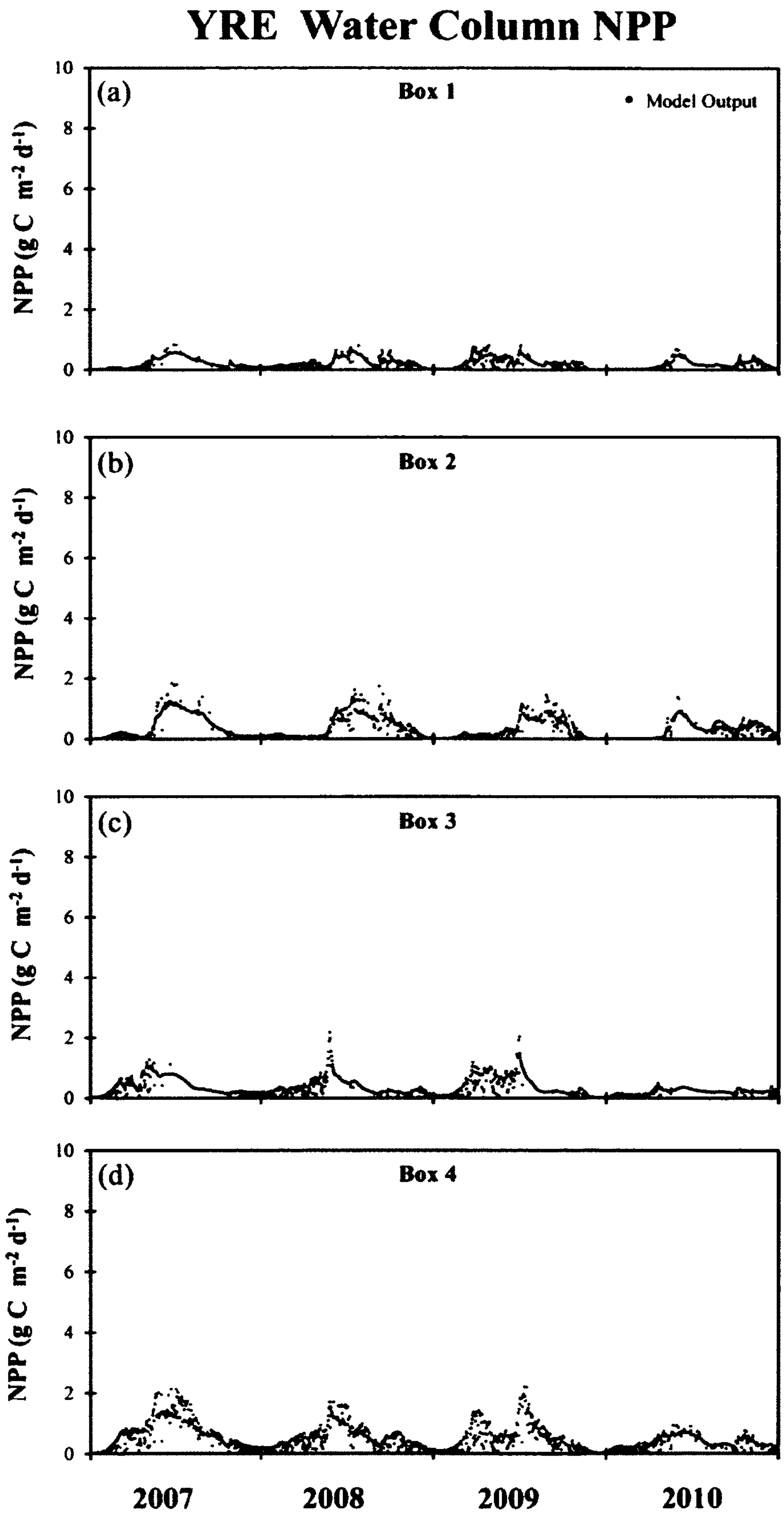
YRE Water Column NPP
(a)
Box 1
• Model Output
(b)
Box 2
(c)
Box 3
(d)
Box 4
NPP (g C m-2 d-1)
0
2
4
6
8
10
2007
2008
2009
2010

Figure A-22. Measured (large points) and modeled (small grey points) surface layer water column net primary production for the lower estuary boxes (5 – 8). Measured rates from Lake et al. (*in review*).

YRE Water Column NPP

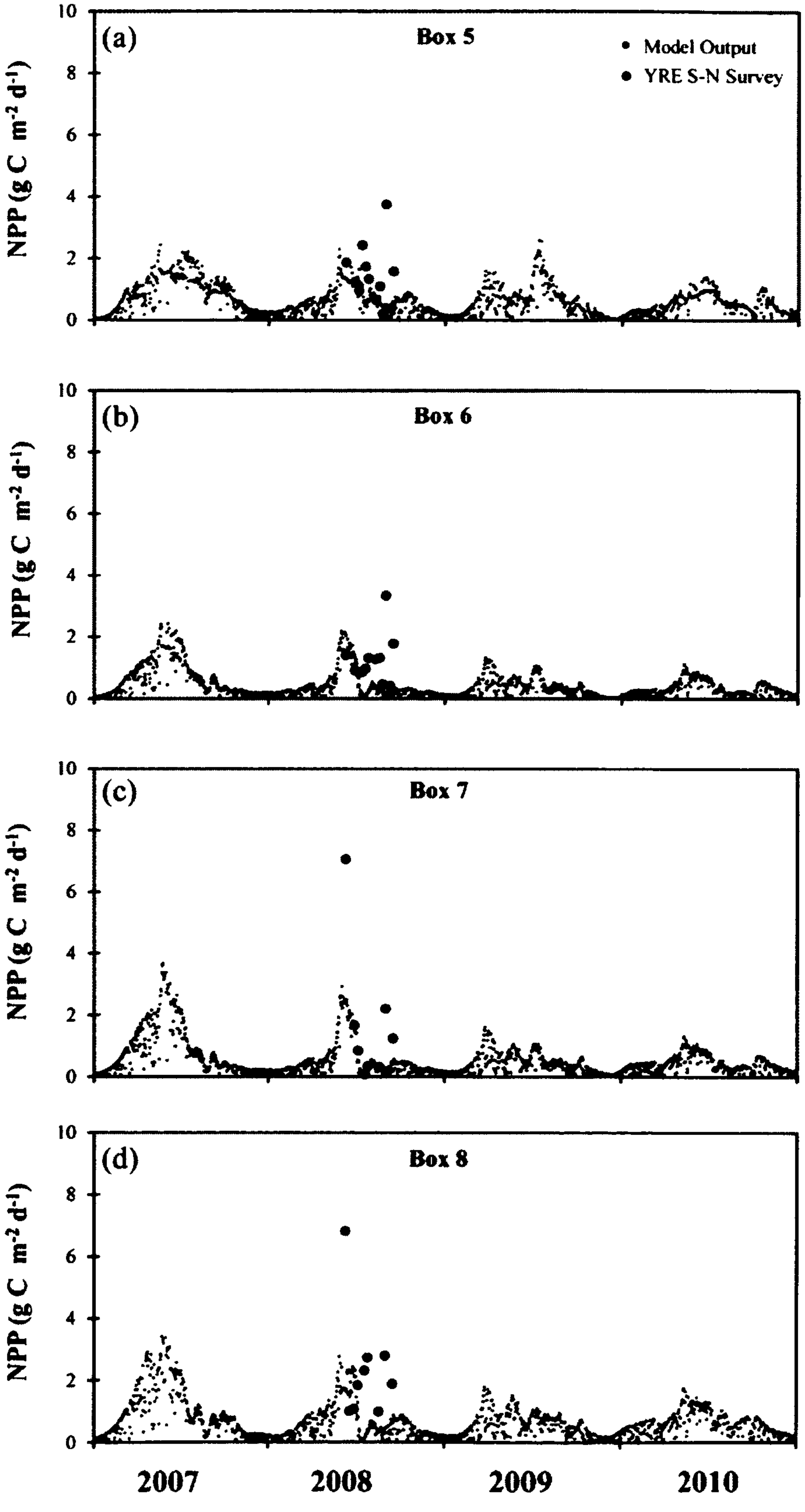

Figure A-23. Modeled (small grey points) surface layer benthic gross primary production for the upper estuary boxes (1 – 4).

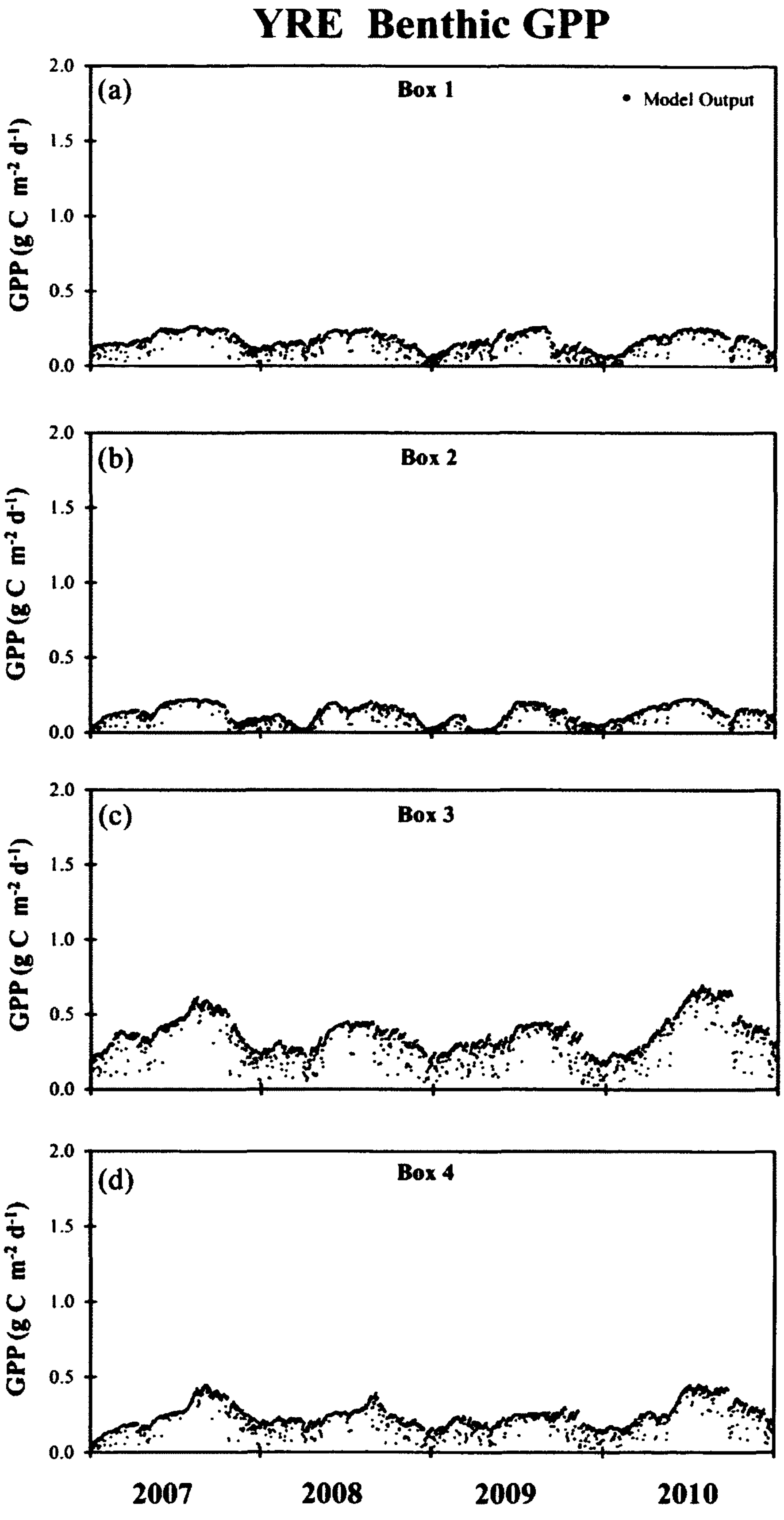
YRE Benthic GPP
(a)
Box 1
Model Output
(b)
Box 2
(c)
Box 3
(d)
Box 4
GPP (g C m-2 d-1)
2.0
1.5
1.0
0.5
0.0
2007
2008
2009
2010

Figure A-24. Measured (large points) and modeled (small grey points) surface layer benthic gross primary production for the lower estuary boxes (5 – 8). Measured rates from Lake et al. (*in review*).

YRE Benthic GPP

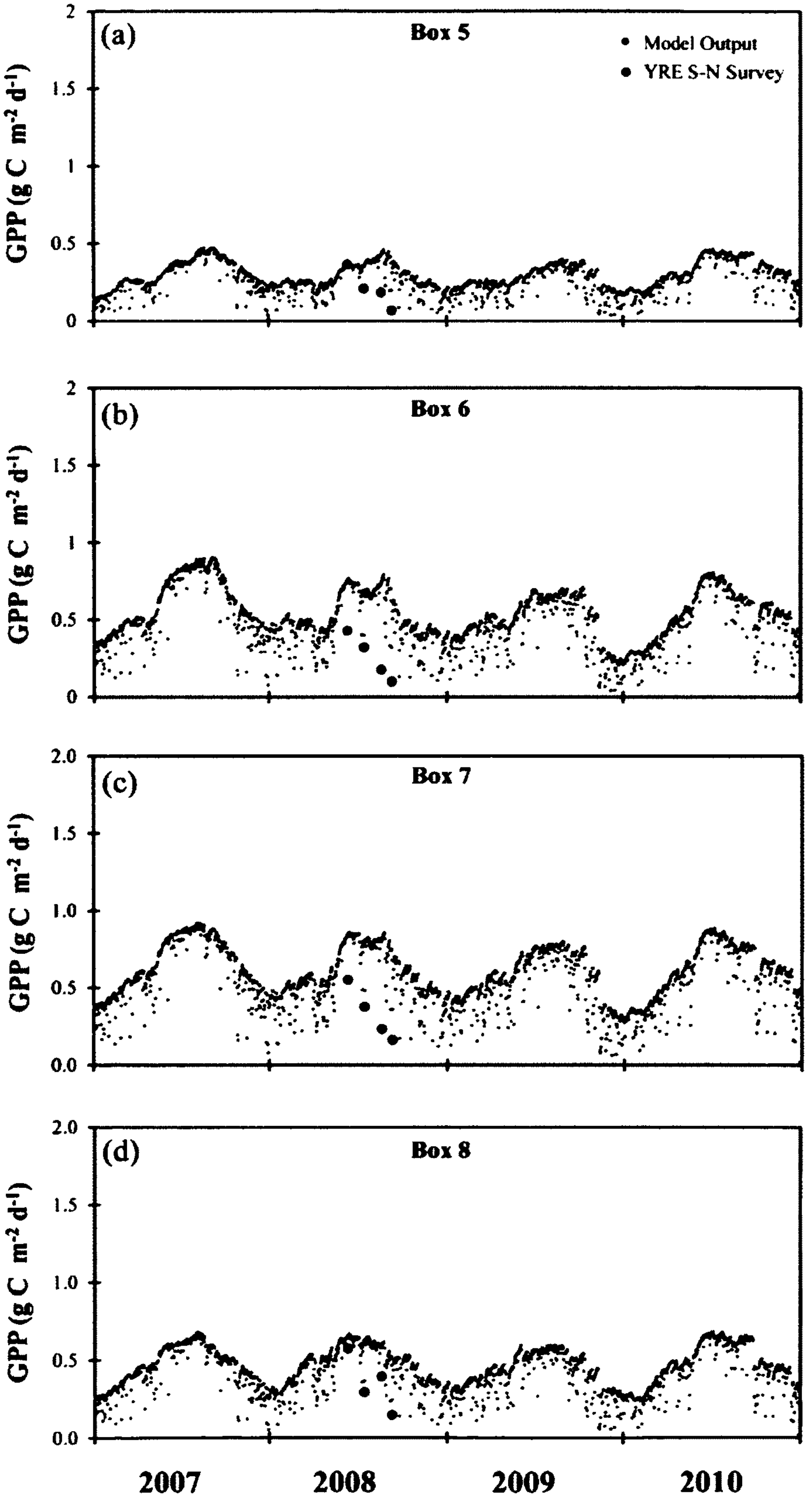

Figure A-25. Modeled (small grey points) surface layer water column respiration for the upper estuary boxes (1 – 4).

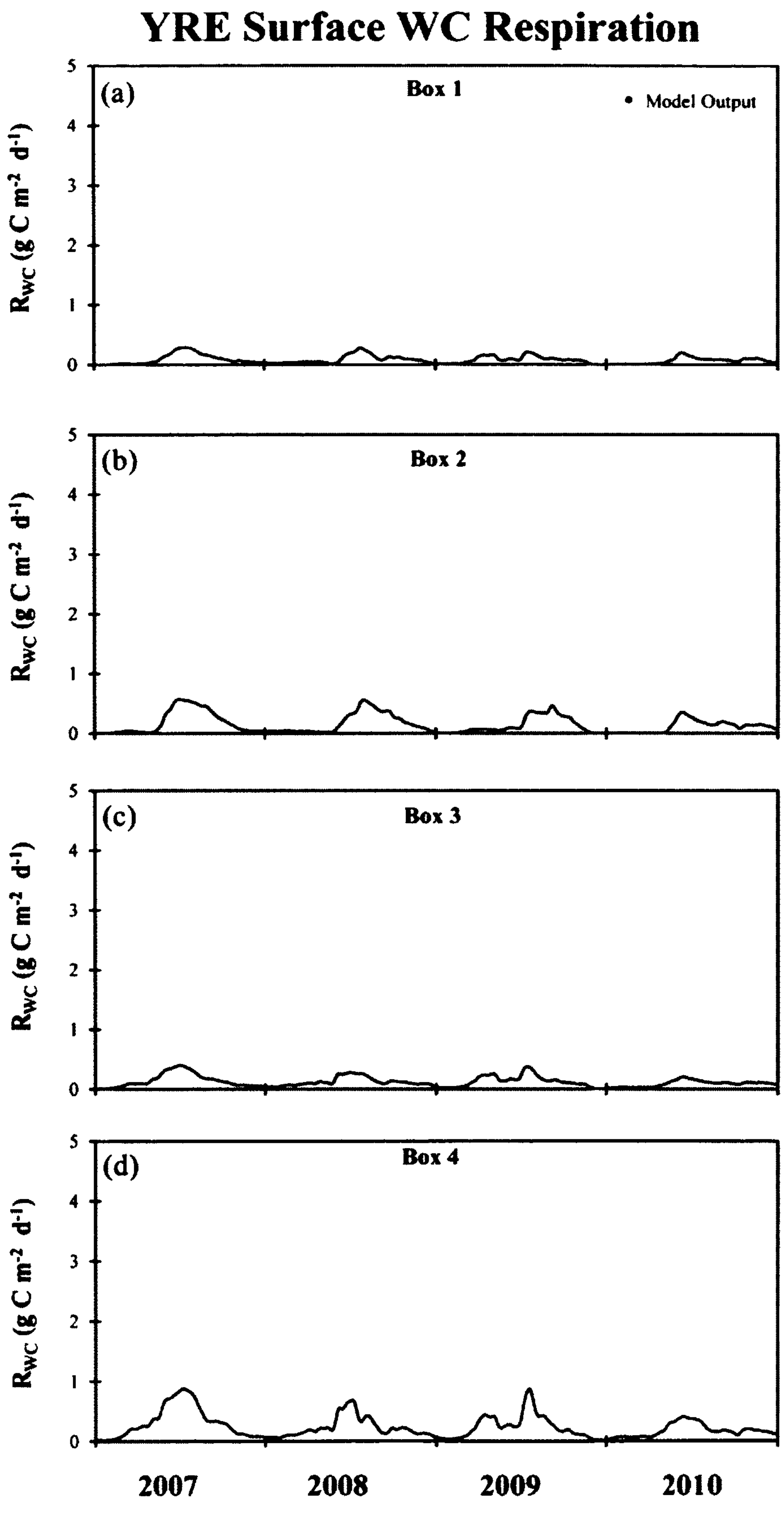
YRE Surface WC Respiration
(a)
Box 1
• Model Output
(b)
Box 2
(c)
Box 3
(d)
Box 4
R$_{WC}$ (g C m^{-2} d^{-1})
0
1
2
3
4
5
2007
2008
2009
2010

Figure A-26. Measured (large points) and modeled (small grey points) surface layer water column respiration for the lower estuary boxes (5 – 8). Measured rates from Lake et al. (*in review*).

YRE Surface WC Respiration

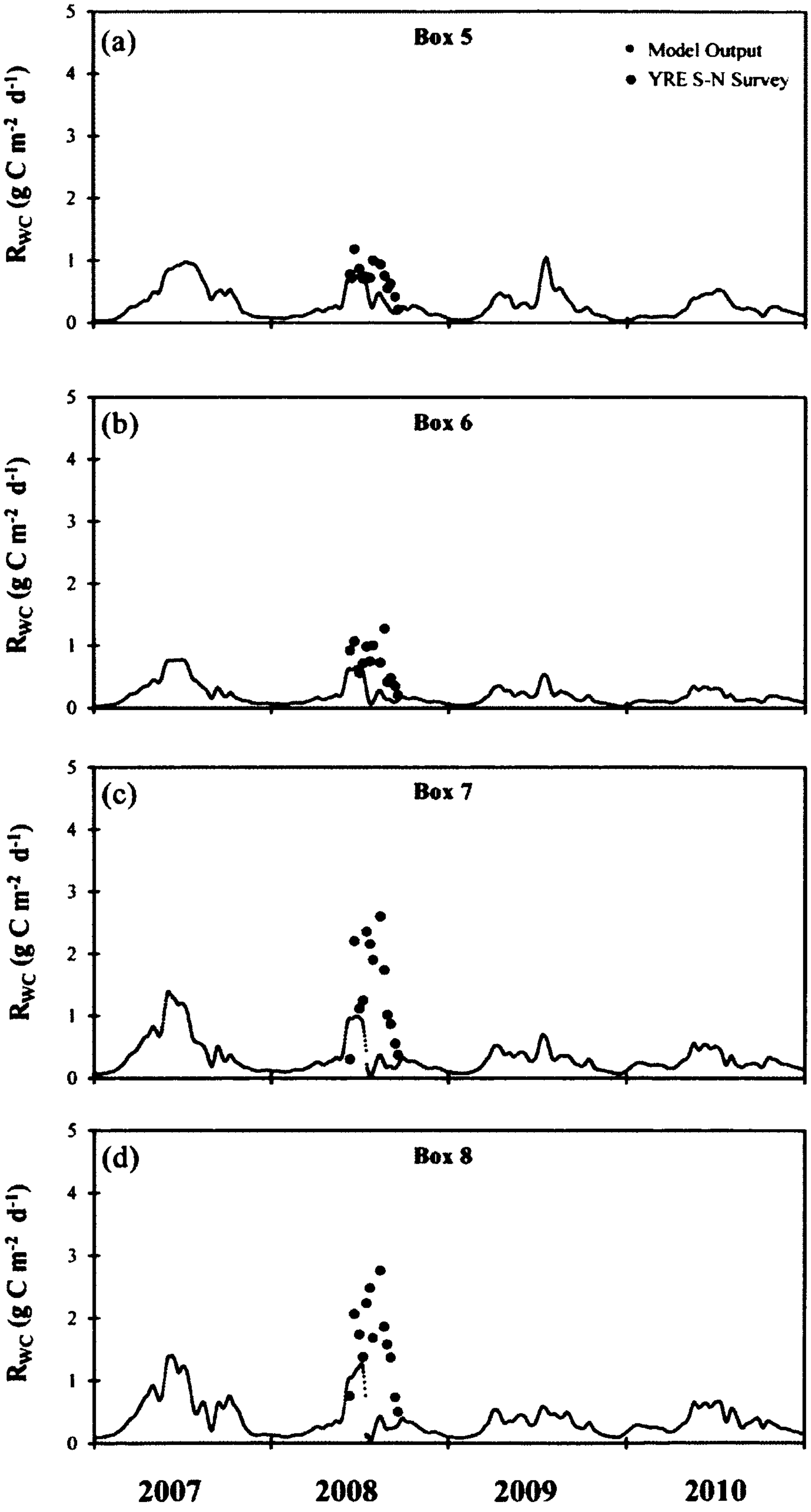

Figure A-27. Modeled (small grey points) bottom layer water column respiration for the upper estuary boxes (1 – 4).

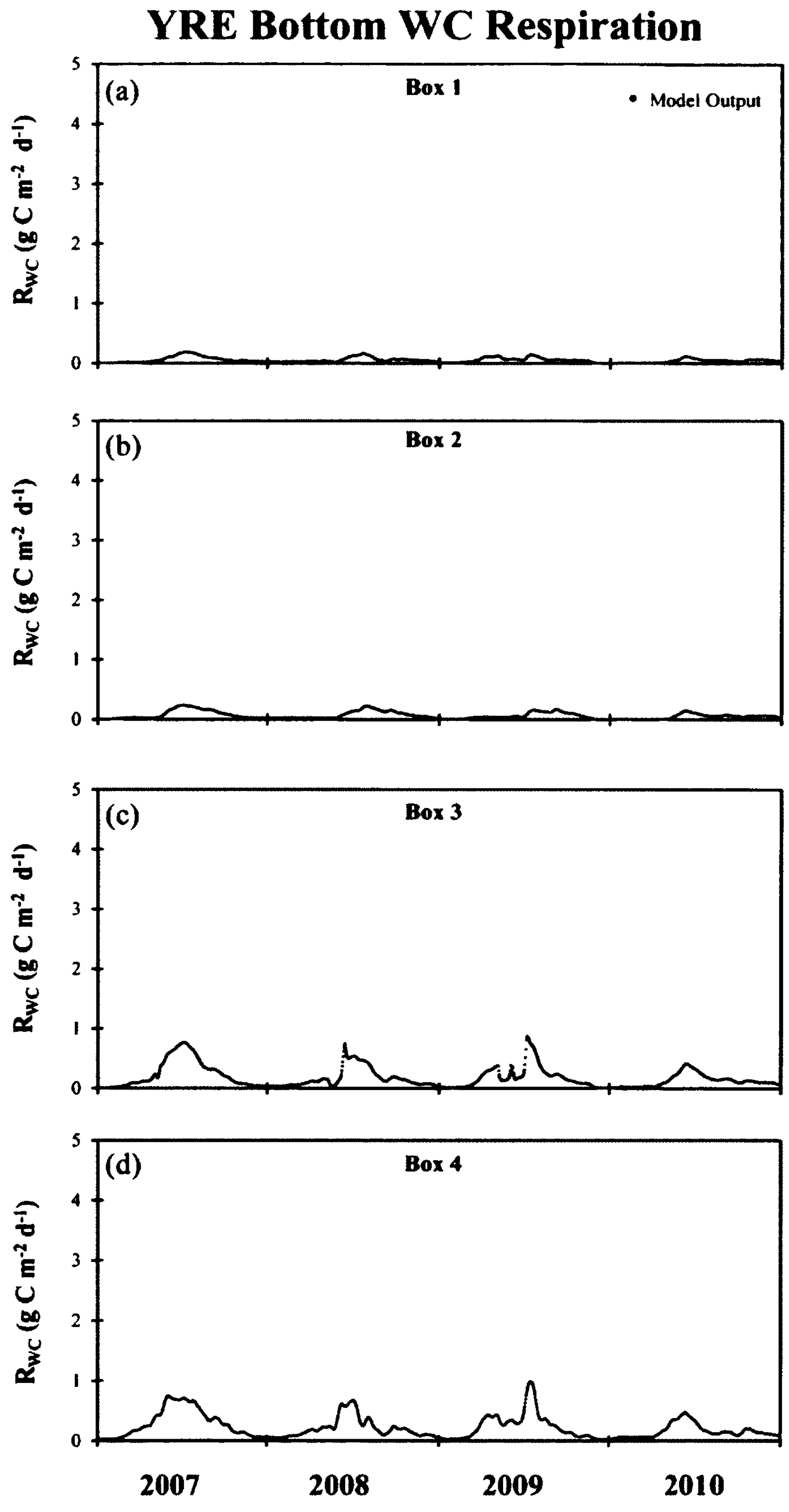
YRE Bottom WC Respiration
(a)
Box 1
• Model Output
(b)
Box 2
(c)
Box 3
(d)
Box 4
R_{WC} (g C m^{-2} d^{-1})
0
1
2
3
4
5
2007
2008
2009
2010

Figure A-28. Measured (large points) and modeled (small grey points) bottom layer water column respiration for the lower estuary boxes (5 – 8). Measured rates from Lake et al. (*in review*).

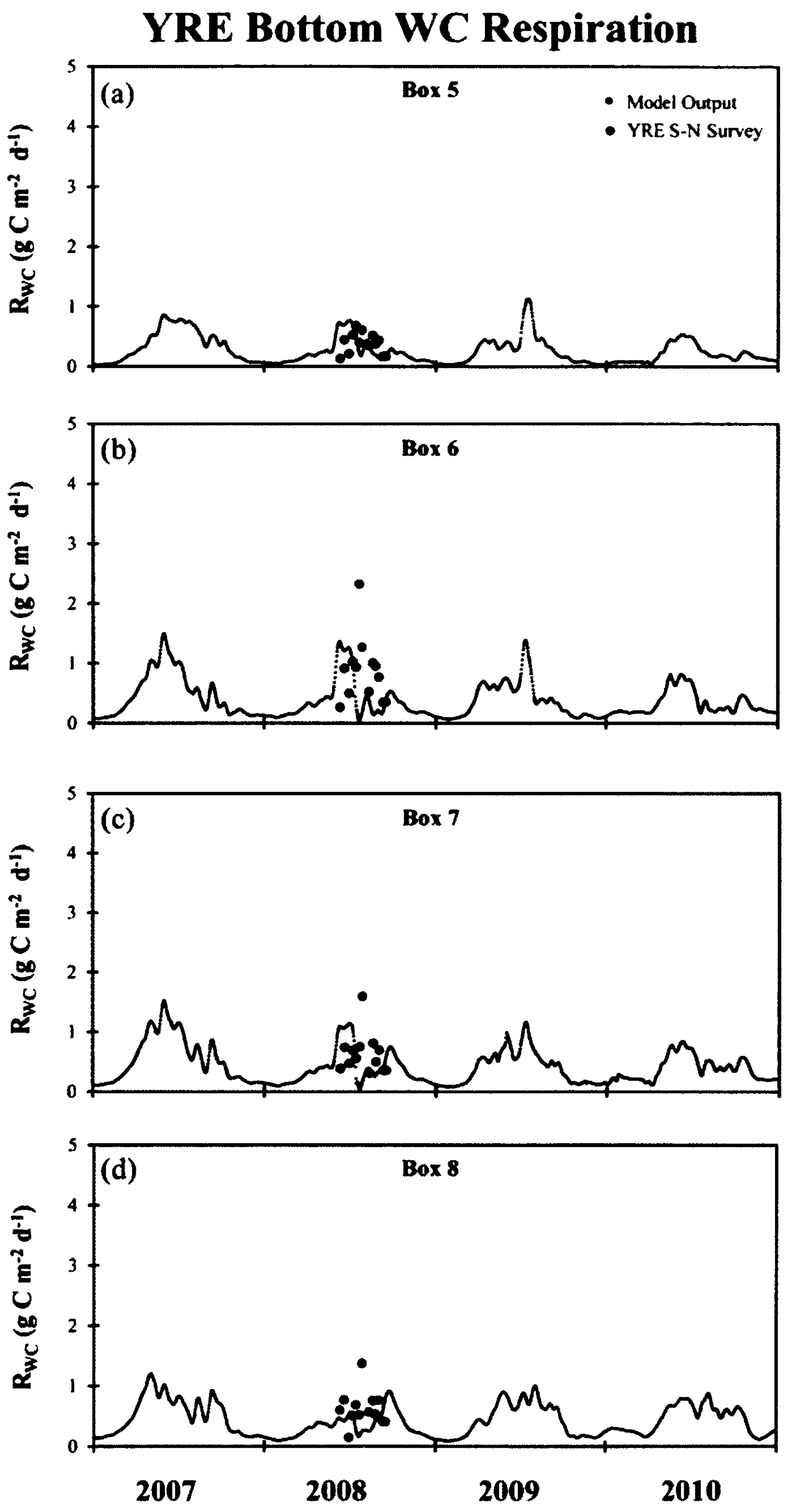
YRE Bottom WC Respiration
(a)
Box 5
Model Output
YRE S-N Survey
(b)
Box 6
(c)
Box 7
(d)
Box 8
R_{WC} (g C m^{-2} d^{-1})
0
1
2
3
4
5
2007
2008
2009
2010

Figure A-29. Modeled (small grey points) surface layer benthic respiration for the upper estuary boxes (1 – 4).

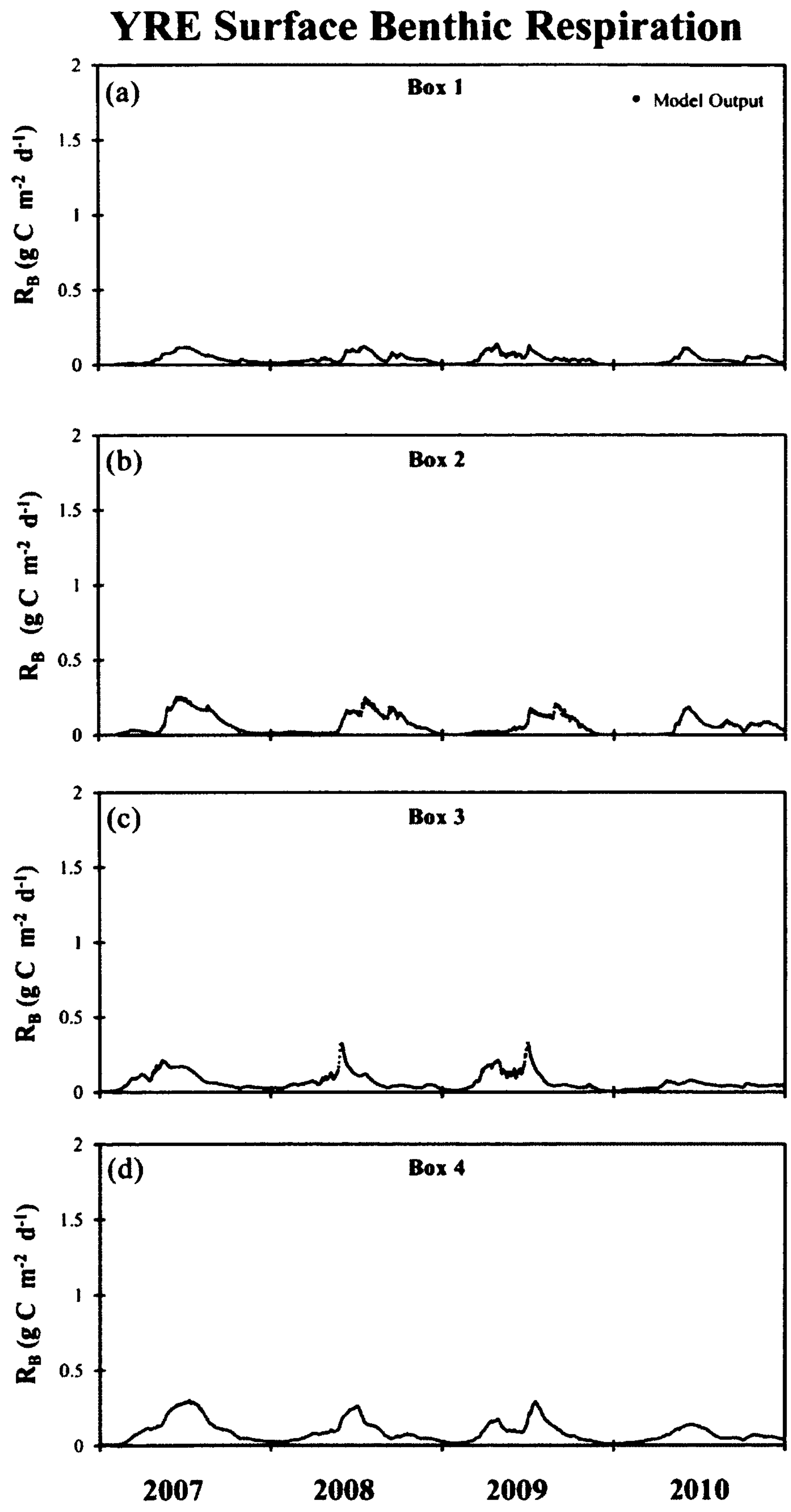
YRE Surface Benthic Respiration
(a)
Box 1
• Model Output
(b)
Box 2
(c)
Box 3
(d)
Box 4
R_B (g C m^{-2} d^{-1})
0
0.5
1
1.5
2
2007
2008
2009
2010

Figure A-30. Measured (large points) and modeled (small grey points) surface layer benthic respiration for the lower estuary boxes (5 – 8). Measured rates from Lake et al. (*in review*).

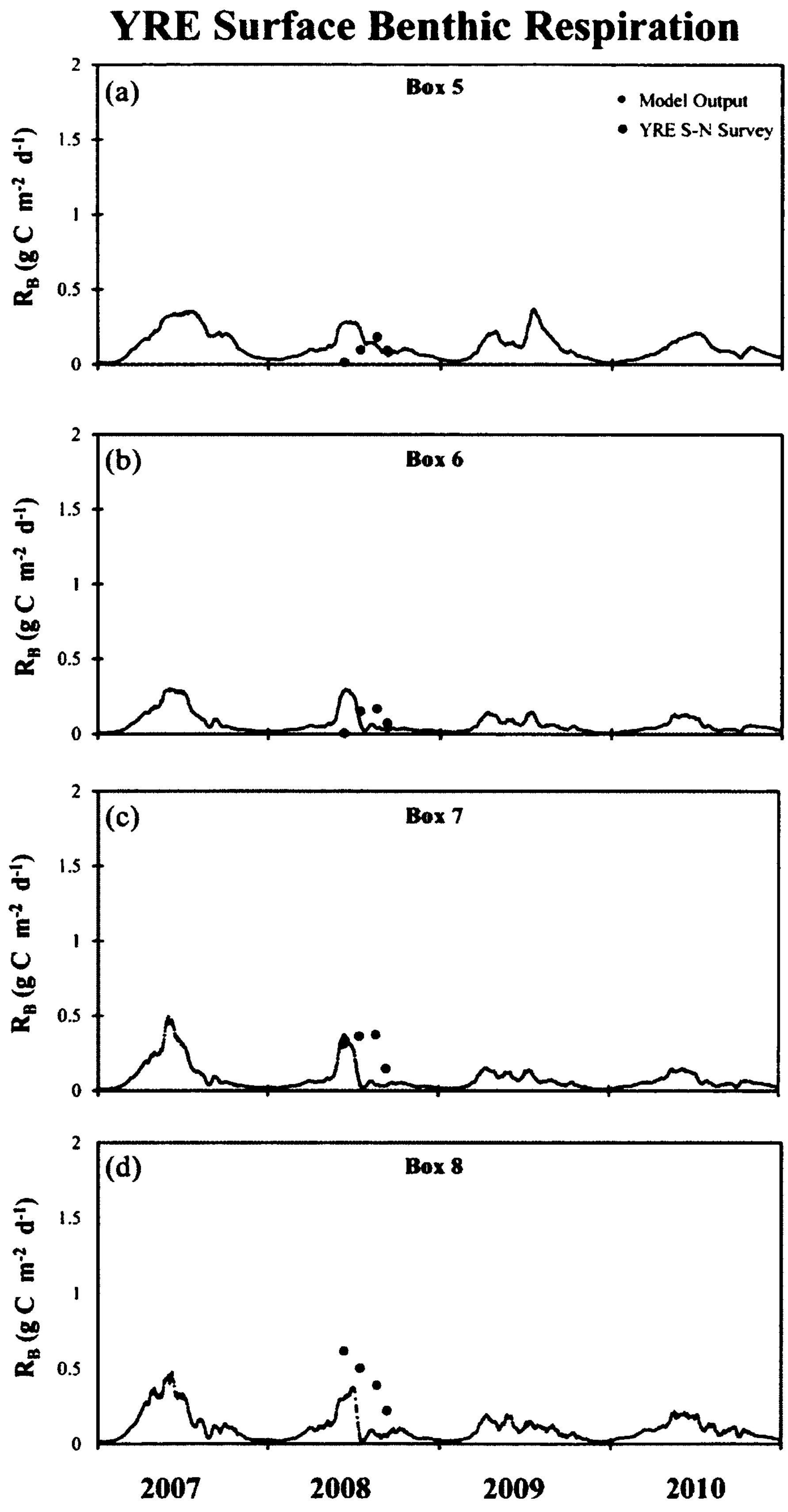
YRE Surface Benthic Respiration

Figure A-31. Modeled (small grey points) bottom layer benthic respiration for the upper estuary boxes (1 – 4).

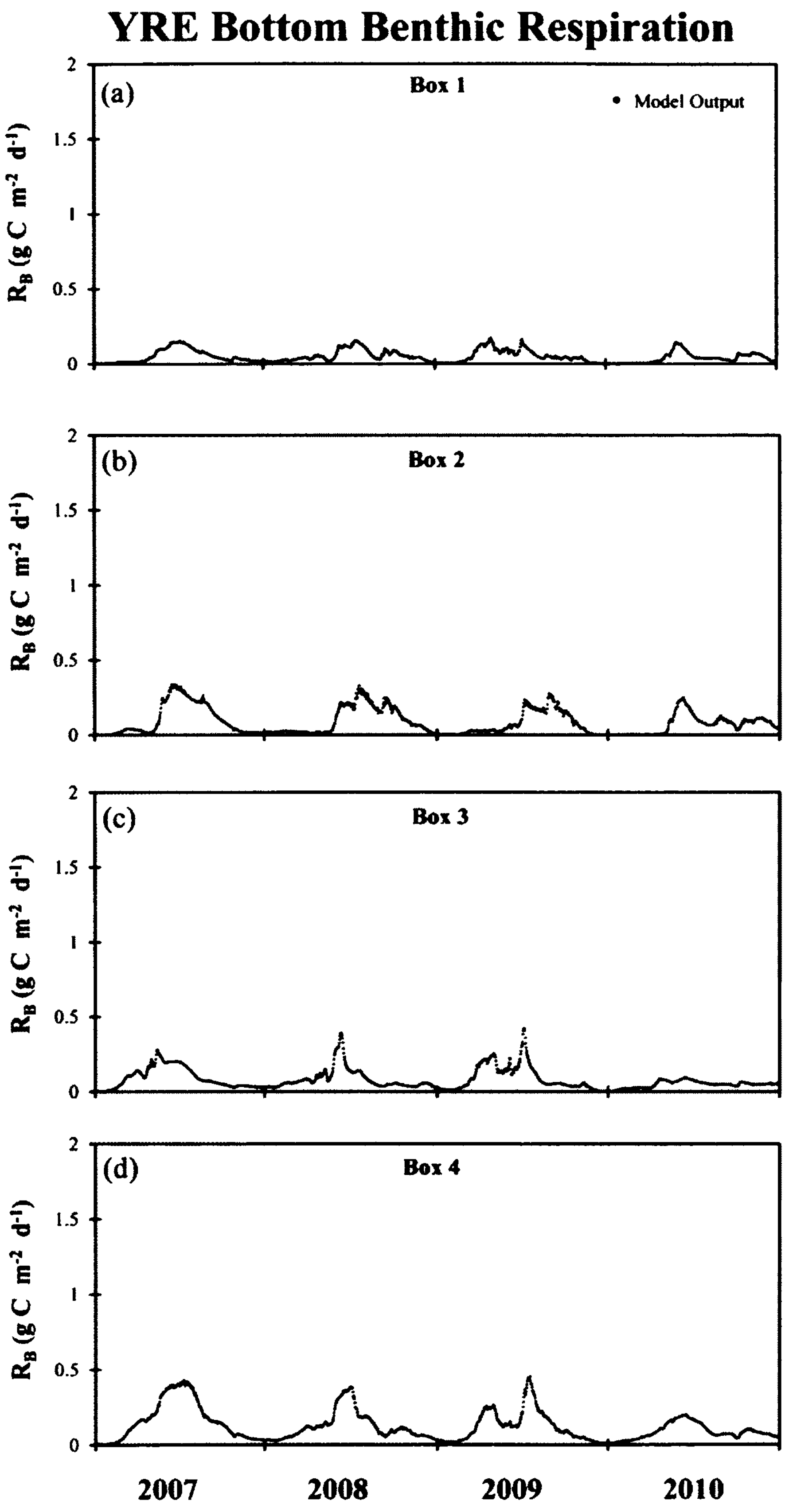
YRE Bottom Benthic Respiration
(a)
Box 1
• Model Output
(b)
Box 2
(c)
Box 3
(d)
Box 4
R_B (g C m^{-2} d^{-1})
0
0.5
1
1.5
2
2007
2008
2009
2010

Figure A-32. Measured (large points) and modeled (small grey points) bottom layer benthic respiration for the lower estuary boxes (5 – 8). Measured rates from Lake et al. (*in review*).

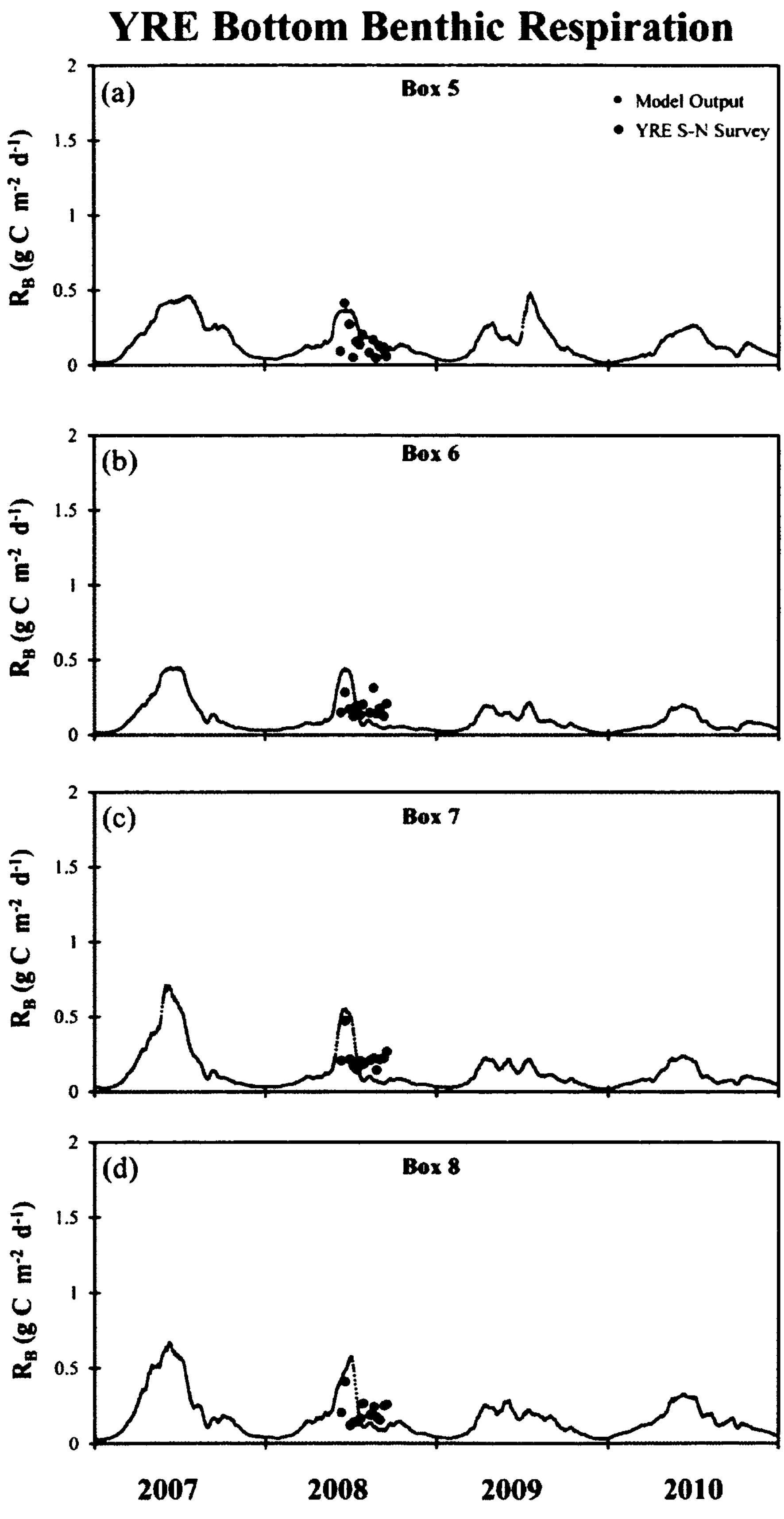
YRE Bottom Benthic Respiration
(a)
Box 5
Model Output
YRE S-N Survey
(b)
Box 6
(c)
Box 7
(d)
Box 8
R_B (g C m^{-2} d^{-1})
0
0.5
1
1.5
2
2007
2008
2009
2010

VITA

Samuel J. Lake

Samuel was born in Hamilton, Ohio on August 1, 1981. After graduating from Fairfield High School in 2000 he went on to earn a double major in Marine Science and Biology from Coastal Carolina University in 2005. After graduation he worked as an Environmental Lab Technician at Coastal Carolina University studying the development of coastal hypoxia in Long Bay, South Carolina. In the Fall of 2007 he moved to Williamsburg, Virginia to attend the College of William and Mary, Virginia Institute of Marine Science. Samuel bypassed into the Ph.D. program and earned his Doctor of Philosophy in Marine Science from the School of Marine Science in May of 2013. He is currently working as a Post-Doctoral Researcher at the Virginia Institute of Marine Science in the Coastal Systems Ecology and Modeling Program Laboratory.